

**School of Electrical and Computer Engineering**

**Optimised Design of Isolated Industrial Power Systems and System  
Harmonics**

**Stjepan Maticevic**

**This thesis is presented for the Degree of  
Doctor of Philosophy  
of  
Curtin University**

**November 2011**

## **Declaration**

To the best of my knowledge and belief this thesis contains no material previously published by any other person except where due acknowledgment has been made.

This thesis contains no material which has been accepted for the award of any other degree or diploma in any university.

Signature: .....

Date: .....

## **ABSTRACT**

This work has focused on understanding the nature and impact of non-linear loads on isolated industrial power systems. The work was carried out over a period of 8 years on various industrial power systems: off-shore oil and gas facilities including an FPSO, a wellhead platform, gas production platforms, a mineral processing plant and an LNG plant. The observations regarding non-linear loads and electrical engineering work carried out on these facilities were incorporated into the report.

A significant literature describing non-linear loads and system harmonics on industrial power systems was collected and reviewed. The literature was classified into five categories: industrial plants and system harmonics, non-linear loads as the source of current harmonics, practical issues with system harmonics, harmonic mitigation strategies and harmonic measurements.

Off-shore oil and gas production facilities consist of a small compact power system. The power system incorporates either its own power generation or is supplied via subsea cable from a remote node. Voltage selection analysis and voltage drop calculation using commercially available power system analysis software are appropriate tools to analyse these systems. Non-linear loads comprise DC rectifiers, variable speed drives, UPS systems and thyristor controlled process heaters. All non-linear loads produce characteristic and non-characteristic harmonics, while thyristor controlled process heaters generate inter-harmonics. Due to remote location, harmonic survey is not a common design practice. Harmonic current measurements during factory acceptance tests do not provide reliable information for accurate power system analysis.

A typical mineral processing plant, located in a remote area includes its own power station. The power generation capacity of those systems is an order of magnitude higher than the power generation of a typical off-shore production facility. Those systems comprise large non-linear loads generating current and voltage inter-harmonics. Harmonic measurements and harmonic survey will provide a full picture of system harmonics on mineral processing plants which is the only practical way to determine system harmonics. Harmonic measurements on gearless mill drive at the factory are not possible as the GMD is assembled for the first time on site.

LNG plants comprise large non-linear loads driving gas compressor, however those loads produce integer harmonics. Design by analysis process is an alternative to the current design process based on load lists. Harmonic measurements and harmonic survey provide a reliable method for determining power system harmonics in an industrial power system.

## **SYNOPSIS**

This work provides an overview of the industrial power system design process and system harmonics. The work explores the impact of non-linear loads implemented on industrial power systems such as off-shore oil and gas facilities, mineral processing plants and LNG plants. The work challenges the design process currently adopted within the industry. Design by power system analysis is proposed as a new design process that would consider and evaluate the impact of non-linear loads in the power system. This approach will lead to optimised system design in relation to voltage and current distortions. The nature of non-linear loads was demonstrated through harmonic measurements and harmonic analysis using commercially available power system analysis software.

## **ACKNOWLEDGMENTS**

There are many people: colleagues, friends and family members, whom I would like to acknowledge and thank for their support and help.

I would like to thank my past and present supervisors for their contribution in guiding me throughout the research work. Firstly, Dr William B Lawrance who encouraged me to start this research and guided me in the first four years. Secondly, but equally gratefully, Professor Chem Nayar who throughout his continuous involvement over the past five years and with his professional guidance managed to provide invaluable directions and helped me to get this research work to the completion stage. Thanks to Professor Nayar, I realised that there is not a single problem, either technical or administrative that may not have a solution, usually a simple one.

I would like to acknowledge a contribution of my friend and colleague, a brilliant electrical engineer Mr Luka Brkic, who expressed a great interest in my research work and throughout our regular conversations about the work and challenges that I have been facing while working on this project provided invisible inner strength which helped me in getting this work done, from start to completion. There are so many human qualities in Luka that will remain a true inspiration for me for the rest of my professional career.

A big thank you goes to my wife Nada, the love of my life and daughters Dr Stjepana Maticevic and Dr Jelena Maticevic and their respective partners Dr Rohan Hockings and Dr David Manners, for their continuous support and understanding over the past 10 years. Also, I would like to thank to all my other family members, both in Croatia and Australia for their encouragement and support.

I would like to thank Mrs Gaye Harvey for her professional editing services and proof reading of the final thesis manuscript.

## **CONTENTS**

<b>ABSTRACT</b>	<b>I</b>
<b>SYNOPSIS</b>	<b>III</b>
<b>ACKNOWLEDGMENTS</b>	<b>IV</b>
<b>CONTENTS</b>	<b>V</b>
<b>LIST OF FIGURES</b>	<b>VIII</b>
<b>LIST OF TABLES</b>	<b>XIV</b>
<b>1. INTRODUCTION</b>	<b>1</b>
1.1 Background	1
1.2 Objectives	3
1.3 Thesis Outline	5
<b>2. LITERATURE REVIEW</b>	<b>8</b>
2.1 Literature Source	8
2.2 Electrical Power Systems for Industrial Plants	9
2.3 Source of Current Harmonics	21
2.4 Practical Issues with System Harmonics	35
2.5 Industrial Power System Harmonics	41
2.6 Mitigation Strategy for Reducing System Harmonics	48
<b>3. ELECTRICAL POWER SYSTEMS ON OFF-SHORE FACILITIES</b>	<b>56</b>
3.1 Codes and Legislation	56
3.1.1 WA Statutory Requirements for Electrical Installations	56
3.1.2 Electrical Design of Off-shore Plants and Non-linear Loads	60
3.2 Power Supply via Subsea Cables	64
3.2.1 System Configuration of an FPSO	64
3.2.2 Power System Configuration of a Wellhead Platform	67
3.2.3 Selection of Supply Voltage and Calculation of Voltage Drop	68
3.2.4 Power System Analysis - Case Study	73
3.3 Non-linear Loads Source of Current Harmonics	75

3.3.1	DC Rectifiers	75
3.3.2	AC UPS Systems	81
3.3.3	VSDs – LV and MV Application	84
3.3.4	Electric Process Heaters	89
3.4	Practical Issues with System Harmonics and Harmonic Analysis Strategies	93
3.4.1	Measurements	93
3.4.2	Harmonic Analysis Strategy	96
3.5	Original Contribution	98
<b>4.</b>	<b>POWER SYSTEMS FOR MINERAL PROCESSING PLANTS</b>	<b>100</b>
4.1	Introduction	100
4.2	Typical Isolated Power System for Gold Processing Plant	101
4.3	Variable Speed Drives for Grinding Mills	102
4.3.1	General	102
4.3.2	Voltage Source Inverters for Ball Mills	102
4.3.3	SAG Mill	105
4.3.4	Cyclo-converters for Gearless Mill Drives	108
4.3.5	Theoretical Background	113
4.4	Practical Issues with System Harmonics – Harmonic Measurements	120
4.4.1	Introduction	120
4.4.2	Methodology	121
4.4.3	Discussion on Harmonic Measurement Analysis	125
4.5	Practical Issues with System Transients	131
4.5.1	Introduction	131
4.5.2	Methodology	134
4.5.3	Discussion on Switching Transient Analysis	136
4.6	Original Contribution	138
<b>5.</b>	<b>ISOLATED POWER SYSTEM FOR AN LNG PLANT</b>	<b>140</b>
5.1	Introduction	140
5.2	Power system description	141
5.2.1	Typical Single Line Diagram	141
5.2.2	Engineering Specifications and Design Process	144
5.3	Non-linear loads	147



5.3.1	Variable Speed Drives and UPS Systems	147
5.3.2	LCI Driven Compressors	147
5.3.1	VSI Driven Compressors	150
5.4	Practical Issues with System Harmonics	154
5.4.1	Mitigation Strategy	154
5.4.2	Filter Selection	156
5.5	Original Contribution	157
<b>6.</b>	<b>CONCLUSIONS AND RECOMMENDATIONS</b>	<b>159</b>
6.1	Original Contribution	159
6.2	Recommendations for Further Work	162
<b>7.</b>	<b>BIBLIOGRAPHY</b>	<b>164</b>
<b>8.</b>	<b>APPENDIX 1 - HARMONIC MEASUREMENTS ON AN INDUSTRIAL PLANT</b>	<b>175</b>
<b>9.</b>	<b>APPENDIX 2 - POWER SYSTEM MODELLING AND HARMONIC ANALYSIS</b>	<b>186</b>
<b>10.</b>	<b>APPENDIX 3 - HARMONIC MEASUREMENTS ON A MINERAL PROCESSING PLANT</b>	<b>197</b>
<b>11.</b>	<b>APPENDIX 4 - SWITCHING TRANSIENTS</b>	<b>213</b>
<b>12.</b>	<b>APPENDIX 5 - HARMONIC FILTER SELECTION STUDY</b>	<b>233</b>

## LIST OF FIGURES

Figure 3-1	Impact on the regulatory process in the oil and gas industry ( <a href="http://www.dmp.wa.gov.au">www.dmp.wa.gov.au</a> )	56
Figure 3-2	North West Shelf production facilities and significant hydrocarbon discoveries ( <a href="http://www.dmp.wa.gov.au">www.dmp.wa.gov.au</a> )	57
Figure 3-3	Maximum demand calculation sheet template	62
Figure 3-4	Configuration of a typical FPSO electrical power system	65
Figure 3-5	Configuration of typical wellhead platform electrical power system	67
Figure 3-6	Nominal $\pi$ cable model	69
Figure 3-7	Subsea cable with distributed constants and equivalent $\pi$ model	71
Figure 3-8	Three-phase, full-wave diode bridge with resistive load; circuit connection, supply line voltages, load voltage, load current, and supply line current (phase a)	77
Figure 3-9	Current harmonic spectrum of 6-pulse full bridge rectifier	81
Figure 3-10	Configuration of typical off-shore platform electrical power system	82
Figure 3-11	Typical UPS battery charger configuration diagram	83
Figure 3-12	Typical UPS schematic diagram	84
Figure 3-13	A simple representation of a VSD system	85
Figure 3-14	Typical configuration of VSI type VSD system	87
Figure 3-15	Typical configuration of CSI type VSD System	89
Figure 3-16	Typical configuration of thyristor controlled process heater	90

Figure 3-17	50% duty cycle of thyristor controlled process heater	91
Figure 3-18	Factory acceptance tests on 60 kVA UPS units	95
Figure 3-19	Factory acceptance tests on 220 kVA UPS units	96
Figure 4-1	Simplified SLD of primary power station and treatment plant	102
Figure 4-2	A voltage source inverter with 12-pulse diode rectifier, 2 quadrant operation	104
Figure 4-3	A voltage source inverter with 6-pulse active front end rectifier, 4 quadrant operation	105
Figure 4-4	3-D Isometric view of gearless mill motor drive	106
Figure 4-5	Possible trajectories of gearless mill drive (Pont, 2005)	107
Figure 4-6	6-pulse cyclo-converter	110
Figure 4-7	6-pulse cyclo-converter feeding three-phase synchronous motor	111
Figure 4-8	12-pulse cyclo-converter feeding 3-phase synchronous motor	112
Figure 4-9	Overview of typical ABB 12-pulse GMD and its components	112
Figure 4-10	Current harmonic spectrum of 6-pulse cyclo-converter (Miyairi, 1979)	114
Figure 4-11	Output voltage and switching functions of cyclo-converter (Miyairi, 1979)	115
Figure 4-12	Fundamental component of output voltage, output current and mode functions (Miyairi, 1979)	116
Figure 4-13:	Front view of Dranetz PowerXplorer PX5	122
Figure 4-14	Test plan for measurements at power station 33 kV switchboard	123
Figure 4-15	Test plan for measurements at concentrator 33 kV switchboard	124

Figure 4-16	Current waveforms on the supply side of SAG mill cyclo-converter	126
Figure 4-17	Full current harmonic spectra of SAG mill cyclo-converter	127
Figure 4-18	Average of one cycle current harmonic spectra of SAG mill cyclo-converter (suitable for ETAP)	127
Figure 4-19	Full current harmonic spectra of the 7 <sup>th</sup> harmonic filter	130
Figure 4-20	Full current harmonic spectra of the 5 <sup>th</sup> harmonic filter	131
Figure 4-21	Voltage and current waveforms at time of energising cyclo-converter transformers	136
Figure 4-22	Subsequent cycles of transformer inrush current	137
Figure 4-23	Back-to-back capacitor switching	138
Figure 5-1	Schematic of Conoco Phillips LNG process (Martinez, 2005)	142
Figure 5-2	Typical LNG plant SLD (Wilson, 2006)	143
Figure 5-3	12-pulse LCI arrangement with harmonic filter (Siemens)	148
Figure 5-4	Thyristor converter power circuit	149
Figure 5-5	24 pulse VSI arrangement (ABB)	152
Figure 5-6	30/36-pulse VSI arrangement (Siemens, Perfect Harmony)	152
Figure 5-7	VSI with reverse conducting IGCTs for a 3.3 kV drive	153
Figure 5-8	VSI with IGBTs for a 3.3 kV motor	153
Figure 8-1	Voltage and current time-plot over 24 hour period	182
Figure 8-2	Voltage and current time-plot over 24 hour period	183
Figure 8-3	Voltage and current time-plot over 24 hour period	184

Figure 9-1	Voltage and current time-plot on rectifier feeder	192
Figure 9-2	ETAP simulation - rectifier feeder current waveform	194
Figure 10-1	Timeplot of electrical parameters	198
Figure 10-2	Voltage harmonics on the 33 kV switchboard	199
Figure 10-3	Current harmonics on inter-connector feeder	199
Figure 10-4	Current harmonics on train 1 feeder	200
Figure 10-5	Current harmonics on train 2 feeder	200
Figure 10-6	Current harmonics on a GT	201
Figure 10-7	Voltage, current and power factor timeplot	202
Figure 10-8	Voltage harmonics	203
Figure 10-9	Current waveform on SAG mill feeder	203
Figure 10-10	Current harmonics on SAG mill feeder	204
Figure 10-11	Current harmonics on the 3 <sup>rd</sup> harmonic feeder	204
Figure 10-12	Current harmonics on the 4 <sup>th</sup> harmonic feeder	205
Figure 10-13	Current harmonics on the 5 <sup>th</sup> harmonic feeder	205
Figure 10-14	Current harmonics on the 7 <sup>th</sup> harmonic feeder	206
Figure 10-15	Voltage, current and power factor timeplot	207
Figure 10-16	Voltage harmonics at the 33 kV switchboard	208
Figure 10-17	Current waveform on SAG mill feeder	208
Figure 10-18	Current harmonic spectrum	209
Figure 10-19	Current waveform on Incomer	209

Figure 10-20	Current harmonic spectrum	210
Figure 10-21	5 <sup>th</sup> harmonic filter harmonic spectrum	210
Figure 10-22	7 <sup>th</sup> harmonic filter harmonic spectrum	211
Figure 11-1	Voltage and current timeplot	214
Figure 11-2	Voltage and current waveforms	214
Figure 11-3	Voltage and current waveforms	215
Figure 11-4	Voltage and current timeplot	216
Figure 11-5	Event #8 voltage and current waveforms	217
Figure 11-6	Event #26 voltage and current waveforms	217
Figure 11-7	Event #31 voltage and current waveforms	218
Figure 11-8	Event #31 waveform close look-up	218
Figure 11-9	Voltage and current timeplot	219
Figure 11-10	Event#202 voltage and current waveforms	220
Figure 11-11	Event#212 voltage and current waveforms	221
Figure 11-12	Event#226 voltage and current waveforms	221
Figure 11-13	Event#259 voltage and current waveforms	222
Figure 11-14	Voltage and current timeplot	223
Figure 11-15	Event#8 voltage and current waveforms	224
Figure 11-16	Event#226 voltage and current waveforms	225
Figure 11-17	Event#73 voltage and current waveforms	226
Figure 11-18	Voltage and current timeplot	227

Figure 11-19	Event#65 voltage and current waveforms	227
Figure 11-20	Event#73 voltage and current waveforms	228
Figure 11-21	Event#118 voltage and current waveforms	229
Figure 11-22	Event#122 voltage and current waveforms	229
Figure 11-23	Event#447 voltage and current waveforms	230
Figure 12-1	Voltage harmonics on SG-502 for case 1	238
Figure 12-2	Voltage harmonics on SG-502 with the single tuned filter	239
Figure 12-3	Harmonic filter parameters – ETAP input data	240
Figure 12-4	SG-502 voltage harmonics with the high-pass single filter	240
Figure 12-5	Voltage harmonics on SG-502 for case 5	242

## **LIST OF TABLES**

Table 3-1	Standard MV power cable electrical parameters	74
Table 3-2	Cable voltage drop and transmission efficiency	75
Table 4-1	Current distortion limits – odd harmonics	125
Table 4-2	Current distortion limits – even harmonics	125
Table 4-3	Current harmonics on the SAG mill feeder	130
Table 4-4	Table 2 of IEEE Std 1159-1995(R2000)	133
Table 8-1	Table 1: Distribution planning levels for harmonic voltages	180
Table 8-2	Current distortion limits as per IEEE Std 519	181
Table 9-1	Harmonic source input data	193
Table 12-1	Power factor for the existing network	237
Table 12-2	Load factor for case 5	241



# **1. INTRODUCTION**

## **1.1 Background**

Western Australia is characterised by a strong resources industry. Mining, mineral processing, oil extraction and LNG gas export business are significant contributors to the Western Australian economy. The total area of Western Australia is 2.6 million square kilometres, with a population of less than 2.3 million. There are many mining and oil and gas plants that are spread around the state. The majority of those are being powered by their own power systems which are isolated and not interconnected into the national grid.

The state of Western Australia has two electrical power grids, one covering Perth and the south east of the state and another the north of Perth in the Pilbara area. The technical requirements on power quality and system harmonics of these two power systems are covered in legislative documents and (Western Power, 2007) Technical Rules.

The purpose of this work is to research practical problems related to the design of isolated power systems and provide guidance on how to optimise a typical industrial isolated power system in relation to system harmonics and system design. Non-linear loads are a source of current harmonics and in order to mitigate the system harmonics, designers of industrial power systems have to understand the underlying issues and apply the most appropriate design methods at various stages of the design process.

This research work was carried out over a period of 8 years, in parallel with normal engineering work on various projects within the oil and gas and mining industry in Western Australia and South East Asia. The work that was carried out during this period is summarised in a chronological order with the generating capacity of the industrial power system shown in brackets:-

- 2001-2003 - Off-shore oil and gas platform (20 MW)
- 2003-2004 - FPSO (25 MW)
- 2004-2006 - Gold processing plant (150 MW)

- 2005-2006 - Coal plant power station upgrade (100 MW)
- 2006-2007 - Gas processing plant (15 MW)
- 2006-2007 - Wellhead platform (0.5 MW)
- 2007-2009 - Chemical processing plant (20 MW)
- 2007-2010 - LNG plant (25 MW / over 400 MW)

On isolated industrial power systems, the power generation is comprised of one or more of the following generator types: gas fired turbines, diesel generators and coal fired steam turbines. Renewable energy sources such as wind turbines and solar power system are not utilised due to the variable nature of the energy source.

The electrical distribution system of an industrial plant is comprised of electric cables and overhead power lines used to distribute power from the generating plant to various load centres. A small compact power system such as an off-shore platform utilises only the electric cables. The loads are connected to electrical switchgear which is used for load switching and isolation purposes. The necessity to improve the safety of electrical switchgear and electrical installations has gained momentum within the industry, and for this reason electrical installations and equipment have to comply with all national and operating plant safety rules.

A modern typical industrial power system will comprise a number of various non-linear loads. This trend has been constantly increasing over last 20 years. Typical non-linear loads found on industrial power systems which were studied in this research work are 6 or 12-pulse rectifiers, AC and DC UPS systems, DC rectifiers, transformer rectifiers (rectiformers), thyristor controlled electric process heaters, LV and MV variable speed drives, cyclo-converters for SAG mill ring motors, LCI load commutated inverters and VSI voltage source inverters for synchronous motor driven compressors. Such a variety of non-linear loads requires careful consideration from the early stages of the design process.

The starting point in this research work was the collection of the relevant literature. Numerous search engines are available via Curtin Library Resources and have been

heavily utilised in this work. The search resulted in the collection of a number of textbooks and technical papers, however only a selected number of highly relevant items is referenced in this thesis. The reference list comprises textbooks, journal papers, proceedings and catalogues, and industry standards and guidelines. A list of references is given in Section 7 titled Bibliography and each reference is further described in Section 2 of this thesis.

This thesis consists of the body of the report and a number of appendices. The appendices incorporate extracts from the technical reports prepared over the last 8 years and are provided in support of the main text in the thesis. The extracts attached in appendices are based on confidential documents prepared directly for various clients and in order to preserve the confidentiality of the reference data, any direct link to the business venture or particular plant has been removed from the text.

## **1.2 Objectives**

Objectives of this research work can be summarised as follows:-

- Summary of the industrial power system design process currently adopted within the industry. Critical evaluation of its suitability in relation to non-linear loads.
- Evaluation of system harmonics at various stages of the design process and comparison of practical issues with theoretical data and methods. Full understanding of the nature and theoretical background of modern day non-linear loads.
- To carry out harmonic measurements on practical real world industrial power systems and analyse the results and to propose new measures to mitigate system harmonics such as consideration for harmonic monitoring via electrical control system.
- To develop a new design process suggesting that industrial power systems should be evaluated for system harmonics at very early stages of design, challenging the current common practice within the industry

- To evaluate front end engineering design practice and propose improvements to address non-linear loads
- To highlight original contribution in this work and present new methods and a system approach towards optimisation of the electrical power system.

The set objectives will be addressed within the body of the report. The original contribution presented in the report will be highlighted at end of each section.

Industrial power systems are best described as power systems established to provide electrical power to industrial plants. The definition of industrial plant according to reference (Institute of Electrical and Electronics Engineers, Inc., 1994) IEEE Std 141-1993 IEEE is an industrial complex comprising industrial facilities and buildings where manufacturing, industrial production, research and development are performed. It does not include commercial buildings such as shopping centres, airports, city offices, or apartment and residential buildings.

The term industrial plant as used in this thesis comprises plant facilities and buildings located in and around the industrial complex used for workshops, offices, laboratories, test stations, storage facilities and accommodation quarters. A typical oil and gas off-shore production facility is comprised of an oil and gas processing plant, production modules and worker accommodation areas. This is described in more detail in Chapter 3. Similarly, an onshore oil and gas or mining industrial plant is comprised of processing plant, plant buildings and off-plot infrastructure such as accommodation village, airport, and general utilities. Onshore industrial plants are described further in Chapters 4 and 5.

The industrial complex requires various systems to support its operation and the electrical power distribution system is one of them. The following electrical design elements are common to all industrial plants:

- Magnitude, quality, characteristics, demand and coincidence or diversity of loads and load factors, associated with industrial processes
- Service, distribution and utilisation voltages and voltage regulation

- Power sources, distribution system, fault current and system co-ordination
- Conformity with regulatory requirements
- Reliability, continuity, safety of personnel and property
- Operation and maintenance

The main interests in this work were isolated electrical power systems which are best described as power systems not interconnected with the national grid. The industrial power systems isolated from the grid are specifically established to provide electrical power supply to industrial plants. They range from a few kW to up to a few hundreds of MW.

### **1.3 Thesis Outline**

This thesis is arranged in the following Chapters:-

Chapter 1 (this Chapter) is an introductory part which describes the purpose and objectives and gives a brief narrative about the work carried out in this research. The research work was carried out on a part time basis and it has complemented full time engineering design work performed on various industrial plants. The experience gained over the work period was incorporated into this thesis through various text, tables, charts and figures. This chapter lists those projects in a chronological order.

Chapter 2 describes the literature search about industrial power systems in the areas of power generation, distribution and electrical loads. The key focus area of this work is the current and voltage harmonics on industrial power systems and the source of harmonics caused by non-linear loads such as electric heaters, variable speed drives, cyclo-converters, LCI and VSI synchronous drives. A literature search was carried out with the aim to find out what types of issue are associated with the focus areas. It starts with a brief summary of literature sources, followed by a summary of the literature related to: electrical power systems for industrial plants; the source of current harmonics in industrial plants; practical issues with system harmonics; industrial power system harmonics; and mitigation strategy for reducing system harmonics. All literature listed in this chapter is directly referenced in the body of the report and is highly relevant to this research work.

Chapter 3 focuses on electrical power systems with an average load of up to 25 MW such as oil and gas off-shore production facilities. Two plant types are described and analysed, firstly an FPSO followed by a wellhead platform. The chapter starts with a description of the design process of an off-shore oil and gas industrial power system. Front end engineering, detail design, electrical engineering specifications, industry standards, and statutory regulations are some of the topics covered in this section. The chapter focuses on the selection of power generation type and the number of units. It explains the design process based on load list calculation and then proposes a new approach based on power system modelling suitable for load flow, short circuit and harmonic studies. The issues associated with subsea cables supplying off-shore facilities are discussed and calculation of the voltage drop of the subsea cable supplying a small load is described. A separate section of this chapter describes various non-linear loads seen as the source of current harmonics, such as AC UPS systems, LV and MV VSD systems, rectifiers and thyristor controlled electric process heaters. The last section includes harmonic measurements on an interconnected industrial plant comprising a large rectifier. It describes a technical solution implemented for the plant expansion project and the harmonic mitigation techniques applied in the design. A list of original contributions is provided at the end of the chapter.

Chapter 4 describes a typical gold processing plant comprising around 100 MW power generation capacity. The plant distribution network consists of cables and transmission lines powering various load centres. The major non-linear load includes cyclo-converters feeding SAG mill synchronous ring motors. Functional description of the SAG mill is briefly described followed by the description of practical cyclo-converters. The analytical formulae of the load waveform for a typical 6-pulse cyclo-converter are presented. In 2005 harmonic measurements and switching transients were carried out on a gold processing plant comprising two SAG mills. The results of the measurements are presented and linked to the power system analysis technique. The hypothesis set out in the previous chapter suggesting that harmonic studies be carried out at a very early stage of the design process is discussed in the context of the harmonic measurement analysis. A list of original contributions is provided at the end of the chapter.

Chapter 5 describes a typical LNG plant comprising its power generation and large electrically driven compressor motors. Such plant would have the capacity of around 500 MW. The chapter describes a practical solution for electrically driven compressors and recommends the type of electrical drive best suited for the plant. LCI and VSI variable speed drives are described and advantages and disadvantages of each type are listed. Special focus is put on the generation of current harmonics on the line side and mitigation strategies for reducing the system harmonics. The timing and scope of harmonic analysis is discussed and compared with current industry practice. Again, a list of original contributions is provided at the end of the chapter.

Chapter 6 is the last chapter and it is comprised of conclusion statements. It summarises material presented in previous chapters and contains design guidelines about the location and selection of non-linear loads in a typical isolated industrial plant. It states original contribution and provides recommendations for further research.

## **2. LITERATURE REVIEW**

### **2.1 Literature Source**

The starting point in this research work was the collection of the relevant literature. This chapter explains the methodology applied in searching various publications related to the subject matter covered in this thesis. It also provides a list of search engines used from the Curtin library resources demonstrating a systematic approach applied during the literature search.

The first source of information was a set of the textbooks held in the Robertson Library located on the Bentley campus at Curtin. The key textbooks located at the Robertson Library were studied and the key words or references found in the textbooks were recorded. Further literature search was carried out utilising the Curtin Library Service, which offered various search engines and data bases of which EngNet Data Base was preferred one. Electronic search on key words such as cyclo-converters, harmonics or filters returned lists of textbooks and technical papers published from research centres mainly in Japan and USA, and selected material was downloaded.

The IEEE offers electronic access to various of its publications via IEEE Explorer, to which Curtin University subscribes. This was utilised to locate a number of transaction papers. Searching was carried out in various ways: subject matter, key words, a word or a phrase in the title or by simply browsing through a particular publication. The following two IEEE journals published over the last 30 years were thoroughly searched and the selected transactions were downloaded in electronic format:-

- IEEE Transactions on Industrial Applications
- IEEE Industry Application Magazine

Reference lists of relevant technical papers were also sources for a key textbooks or technical papers explaining fundamental principles or formulae directly related to the concepts presented in those works.

The material collected as part of the literature search is grouped into five categories:-



- **Electrical Power Systems for Industrial Plants** – This collection consists of technical papers relating to industrial power systems. The focus is directed to isolated power systems and various issues relating to the power quality, especially system harmonics. The industrial power systems of interest are oil and gas off-shore platforms, FPSOs, LNG plants and large mining or mineral processing plants.
- **Source of Current Harmonics** – This group incorporates literature which describes devices and components of the power system known to be sources of current harmonics. The current harmonics are produced by non-linear static loads such as rectifiers, variable speed drives and cyclo-converters. The literature collected describes the control and switching philosophy of various static loads and the mechanism leading to generation of current harmonics.
- **Practical Issues with System Harmonics** – The focus of this collection is based on industrial power systems and particularly on isolated systems. Any practical issues recorded in the literature such as vibration, nuisance tripping of circuit breakers, overheating of power distribution system components and overloading of power generation were the focus of the literature search.
- **Industrial Power System Harmonics** – This literature collection describes industrial power systems and power system harmonics. Papers relating to harmonic measurement techniques and power quality assessment methodology are also included.
- **Mitigation Strategy for Reducing System Harmonics** – This literature focuses on mitigation strategies for reducing the impact of current harmonics on the system. Areas of system design such as functional location of harmonic filters, type of harmonic filters and its use are explained in these works. The focus is on the industrial power systems.

## **2.2 Electrical Power Systems for Industrial Plants**

The electrical power system for industrial plants in Western Australia must provide the level of safety mandated by statutory legislation, such as Western Australian Electricity Act 1945 and its Regulations. The equipment used in the power system

has to meet a minimum technical standard in order to provide a prescribed level of efficiency and power supply reliability. The design redundancy, availability of supply and equipment reliability are the factors controlled by the operator. The following list gives the key standards and textbooks used as a starting point in the design of an industrial power system.

1. (Standards Australia International, 2007), known as AS/NZS 3000 Wiring Rules is a prescriptive standard published by Standards Australia. Compliance with AS/NZS 3000 is mandated through Western Australian Electricity Act 1945 and its regulations. The standard is applicable to all domestic and commercial electrical installations in Western Australia, such as mining plants and oil and gas installations. It applies to both on-shore and off-shore facilities, provided they are located within Western Australian state waters. Commonwealth of Australia territorial waters are governed by the Australian Commonwealth legislation: Petroleum (Submerged Lands) Act 1967 (PSLA). The PSLA does not reference AS/NZS 3000 and operators installing equipment within the Commonwealth waters may specify their own standards for electrical equipment.
2. (Institute of Electrical and Electronics Engineers, Inc., 1994) titled IEEE Std 141-1993 IEEE Recommended Practice for Electrical Power Distribution for Industrial Plants, provides recommended practice and guidance for the design of electrical power systems on industrial plants. It is applicable to both isolated and inter-connected systems. The Standard references a number of IEEE Standards, engineering textbooks and other materials and would help engineers to design a reliable industrial power system. The following two reference standards are complementary to IEEE Std 141: 1) - (Institute of Electrical and Electronics Engineers, Inc., 1992) IEEE-Std 519-1992 IEEE Recommended Practices and Requirements for Harmonic Control in Electrical Power System and 2) - (Institute of Electrical and Electronics Engineers, Inc., 1998) IEEE Std 399-1997 IEEE Recommended Practice for Industrial and Commercial Power System Analysis. Chapter 9 of this reference deals with harmonics in power systems and provides a basic introduction to the source of harmonics and harmonic mitigation strategies. While not specifically related to an isolated

power system, the basic principles for designing any industrial power system are also applicable to an isolated power system. Consequently, this textbook is the relevant reference and a good starting point in the design of the industrial power systems.

3. (AREVA T&D, 2005) Network Protection and Automation Guide, Edition 2005 is the latest revision of the industry standard for the design of electrical protection schemes, formerly published by ALSTOM and earlier, General Electric Company. The textbook describes protection schemes used on electrical power systems. Chapter 18 describes protection principles of commercial and industrial power systems. Protection schemes applied in this chapter are widely used on isolated power systems. (AREVA T&D, 2005) provides two chapters dedicated to current and voltage transformers, which are highly relevant to the study of harmonics especially harmonic measurements. Both ratio and angle errors of the instrument transformers are described and the impact on the accuracy of the protection and measurement scheme are discussed.
4. (Khan, 2008) provides an in-depth systematic approach to the design of industrial power systems. The textbook describes all components of an industrial power system, such as power generation, transformers, cables and various loads. Sections 15 and 16 are related to power system capacitors and non-linear loads in the system. Design guidelines and specifications for the purchase of equipment and devices are given for each component of an industrial power system.

The following papers address non-linear loads on industrial plants. As the focus of this thesis is on non-linear loads and system harmonics, the selected papers are directly related to those areas. Implementation techniques and operating modes of such loads are a challenge to operators. Experience gained through practical operation and application of such loads is valuable to designers and operators of industrial plants.

5. (Timple, 1982) produced one of early papers on the application of cyclo-converters introduced into the steel industry. This paper compares

performances of cyclo-converter drives with traditional DC drives used in the rolling mills. The paper describes the principles of operation of a 6-pulse non-circulating current mode cyclo-converter utilising thyristor switches connected in anti-parallel configuration. Cyclo-converters are expected to perform in a similar way to a reversing converter used in DC drives with regards to current waveform, dynamic control, reliability, cost and system harmonics. The control system described in the paper is field-oriented stator current principle (or flux vector control) which can be used for both synchronous and induction motors. The author highlights the following advantages of cyclo-converters: synchronous or asynchronous standard machine option available, no additional flux-sensing devices required in the motor, choice of voltage and current levels, operation possible in weak fields, natural commutation, robust line-commutated converters (as for DC drives), efficiency better than comparable DC drives, investment cost lower than a double-motor DC drive. Results of measurements on a 1.2 MW AC drive are presented in the paper, concluding that dynamic properties of AC are equivalent to DC drives. The paper suggests that the application of cyclo-converters could be extended to high capacity drives running at slow speed.

6. (Colby, 1985) focuses on LCI converters and states that the commutation of the LCI converter is achieved by the induced EMF of the synchronous machine. The authors compute various steady state parameters using a state space analysis of synchronous motor drive such as current, voltage, and torque waveforms. Steady-state operating points are defined by the firing angle, commutation overlap angle, and the ratio of average field current to DC link current. Analytical formulae and sample calculations for a 4500-hp LCI drive were presented. The equations were based on digital computer-based state space solution of the synchronous machine. Results of digital simulations showing inverter voltage, electromagnetic torque, field current and DC link current were provided.
7. (Ishihara, 1986) compares three mill drive systems for application in the steel mill industry: 1) DC motor-thyristor Leonard using voltage and field control, 2) induction motor – cyclo-converter drive 3) synchronous motor – load

commutated inverter. The results of the comparison show that AC motors compared with DC motors have the following advantages: 1) easy maintenance, 2) overall efficiency, 3) overload characteristics, and 4) resistance to shock. The cyclo-converter fed induction motor does not generate any torque ripple and is suitable for low-speed reverse-operation large-capacity mills (3-5 MW). The synchronous motors driven by LCI converter are suitable for high speed non-reverse operation large capacity mills (above 6 MW). LCI's utilise motor EMF for commutation which is affected by armature reaction leading to a low overload factor. The cyclo-converter is the most suitable for steel mill application. The disadvantages are that these drives have poor input power factor and generate input harmonics. The authors evaluate design aspects of the cyclo-converter drive system and propose measures to improve the design of cyclo-converter, motor and harmonic suppression systems. Some of the proposed measures such as rotor splitting and installation of harmonic filters are commonly used with cyclo-converters driving induction motors.

8. (Azbill, 1990) describes practical issues with LCI drives experienced in operation. The experience described in this paper was collected in late 80's, at the time when LCI drives were starting to be applied in process plants. The experience gained and described in this paper relates to project execution and installation, start-up and operation of 7000 hp (2 pole) and 3600 hp (4 pole) synchronous motors driven by LCI drives. The paper describes the project lifecycle and gives a simplified single line diagram of the system, complete with harmonic filters which on this plant were installed at 13.8 kV voltage level. This paper then provides lessons learnt: a) Project strategy, project timeline; b) Installation of motors, controllers, harmonic filters; c) Commissioning and checkouts, interference and spare parts; d) Operation; e) Performance after start-up including shut down history and troubleshooting. Finally, the paper concludes that the new technology presented many challenges when applied for the first time. The authors recommend that training in the principles and operation of the unit should be approached in early stages of project implementation. The paper is positive in its approach and recommends continuing use of the LCI technology.

9. (IEEE/Cigre, 1997) produced a joint paper prepared by the IEEE Task Force on Inter-harmonics and the CC02 (Cigré 36.05/CIREN WG 2) Voltage Quality Working Group. This is a significant paper which summarises the current situation with inter-harmonics and provides a starting point for developing engineering guidelines and limits for inter-harmonics in power systems for future inclusion in IEEE 519, IEC-61000 and other relevant standards. Definition of harmonics, inter-harmonics and sub-harmonics is given in the introduction. A system comprised of inter-harmonics may not provide a periodic waveform, which creates issues with inter-harmonic measurements. The paper lists and describes sources of inter-harmonics. These are non-linear loads as follows: cyclo-converter, arcing load, induction motors, induction motors with wound rotor using sub-synchronous converter cascades, integral cycle control devices (typical applications are ovens, furnaces, die heaters, and spot-welders). The impact of inter-harmonics on a power system is characterised as: heating effect, CRT flicker, torsional oscillations, overload of series filters, communication interference, ripple control interference and CR saturation. Measurements of inter-harmonics with traditional equipment may not be feasible, as the waveforms consisting of just two frequency components that are not harmonically related may not be a periodic function. Hanning windows applied in harmonic FFT analysis need to be modified using zero padding technique to enable determination of inter-harmonics. Another technique is to apply a 10 waveform (50 Hz system) window, and use a phase locked loop, or to minimise signals being registered in frequency bins due to end-effect errors. Some analysis methods of inter-harmonics groups were proposed. The mitigation strategy is to employ harmonic filters comprising damping resistors. For this reason the second and third order filters are the best choice.
10. (Kennedy, 2002) describes current issues with power transformers supplying static semiconductor rectifier circuits which have phased out old mercury-arc rectifiers. The level of harmonics produced by semiconductor circuits is higher than with the old technology. Power transformer design requires different specification data than the traditional transformers designed for fundamental frequency. Two IEEE standards are discussed in the paper: 1) IEEE Standard

Practices and Requirements for Semiconductor Power Rectifier Transformers and IEEE C57.18.10-1998 and 2) IEEE Recommended Practice for Establishing Transformer Capability When Supplying Non-sinusoidal Load Currents, IEEE C57.110-1999. The term harmonic loss factor as introduced by the IEEE is explained. It takes into consideration winding eddy-current harmonic losses and other stray losses. These two types of transformer losses are most affected by harmonic currents. The losses calculated by using the harmonic loss factors are used when the thermal tests are performed. The heat run test for rectifier transformers is performed at fundamental frequency and the current applied during the test takes into consideration higher losses. The author recommends that each transformer is supplied with an earth screen, between the primary and secondary windings, in order to provide capacitive decoupling of the primary and secondary windings. Transformers with high impedance and closely coupled with vacuum circuit breakers and exposed to frequent switching will be subjected to switching transients. These transients will create resonant conditions within transformer windings and over-voltages in the middle of the winding causing insulation breakdown. The solution is the installation of surge arresters and a resistor-capacitor circuit between the breaker and transformer.

11. (Tischler, 2003) explains the operation of the GMD cyclo-converter under fault conditions. The case studies are supported with measurement and waveforms recorded during the fault conditions. The paper describes principle of operation of a 6-pulse non-circulating current cyclo-converter and shows simulated voltage and current waveforms of cyclo-converter and the motor. The waveforms presented are signatures of the healthy motor drive. The first case study examines the situation when the power supply is lost. Simulation results show that as soon as an under-voltage condition is detected, the thyristor triggering circuit will be blocked. The EMF of the motor will force the thyristor and transformer currents to fall to zero. The mill will continue turning until a mechanical brake is applied or the motor is stopped due to friction. The lubrication system will support the drive until it is stopped. Another three variants of power loss are also presented: transformer feeder circuit breaker opens without signal to gearless drive system, power outage without immediate

voltage reduction, and run-through during short power outages. The ride through feature is supported for up to 200 ms. The second case study examines the triggering of the wrong thyristor in an anti-parallel bridge. When this happens the short circuit current is limited by transformer reactance and the trigger current is blocked and extinguishes the current within milliseconds. Where there is an earth fault in cables or motors, simulation shows that normal operation will continue as there is no second connection to earth. The earth fault relay will detect the fault and shut down the mill drive. When the thyristor fails to block reverse voltage, this situation will be seen as a transformer short circuit which will be detected by the over-current relay, thyristor triggering will be blocked and the supply side circuit breaker will be tripped. All currents will decrease to zero. In the case of the short circuit at motor terminals, the overcurrent protection blocks the triggering of the thyristors preventing further switching of the thyristors. The short circuit current will flow through the thyristor for half a cycle and will reduce to zero. The fault current will flow until the motor is stopped or the field is removed. The stator fixing bolts need to be designed to sustain the short circuit force. The paper concludes that the design of cyclo-converter circuit for GMD application is robust.

12. (Kleiner, 2003) states that traditionally, refrigeration compressors on LNG plants are gas turbine driven. Electrically driven helper motors are inbuilt into a rotating string to accelerate the gas turbine to the speed when gas turbine firing starts and also to cover the shortage of power during high ambient temperatures. The helper motors are rated up to 20 MW and consist of a synchronous motor and a variable frequency drive suitable for four quadrant operation. The paper reports that the only suitable technology for such power ratings is the load commutated inverter (LCI) drive, consisting of thyristors (SCRs) as power semiconductor switching elements. Synchronous motors are 2-pole motors, including cylindrical laminated rotor, stator windings and brushless exciters specifically designed for LCI drives. Based on the current experience, the authors propose that the size of helper motors is increased to up to 100 MW and the gas turbine is completely eliminated from the rotating string. This would result in an all electric drive LNG plant, which is currently being designed in Germany. Elimination of the gas turbine improves the



availability of the compressor. In the case where a gas turbine is utilised, the LCI can be used to inject the energy back into the system if there is excess power.

13. (Martinez, 2005) explains the advantages of the electrically driven compressor and compares it with the traditional gas turbine driven compressor currently widely accepted in the industry. The terms "production availability" and "production efficiency" are explained and used throughout the paper to justify implementation of all-electric motor drives. The paper explains implementation strategy of electric drives into the proprietary Conoco Phillips optimised cascade LNG process incorporating LNG trains with production capacity of 3 to 5 Mtpa. A comparison between the plant utilising frame 7E gas turbines and the plant utilising electric drives is explained. A study into electric drive technology evaluates two different converter types: LCI (Load Commutated Inverters) and GCT (Gate Commutated Turn off Thyristors). The study shows that GCT design is more favourable than LCI technology due to reduced input harmonic content and superior ride through capabilities. It recommends that full VSD compared with starter VSD is implemented for motor starting. Results of the study into power plant design to support such a large load are presented in the paper. It concludes that a simple cycle power plant is the least complicated to operate, requires shortest installation time and is the lowest cost in comparison with a combined cycle plant. The combined cycle plants offer greater thermal efficiency (48% -vs- 33%) and can be supplied in larger units. The economic comparison between gas turbine driven compressors and all electric motor drives shows that the difference is marginal. The technology is available, but there are many factors that will influence the final selection.
14. (Hazel, 2006) describes the Electrical Network Monitoring and Control System (ENMCS) and importance of providing appropriate training to operation personnel. Insufficient training can lead to operator errors and costly system shutdowns, such as one experienced at a chemical process plant in France. After the incident the management requested better training. The authors describe experiences gained during the implementation of better training policy into the ENMCS at this particular plant. A training simulator was added into

the ENMCS system providing a safe training environment. The training improved operator confidence, enabling effective circuit breaker switching as part of yearly maintenance activities.

15. (Norrga, 2008) describes an AC/DC converter comprising a two-phase by three-phase cyclo-converter in the front end, separated from the voltage source AC/DC converter by an isolating transformer. PWM control of the output voltage is achieved via a new control circuit. During the low load operation of the converter, commutation is difficult as the snubber capacitors used to help with commutation are not sufficiently charged. The cyclo-converter is used to momentarily short circuit the transformer; then a quasi-resonant commutation of the voltage source converter could be achieved down to zero load. A 40 kVA model prototype was built and tested confirming that the proposed circuit is technically feasible.
16. (Ravani von Ow, 2010) evaluates various AC drive technologies for grinding mills. The paper describes cyclo-converters and voltage source inverters comprising Direct Torque Control (DTC). The paper describes a brief history of the development of AG, SAG and Ball mills which are used for grinding operations. GMDs are employed in the power range from 12 MW to 36 MW. The paper reports that currently AC drive technology has taken momentum and that cyclo-converters are the most effective and compact drive solution for GMDs. This is due to the high efficiency of a direct drive, the flexibility of selecting the optimal motor voltage, compact design, excellent performance at low speeds, and high starting torque. The operational frequency of GMD is from 0.3 Hz up to about 5-6 Hz. In a cyclo-converter, the energy can be transferred in either direction directly without a DC link. The cyclo-converter is a line-commutated converter, as the reactive power required to transfer the current between bridge legs during the commutation is obtained from the supply side of the converter. The paper also describes the system topology of a multilevel voltage source inverter for a dual pinion mill drive with induction machines.
17. (Bomvinsinho, 2010) reports on and describes the advantages of the new controller used on ABB GMD drives. The new controller is based on ABB AC

800PEC platform. The paper selects a typical 6-pulse cyclo-converter with no circulating currents topology and explains electrical protection features of the AC 800PEC controller. The protection functions for a cyclo-converter are differential protection, over-current and over-voltage protection at supply and load sides, over and under frequency protection and under-voltage protection at the supply side and thyristor short circuit detection. The controller includes ring motor protective functions and the transient recorder. It supports 'Ride Through' capability for up to 200 Ms and 85% of the supply voltage. The controller supports air gap supervision (static - on stator and rotating - on rotor). The protective and diagnostics functions inbuilt into the new controller will prevent extensive damage developing in the system, thus increasing the reliability and availability of the GMD system.

Interconnected power systems linking off-shore platforms and the application of subsea cables have been given a special focus in this research. The following papers describe such systems and are a good starting point for understanding the issues relevant to such applications.

18. (Fielding, 1991) describes an interconnected power system comprising three off-shore platforms. Two platforms include power generation and the third platform does not include any generation. All three platforms are interconnected via 33 kV subsea cable and step-up/step-down transformers. In one case study presented in the paper the authors evaluate power management functions inbuilt into the system. They provide results of the load flow and the transient stability study for three-phase fault at 13.8 kV bus. They evaluate a loss of power generation scenario and provide requirements for the spinning reserve. In conclusion, the authors confirm that interconnection of off-shore platforms will result in an increased power factor, which has economical advantages.
19. (Liang, 2009) investigates the technical, operational and maintenance issues of subsea cables for the off-shore oil and gas industry. Increasingly over the last decade off-shore installations have been powered up via subsea cables and the main concern is the introduction of parallel resonance into the system. The authors investigate such issues on an interconnected system supplying four

platforms. Variable frequency drives, which account for up to 98% of total load, generate system harmonics which can create parallel resonance with a long subsea cable. A mitigation strategy for reducing harmonic resonance is discussed and an optimised solution based on power system study is proposed.

20. (Liang, 2010) focuses on the use of subsea cables and their application in electrical submersible pumps for the off-shore industry. Submersible pumps are used to pump the oil from the wells in deep waters. The reliability of the power supply and the electrical submersible pumps has to be high as these installations are usually in-accessible once they are installed. The subsea cables connected to variable frequency drives either to the supply side or the load side, will create resonance conditions at the motor. The author presents case studies that were carried out into parallel resonance, series resonance and motor starting and provides recommendations for the optimised system design. The first case study investigates the system where the subsea cable was connected to the supply side of a set of VSD feeding submersible pumps. The length of the subsea cable ranged from 1 to 35 km. Harmonic analysis and resonance study were performed using an ETAP power system analysis software package. This study found that a 25 km long cable will create parallel resonance conditions at either 5<sup>th</sup> to 11<sup>th</sup> harmonic, depending on cable parameters. The mitigation strategy is to select VSD with higher number of pulses and consider various cable types. Harmonic analysis is an essential part of the design process. The second study case considers installations where the subsea cable is connected to the load side of variable frequency converter. A system with no load filters will create series resonance. This situation is mitigated with the installation of load side filters. In conclusion the author provides steps and methodology for designing a subsea electrical submersible pump system.
21. (Verma, 2010) describes technical issues experienced with the application of variable speed drives feeding submersible pumps in oil exploration. The common issues related to the static loads are discussed in the introductory part of the paper. The harmonics generated by such devices cannot be filtered using passive filters and the application of active filters is not reliable enough in this

application. The author proposes the installation of a power conditioner on the primary side of the VSD circuit. A new control scheme is developed and employed within the power conditioner which provides optimal power supply to a number of VSDs connected to the same bus.

### **2.3 Source of Current Harmonics**

The non linear loads such as AC UPS Systems, VSDs, electric process heaters, DC motors, cyclo-converters, LCI and VSI compressor drives are sources of current harmonics. The literature search was focused on non-linear loads in industrial power systems. It included both isolated and interconnected industrial power systems because of the fact that various non-linear loads are installed on both system types. Particular attention was directed to non-linear loads typically found on oil and gas plants and mineral processing facilities. Another area of interest was the literature describing Fourier Analysis as this method is used in analysis of the harmonics generated by non-linear loads. The following list of textbooks provides fundamental theory and background on Fourier Analysis and frequency converters:-

1. (Schaefer, 1965) This is an early textbook explaining in detail rectifier circuit topologies and load side voltage and current characteristics. The first section describes various topologies and rectifier circuit connections. The emphasis is on the design of rectifier circuits and supply side transformers. The circuit and transformer topologies for single-phase, 2, 3, 6 and 12-pulse midpoint and bridge connections are thoroughly described and supported with analytical formulae. The principle of operation of an inter-phase transformer is explained and guidelines for inter-phase transformer design are given for various rectifier circuit topologies. This is an essential textbook for designers of rectifier circuits and designers and manufacturers of power and inter-phasing transformers. The second section focuses on DC characteristics of various rectifier topologies. The textbook explains DC voltage waveforms, commutating reactance and commutation angle, voltage and current ripple for both inductive and capacitive loads.
2. (Paice, 1996) This is a classic textbook on power harmonics. Its main theme is system harmonics generated by power electronic converters. It starts with

explanation of harmonic requirements on electrical power system and summarises the concept of voltage distortion, line notching calculation, limits and mitigation strategies, current distortion and transformer sizing and definition of terms relevant to harmonics. The author introduces two types of power sources; type 1 which provides a fully balanced power supply and type 2 which provides an unbalanced and distorted power supply. Of special interest is an analysis of a type 2 power source on static converters. Understanding that an unbalanced power supply will create the third harmonic component on the supply network, or that pre-existing harmonics will impact on the supply side DC component is fundamental to the study of system harmonics. The bulk of the textbook material investigates the simplest method used to eliminate harmonics and a multi-pulse system achieved via shifting transformers. The paralleling of two or more rectifier circuits will create circulating current and will require an inter-phasing transformer to reduce its effect. The effect of various transformer configurations on transformer rating is explained. Chapter 7 provides an overview of harmonic calculation and gives formulae for calculating transformer K factor, followed by the text discussing harmonic mitigation techniques employed to meet harmonic standards and describes methodology for the design of passive and the selection of the active harmonic filters. The last chapter provides the results of harmonic measurements on the supply side of various rectifier circuits such as the 6-pulse rectifier with and without input capacitors and the 12-pulse with autotransformer configuration.

3. (Howell, 2001) in his textbook *Principles of Fourier Analysis* explains the classical theory of Fourier series and provides methods and formulae used to derive harmonic series for various wave-shapes. This is especially useful when describing sources of current harmonics. He explains the generalised method of Fourier transforms, showing that classical theory is a special cases of the generalised theory. The notations and conventions used in this textbook are adopted and followed in thesis. Part I of the textbook is preliminary material and part II describes Fourier series. Part II is a significant for this thesis as it is directly related to trigonometric functions.

4. (Shepherd, 2004) provides an overview of static power circuits and gives analytical formulae for the supply side and load side voltage and current waveforms. Harmonic analysis is based on circuit theory and Fourier transform. The textbook is divided into four parts, covering AC to DC Converters (Rectifiers), DC to AC Converters (Inverters), AC to AC Converters and DC to DC Converters. Part 1 explains power switching philosophy and semiconductor switches such as the diodes, thyristors (GTO) and power transistors (IGBT). An introduction to power converter circuits starts with single-phase uncontrolled and controlled rectifier circuits then moves to three-phase half wave and full wave uncontrolled and controlled bridge rectifier circuits. Current and voltage equations derived in the beginning are gradually expanded to include more complex circuits. The last sections of Part 1 explain the concept of Pulse Width Modulation (PWM) technique applied to controlled rectifier circuits. The formulae derived in this part include inductive and capacitive passive loads. Part 2 of this textbook starts with the three-phase naturally commutated controlled bridge inverters theory and then expands into step wave and pulse width modulation controlled inverter circuits. A separate section describes the effect of PWM waveforms when applied to induction motors. Part 3 provides an introduction to frequency converters, starting with phase controlled cyclo-converters and then moving to envelope and matrix converters. Phase controlled cyclo-converter theory is explained and system topology presented for both 6-pulse and 12-pulse non-circulating and circulating current design. Formulae for the output voltage and input current, power factor and displacement factor are given for selected topologies. The text also includes a large number of worked numerical examples at the end of each chapter, with answers. Overall the book provides a good introduction to the theory of power electronic circuits.

Technical papers summarised in below text focus on various aspects of non-linear loads such as cyclo-converters, DC rectifiers and variable speed drive converters. Early papers on cyclo-converters are of special interest as they provide analytical formulae and help in understanding the theoretical background of these complex devices:-

5. (Miyairi, 1979) published an early paper in the area of cyclo-converters and derived analytical formulae for load side current harmonics. Analytical results are compared with the results of digital simulation and practical experimental values and show full correlation between analytical results and digital simulation. A set of analytical formulae is derived for the three-phase 6-pulse naturally commutated circulating current free cyclo-converter. The authors are specifically interested in analytical formulae for the load side current harmonics and the rms voltages between the bridge converter and the cyclo-converter. They observe that the mean voltage at DC terminals of the bridge converter is equal to the rms value of the fundamental output voltage of the cyclo-converter. Also, they conclude that the rms values for  $6mf \pm nf_o$  ( $m=1, 2, 3 \dots n = 1, 3, 5 \dots$ ) harmonic families of the output voltage of the cyclo-converter coincide with the rms voltage of  $6mf$  harmonic components in the bridge converter. For this reason a 6-pulse bridge converter could be considered a special case of the cyclo-converter.
  
6. (Tadakuma, 1979) published an early paper investigating output current responses in six-phase and twelve-phase cyclo-converters used large synchronous motors. Output current offset and phase deviations are significant during higher output frequency operation. The pulsating ripple current causes torque pulsations of the synchronous motor. The paper presents a compensation method which aims to improve current response performance. In a higher output frequency operation, the cyclo-converter output current comprises offset current, phase deviation and pulsation all of which together have a negative effect on the cyclo-converter control circuit. To improve current responses this paper proposes a compensating method which is based on speed control. 6-pulse and 12-pulse cyclo-converter digital simulation results are presented and the 12-pulse waveforms are compared with experimental results. The paper concludes that the output current can be improved by applying a compensating circuit instead of a high gain loop.
  
7. (Chattopadhyay, 1980) carried out digital simulation of cyclo-converter fed induction motor and the results of his work are presented in a paper, which analyses a drive system comprising a three-phase induction motor and a half



wave phase-controlled thyristor cyclo-converter. The model is represented with combined motor equations expressed in d-q axis and thyristor switching matrix which includes the discontinuities in the stator current due to opening of stator phases. The combined model was used as the basis in developing a digital computer program for dynamic and steady-state performance simulation. The results obtained by digital simulations are compared with measured results on a model. The technique presented in the paper is a generic method, which can be expanded to more complex systems.

8. (Akagi, 1981) published a significant paper in development of the cyclo-converters as it derives theoretical formulas for effective amplitude of input current harmonics assuming that the output current waveform is sinusoidal. Prior papers provided insight into line side harmonics based on digital simulations. The formulae are expanded to an externally commutated thyristor amplifier producing an output voltage of arbitrary periodical waveform. The analytical formulae are derived for a three-phase 6-pulse non-cross current type cyclo-converter. Derivation method is based on Fourier periodic function analysis and the current switching matrix applicable to the supply side. The derivations show that the fundamental input reactive power of the cyclo-converter is independent of the load fundamental power factor. However, it is a function of the output voltage waveform and the output current amplitude.
  
9. (Wade, 1983) looks into various reliability issues associated with the application of large LCI drives in the paper industry. The author addresses various design redundancy issues such as duplicated control system power supplies and various cooling fan arrangements. In addition, the paper examines negative effects of LCI drives such as system harmonics and pulsating currents. The paper recommends that power system analysis and harmonic studies are carried out in the planning stage. If resonance is found to be a problem then various harmonic mitigation strategies should be applied. The simplest one is to consider phase multiplication, that is, to increase 6-pulse to 12-pulse design. The installation of harmonic filters is another mitigation strategy. LCI converters produce pulsating frequency at motor terminals which is 6 times the nominal frequency. The magnitude of the ripple torque is low; however, it is

always present within the motor. The LCI drive within its speed range will have one or more speeds at which the natural frequencies of the drive and the driven machine system will coincide. To avoid this occurrence it is recommended that torsional analysis is carried out at the drive design stage and rectified before the drive system is built. Torsional vibration problems on LCI drives are usually caused by elastomeric compliant couplings with high damping characteristics. This can be mitigated by providing damping couplings with different coefficient of dumping and elasticity.

10. (Shahrodi, 1985) describes a 6-pulse bridge rectifier circuit and the generation of current harmonics on the supply side. Injection of current harmonics on the primary side is mitigated by the installation of an input harmonic filter. However this filter will impact on the operation of the bridge rectifier. The author presents two methods of calculating current harmonics in the line side with and without load side ripples taken into consideration. Major effects of the input filter are reduction of the input current distortion, reduction of the output ripple, and improvement of the power factor.
11. (Hill, 1991) describes the dynamic behaviour of a 12-pulse circulating current cyclo-converter. The difference between circulating and non-circulating current cyclo-converter designs is briefly explained. The main advantage of the circulating current cyclo-converter is that it provides a higher ratio between output and input frequencies compared with non-circulating current design which limits this ratio to one third. The circulating current design eliminates a dead time of approximately 1 ms which prevents the current flow in part of the circuit that is not conducting. The negative effects of the circulating current design are the generation of significant losses and poor input side power factor. A 6-pulse cyclo-converter converts three-phase 50 Hz power source to a three single-phase variable frequency output via four three-phase 6-pulse thyristor converters. A reactor in each half will limit the circulating current. The paper describes control strategy employed in the design of this type of cyclo-converter. A proportional controller used for minimising controller wind-up during disturbance and feed forward technique that cancel out the load current disturbance are employed in the design. Shapes of circulating current and

converter current are measured on the prototype, showing the pulsating nature of the circulating current. Dynamic modelling shows that the circulating current is influenced by the load current, the higher the load, the higher the circulating current. The circulating current is difficult to regulate and for this reason it is difficult to regulate the input power. However, the circulating current cyclo-converter offers higher output frequencies than non-circulating current design.

12. (Neft, 1992) describes the design principles of a nine-switch (3 switches per phase) forced commutated cyclo-converter (matrix converter) developed for four quadrant motor drive application. The design principles were applied to a 30 HP vector controlled induction motor drive. The design is based on high frequency switching of the power switches in order to provide separation of distorted waveforms from the fundamental component. The switching technique presented in the paper is based on PWM modulated waveshape which was selected at 2880 Hz. The switching technique is based on virtual DC-link where only one of the switches per phase is conducting, either in positive or negative waveform. The rectifier action is based on two sets of switch control functions for switches in each group. The “positive” set would generate a predominantly positive group output voltage relative to mains neutral. The “negative” set would generate negative voltage. The difference between the positive and negative group output voltages will define a virtual DC-link voltage. The switch type used in this work is based on bipolar transistor wired in full bridge rectifier. The other switches could have been GTOs or MOSFETs. The higher frequency components on the line side of the converter were filtered with a high frequency tuned filter. The results of measurements carried out on a 30 hp drive show the input current waveform distortion was less than an ideal 12-pulse rectifier waveform and also that the constant power flow and the quality of the input current waveform were maintained over the entire speed range. This paper is significant as it shows that control technique plays an important role in the principle of operation of matrix converters.

13. (Kusko, 1993) presents the application of 6-pulse converters supplying DC motors used for elevators and lifts. The drive has to operate in four quadrant mode and a typical rectifier will comprise two 6-pulse dual converters. The 6-pulse thyristor controlled rectifiers produce voltage notches and current harmonics in the supply side. They also generate current waveform ripples on the DC side. The ripples cause additional audible motor noise resulting from the magnetic noise from the armature core laminations and mechanical resonance of the stator frame. The mechanism of generating distortion in the power system is described in detail. In addition the paper describes a 2-pulse midpoint converter using thyristor armature reversing switches for four-quadrant elevator drive service, including construction and harmonic measurements. 12-pulse rectifiers compared with 6-pulse dual units will reduce audible noise. Measures for reducing primary side distortions such as: source impedance, power harmonic filters and increase of pulse numbers are discussed and presented in the paper.
14. (Sakui, 1994) presents an analytical method for calculating harmonic currents in a three-phase diode bridge rectifier with DC filter. The equations for the harmonic currents are derived for two cases: continuous and discontinuous DC load current. In both cases the authors took into consideration the effect of both AC and DC side impedances. The formulae presented in the paper are compared with the results of time-domain simulation method which demonstrates good correlation between the two sets of results.
15. (Zargari, 1997) deals with the medium voltage thyristor bridge rectifier circuit. The author is concerned that conventional topologies of utilising 6, 12 and 18-pulse rectifiers would result in a poor input harmonic current profile and low load-varying input displacement factor (IDF). The paper proposes modifications to a conventional 18-pulse rectifier circuit by adding a GTO across each 6-pulse bridge circuit. The purpose of a GTO is to short out the 6-pulse bridge circuit. The author claims that the short circuiting would provide lower voltage level, decrease the delay angle and improve the power factor. Experimental results on a 12-pulse 10 kVA system are used to verify the proposed system topology. The paper provides a table showing a number of

components required for 6, 12 and 18-pulse bridge rectifiers and then shows that the proposed scheme for the 18-pulse rectifier will result in an extra 2 GTOs added into the rectifier circuit. The DC rectifier voltage is a function of the number of 6-pulse bridge circuits and the delay angle. The primary side harmonics are the function of bridge rectifiers left in the circuit and are not coincidental with the typical harmonics for 6 or 12-pulse harmonics. In the case where one bridge is short circuited in an 18-pulse rectifier circuit, the line side current harmonics are higher than the 12-pulse rectifier harmonics and incorporate all odd-order harmonic spectrum. This was done for the following DC voltage switching criteria:  $0.66V_n$  for short circuiting one bridge,  $0.33V_n$  for short circuiting two bridges in a three bridge configuration for the 18-pulse rectifier. The author proposes that phase shifting of the three secondary windings of transformer for an 18-pulse configuration is 20 degrees.

16. (Bernet, 2000) compares and evaluates two different product types: a 1.14 MVA two-level PWM Voltage Source Inverter (VSI) and a 6 MVA three-level voltage source converter with active front end applying (3300V,1200A) IGBT modules and 4.5kV IGCTs. The author discusses the design and the characteristics of a commercially available IGCT neutral point clamped PWM voltage source converter for medium voltage drives, summarises recent developments in traction converters and provides state of the art and trends in the development of semiconductor power switches.
17. (De Rosa, 2003) describes a computational model of a high power variable speed drive developed for EMTP program. The authors developed two different models, one representing line commutated inverters and another representing voltage source inverters (PWM inverter). They evaluated model accuracy and computational efficiency of the models and reported on a significant reduction in computational burdens. The models were applied for simulation of the probabilistic analysis of waveform distortion.
18. (ABB, Switzerland, 2004) in Part 1 of “Manufacturer’s Guide to Standard MV VSD drives” focuses on purchasing decisions such as reliability, efficiency, cost, various technologies, commissioning and maintenance and performance.

Various performance issues are defined such as harmonics, torque pulsation, noise, motor control, voltage fluctuations and ride-through capability.

19. (ABB, Switzerland, 2004) The second part starts with a description of the main components of variable drive systems. It describes requirements that should be considered on the supply and load side of the VSD. An overview of drive system topologies currently used within the industry is presented. The paper lists advantages and disadvantages of VSIs (Voltage Source Inverters), both single and multilevel type, CSIs (Current Source Inverters), LCIs (Load Commutated Inverters), slip energy recovery drives and cyclo-converters. The paper provides an overview of motor control platforms such as PWM (Pulse Width Modulation), Scalar Control, Flux Vector Control and Direct Torque Control. It encourages engineers to select standard types instead of engineered drives. The right combination of drive topology and control platform will improve the performance of drive systems.
20. (Mendes de Seixas, 2004) describes AC-DC converter for telecommunication applications. Typical requirements imposed on such converters are galvanic isolation between AC and DC supply and regulated DC supply. The author states that while single-phase AC-DC converters are well developed, the solution applicable to single-phase supplies cannot be applied to three-phase units. The author describes a solution for medium voltage converters supplied from three-phase power supply. The paper describes circuit topology comprising an 18-pulse star-connected autotransformer which provides natural power factor correction and feeds three full bridge 6-pulse rectifiers displaced by 20 degrees. The DC links are not paralleled, thus avoiding need for inter-phase transformers. Each DC link comprises an L-C circuit which is used to supply full bridge converters. Converters use transistors for switching and the phase-shifted pulse width modulation technique is employed in the switching circuit. This arrangement reduces commutation losses. Each full bridge converter supplies a high frequency transformer having two secondary windings. The transformers provide galvanic isolation between supply side and DC regulated circuits. The secondary windings are interconnected in a single DC supply circuit. The full bridge converters are synchronised through a

conventional voltage controller. The paper then analyses each functional component of the circuit. It starts with the autotransformer, providing vector diagrams and conventional Fourier analysis of input current and input voltage. It shows that current harmonics on the supply side are the characteristic harmonics of an 18-pulse rectifier, i.e.  $(n \pm 1) \times 18$ , where  $n$  is an integer starting from 1. The remaining component of the circuit is also described, touching on PS-PWM technique, current balancing and output command strategy. The concept of synchronisation of the bridge rectifier is briefly described. The paper then provides a list of the most important circuit components for the 12 kW prototype unit and the results of measurements on the prototype. The results show that primary side current harmonics are low and correlate with conventional Fourier analysis results.

21. (Kwak, 2005) proposes a new configuration for variable frequency drives for induction motors. It includes a combination of load-commutated and voltage source inverters. The proposed scheme does not require a capacitor on the load side used for forced commutation. The quality of the output current is improved and it offers a faster dynamic response. The scheme eliminates motor circuit resonance and motor torque pulsation. It was tested in the laboratory on 1 horse-power drive and digital simulation was carried out on a 50 horse-power induction motor. Conventional LCI-based induction motor drives have a thyristor-based topology and in order to provide natural commutation for thyristors, the LCI has to be loaded with a leading power factor in all operating regions. This is achieved by the installation of capacitor banks. For example synchronous motors do not require capacitors as the leading power factor can be achieved via the excitation control circuit. The capacitors can excite resonance within the motor circuit and cannot provide leading power factor at low loads. In the proposed scheme, the capacitor bank is replaced with a VSI converter powered up from a DC circuit. The leading power factor is provided by the VSI for the entire speed and load range. Fast dynamic response is achieved by VSI operation.
22. (Pont, 2005) and (Rodríguez, 2005) published two papers originating from the same team of engineers, and describing practical issues experienced on an

industrial power system having four gearless motor drives. The papers describe the principles of operation and design constraints of a SAG mill and provide formulae for calculating the critical speed of the drive. The paper explains vector control of a ring motor with two separate stator windings driven by a 12-pulse cyclo-converter. It also describes plant distribution system and explains the harmonic filter switching sequence implemented on the plant to compensate the power factor and mitigate system harmonics. Power quality issues with system harmonics are described and the results of the total harmonic distortion at 220 kV point of common coupling are presented. The paper provides results of analysis of cyclo-converters and load-commutated inverters and assesses impact on the power grid, driven motors and the control scheme. (Pont, 2005) describes the instrument installed inside the mill to detect the acoustic noise of damaged liners. Early detection of a damaged liner will prevent unplanned shutdowns.

23. (Kwak, 2006) discusses practical issues of VSI and CSI variable speed drives and evaluates their advantages in relation to type of various switching devices. Shortcomings identified with the existing design of CSI lead to the development of a new multilevel converter topology based on the CSI module. Multilevel CSI units improve current waveform and inject a reduced level of harmonics back into the supply side. The proposed configuration is a combination of GTO based CSI and thyristor Load Commutated Inverter (LCI). The leading power factor on the supply side feeding an induction motor is achieved with the installation of a capacitor bank on the load side. The proposed multilevel inverter will generate reduced input line harmonics compared with traditional LCI type converter. The concept was confirmed with both simulations and experimental results.
24. (Wiechmann, 2007) compares three types of MV converters that could be considered for application in SAG and ball mill grinding operation. Grinding mills operate at speeds between 10 rpm down to 0.28 rpm, depending on the mode of operation. They also require a 150% nominal torque at start. The author concludes that the most favoured drive is a cyclo-converter utilising thyristor switching. They are the most cost effective, require minimum indoor



space and provide good dynamic response at low speeds. The main disadvantage is that they have a poor power factor and produce current harmonics and for this reason require harmonic filters. The second type is Voltage Source Converter including 3 Level NPG Voltage Source Inverter and HV-IGBT/IGCT switching devices. This drive requires current de-rating at motor operating frequencies smaller than 3 Hz. The third type is the Robicon Perfect Harmony, consisting of a series of low voltage modules assembled in an MV stack. The LV modules comprise voltage source converters with a diode rectifier, while inverters are comprised of IGBT inverters. The main disadvantage of Perfect Harmony drives is that they require current de-rating at low frequency and have a very large footprint.

25. (Ahrens, 2007) focuses on a GMD and its potential in optimisation of the grinding process. The paper describes GMD functionality and technical features in comparison with other drive solutions. Paper provides a brief history and an overview of a typical GMD system. It describes a typical GMD motor design and the principle of operation of the cyclo-converter. A 6-pulse system is used as an example. The GMD application is compared with: fixed speed drives, slip ring motors, synchronous motors and variable speed drives (slip energy recovery drives), LCI drives, voltage source inverters, cyclo-converters and GMDs. The paper lists a number of drive selection criteria that should be considered when selecting drive type: energy and cost savings, maintenance, space, alignment, frozen charge, inching, creeping and positioning, load sharing and supervision. In conclusion it is stated that gearless mill drives are still the primary choice for many grinding applications in the minerals and mining industries, especially for large SAG and ball mills.
26. (Zhezhelenko, 2007) Inter-harmonics generated by direct frequency converters create additional losses in the power system and require harmonic filters designed for inter-harmonic filtering. Static frequency converters are a source of inter-harmonics caused by modulation of non-sinusoidal waveforms which include harmonics of integer orders and which are due to the presence of low frequency fluctuations of non-linear loads. A set of formulae for generation of inter-harmonics in the system of the three-phase to single-phase cyclo-

converter is provided and also, formulae for calculating additional losses of system components due to the presence of inter-harmonics are given. A proposed mitigation strategy for reducing system harmonics is to install filters, either second or third order filters. First order filters are not effective in reducing the inter-harmonics.

27. (Jorg, 2007) provides a brief summary of energy consumption via electric motors and states that 30% of total generated energy is consumed by electric motors. For this reason, improving the efficiency of electric motor drives has significant economic benefits. Only 10% of motors are powered via variable voltage variable frequency converters. The application of variable speed drives offers energy savings. For this reason, ABB product development team have developed a more efficient MV voltage drive comprising 5-level frequency converters. Traditionally, MV frequency converters of VSI type were two-level, comprising of two capacitor banks connected to a DC bus. The output voltage was connected to large capacitor. Traditional control method was PWM. The highest output voltage for two-level topology is 2.3 kV. The five-level concept utilises larger number of capacitors and switches, ABB's five level design comprises five different voltage levels which offer a total of nine levels phase to neutral. The five-level design improves supply voltage waveform, very close to sinusoidal. The outcome is that a standard motor without de-rating can be used.
28. (Ewanchuk, 2009) evaluates a new inverter drive system topology comprising six-switch three-phase inverter drive system. This system is specifically developed for high-speed low-voltage motor application. Conventional voltage source inverter topology puts limits on maximum switching frequency. Increased switching frequency will result in high load harmonic currents, causing excessive rotor heating. The proposed topology offers higher fundamental PWM frequency waveforms and reduced harmonic content, and was tested experimentally on a 15 horse-power 18000 rpm induction motor.
29. (Suh, 2009) looks into the possible application of integrated gate commutated thyristors (IGCTs) in high-current high-power rectifier systems. Traditionally, the high-power rectifier systems were based on either phase-controlled

thyristors or IGBT technology. The author proposes a new configuration consisting of a front-end diode rectifier and three-level step-down DC/DC converter. The proposed three-level design provides a wider operating range of continuous conduction mode, resulting in a higher average output current of less ripple size than two-level design. To confirm feasibility of the proposed configuration, the author built a prototype of a 5 kA 3.1 MW rectifier and provides both simulated results using MATLAB and test results. The results show that the proposed design provides a smooth output DC current with reduced high-frequency harmonics. This is a better solution in comparison with IGBT technology which generates the high-frequency harmonics. It is likely that the application of IGCT technology will find its use in low- and medium-voltage high-power rectifier systems.

## **2.4 Practical Issues with System Harmonics**

In this section, the focus is directed to industrial power systems, and isolated systems. Any practical issues such as vibration, nuisance tripping of circuit breakers, overheating of power distribution system components and overloading of power generation are covered. It also references technical papers which explain harmonic measurement techniques.

1. (Arrilag, et al., 2007) This is the second edition of what was the first textbook published by John Wiley in the area of power system harmonics, following the first international conference on power system harmonics which was held in Manchester in 1982. Its aim is to provide a general understanding of power system harmonics generation, their effects, monitoring, analysis and mitigation techniques. It takes into consideration the main developments in power electronics in the power industry over the last two decades. The first chapter explains the mechanism of harmonic generation caused by static switches, reviews international standards such as the IEC 61000 series and IEEE 519 and includes the definition and formulae of most common harmonic indices. The second chapter describes harmonic analysis technique based on Fourier Analysis. The theory of DFT, FFT, window functions and Nyquist frequency, and aliasing are explained. The authors provide an introduction to inter-harmonic analysis. Electrical devices generating harmonic currents are

described in the third chapter, starting with transformers and rotating machinery, and expanding to arcing devices, current and voltage source converters, thyristor controlled reactors and AC regulators. The effect of harmonic distortion on rotating machines, static plant, consumer equipment and protection systems is explained in a separate chapter. Harmonic monitoring is an important part of harmonic assessment and the textbook discusses the requirements for harmonic monitoring, explaining measurement requirements, transducers, harmonic measuring instruments and the presentation of harmonic measurement results. The measurement technique presented is in line with the requirements in IEC 61000 4-7, which describes the techniques for measuring harmonic distortion in a power system. There is a section on how to monitor and measure inter-harmonics. Harmonic elimination technique, explaining application and selection of various passive filter types, is in another section. The last two chapters are devoted to the calculation and analysis of harmonics in the power system.

2. (Fukao, 1987) argues that industrial power systems operating at frequency up to 500 Hz would enable plants with higher speed fans and process motors which would result in potential savings. The paper proposes that a circulating current cyclo-converter operating in discontinuous mode is employed to link a commercial 50 Hz system and an industrial 500 Hz system. In discontinuous mode, only the circulating current is exchanged every half cycle and only the discontinuous current flows in other half of the converter. The outcome is that the size of circulating current reactor can be reduced. The paper derives formulae for primary and secondary side current waveforms and reactive power. The analytical formulae were confirmed with experimental results obtained in the laboratory.
3. (Quirt, 1988) introduces and explains voltages to earth found in LCI (Load Commutated Inverters) converters. This voltage is a function of the rectifier firing angle, motor voltage and line side transformer voltage and can be as high as 2.4 times nominal line to neutral voltage. LCI converters come with a single reactor (positive) and double reactor (both positive and negative buses). In the case of the single reactor, the dominant waveform harmonic in the DC

circuit is the 3<sup>rd</sup> harmonic; with the double reactor it is the 6th harmonic, as demonstrated with analytical formulae derived and presented in the paper. The line to earth voltage will be reduced by almost 50% with dual reactors for firing angles higher than 40°. The observations made on LCI drives are applicable to CSI drives incorporating a DC link with smoothing reactors.

4. (McSharry, 1988) describes design, fabrication, and back-to-back testing of a 14,200 hp two-pole, cylindrical-rotor synchronous motor. The author describes the basic principles of an LCI converter and the effect of current harmonics, and oscillating ripples on a synchronous motor. It is pointed out that line-to-earth voltages are higher on LCI drives than on other drives. Comparison between 6-pulse and 12-pulse topology, and an evaluation of stator harmonics and their impact on rotor losses are presented in the paper. Dual winding stator design is selected as it reduces the impact of LCI ripples on the motor. Rotor design is based on traditional motor design and the negative effects created by the LCI drive are addressed. The standard design is evaluated applying finite difference and finite element methods to redesign slot and skew wedges. The retaining ring is changed to nonmagnetic steel material to eliminate induced currents. The standard stator design is modified to accommodate LCI effects. Selection of the number of stator slots, air gap dimensions, stator ventilation arrangement, constant ratio of V/Hz are considered during stator design to achieve optimal design for LCI application. A full temperature rise test was carried out on stator and rotor in back-to-back test configuration. Motors were coupled and one was operated as motor and other as generator. The test was carried out for both 6-pulse and 12-pulse configuration and results of the heat run are compared with calculated values. The authors emphasise the benefits of back-to-back testing in order to verify the design parameters of the synchronous motor for LCI drive operation.
5. (Chu, 1989) presents the results of harmonic measurements on a power system containing a 15 MVA three-phase static frequency converter supplying a single-phase 25 Hz network. The results of the measurements show a strong presence of current harmonics, both sub-harmonics and inter-harmonics, especially in the range below 500 Hz. At light loads, the magnitude of some of

the characteristic harmonics such as 10 Hz and 110 Hz exceeded the amplitude of the fundamental frequency (60 Hz). The paper describes configuration of the power system comprising 66 kV and 13.2 kV voltage levels. The measurements were carried out on the system with a static frequency converter out of operation, to determine baseline harmonics. The current harmonics were measured on two supply lines at 13.2 kV and 66 kV levels. Voltage harmonics were measured at both 13.2 kV and 66 kV buses. Both oscilloscope and harmonic analysers were used for harmonic measurements. The measurements were taken over a period of 24 hours, with varying loads. The characteristic harmonics were calculated using theoretical formula and the measurements confirmed that those harmonics were dominant. The impact of current harmonics on shunt capacitors is evaluated and it is concluded that the possibility of parallel resonance should be investigated prior to installation of any shunt capacitors, as parallel resonance on shunt capacitors could make the power factor worse. The paper recommends that the impact of current harmonics should be evaluated at various voltage levels which could lead to more consistent harmonic limits at different voltage levels. The paper recommends continued research into the impact of current harmonics caused by frequency converters, in order to establish a standard on harmonic distortion to be imposed on consumer equipment.

6. (Winn, 1989) explains the methodology for carrying out harmonic measurements on power systems using the digital storage oscilloscope. The oscilloscope can be connected to existing voltage or current transformers and digital current and voltage waveforms can be captured and stored in the oscilloscope. The Fast Fourier Transform (FFT) algorithm can be used to process stored data. IEEE-519 standard recommends 60 dB as the sampling dynamic range for capturing voltage and current waveforms. A sampling time has to be a minimum 10 kHz. Digital oscilloscopes have a sampling time of 100 kHz. The digital oscilloscope described in this paper can store up to four channels at the same time and has a connection to a PC. Previous work established that CTs and VTs have sufficient accuracy to measure harmonics up to 5 kHz. As a current sensor a clip-on CT can be used to measure the secondary current of the CT. A clip-on CT is also accurate up to 5 kHz. The

author describes sampling requirements for the FFT algorithm and discusses Nyquist's criterion for identifying a frequency of sampling points, saying that sampling rate must be twice the frequency for an accurate harmonic assessment. The highest frequency that could be determined by the FFT algorithm is called the Nyquist frequency; all higher frequencies will show an aliasing effect. The measurements at 60 Hz system for up to 71<sup>st</sup> harmonic and to avoid aliasing, according to the Nyquist criterion must be sampled at 8520 Hz minimum ( $71 \times 60 \times 2$ ) or at 117.37  $\mu$ s between points. Windowing of sampled signals is required for accurate results from the FFT algorithm. The paper states that when transient conditions occur, the sampling rate has to be increased to observe transient waveforms. Transient waveforms require more cycles in a window. The four cycles normally used for harmonic FFT analysis need to be increased when analyzing transient recordings.

7. (Sutherland, 1995) explains harmonic measurement techniques for each of the following applications: harmonic filter design and capacitor bank applications, verification of the design and installation of harmonic filters and capacitor banks; compliance with utility harmonic distortion requirements. The selection of a harmonic measurement approach depends on which application has been selected, as each of them will have its own measurement technique. The measurement process starts with selection of equipment and an appropriate technique. Harmonic current measurements at feeders are used to trace harmonic currents to the source of harmonics. The measurements should be made on all three phases due to current imbalance. Three-phase voltage harmonics measurements are carried out at buses, usually at the point of common coupling. Current and voltage waveforms are detected with VTs and CTs and probes and harmonic measurements are usually carried out utilising the existing instrument transformers. The accuracy of CTs is about 3% at frequencies up to 10 kHz and accuracy of VTs is about 3% up to 5 kHz. Current probes have an accuracy of 0.5 to 2% at frequencies up to 10 kHz. Harmonic measurements are normally carried out by spectrum and harmonic analysers. The paper suggests that measurements are carried out up to 25<sup>th</sup> harmonics. The selected instrument should be suitable for an accuracy of 5% of the harmonic limit. The instrument should have dynamic range such that the

smallest detectable variations are not larger than the smallest instrument resolution. Spectrum analysis is done using the FFT algorithm based on windowing technique. Waveforms captured during measurements are stored as raw data on a memory storage device and used for detailed analysis.

8. (Andrews, 1996) describes a process of harmonic measurements, analysis and power factor correction in a steel manufacturing facility. Harmonic measurements were carried out on the plant to establish base system harmonics and power factor. The author describes the mechanism of harmonic current generation by arc furnaces and 6-pulse rectifiers and proposes harmonic spectrum tables be used as input data in harmonic analysis. In conclusion, he points out that harmonic analysis and filter design involve short circuit and/or power flow studies as preliminary work and recommends that an unbalanced detection scheme be used to detect current imbalance and then initiate tripping of capacitor feeder breaker in order to disconnect the capacitor bank from the system in the event of one or more fuse operations or failed capacitor units. This will protect remaining capacitor cans from excessive over-voltages. Capacitor failure will shift the tuning frequency to higher value.
9. (Kadar, 1997) presents a method for the correction of voltage and current harmonic measurement errors caused by current and voltage transformers. Real-time power quality analysers are used for measurements and if not compensated, can produce inaccurate results. The paper proposes a compensation scheme based on digital filters. An example case of the reduction of measurement error from uncompensated to compensated is presented, showing that the measurement error introduced without compensation could be up to 1000 compared with the compensated method. Current transformer error can be greater than 3% at frequencies up to 10 kHz. Voltage transformer error can be greater than 4% for frequencies of up to 10 kHz. The compensation model described in this paper is accurate for frequencies below 20 kHz.
10. (Kleiner, 2003) Traditionally, refrigeration compressors on LNG plants are gas-turbine driven. Electrically-driven helper motors are inbuilt in a rotating string to accelerate the gas turbine to the nominal speed when firing starts and also to cover the shortage of power during high ambient temperatures. The



helper motors are rated up to 20 MW and consist of a synchronous motor and a variable frequency drive suitable for four quadrant operation. The paper reports that the only suitable technology for such power ratings is the Lad Commutated Inverter (LCI) drive, with thyristors (SCRs) as power semiconductor switching elements. Synchronous motors are 2-pole motors, including a cylindrical laminated rotor, stator windings and brushless exciters specifically designed for LCI drives. Based on current experience, authors propose that size of helper motors is increased to up to 100 MW and the gas turbine is completely eliminated from the rotating string. An all-electrical-drive LNG plant is currently being designed in Germany. Elimination of the gas turbine will improve availability of the compressor. In the case where a gas turbine is utilised, the LCI can be used to inject the energy back into the system when there is an excess of power.

## **2.5 Industrial Power System Harmonics**

This section provides a list of literature that describes industrial power systems and power system harmonics found in such systems.

1. (Institute of Electrical and Electronics Engineers, Inc., 1992) IEEE-Std 519-1992 is an industry standard on the subject of power system harmonics. The document explains harmonic generation principles and commutation phenomena. It lists and describes electrical devices which are seen as sources of current harmonics in the system. The devices described in the textbook are: converters, arc furnaces, static VAR compensator, inverters, phase controlled converters, cyclo-converters, switched mode power supplies and pulse width modulated drives. The document describes the effects of system harmonics on various devices such as rotating machines, transformers, power cables, electronic equipment, metering and protection, static power converters and telephone lines. It then explains the concept of reactive power compensation and harmonic current control. Harmonic analysis and harmonic measurement techniques are described in separate chapters. The main contribution of this standard are recommended practices for individual users and utilities. Individual users are responsible for harmonic generation and the standard provides recommended limits for current distortions, commutation notches and

flickers. The standard provides a table listing the current distortion limits for general distribution systems (120 V through 69 kV). The utilities are concerned with voltage distortion limits and the standard provides a voltage distortion limit table. The last chapters of this standard provide a methodology for evaluating new harmonic sources, which includes harmonic analysis, harmonic measurement and development of solutions for harmonic problems.

2. (Institute of Electrical and Electronics Engineers, Inc., 1995) IEEE Std 1159-1995(R2001) details a recommended practice for measuring and interpreting power quality parameters defined on electrical power systems. The signal that is captured by the measuring instruments is limited to 100 VAC and nominal frequency ratings range from 45 Hz to 450 Hz. The standard provides a list of recommended terms (flicker, harmonic content, for example) with a definition of each of term. It also provides a list of terms that should be avoided (blackout and spike, for example). It describes power quality phenomena and in Table 1 gives a list of principal phenomena causing electromagnetic disturbances as classified by the IEC. Each power quality phenomenon is described. For example, the phenomenon “oscillatory transient” is fully described and discussed, supported with a number of waveforms and graphs. Waveform distortions and harmonics, inter-harmonics and notching are discussed. The standard describes monitoring objectives and the effect of power quality phenomena on the power system. Measurement instruments, current sensors, voltage and current transformers are discussed and recommendation for the selection of connection points is given. The standard sets criteria for monitoring duration and provides guidelines for interpretation of the measurements. Table B.1 contains the relevant NEMA/ANSI standards applicable for various power system topics such as harmonics, disturbance, monitoring, and mitigation equipment.
3. (Standards Australia International, 2001) AS/NZS 61000.3.6:2001: This standard is part of an AS/NZS 61000 series, which is based on IEC 61000 series, and focuses on disturbances in MV and HV supply networks. Part 3-6 sets the guidelines and explains the principles that would need to be followed when connecting large non-linear loads producing harmonics and sub-

harmonics to an interconnected power system. The standard focuses on limiting voltage harmonics on the supply network and provides compatibility levels on LV and MV networks. It provides planning levels of voltage harmonics on MV and HV networks. The compliance with set limits is achieved by assessing injected current harmonics and their impact on network voltages. Harmonic measurements should be carried out over a period of at least one week. The evaluation approach is based on three stages: 1) Simplified evaluation of disturbance emission, 2) emission limits relative to actual network characteristics and 3) acceptance of higher emission limits. In summary, the process includes the assessment of harmonic current injected from non-linear loads under worst operating conditions, followed by the assessment of the network impedance and calculation of voltage distortion. The calculated levels are then compared with the compatibility and planning values as listed in tables 1 and 2 of the standard. The reason for such an approach is that the harmonic currents are injected into the network from various non-linear loads and depending on system impedance this will affect the level of voltage harmonics in the system. The standard also sets criteria for reducing interference to the telecommunication network caused by current harmonics. It provides a comprehensive bibliography.

4. (Standards Australia International, 2001) AS/NZS 61000.3.7:2001 Part 3-7 sets the principles for harmonics, inter-harmonics and flicker measurements that need to be followed when connecting large flicker-producing loads to interconnected power systems. Both compatibility and planning levels for flicker severity factors are specified, with a view to using short- and long-term factors to limit flickers on the network. The evaluation approach is based on three stages similar to those given in AS/NZS 61000.3.7:2001 Part 3-6.
5. (Standards Australia International, 2003) HB 264-2003 Power Quality handbook published by Standards Australia provides recommendations for the application of AS/NZS 61000.3.6 and AS/NZS 61000.3.7. In addition, the handbook provides methods for establishing harmonic and flicker planning levels. In summary the measurements on the power system should be carried out before and after the implementation of non-linear and fluctuating loads.

The results should be used to review the assessment methodology as proposed in these two standards. This handbook is intended as a supporting document to the National Electricity Code.

6. (Sankaran, 2002) This textbook reports on practical power quality issues experienced on various power systems. It is divided into 9 chapters covering the areas of harmonics, system transients, electromagnetic interference and then provides practical solutions to various problems. The book explains power quality issues in a simple way, supported with graphs, waveforms and examples. And also covers power frequency disturbances such as voltage sags and flickers. Static uninterruptible power supplies are usually required to solve such problems on low voltage networks. Sub-cycle disturbances in the power system are classified as system transients, which are created by switching off the power system components. Voltage and current harmonics are special types of system disturbances that can be analysed using Fourier analysis. A complex composite waveform can be expressed as the sum of sinusoidal functions, which if different from the fundamental frequency, is referred to as harmonics. The harmonics in the system are characterised with positive, negative or zero sequence of rotation. The power quality factors such as total and individual harmonic distortions are described and tables of individual current harmonic distortion for various loads are tabulated. The book describes the effect of harmonics on power systems and recommends mitigation strategies. System earthing arrangements and system power factors are dealt with in separate chapters. Electromagnetic interference, and measuring and solving power quality problems are discussed in the final chapters.
7. (Das, 2002) This is a classical textbook on power system analysis covering short circuit and load flow analysis. Of special interest are the last five chapters covering the areas of harmonic generation and harmonic analysis. Harmonic generation is associated with non-linear loads and the book discusses such topics as nonlinear loads, sub-harmonic frequencies, static power converters, arc furnaces and cyclo-converters. The effects of harmonics on power system components are covered in a separate chapter describing harmonic resonance and voltage notching, and their effect on rotating machines, transformers,

cables, capacitors, overloading of neutral conductor, protective relays and meters, circuit breakers, and fuses and telecommunication lines. The last two chapters describe harmonic analysis methods and network modelling techniques. Harmonic mitigation strategies are mainly associated with selection and design of passive filters. Active filters are briefly mentioned. The book describes design procedures and methods for the selection and design of harmonic filters: band pass, double tuned and damped filters.

8. (De La Rosa, 2006) in his textbook *Harmonics and Power Systems* describes harmonics in industrial power systems. The first chapter provides a definition of harmonics and various network parameters used in defining power system quality. Chapter 2 details various harmonic sources which are commonly found in an industrial power system. Chapter 3 provides an overview of industry standards which specify harmonic distortion limits. Chapter 4 describes the effects of harmonic currents on power system equipment. The emphasis is on the understanding of harmonics which create pulsating torques and cause excessive vibration. Chapter 5 describes the principles of harmonic measurement and the most effective way to monitor system harmonics. Chapters 6 and 7 discuss minimising system harmonics with mitigation techniques such as the installation of passive harmonic filters and the application of power converters with a higher number of pulses. Chapter 8 describes the elements of an electrical power system and their importance on the propagation of power system harmonics. Chapter 9 covers losses in an electrical power system due to system harmonics.

The following technical papers describe the generation of harmonics, their effects on system components and mitigation strategies applied on industrial power systems:-

9. (Amemiya, 1978) provides a classification of static frequency converters in relation to thyristor controlled rectifier circuits: type A - single circuit symmetrical control; type B - single circuit asymmetrical control; type C - cascade circuit - asymmetrical control, equal voltage division type; and type D - cascade circuit - asymmetrical control, unequal voltage division type. Type D is developed and described in this paper. The system consists of a single-phase input transformer and multi-winding secondary bridge rectifiers connected in

series. The type D cyclo-converter utilises secondary windings with a different number of turns and voltages. This creates different voltage amplitudes on the rectifier bridges. The proposed system improves the input power factor. The paper provides derivation formulae of line and secondary side voltage and current waveforms. The theory presented in the paper was confirmed with a prototype. The single-phase arrangement can be easily expanded to the three-phase system.

10. (Peeran, 1995) prepared a technical paper for distribution system designers, to help them select and specify harmonic filters for the variable frequency drives after obtaining the necessary information from the VSD manufacturers. The author recognised a need for carrying out harmonic study for the overall power system at the system design stage. The paper provides a simplified formulae for calculating harmonic THD (total harmonic distortion) and HF (harmonic filter) factors. Table II in the paper comprises tabulated input harmonic currents, THD (i) and harmonic factor for various variable frequency types. This is a useful information that can be used as a starting point in system analysis when information from the supplier is not readily available. In addition to characteristic harmonics, non-characteristic harmonics are also present due to slight irregularities in the conduction of the converter devices and unbalanced phase voltages. Harmonic currents drawn from the source are dependent on VSD design (LCI, CSI, VSI or PWM). Front end controlled VSDs include thyristors and GTOs. PWM type VSD includes a diode rectifier. LC, single-tuned filters are widely used to mitigate characteristic harmonics. Simple formulae, detuning principles and a set of voltage attenuation curves for various filters are given in the paper. The author provides a simplified filter design procedure supported with a working example. He also provides key sections that should be used when specifying harmonic filters for VSD application.
11. (Thasananutariya, 2009) describes the design process in carrying out harmonic study and evaluation of system harmonics for a low-voltage variable-speed drive system in an industrial plant. The process starts with the analysis of VSD input current and input harmonics. The harmonic study process comprises 5

steps: collect data and establish system topology; calculate short circuit current at the point of common coupling and establish parameters of equivalent supply network; calculate the resonance frequency of the system; establish harmonic sources and harmonic current either by carrying out measurements or using vendor data; and finally, calculate system harmonics and compare with recommended levels. The paper describes a case study and shows the results of calculations and measurements. In conclusion the author recommends that a single-tuned filter combination be installed when the harmonic limits, as recommended by IEEE 519 are exceeded. The VSDs up to 200 kVA utilising 500 kVAr input filters do not produce significant level of system harmonics and improve the power factor from 0.77 to 0.96.

12. (Dionise, 2010) describes a high-voltage, anode foil manufacturing facility and quality problems with the harmonic filters which were experienced in operations. The industrial power system is supplied from the grid. The plant comprises twenty rectifiers spread over two buses with a total capacity of approximately 25 MVA. Each bus is equipped with a set of harmonic filters tuned to rectify characteristic harmonics. The disturbances that occurred on the main grid resulted in damage to rectifiers and caused failures of filter components resulting in unexpected plant shutdown. The paper describes a power quality investigation that was carried out after the incident and explains the methodology used for analysis. Field harmonic measurements were carried out and the results of the measurements were used to confirm results of the model used to analyse system harmonics. Harmonic analysis established that one of the filters was detuned and proposed a new tuning frequency. Transient simulations using EMTP were carried out to determine over-voltages that are generated with capacitor bank switching actions. Simulation showed that back-to-back switching current can be reduced to safe levels by applying 12 kV surge arresters at harmonic filters and key feeders.
13. (Salor, 2010) This is a comprehensive paper summarising research methodology and the results of analysis into power quality issues of the Turkish national power grid caused by the steel mill industry. The steel mill industry in Turkey represents 10% load of the national grid having generation

capability of 40 GW. The power quality investigation was based on field measurements as per IEC 61000-4-30. The measurements indicated the presence of inter-harmonics and voltage flicker problems occurring at points of common coupling and Static Var Compensator (SVC) systems in plants. The measurement data were collected with the use of GPS receiver synchronization modules attached to the mobile PQ measurement systems. Based on the field measurements the author concludes that SVC systems cause inter-harmonic amplification problems around the second harmonic. This requires the development of a new approach and methods for solving the system issues.

## **2.6 Mitigation Strategy for Reducing System Harmonics**

The literature search was focused on mitigation strategies and methodology for reducing the impact of current harmonics on the system. Areas of system design such as functional location of harmonic filters, and type of harmonic filters and their use was explained in this literature search. Again industrial power systems were of primary interest.

1. (Benedict, 1992) This is an introductory report summarising various types of losses in electrical power systems. It was prepared by a group of students at Purdue University as part of a class project on losses. Our interest is the first section which describes losses on transmission lines, and is directly linked with our investigation into subsea cables. Chapter 4 describes uninterruptible power supply systems which are discussed in Chapter 3 of this thesis.
2. (Arrilag, et al., 2000) This book describes harmonic analysis in power systems. It is based on analytical formulae and advanced algorithms developed in the area of harmonic analysis. Introductory parts include harmonic modelling philosophy and description of Fourier analysis. The main part of the textbook is devoted to modelling of the linear components and harmonic analysis of static converters in the frequency domain. The last two chapters describe modelling of non-linearities in the harmonic domain. The application of such models is used in advanced harmonic flow studies. Harmonic analysis described in this book is oriented towards large interconnected power systems.



3. (Natarajan, 2005) in his textbook *Power System Capacitors* explains the basic principles of power system capacitors. The textbook is divided into twenty three chapters, starting with basic principles of power system capacitors. Chapter 7 discusses the location of shunt capacitors. Chapter 12 explains power system capacitors for motor operations and Chapter 14 explains the principle of static VAR compensators, which are used to control power factors in electrical power systems. Chapter 20 describes harmonic filtering principles. The last chapter explains problems associated with induced voltages in control cables located in the vicinity of HV power cables. The textbook is arranged in a structured way, explaining the most basic principles first and then moving towards more complex issues. The methodology explained in Chapter 20, describing harmonic filtering principles was followed in developing practical solutions for harmonic mitigation strategy explained in this thesis.

In addition to the selected textbooks, the following technical papers focus on system harmonic mitigation strategies:-

4. (Wade, 1983) describes special features built into the design of LCI drives applied in the paper industry to drive large fan motors. The paper provides examples of various circuit configurations, addressing design redundancy and describing component de-rating requirements. At the time the paper was presented, LCI drive was an emerging technology and there was concern about its impact on the reliability of boiler fan drives. Various LCI circuit configurations are presented in the paper: two 70-percent fans with 6-pulse LCI drives; single fan with dual-channel 12-pulse LCI drive or several fan or pump drives, each with a 6-pulse LCI drive and "flying spare" directly impact onto drive reliability. Auxiliary supply redundancy ensures the drive's reliability. The paper concludes that LCI drives offer the level of reliability required by the paper mill industry and this is a positive aspect of LCI drive technology. The negative effect of the LCI drives is that they produce non-linear waveforms in the supply side of the network resulting in current and voltage harmonics on the system. The paper proposes various mitigation strategies. The first method is phase multiplication, or phase shifting. The second mitigation strategy is the installation of harmonic filters. The most common method is to

install shunt LC filters, located at the harmonic source (on the primary side of the converter isolation transformer) and tuned to the series resonance critical frequency. In the case of large 6-pulse systems, the most effective method is the installation of the 5<sup>th</sup> and 7<sup>th</sup> harmonic filters. Another issue reported in the paper is motor torque pulsation causing torsional vibration problems. As a mitigation strategy, it is recommended that torsional analysis of the system is performed and modification of the drive couplings is carried out before the drive is installed. In conclusion, the paper refers to LCI drives as ‘the electric drive of the 1980s’.

5. (Hammond, 1988) conducted one of the early studies of system harmonics. The paper describes an industrial power system supplying a water treatment plant. The system incorporates its own power generation and can operate as an isolated power system. In addition, the power system is connected to the power grid and can operate in parallel with the grid. Different modes of operation mean that the input impedance and kVAr are changing. The maximum power supply capacity is not more than 2.5 MW, so this is a typical small power system which has difficulty complying with harmonic limits prescribed by IEEE 519 due to its high supply impedance. However, most designers reference the 5% limit on individual current harmonics, as suggested by IEEE 519, irrespective of system impedance. The paper describes filter selection and design for systems with very low input impedance. The system loads incorporate a number of current source VSDs, with some of them including harmonic filters. The paper states that for filter design and the selection of filter capacitors, the minimum and maximum kVAr of generators have to be considered. For this particular plant, the designers selected 2<sup>nd</sup> order high pass filters, the justification for which is that there are no issues with filter tuning and they are more effective in attenuating notches than the trap (first-order, single-tuned) filters. The paper then describes problems experienced during factory testing. The particular test station did not offer the same load and the same input impedance as found in the plant. The test facility was modified to simulate the real plant as closely as possible by adding appropriate input impedance and reactive load. The purpose of this set-up was to confirm correlation between time-domain simulations and test results. In addition, a

frequency domain simulation was performed once the filters were installed. Some discrepancies between measured and calculated data were noted, and attributed to different system impedance being used in simulations and for measurements. This paper is of special interest for us as it looks into harmonic issues on small power systems. In practice, some industrial plants have water treatment or similar smaller plants located over ten kilometres distant from the main plant, and the issues described in this paper are typical for such systems. The paper identifies specific problem, proposes design methodology and solutions and then reports on harmonic measurements, both in the factory and in the field, to prove the system design.

6. (Merhej, 1994) describes the Congo Yombo Development Phase I project, comprising an FPSO, two off-shore platforms and a number of submersible pumps used to lift crude oil. The electrical submersible pumps are fed via variable frequency converters which generate harmonics, and impact on the reliability of the electrical distribution system. The study confirmed that the level of harmonics on the installation was well above the levels recommended by IEEE-519 for the reliable operation of the system. Mitigation strategy consisted of the installation of 12-pulse variable speed drives and harmonic filters. The author describes the design process that led to the installation of tuned MV harmonic filters, thus reducing the 5th, 7th, 11th and 13th harmonics. The notching effect was mitigated by selecting an appropriate transformer impedance in the 12-pulse variable frequency drives. In conclusion, the author states that no system design of this type should be attempted without a complete computer model to verify the system performance.
7. (Choi, 1996) The author presents a new topology for a 12-pulse DC rectifier system incorporating an active, inter-phase reactor. The proposed system injects less than 1% THD back into the supply system. The energy required for the active inter-phase reactor is 50% of rectifier nominal capacity. This power can be reduced down to 18% by employing an autotransformer as the inter-phase transformer. The theoretical background and analytical formulae for the

proposed system are presented in the paper and followed by a simulation to verify the new concept.

8. (Esmail, 1996) discusses various topologies of low-cost high-quality low-harmonic AC-DC rectifiers. He introduces and describes two new classes of low-cost three-phase AC-DC high power factor, low-harmonic controlled rectifiers. The two new types are derived from DC-DC topologies using a simple transformation. The first class is based on boost-type input, DC-DC converters, with input inductors operating in the discontinuous current mode. The second class is based on buck-type input, DC-DC converters with the input filter capacitors operating in the discontinuous conduction mode. The paper presents various topologies of these two types of rectifiers. Several topologies are then simulated to prove that the proposed, low-cost rectifiers provide low harmonics and a high power factor on the supply side.
9. (McGranaham, 1999) focuses on the application of the revised IEEE 519 harmonics standard to industrial plants incorporating variable speed drives. The paper describes characteristic harmonics which are generated by VSDs. Variable speed drives are split into two types: high distortion current waveform (PWM voltage source inverter types with no harmonic filters or chokes), and normal distortion current waveform (DC drives, large AC drives with current source inverters, and voltage source inverters with added chokes in the DC link for current smoothing). Adding a choke in the DC link will provide a significant impact on source harmonics and for this reason some manufacturers include this choke as a standard component. The requirements for control of the harmonic currents are developed as a function of the ASD characteristics, overall plant loading level, power system characteristics, and power-factor-correction requirements. For harmonic mitigation, the author discusses the use of filters and provides filter design procedures.
10. (Daniel, 1997) analyses a typical PWM rectifier circuit, feeding a capacitive load, and discusses the limits for harmonic generation as prescribed by IEEE and IEC standards. A new control method which would result in reduced input current harmonics was developed. Capacitive load rectifier circuit will draw the current from the supply circuit only when the instantaneous voltage of the

supply side is greater than the voltage across the DC-link capacitor. The supply current is pulsed and the 5<sup>th</sup> harmonic is dominant. IEC 555-2 limits the 5<sup>th</sup> harmonic absolute limit at 1.14 mA/W, with a relative limit of 1.9 mA/W for equipment with an input power range from 50 to 600 W. The new approach presented in this paper utilises a new circuit and a control strategy based on the actual load of the rectifier for units up to 10 kW. The control strategy utilises switches which conduct only for a short duration in the mains cycle. The switching devices used in the experiment were IGBTs.

11. (Steinke, 1999) covers the practical issue of medium-voltage, source inverters utilising GTOs in the inverter circuit and PWM control technique. The dv/dt over-voltages caused by GTOs on the load side require a special motor design. The intention of this paper is to show that by installation of an LC filter between the inverter and the motor, it is possible to use a standard motor design in a variable speed drive application. Research into technical aspects of this proposal showed that LC filters would be energised by resonant frequency. Installation of a damping resistor has an impact on motor and converter power. The paper provides theoretical formulae and vector diagrams showing the effect of an LC circuit on the power requirements of the motor and the converter. The preferred location of damping resistors is in the inverter circuit. As the LC filter compensates reactive power of the motor, applications with the LC filter require less power in the inverter circuit.
12. (Shimizu, 2000) presents a new design for a single-phase, pulse-width modulation (PWM), voltage-source rectifier. The new topology does not create input current harmonics commonly found on DC rectifiers. It delivers a zero-ripple output current. The rectifier comprises a conventional single-phase PWM voltage-source rectifier, an inductor and a couple of additional switches. The input current control is achieved by utilising the conventional PWM current control technique. For the reduction of DC ripples, the authors presents two control methods using microprocessor technology, the DC inductor method and the AC inductor method. The proposed topology was confirmed experimentally and is applicable to devices in which the batteries are connected

in parallel such as DC line uninterruptible power systems and DC power supplies.

13. (Schmidtke, 2009) describes utility-generated harmonics and transients on multiple harmonic filters over six-phase expansion in a 170 MW plant. To establish the level of harmonic currents drawn from the utility, the paper proposes a three-step method to determine system harmonics. 1) Measure voltage and current harmonics at the point of common coupling, with both rectifiers and capacitors switched off. This will establish base line utility harmonics. 2) Continue the measurements with only the capacitor switched on and 3) with both the capacitor and the rectifiers switched on. If the results between measurements 2) and 3) are similar then the current harmonics are drawn from the utility. Transient over-voltages detected on the plant filters were caused by utility capacitor switching. By energising larger capacitor banks first, potential switching ripples can be minimised. In case of a large rectifier load being tripped and capacitor banks remaining connected, the steady state voltage can rise above allowed levels. Rapid filter bank tripping is recommended to mitigate damage to the filter from prolonged exposure to high voltages.
14. (Verma, 2010) describes a genetic algorithm technique for the design of tuned filters. The genetic algorithm technique is based on a stochastic global search method which utilises the principle of natural selection and genetically developed offspring. The application of harmonic filters in off-shore oil and gas industry is based on shunt filters. This is still seen as the most common solution on medium and high voltage systems. Low voltage systems have started to utilise active harmonic filters. On off-shore platforms, the reactive power requirements on the system are reduced due to the capacitive effect of submersible cables. This paper describes the design of passive filter conforming to the IEEE 1531 standard considering reduced reactive power requirements. The main objective in the proposed design algorithm is the minimisation of net source rms current with the insertion of a passive filter. The passive filter designed using this methodology was simulated via MATLAB.

15. (Guyomard, 2010) reports on practical experience gained over 20 years of operation of large compressor motors driven by LCI converters. The compressors were in the range of 20 to 40 MW. The data were collected from four major plants coded by phantom names. The compressors were installed and commissioned in late 1980's and were expected to operate continuously over a period of six years before a shutdown. A typical LCI drive incorporated an isolating transformer, LCI thyristor converters and a synchronous motor. Experience showed that on one drive, an isolating transformer that was loaded to its nameplate data failed several times in operation and was eventually replaced with a new unit. One of the compressor motors failed due to excessive overheating and was replaced with a new rotor. Overheating of single-core power cables due to circulating currents in cable armour was also reported. The author proposes a practical solution, suggesting that major components of the compressor drive system such as transformer, cables, converter and motor should be de-rated. He proposes that the thyristors are designed for 120% of the nominal current, cables up to 130% and all other components for an increased factor of at least 10%. The proposed derating factors should be added over and above the factors used for future expansion and removing bottlenecks. This is a very practical approach and probably the simplest way of dealing with system harmonics on the plants comprising large LCI drives. This approach increases the reliability of the plant; however it does not lead to system optimisation.

### 3. ELECTRICAL POWER SYSTEMS ON OFF-SHORE FACILITIES

#### 3.1 Codes and Legislation

##### 3.1.1 WA Statutory Requirements for Electrical Installations

The Government of Western Australia, Department of Mines and Petroleum has a regulatory role in the mining and petroleum sector in WA. The department publishes regular facts and figures, including statistical data on the current activities within the mining and petroleum (oil and gas) sectors. The department web site [www.dmp.wa.gov.au](http://www.dmp.wa.gov.au) contains the most recent and up to date information about resource projects in WA. The petroleum industry in Western Australia represents almost a third of the total value of Western Australia's resource industry. Figure 3.1 below, extracted from Department of Mines and Petroleum publication (Department of Mines and Petroleum, 2010) shows the impact of regulatory process in the oil and gas sector.

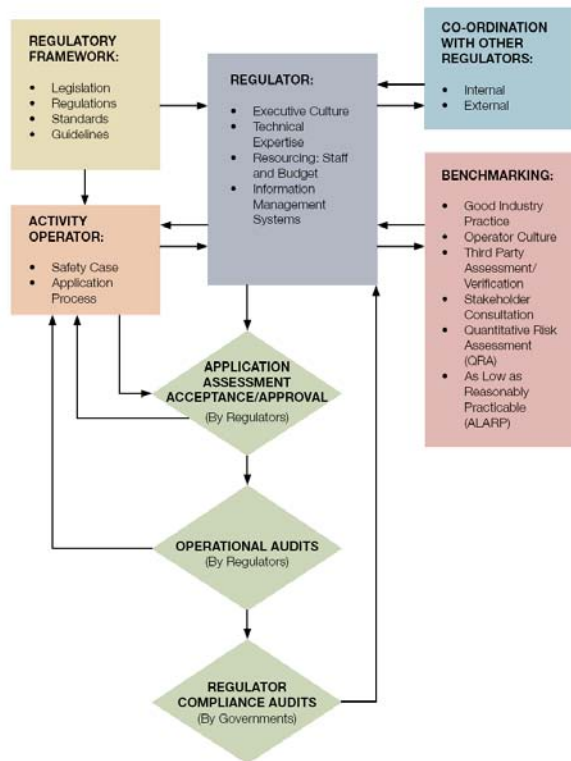


**Figure 3-1** Impact on the regulatory process in the oil and gas industry  
([www.dmp.wa.gov.au](http://www.dmp.wa.gov.au))



The regulatory process in Figure 3.1 applies to the oil and gas facilities located onshore in Western Australia and off-shore facilities located within the state waters. State waters are defined as beginning from the High Water Mark and to a distance of three nautical miles seaward. Commonwealth waters are defined as the waters beyond three nautical miles to a distance of 200 nautical miles from the low water mark. Refer to Figure 3.2 showing location of oil and gas production facilities in the North West Shelf development, off the coast of Western Australia. The red and purple lines show delineation between the Commonwealth and State waters. The Figure 3.2 shows that major off-shore oil and gas exploration facilities are located in Commonwealth waters.

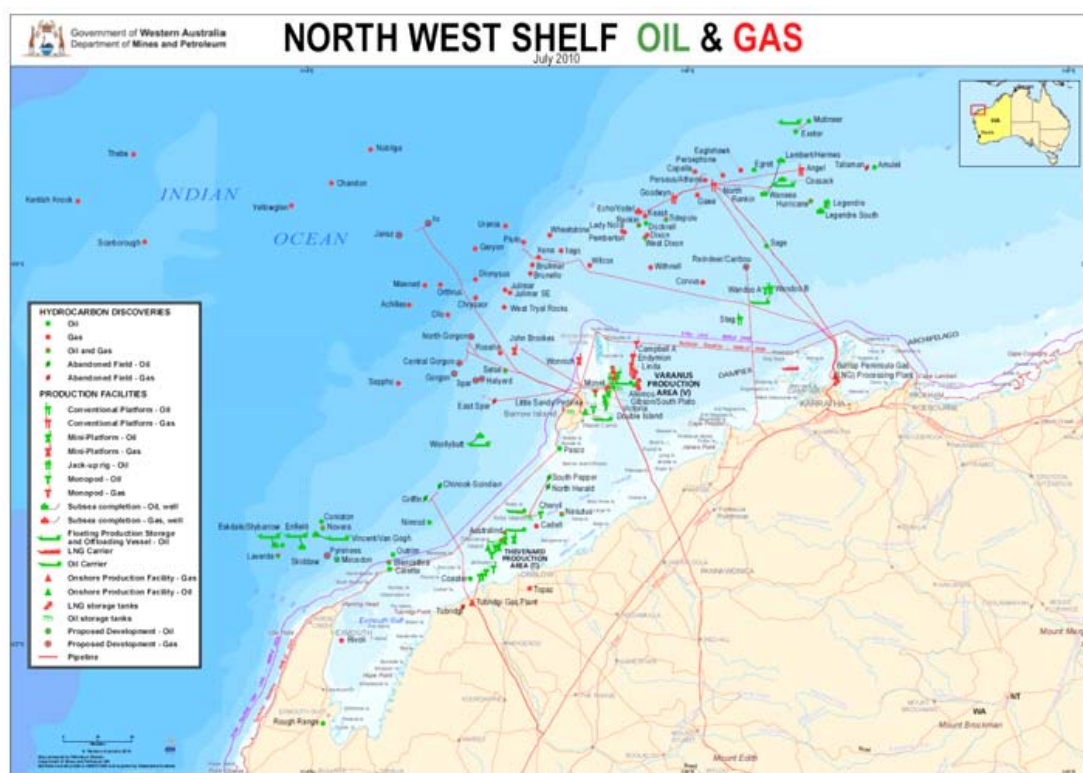


**Figure 3-2 North West Shelf production facilities and significant hydrocarbon discoveries (www.dmp.wa.gov.au)**

In Western Australia, all persons designing, constructing, operating and maintaining electrical installations including electricity generation, transmission and distribution systems and industrial electrical installations must comply with the electricity technical and safety legislation. Energy Safety WA, a Division of the Department of Consumer and Employment Protection, is responsible for the technical and safety

regulation of the whole electrical industry in Western Australia. Energy Safety is an independent regulator through the statutory functions of the Director of Energy Safety, created by Part 2 (s.5 –s.9) of the Energy Co-ordination Act 1994.

All electrical works including design, installation, testing, commissioning and operation must be carried out in accordance with the requirements of the Western Australian Government Act and supporting Regulations:- Electricity Act 1945, Electricity Regulations 1947, Electricity (Licensing) Regulations 1991, Electricity (Supply Standards and System Safety) Regulations 2001.

The Electricity Regulations 1947 covers electrical worker safety and the supply of electricity to consumers including obligations to inspect consumer installations. These regulations also cover requirements for the safety approval of certain types of electrical equipment and the energy efficiency requirements. The Electricity (Licensing) Regulations 1991 cover the standards of electrical work on a consumer's installations and licensing of electrical workers and contractors. Part 5 of the Regulations provides a list of relevant Australian Standards. It also references WA Electrical Requirements.

Note: WA Electrical Requirements are published by the Director of Energy Safety WA under the provision of regulation 49 of the Electricity (Licensing) Regulations 1991. The WA Electrical Requirements specify supply service rules, which are related to supply connection requirements. The WA Electrical Requirements also stipulate any Western Australian variations to the Wiring Rules (AS/NZS 3000) and any other standards as referenced by the Electricity (Licensing) Regulations 1991. The Electricity (Supply Standards and System Safety) Regulations 2001 apply to electricity infrastructure that forms part of a network and cover requirements for network safety.

Electrical installations located off-shore, outside the Western Australian State waters, are located within Commonwealth of Australia territorial waters and are governed by Australian Commonwealth legislation: Petroleum (Submerged Lands) Act 1967 (PSLA).

The following standards are referenced in Part 5.0 of Electricity (Licensing) Regulations 1991, thus making them mandatory in Western Australia:- AS/NZS 3000 “Electrical Installations (known as Wiring Rules); AS 2067 “Switchgear assemblies and ancillary equipment for alternating voltages above 1kV”, AS/NZS 2381 “Electrical equipment for explosive atmosphere – Selection installation and maintenance”, AS/NZS 2430 “Classification of hazardous areas”, AS 3004 (Sections 1 and 2 only) “Electrical Installations – marinas and pleasure craft at low voltage”, AS/NZS 3008 “Electrical installations – selection of cables”, AS/NZS 3010 (Part 1) “Electrical installations – Generating sets”.

The Electricity (Supply Standards and System Safety) Regulations 2001 Schedule 2 nominates a series of standards, which when followed, guide design engineers in achieving a safe design and may be used as evidence that safety objectives have been met. Those standards are not mandatory. Refer to the relevant sections of The Electricity Regulations 2001 for a detailed list of those standards.

The WA Electrical Requirements document describes requirements for high voltage installations. Section 7.1 states that high voltage installations must be designed by persons with engineering competence and an understanding of the effects of voltages exceeding 1 kV and associated high load and fault current to ensure safety of personnel. In addition, Section 7.3 of the Requirements states that a consumer’s high voltage installation design proposal is to be certified, by a professionally qualified electrical engineer, as compliant with the requirements of the Electricity (Licensing) Regulations 1991. A high voltage design proposal comprising SLD, load details, protection relay, VT, CT details, and earthing system design is to be submitted to the Network Operator before equipment is purchased and construction starts.

WA Electrical Requirements Section 1 Introduction, (noting that WA Electrical Requirements is referenced in Regulation 3 of the Electricity (Licensing) Regulations 1991), specifies that on isolated power systems, Energy Safety is deemed to be the Network operator, for activities such as for submission of Notices. This requirement does not apply to the submission of HV proposals. However, the electrical installations must comply with the relevant requirements of the Electricity (Licensing) Regulations 1991 and WA Electrical Requirements.

The WA Electrical Requirements document does not provide the definition of ‘a professionally qualified electrical engineer’. The following ruling is proposed for implementation in company standards.

A professionally qualified electrical engineer is an engineer registered on the National Professional Engineer Register (NPER). This registration can be achieved through the Institution of Engineers Australia, (IEAust).

### **3.1.2 Electrical Design of Off-shore Plants and Non-linear Loads**

The electrical design process applicable to off-shore oil and gas production facilities such as FPSOs, off-shore platforms and wellhead platforms is structured around equipment list and load balance calculations. The design process which is suitable to linear systems has been in use for more than 30 years. In the meantime non-linear loads have constantly been increasing by the application of variable speed drives and power electronic circuits, however the design process has not been adjusted to reflect this trend.

It has been observed, that the design approach applied in the oil and gas industry is very conservative resulting in system design that is not optimised. An alternative design process that will lead to the design process taking into consideration non-linear loads from the early stages of design development leading to better design and optimisation has to be developed.

There are many textbooks and journal papers addressing design aspects of an industrial power system. The relevant list of such publications is presented and described in Section 2.2 of this thesis.

The design process currently in use within the industry can be described as "Design by Load Balance Calculation". A set of maximum demand calculation sheets is used to summarise all major loads and is considered as a key document which is regularly updated and revised throughout the project. A maximum demand summary figure is calculated for each LV and MV switchboard using the maximum demand calculation sheets. The figures are then used as bases for the sizing of switchboards, transformers, cables and power generation. This is an important tool; however the

question is whether an alternative methodology could lead to better design that is optimised.

The maximum demand spreadsheet is arranged around load centres represented via single line diagrams, one calculation worksheet per switchboard. Calculation of maximum demand is a simple task; the formulae used are based on basic algebraic manipulations. Each load fed from the switchboard via a single feeder is represented with a single entry line in the calculation sheet. Each individual load is analysed separately and the diversity factor is applied by assigning load duty: continuous, intermittent or stand-by. The quality of maximum demand calculation is directly linked with the quality of input data provided by the process team. The design input is based on the following information; process instrument and piping diagrams (P&IDs), lighting layout drawings, instrument supplies. A sample calculation sheet is given in Figure 3-3. Maximum demand calculation formulae which are listed on the power balance calculation sheet are repeated below for clarity. It can be seen that the simplified formulae for calculating maximum demand figures are developed for the fundamental frequency, thus reflecting the linear loads:-

$$\sum S_c = \sum P_c + \sum Q_c \quad (3-1)$$

$$\sum S_i = \sum P_i + \sum Q_i \quad (3-2)$$

$$\sum S_s = \sum P_s + \sum Q_s \quad (3-3)$$

where

- $\sum S, \sum P, \sum Q$  are the sum of apparent, active and reactive components
- $c, i, s$  are continuous, intermittent and standby indices

DESIGN BY LOAD LIST  
TEMPLATE

LOAD LIST

DOCUMENT No.  
REVISION

EQUIPMENT										CONSUMED LOAD						NOTES	REV								
Item	Tag No.	Description	V.M.	Essential	Non-Essential	Freezing	Module Type	Absorb Load	Equip. Rating	Load Factor A/B	B/E at LFC	Power Factor at LFC	Load Duty	Continuous				Intermittent		Standby					
														[A]	[B]			[C]	[D]	[E]	[F]	[G]	[H]	[I]	[J]
1																									
2																									
3																									
4																									
5																									
6																									
7																									
8																									
9																									
10																									
11																									
12																									
13																									
14																									
15																									
16																									
17																									
18																									
19																									
20																									
21																									
22																									
23																									
24																									
25																									
Total Σ																									

NOTES

1)  $S = \sqrt{P^2 + Q^2}$  where  $P = \text{Real Power}$ ,  $Q = \text{Reactive Power}$

2) Diversity factors  $x, y, z$  are defined as follows:  $x = 1, y = 0.3, z = 0.1$

3)  $y \times 25$  cannot be less than the largest intermittent load

4)  $z \times 25$  cannot be less than the largest standby load

Maximum normal running load ( $x \times \Sigma S + y \times \Sigma P$ )	0.0 kW	0.0 kVA
	0.0 kVAh	0.0 kVAh
Peak load ( $x \times \Sigma S + y \times \Sigma P + z \times \Sigma S$ )	0.0 kW	0.0 kVA
	0.0 kVAh	0.0 kVAh

Figure 3-3 Maximum demand calculation sheet template

Maximum demand is calculated as:-

$$P_M = 1.1 \times \sum P_c + 0.3 \times \sum P_t \quad (3-4)$$

$$Q_M = 1.1 \times \sum Q_c + 0.3 \times \sum Q_t \quad (3-5)$$

$$S_M = \sqrt{P_M^2 + Q_M^2} \quad (3-6)$$

where multiplying factors 1.1 and 0.3 are the empirical values.

Maximum demand calculation starts at a very early stage of the design process and once the design process is complete the load list is the key document used for controlling design changes. Transformer sizing, switchboard sizing and feeder cable sizing calculations are all based on the load list figures. When the design has advanced almost to completion phase, then we model the system and run power system studies to verify system configuration and design. Adjustments are then made on the power balance calculation sheets.

The following design process called "Design by Power System Analysis" is proposed as an alternative process which takes into consideration non-linear loads. The application of this approach will lead to system optimisation. The salient points of the Design by Analysis process are as follows:

1. The starting point is the development of a load list for each load centre. The load centre is an area where load can be supplied from a single node. Using a power system analysis tool such as ETAP, a model of the power system is developed. The model can be used to calculate load flow, fault levels and voltage and current harmonics.
2. Design of industrial power systems should be based on power system analysis using software such as ETAP. Load lists and equipment lists can then be generated from power system analysis printouts.
3. Power system models should be configured around single line diagrams. However, every individual load down to the LV voltage level has to be modelled. Each feeder should include information on switching device, power cable and final load, either static or rotating.

4. All loads should include harmonic sources, especially non-linear loads such as rectifiers or variable speed drives.
5. Load flow and short circuit studies should be complemented with harmonic studies in the early stages of the design process.

The hypothesis developed in this section states that non-linear loads have to be taken into consideration and that design by power system analysis will result in better controlled design. This approach will lead to optimised design of the electrical power system. The Design by Analysis approach applies to all industrial power systems.

For the systems which undergo major expansion, the power system model should be developed first. The model should then be updated with new components and power system studies run for various study cases. Load list calculation should be bypassed and the power system model used as starting tool.

A case study is presented in Appendices 1 and 2 of this thesis. Appendix 1 describes the data collection process and the harmonic survey results. Appendix 2 describes the model verification process.

## **3.2 Power Supply via Subsea Cables**

### **3.2.1 System Configuration of an FPSO**

The design of an electrical power system on a typical industrial plant such as an FPSO starts with the development of the system key single line diagram (SLD). The purpose of this diagram is to show the configuration of the electrical power system on a single page and to gain a high level overview of the system.

A typical key SLD of FPSO is shown on the diagram in Figure 3-4. The power system is an isolated power system and is not interconnected with any other power system. Development of the key SLD is run in parallel with the development of load lists, which are described in Section 3.1.2. The diagram in Figure 3-4 shows the following major components:-

- MV switchboard comprising main power generation, MV motor feeders and a transformer feeder



- LV distribution system consisting of a main production switchboard – this is a two-section board which comprises production loads not critical for the production. These loads do not require a back-up generator.
- Offloading area switchboard – this is a two-section board comprising all loads located in the offloading area.
- Turret switchboard – this is a two-section board which supplies all turret loads and loads adjacent to the turret.
- Shipping switchboard - this is a two section board supplying the shipping system.

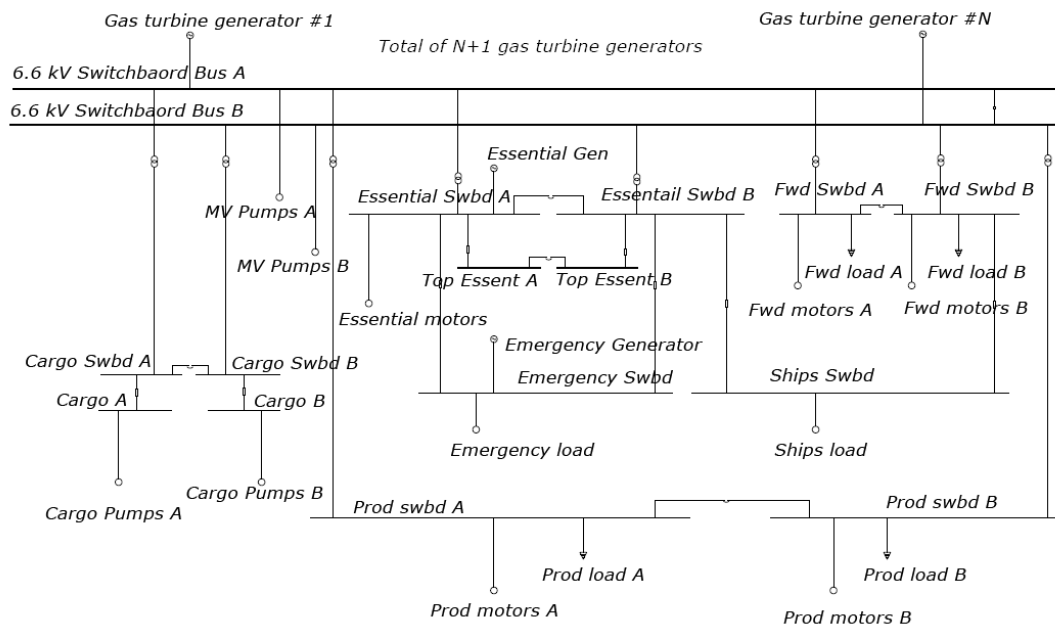


**Figure 3-4 Configuration of a typical FPSO electrical power system**

The FPSOs electrical power system as shown in a typical SLD is designed so it can be operated in various modes:

- Shipping mode – In this mode of operation the turret is disconnected from the vessel. The main power generation is shut down and the ship propulsion system is powered via the ship diesel generator.
- Production mode - The vessel is moored off-shore close to the oil and gas field, the turret is connected to the inlet pipeline, and oil or gas is flowing into

the process system. In this mode, the shipping diesel generator is shut down and the power system is supplied via the main power generation.

- Offloading mode – The storage oil is transferred from the vessel into barges. Offloading is carried out in parallel with operating mode and the maximum demand is at its peak.
- Emergency mode – The main power generation is shut down and the power system is supplied via essential diesel generators.

In addition to the above switchboards, the LV distribution system is provided with an essential switchboard comprising those loads which require back-up generation. The essential switchboard feeds all individual feeders and incorporates feeders to various other switchboards that require back-up supply. Those loads are important for the safe operation of the system. The loads on this board incorporate all essential loads from all functional areas.

Supply to a two-section switchboard is arranged in a secondary selective system configuration, described in (Institute of Electrical and Electronics Engineers, Inc., 1994). The bus tie circuit breaker is normally open. If one of the transformer feeders fails, the bus coupler breaker is closed and both sections of the board are supplied via a single transformer feeder. This will interrupt the power supply to half the board. If maintenance is required on one of the feeders, then the bus coupler is firstly closed for temporary paralleling operations and then the feeder scheduled for maintenance is switched off.

The main switchboard incorporates a set of busbars, circuit breakers, current and voltage transformers, protection relays and low voltage control compartments. All the components are enclosed in functional compartments and assembled into a medium voltage switchgear assembly. The nominal voltage level selected for the MV system is 6.6 kV, 50 Hz.

The 6.6 kV switchboard is a two-section board comprising a bus coupler breaker and a number of feeder circuits. Each feeder is equipped with a switching device, either a circuit breaker or a fuse vacuum contactor FVC combination. The circuit breakers

are used on generator feeder circuits and transformer feeders, while FVC's are used in motor drive feeders due to the need for frequent switching.

The outgoing circuits comprise fused vacuum contactor panels arranged in a compact assembly. Incomer panels, section coupling panels and transformer feeders incorporate circuit breakers which can be withdrawn. Facilities are provided to apply a trip on all outgoing VCBs and latched FVCs on each bus bar section, for a short time, when the CBs feeding that section are open.

### 3.2.2 Power System Configuration of a Wellhead Platform

Wellhead platforms are small facilities used in the exploration of oil and gas fields. The maximum demand on these platforms ranges from a few hundred to a few thousand kilowatts. A typical configuration of the electrical distribution system on a wellhead platform is shown in Figure 3.5.

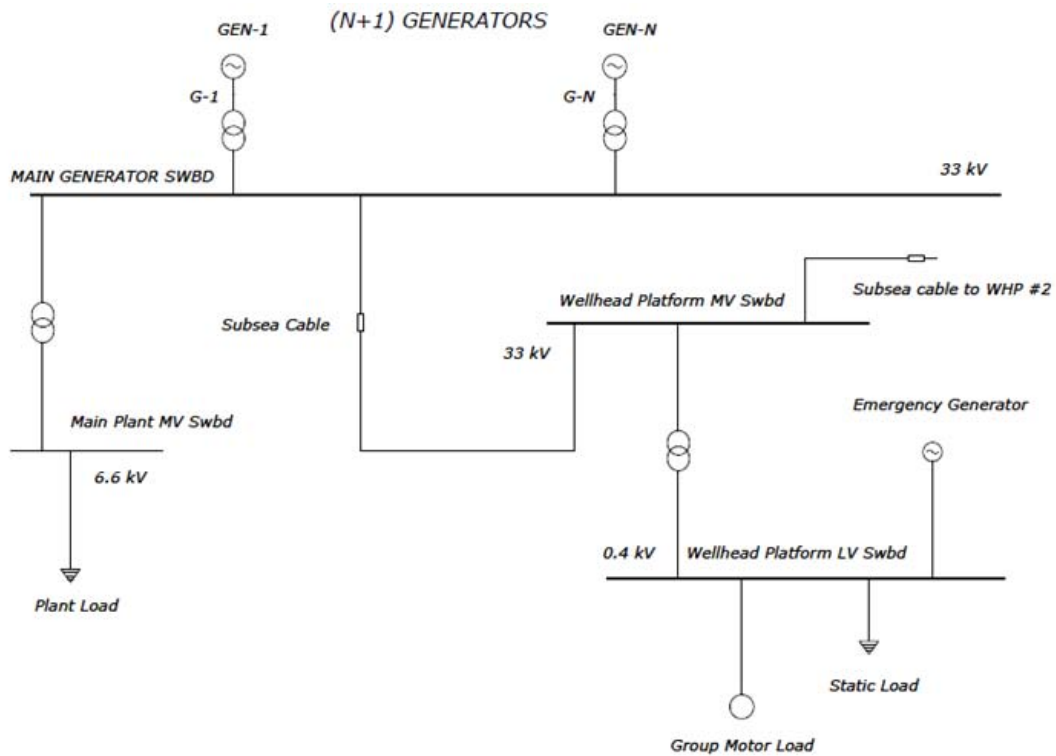


**Figure 3-5 Configuration of typical wellhead platform electrical power system**

The power supply to the platform is directed via a 33 kV subsea cable. The cable is a part of a subsea umbilical assembly which comprises chemical lines, fibre optic

cables and a gas pipeline. The umbilical is raised to the platform and secured via a cable riser. The power cable is connected at 33 kV switchgear which consists of two outgoing feeders, one provides power to the wellhead platform and the other is used to provide further distribution to a ring main system. The LV (400 V) distribution system on the platform is powered via a step-down transformer. The low voltage switchboard consists of a number of outgoing circuits supplying various loads. All motor loads are grouped together and represented as a lumped motor load. All feeder loads, such as feeders to various distribution boards, UPS and the battery charger system are grouped together and shown as a lumped feeder load. An emergency diesel powered generator is provided and is connected to the LV switchboard, in case the back-up power is required.

The design of the electrical power system follows the principles described in Sections 3.2.3 and 3.2.4. As the wellhead platform is supplied via a subsea cable that can be as long as fifty kilometres, a typical design challenge is to select the optimal supply voltage level and calculate the voltage drop of the subsea cable under various loads.

### **3.2.3 Selection of Supply Voltage and Calculation of Voltage Drop**

This section describes two models commonly used in representing subsea cables in power system analysis and evaluates the impact on the selection of the supply voltage and voltage drop calculation.

An appropriate design for cable modelling and system analysis is important when selecting the supply voltage and calculating voltage drop of a subsea cable system. Oversimplification of the distribution circuit based on a cable model which neglects cable capacitance can result in inaccurate voltage drop calculation and an inappropriate voltage level that can have a negative impact on the results of harmonic analysis.

For example, (Liang, 2010) and (Liang, 2009) presented power system analysis of a subsea cable system using a lumped  $\pi$  circuit for subsea cables. The cable lengths were from 5.8 to 11 kilometres. Power system analysis calculations were carried out using ETAP, a commercially available power system analysis software package. Let us evaluate if the methodology applied by (Liang, 2009) can be applied to the

selection of the supply voltage and voltage drop calculation. The evaluation will recommend a practical approach that should be applied in static power system analysis for the industrial system comprising subsea MV distribution systems.

The subsea cables are represented with a combination of impedance and admittance in power system analysis. Impedance comprises resistance and reactance and admittance comprises the shunt capacitance and conductance. Reference (Institute of Electrical and Electronics Engineers, Inc., 1992) IEEE Std 519 recommends that for low frequencies and short lines simple series impedance is sufficient to represent lines. The same reference states that when performing harmonic studies where frequencies above the 25<sup>th</sup> harmonic are important, shunt capacitance should be included in cable models.

Reference (Institute of Electrical and Electronics Engineers, Inc., 1998) states that cable models can be represented with the overhead line models. The relative values of reactance are different between cables and transmission lines. The same reference provides a table comparing cable and transmission line inductive reactance and shunt capacitance for two voltage levels, 69 kV and 13.8 kV. The table shows that cable inductive reactance is about one quarter that of the line and the capacitive reactance is thirty to forty times that of the line. Based on this comparison, it is suggested that for fundamental frequencies, the medium line model or what is known to be a nominal  $\pi$  model (see Figure 3.5) should be used for cables in the order of approximately 1.5 kilometres in length.

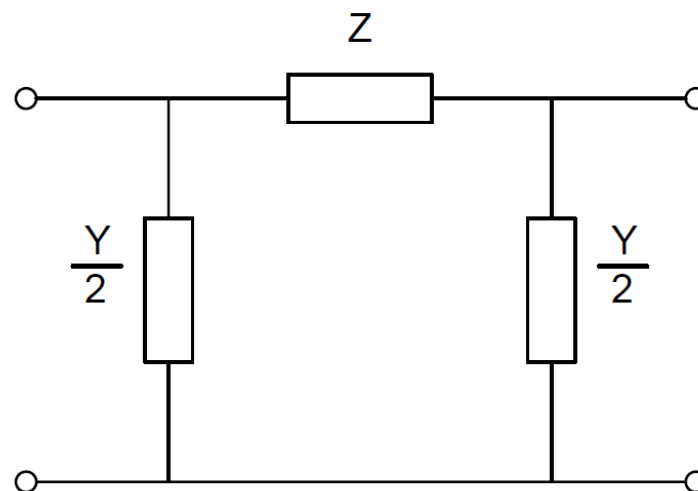


**Figure 3-6**

**Nominal  $\pi$  cable model**

The  $\pi$  model can be represented as a two-port network described with four coefficients ABCD known as the generalised circuit constants of the transmission line. For calculating voltage drop, the following equations can be used to calculate the voltage and current at length  $l$  from the load side (receiving end) of the cable.

$$\begin{bmatrix} V(l) \\ I(l) \end{bmatrix} = \begin{bmatrix} A & B \\ C & D \end{bmatrix} \times \begin{bmatrix} V_R \\ I_R \end{bmatrix} \quad (3-7)$$

The following trivial identity for voltage and current at the sending end is shown for clarity in order to emphasise that voltage and current of the cable at the length  $L$  are identical to the voltage and current at source (sending end). The total line current of the subsea cable is dependent on where it is calculated along the cable length.

$$\begin{bmatrix} V_S \\ I_S \end{bmatrix} = \begin{bmatrix} V(L) \\ I(L) \end{bmatrix} \quad (3-8)$$

The variables in equations (3-7) and (3-8) have the following meaning:

- $l$  is cable length measured from load end [km]
- $L$  is total cable length from sending to receiving end [km]
- $A = \frac{ZY}{2} + 1$  ;  $B = Z$
- $C = Y \left( 1 + \frac{ZY}{4} \right)$  ;  $D = \frac{ZY}{2} + 1$
- $Z = r + jx$  series impedance of the line [ $\Omega/\text{km}$ ]
- $Y = g + jb$  shunt admittance of the line [S/km]

As the nominal  $\pi$  model is recommended for cables up to 1.5 kilometres in length, it is then logical to expect that the cables with lengths greater than 1.5 kilometres should be modelled using an equivalent long line circuit model with distributed constants. A long line circuit and its equivalent  $\pi$  model are shown in Figure 3.6, below.

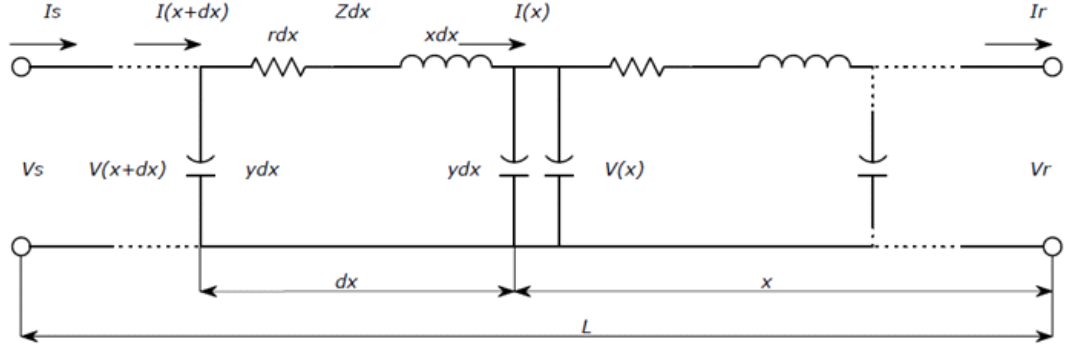


**Figure 3-7 Subsea cable with distributed constants and equivalent  $\pi$  model**

The subsea cable model represented as the equivalent  $\pi$  circuit of a long line is derived and fully described in (Grainger, et al., 1994). A short form derivation is presented as follows:-

From Figure 3.6, assuming that  $\Delta x \rightarrow 0$  we can write the following differential equations using Kirchhoff's voltage and current laws:-

$$\frac{dV(x)}{dx} = -ZI(x) \quad (3-9)$$

$$\frac{dI(x)}{dx} = -YV(x) \quad (3-10)$$

Finding the second derivation of (3-9) and substituting into (3-10), we get the following 2<sup>nd</sup> order differential equation in implicit form:-

$$\frac{d^2 V(x)}{dx^2} = -ZYV(x) \quad (3-11)$$

Let us define  $\gamma = \sqrt{ZY}$ , substitute it in (3-11) and express the 2<sup>nd</sup> order differential equation in explicit form:-

$$\frac{d^2 V(x)}{dx^2} - \gamma^2 V(x) = 0 \quad (3-12)$$

The general solution of the 2<sup>nd</sup> order differential equation (3-12) is of the form

$$V(x) = A_1 e^{\gamma x} + A_2 e^{-\gamma x} \quad (3-13)$$

The constant  $\gamma$  is called the propagation constant and is a complex quantity of the following form

$$\gamma = \alpha + j\beta \quad (3-14)$$

The real part  $\alpha$  of the propagation constant is called the attenuation constant. The quadrature part  $\beta$  of the propagation constant is the phase constant. We can calculate the current along the line by rearranging equation (3-9) and substituting into (3-13):-

$$I(x) = \frac{Y}{z} (A_1 e^{\gamma x} + A_2 e^{-\gamma x}) \quad (3-15)$$

Let us introduce  $Z_c$  called the characteristic impedance of the line and rearrange the identity  $\frac{Y}{z} = \sqrt{\frac{Y}{z}} = \frac{1}{Z_c}$ . The constants  $A_1$  and  $A_2$  can be evaluated by using the conditions at the receiving end of the line, when  $x = 0 \rightarrow V(0) = V_R$  and  $I(0) = I_R$

$$A_1 = \frac{V_R + Z_c I_R}{2} \quad \text{and} \quad A_2 = \frac{V_R - Z_c I_R}{2} \quad (3-16)$$

The equations for voltage and current become:-

$$\begin{aligned} V(x) &= \cosh(\gamma x) V_R + Z_c \sinh(\gamma x) I_R \\ I(x) &= \frac{1}{Z_c} \sinh(\gamma x) V_R + \cosh(\gamma x) I_R \end{aligned} \quad (3-17)$$

The equation (3-17) is the equivalent  $\pi$  model circuit equation, refer to Figure 3-6 and equation (3-7). When  $x = l \rightarrow V(l) = V_S$  and  $I(l) = I_S$ , equation (3-17) can be rewritten in terms of a two-port network:

$$\begin{bmatrix} V_S \\ I_S \end{bmatrix} = \begin{bmatrix} A & B \\ C & D \end{bmatrix} \begin{bmatrix} V_R \\ I_R \end{bmatrix} \quad (3-18)$$

where the constants A, B, C and D are as follows:-

$$\begin{aligned} - \quad A &= \cosh(\gamma l) & ; & \quad B = Z_c \sinh(\gamma l) \\ - \quad C &= \frac{1}{Z_c} \sinh(\gamma l) & ; & \quad D = \cosh(\gamma l) \end{aligned}$$

Alternatively, inverting the two port matrix we get equation (3-19)

$$\begin{bmatrix} V_R \\ I_R \end{bmatrix} = \begin{bmatrix} D & -B \\ -C & A \end{bmatrix} \begin{bmatrix} V_S \\ I_S \end{bmatrix} \quad (3-19)$$



The value of the current can then be calculated at the receiving end for a given power factor. The voltage drop across the subsea cable expressed as percentage is calculated by comparing the voltage level at the sending end ( $V_S$ ) and receiving end ( $V_R$ ) of the two-port network.

$$\Delta V = \frac{V_S - V_R}{V_S} \times 100 \quad (3-20)$$

As suggested by (Standards Australia International, 2007) AS/NZS 3000, the voltage drop between the point of supply and any point of the electrical installation shall not exceed 5 percent of the nominal voltage at the point of supply. The transmission efficiency is calculated as follows:

$$\eta = \frac{P_R}{P_S} \times 100 \quad (3-21)$$

The transmission efficiency ( $\eta$ ) of the subsea cable is calculated by comparing the active power level at the sending end ( $P_S$ ) and receiving end ( $P_R$ ) of the two port network.

### 3.2.4 Power System Analysis - Case Study

The purpose of this case study was to calculate voltage drop and power transmission efficiency using nominal  $\pi$  (medium line) and distributed parameter cable models (long line). The calculation should determine which model is the most suitable for analysis of industrial power systems. The voltage drop and transmission efficiency calculation was carried out using analytical formulae presented in the previous section. The results of the calculation are presented in tables and assist in determining which cable model should be used when analysing subsea power distribution network.

The configuration of the supply system used in the analysis reflects a typical wellhead platform supplied via a subsea cable and described in Section 3.2.2. The wellhead platform is supplied via a subsea cable from a remote power supply node. The length of the subsea cable was assumed to be 45 kilometres. The total load on the platform was varied from 0 to 3000 kVA in steps of 500 kVA with a constant power factor of 0.8 leading. Analysis was carried out for the IEC standard medium

voltage levels 11, 22 and 33 kV. The cable cross sectional area was assumed to be 70 mm<sup>2</sup> and cable insulation was XLPE.

Cable data were taken from the manufacturer's catalogue and are listed in Table 3.1. The results of analytical calculation based on two models are listed in Table 3-2.

Voltage (kV)	Cross Section (mm <sup>2</sup> )	Rating (A) Laid in ground	Resistance at 90°C (μΩ/m)	Reactance at 50 Hz (μΩ/m)	Maximum Capacitance (pF/m)
11	70	270	343	130	288
22	70	270	343	141	200
33	70	270	343	151	154

**Table 3-1 Standard MV power cable electrical parameters**

S <sub>R</sub> [kVA]		11 kV		22 kV		33 kV	
p.f. = 0.8		$\pi$	<b>D-<math>\pi</math></b>	$\pi$	<b>D-<math>\pi</math></b>	$\pi$	<b>D-<math>\pi</math></b>
0	V <sub>d</sub> [%]	-1.15	-1.17	-0.88	-0.89	-0.73	-0.73
	$\eta$ [%]	0.00	0.00	0.00	0.00	0.00	0.00
500	V <sub>d</sub> [%]	5.10	5.08	0.78	0.77	0.03	0.02
	$\eta$ [%]	95.06	94.46	97.61	96.10	96.76	95.23
1000	V <sub>d</sub> [%]	10.65	10.63	2.39	2.38	0.77	0.77
	$\eta$ [%]	89.13	88.89	97.49	96.88	98.29	97.48
1500	V <sub>d</sub> [%]	15.61	15.58	3.95	3.94	1.51	1.50
	$\eta$ [%]	83.44	83.35	96.20	95.81	98.23	97.69
2000	V <sub>d</sub> [%]	20.06	20.03	5.46	5.45	2.23	2.22
	$\eta$ [%]	78.33	78.32	94.67	94.39	97.78	97.38
2500	V <sub>d</sub> [%]	24.08	24.05	6.93	6.92	2.94	2.94
	$\eta$ [%]	73.78	73.82	93.08	92.87	97.18	96.86

$S_R$ [kVA]		11 kV		22 kV		33 kV	
3000	Vd [%]	27.73	27.69	8.36	8.34	3.65	3.64
	$\eta$ [%]	69.71	69.79	91.48	91.33	96.50	96.24

**Table 3-2 Cable voltage drop and transmission efficiency**

The results in Table 3-2 show that voltage drop calculation results are within +/- 0.5% between nominal  $\pi$  and Distributed (D- $\pi$ ) models. The transmission efficiency results are within +/-2%. For practical purposes in an industrial environment both levels of accuracy are acceptable. For this reason it is recommended that simplified model, based on nominal  $\pi$ , is utilised in power system analysis. This is in line with the approach adopted by (Liang, 2009).

### 3.3 Non-linear Loads Source of Current Harmonics

#### 3.3.1 DC Rectifiers

Non-linear loads can be classified into two groups. The first group are loads fed directly from the primary supply system and comprising electromagnetic circuits such as transformers, induction and synchronous motors and air-cored reactors. The magnetic circuit in those devices is made of magnetic steel characterised with hysteresis and a non-linear magnetising curve. The properties of such loads are explained in (Arrilag, et al., 2007). These loads produce voltage and current harmonics mainly during the switching operations and are not further explained.

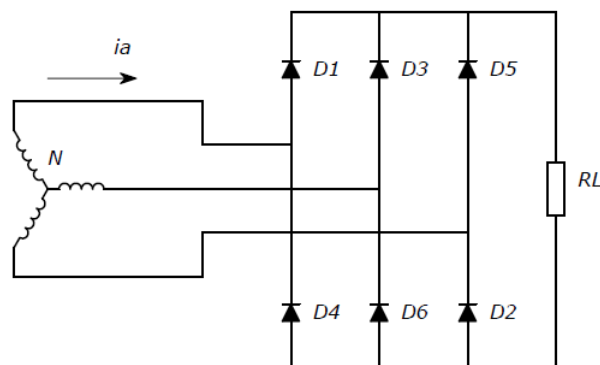
The second group are the loads fed via power converter circuits incorporating static switches used to control power flow. The switching sequence of the static switches is an effective way to control power flow; however, this operation produces irregular voltage and current wave shapes. The result is the presence of current and voltage harmonics in the power system. The most common loads on off-shore facilities are converter circuits found in UPS systems, electric heater control panels, DC drilling motors, LV and MV VSDs.

In harmonic analysis non-linear loads are represented as a source of current harmonics. On an industrial power system, DC rectifiers may be installed as stand-alone devices or they may be an integral part of static converters utilising a DC link.

The two most common types of rectifiers are uncontrolled and phase controlled. Uncontrolled rectifiers use diodes as switching devices, while phase controlled rectifiers utilise thyristor controlled switches. (Shepherd, 2004) describes various types of rectifier circuits. (Schaefer, 1965) explains design issues with interposing transformers in the case where two or more bridge rectifiers are paralleled.

In the following text, the methodology for calculating harmonic currents on the supply side of the rectifier is explained on an ideal three-phase 6-pulse rectifier circuit. The 6-pulse rectifier circuit and voltage waveforms on the primary and secondary side of the rectifier are shown in Figure 3-8. An analytical description of voltage and current waveforms of DC rectifiers and the mechanism of harmonic current generation are based on the material presented by (Shepherd, 2004). The approach used to analyse the 6-pulse rectifier can be extended to 12, 18 and 24-pulse circuits.

In Figure 3.8, diodes D1, D3 and D5 are part of the upper bridge while D2, D4 and D6 are part of the lower bridge. The natural commutation of the diodes is achieved by the natural cycling of the supply voltage. To avoid short circuits on the primary side and to enable a flow of load current, only one diode in the upper part and one diode in the lower part should be conducting at any time. For the resistive loads and assuming ideal commutation, Figure 3.8 shows voltage and current waveforms on the load and primary sides of the rectifier.



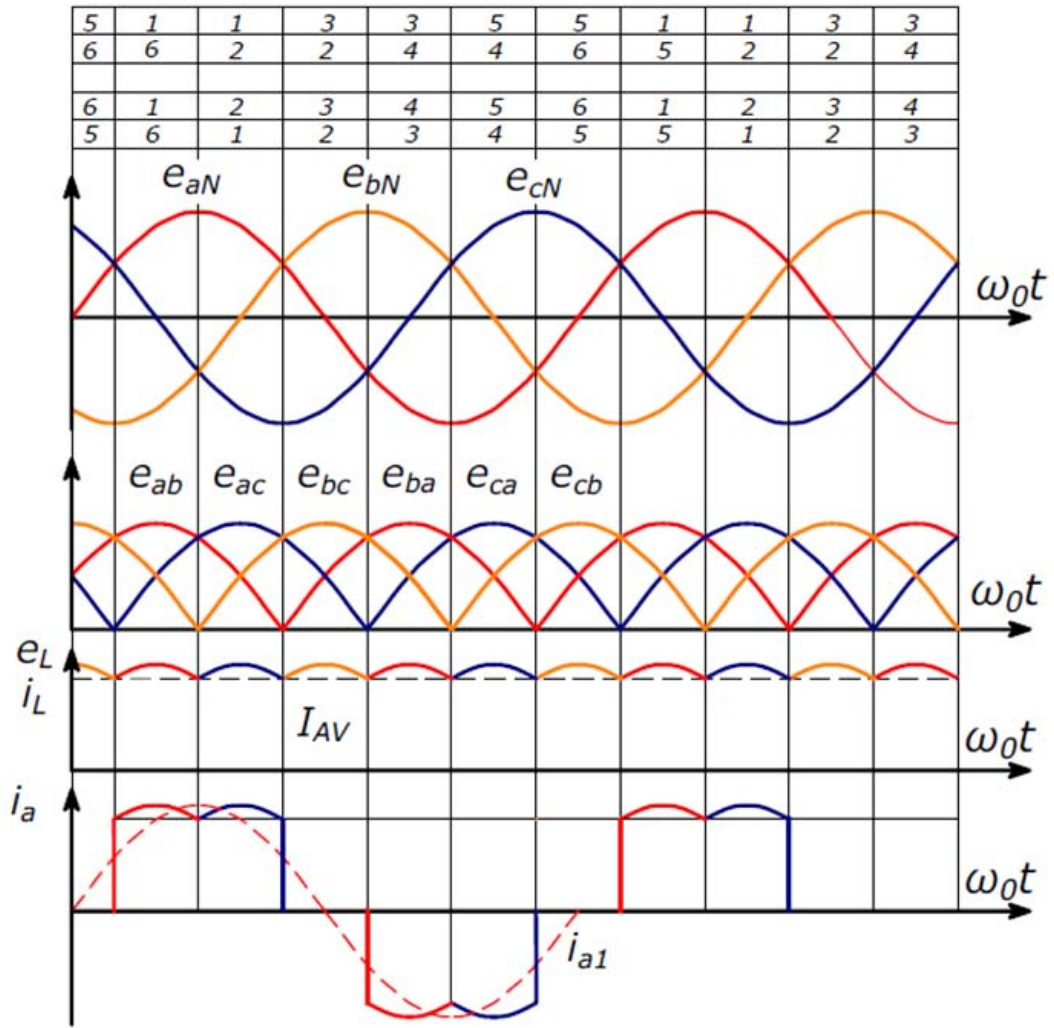


**Figure 3-8 Three-phase, full-wave diode bridge with resistive load; circuit connection, supply line voltages, load voltage, load current, and supply line current (phase a)**

The following derivation will be carried out for phase A. To begin analytical derivation, we need to perform a qualitative analysis of the rectifier circuit and determine voltage and current waveshapes on the primary and secondary side of the circuit. In this case, the supply side voltages are sinusoidal with a phase shift of  $120^\circ$ . Voltage waveforms over a period can be expressed as follows:-

$$e_{aN} = E_m \sin \omega_0 t$$

$$e_{bN} = E_m \sin(\omega_0 t - 120^\circ)$$

$$e_{cN} = E_m \sin(\omega_0 t - 240^\circ) \quad (3-22)$$

where fundamental period  $T_0 = 2\pi f_0$ . The primary side current of the A phase can be described as follows:-

$$i_a(t) = \begin{cases} 0, & 0 \leq t \leq \frac{T_0}{6} \\ -I_m \sin(3\omega_0 t), & \frac{T_0}{6} \leq t \leq \frac{2T_0}{6} \\ I_m \sin(3\omega_0 t), & \frac{2T_0}{6} \leq t \leq \frac{3T_0}{6} \\ 0, & \frac{3T_0}{6} \leq t \leq \frac{4T_0}{6} \\ -I_m \sin(3\omega_0 t), & \frac{4T_0}{6} \leq t \leq \frac{5T_0}{6} \\ I_m \sin(3\omega_0 t), & \frac{5T_0}{6} \leq t < T_0 \end{cases} \quad (3-23)$$

The current  $i_a$  is a periodic function and according to (Howell, 2001), any periodic function can be expressed as the sum of harmonic components using a trigonometric Fourier series expansion:-

$$x(t) = a_0 + \sum_{n=1}^{\infty} a_n \cos(n\omega_0 t) + \sum_{n=1}^{\infty} b_n \sin(n\omega_0 t) \quad (3-24)$$

$$a_0 = \frac{1}{T_0} \int_{t=0}^{t=T_0} x(t) dt \quad (3-25)$$

$$a_n = \frac{2}{T_0} \int_{t=0}^{t=T_0} \cos(n\omega_0 t) x(t) dt \quad (3-26)$$

$$b_n = \frac{2}{T_0} \int_{t=0}^{t=T_0} \sin(n\omega_0 t) x(t) dt \quad (3-27)$$

Substituting (3-23) into Fourier series, the coefficient  $a_n$  and  $b_n$  are calculated as follows:-

$$a_{na} = \begin{cases} 0 \\ + \int_{T_0/6}^{2T_0/6} -I_m \sin(3\omega_0 t) \cos(n\omega_0 t) dt \\ + \int_{2T_0/6}^{3T_0/6} I_m \sin(3\omega_0 t) \cos(n\omega_0 t) dt \\ + 0 \\ + \int_{4T_0/6}^{5T_0/6} -I_m \sin(3\omega_0 t) \cos(n\omega_0 t) dt \\ + \int_{5T_0/6}^{T_0} I_m \sin(3\omega_0 t) \cos(n\omega_0 t) dt \end{cases} \quad (3-28)$$

$$b_{na} = \begin{cases} 0 \\ + \int_{T_0/6}^{2T_0/6} -I_m \sin(3\omega_0 t) \sin(n\omega_0 t) dt \\ + \int_{2T_0/6}^{3T_0/6} I_m \sin(3\omega_0 t) \sin(n\omega_0 t) dt \\ + 0 \\ + \int_{4T_0/6}^{5T_0/6} -I_m \sin(3\omega_0 t) \sin(n\omega_0 t) dt \\ + \int_{5T_0/6}^{T_0} I_m \sin(3\omega_0 t) \sin(n\omega_0 t) dt \end{cases} \quad (3-29)$$

We note the following trigonometric identities and rearrange (3-28) and (3-29)

$$\sin(mx) \cos(nx) = \frac{1}{2} [\sin(m+n)x + \sin(m-n)x] \quad (3-30)$$

$$\sin(mx) \sin(nx) = \frac{1}{2} [\cos(m-n)x - \cos(m+n)x] \quad (3-31)$$

$$a_{na} = \frac{I_m}{2\pi(3+n)} \begin{Bmatrix} 2 \cos \left[ \frac{2}{3}\pi(3+n) \right] \\ - \cos \left[ \frac{1}{3}\pi(3+n) \right] \\ - \cos[\pi(3+n)] \\ + 2 \cos \left[ \frac{5}{3}\pi(3+n) \right] \\ - \cos \left[ \frac{4}{3}\pi(3+n) \right] \\ - \cos[2\pi(3+n)] \end{Bmatrix} + \frac{I_m}{2\pi(3-n)} \begin{Bmatrix} 2 \cos \left[ \frac{2}{3}\pi(3-n) \right] \\ - \cos \left[ \frac{1}{3}\pi(3-n) \right] \\ - \cos[\pi(3-n)] \\ + 2 \cos \left[ \frac{5}{3}\pi(3-n) \right] \\ - \cos \left[ \frac{4}{3}\pi(3-n) \right] \\ - \cos[2\pi(3-n)] \end{Bmatrix} \quad (3-32)$$

$$b_{na} = \frac{I_m}{2\pi(3+n)} \begin{Bmatrix} 2 \sin \left[ \frac{2}{3}\pi(3+n) \right] \\ - \sin \left[ \frac{1}{3}\pi(3+n) \right] \\ - \sin[\pi(3+n)] \\ + 2 \sin \left[ \frac{5}{3}\pi(3+n) \right] \\ - \sin \left[ \frac{4}{3}\pi(3+n) \right] \\ - \sin[2\pi(3+n)] \end{Bmatrix} - \frac{I_m}{2\pi(3-n)} \begin{Bmatrix} 2 \sin \left[ \frac{2}{3}\pi(3-n) \right] \\ - \sin \left[ \frac{1}{3}\pi(3-n) \right] \\ - \sin[\pi(3-n)] \\ + 2 \sin \left[ \frac{5}{3}\pi(3-n) \right] \\ - \sin \left[ \frac{4}{3}\pi(3-n) \right] \\ - \sin[2\pi(3-n)] \end{Bmatrix} \quad (3-33)$$

Equations (3-27) and (3-28) are used to calculate coefficients  $a$  and  $b$  of the Fourier series. The general expression of the supply current of phase  $a$  is expressed in the following equation:-

$$i_a(t) = a_0 + \begin{cases} a_1 \cos(\omega_0 t) \\ + a_2 \cos(2\omega_0 t) \\ + a_3 \cos(3\omega_0 t) \\ + a_4 \cos(4\omega_0 t) \\ + a_5 \cos(5\omega_0 t) \\ + a_6 \cos(6\omega_0 t) \\ + a_7 \cos(7\omega_0 t) \\ + \dots \end{cases} + \begin{cases} b_1 \sin(\omega_0 t) \\ + b_2 \sin(2\omega_0 t) \\ + b_3 \sin(3\omega_0 t) \\ + b_4 \sin(4\omega_0 t) \\ + b_5 \sin(5\omega_0 t) \\ + b_6 \sin(6\omega_0 t) \\ + b_7 \sin(7\omega_0 t) \\ + \dots \end{cases} \quad (3-34)$$

The evaluation of the Fourier coefficient in (3-32) and (3-33) show that all even coefficients (2, 4, 6, 8, 10, etc.) are equal to zero. In addition, all coefficient multiples of 3 (3, 6, 9, 12, etc.) are also equal to zero. This leaves only the 5<sup>th</sup>, 7<sup>th</sup>, 11<sup>th</sup>, 13<sup>th</sup>, etc. coefficient at non-zero values. The harmonic spectrum can be expressed as:-

$$f_0(p \pm 1) \quad (3-35)$$

where  $p$  is the number of voltage pulses on the secondary side and  $f_0$  is the system fundamental frequency. The equation (3-34) could then be written as follows:-

$$i_a(t) = a_0 + \begin{cases} a_1 \cos(\omega_0 t) \\ + a_5 \cos(5\omega_0 t) \\ + a_7 \cos(7\omega_0 t) \\ + a_{11} \cos(11\omega_0 t) \\ + a_{13} \cos(13\omega_0 t) \\ + a_{17} \cos(17\omega_0 t) \\ + a_{19} \cos(19\omega_0 t) \\ + \dots \end{cases} + \begin{cases} b_1 \sin(\omega_0 t) \\ + b_5 \sin(5\omega_0 t) \\ + b_7 \sin(7\omega_0 t) \\ + b_{11} \sin(11\omega_0 t) \\ + b_{13} \sin(13\omega_0 t) \\ + b_{17} \sin(17\omega_0 t) \\ + b_{19} \sin(19\omega_0 t) \\ + \dots \end{cases} \quad (3-36)$$

The magnitude of each harmonic component is inversely proportional to  $n$ , where  $n$  is the harmonic number. We can see that the 6-pulse rectifier will generate only a limited number of harmonics, and that the magnitude will be inversely proportional to the harmonic number. These are theoretical values. In practice these values are higher. The above derivation is applicable to ideal circuits, ignoring circulating currents and the effect of commutation. The commutation mechanism and voltage notching are described in (Institute of Electrical and Electronics Engineers, Inc., 1992) and (Shepherd, 2004). The most reliable way of determining input harmonic currents is to carry out harmonic measurements.

Figure 3-9 shows the amplitude of harmonic components on the load side for the 6-pulse phase controlled rectifier (Miyairi, 1979). The graph shows that the DC



component is dominant, however, the load side will comprise pulsating harmonics, multiples of fundamental frequency and a number of pulses. For a 6-pulse rectifier that will be  $n \times p \times f_2$ .

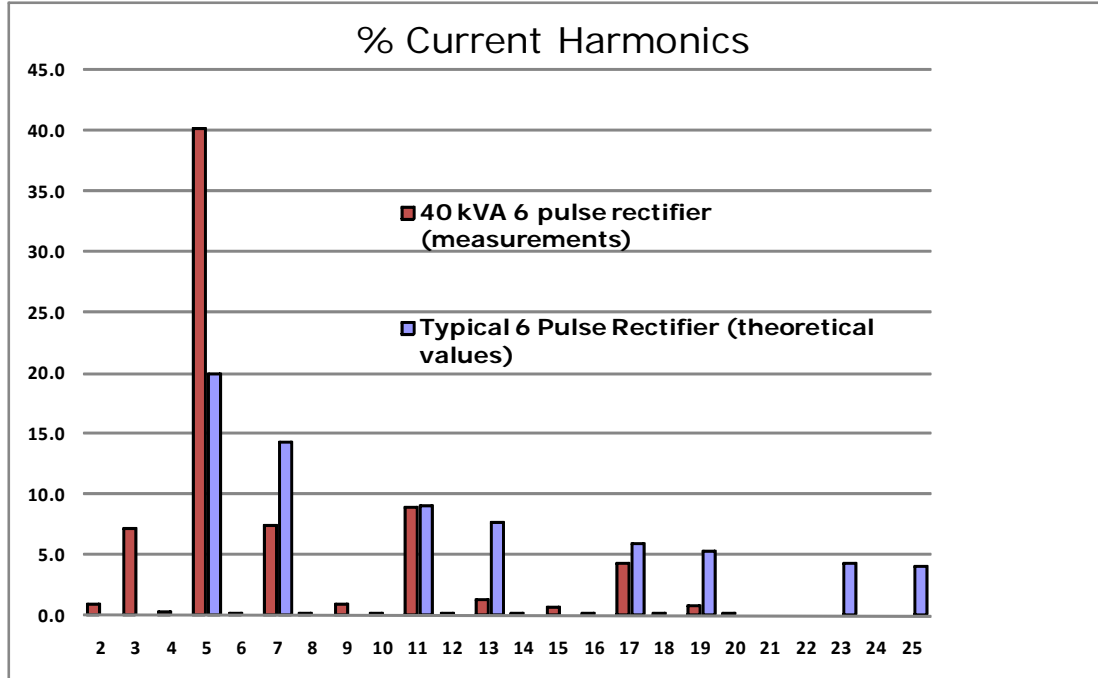


**Figure 3-9 Current harmonic spectrum of 6-pulse full bridge rectifier**

The derivation of formulae for 6-pulse rectifiers can be extended by analogy to higher pulse units, such as 12-pulse and higher. Refer to Section 2 of this thesis for an extensive literature review list.

### 3.3.2 AC UPS Systems

On off-shore facilities, all critical or vital loads are supplied via a fully redundant Uninterruptible Power Supply (UPS) system. The UPS system supplies 5-10% of a total facility load. Typically, an AC UPS system comprises one or two independent, fully segregated, 100% rated UPS units. Refer to Figure 3-10 for a typical configuration of the AC UPS system.

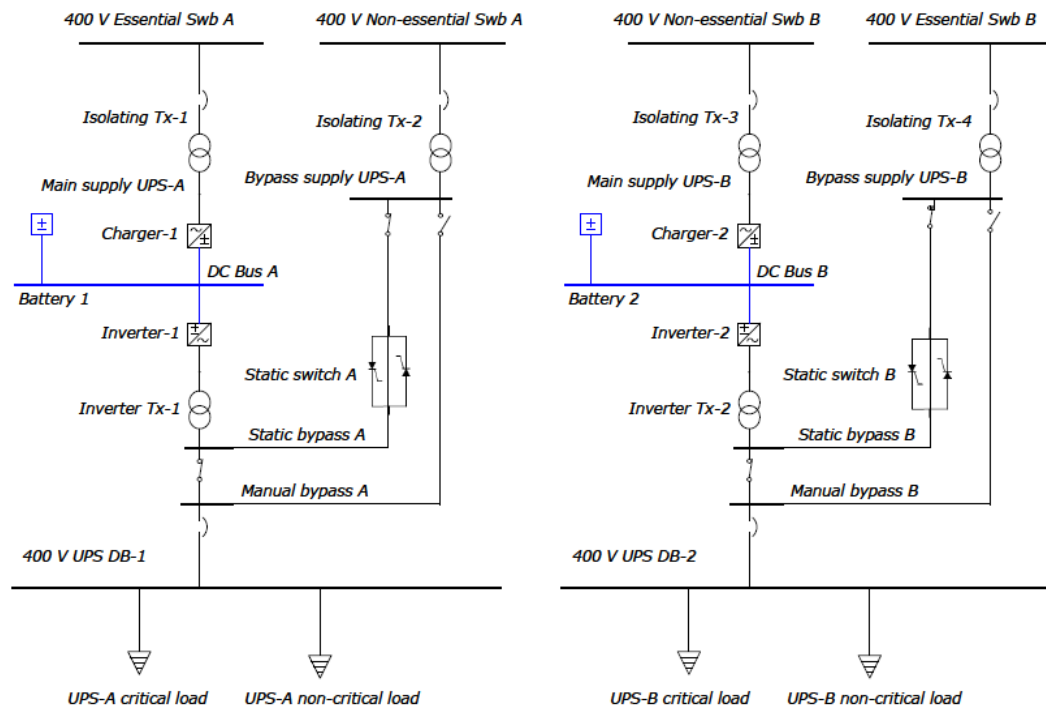


**Figure 3-10 Configuration of typical off-shore platform electrical power system**

The AC supply circuits derived from the two UPS units do not normally operate in parallel with each other. The critical supply distribution boards provide dual supplies to each critical load. Each UPS unit comprises main supply, bypass supply and maintenance bypass. In normal mode of operation, the power is supplied via normal supply. When there is an inverter fault, the power is automatically switched via a static switch to the bypass supply. The maintenance bypass is used when carrying out maintenance of the UPS unit; the power is directly fed from the mains board. It should be noted that only normal supply mode will provide the level of voltage regulation and is the mode that is utilised most of the time.

The AC UPS units are the solid state, double conversion and microprocessor-controlled type. The main supply comprises a rectifier, a DC link and an inverter part. Bypass supply comprises direct supply from the mains. The AC input of the rectifier is a three-phase three-wire design and the bypass supply is a three-phase four-wire or one-phase two-wire configuration, as appropriate. The neutral of the output is solidly earthed.

The UPS rectifier is the front end part of the UPS unit. The most common rectifier circuit is three-phase full wave controlled bridge rectifier circuit. It is supplied from the mains supply via an isolation transformer. The three-phase power supply is rectified from an AC voltage into the DC voltage. The DC voltage is smoothed via a DC inductor and this portion of the power flow is fed into the DC battery bank. Refer to Figure 3-11 for a typical configuration of the UPS rectifier and battery charger circuit.

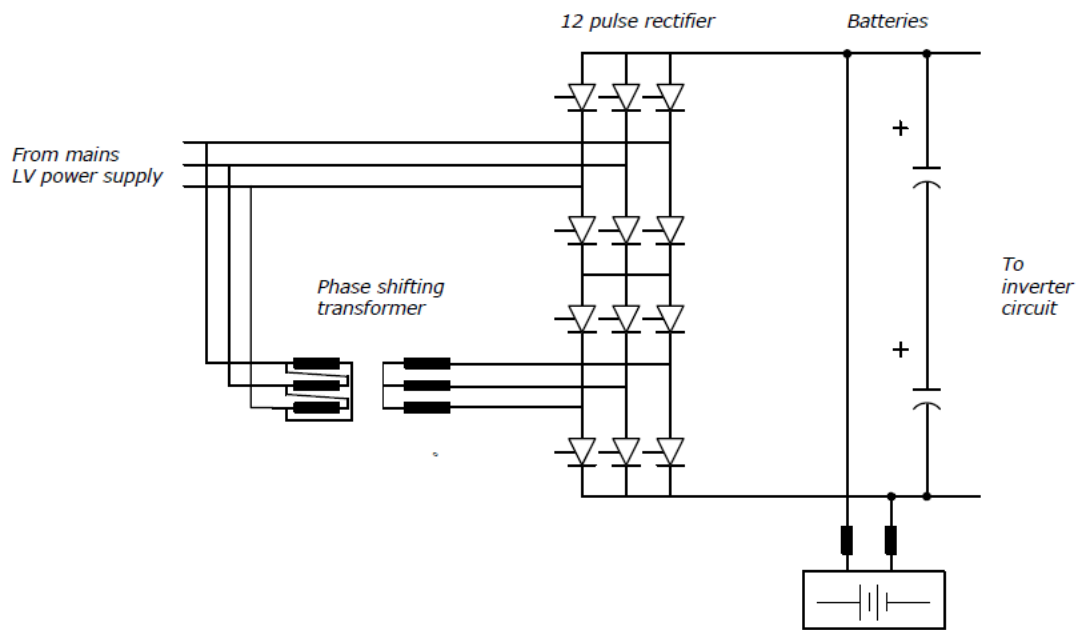


**Figure 3-11 Typical UPS battery charger configuration diagram**

The rectifier elements are thyristor controlled static switches and commutation is achieved naturally by the line side of the system. The battery bank placed between the rectifier and inverter provides a constant source of voltage to the inverter circuit. The inverter operates as a VSI inverter. It usually incorporates IGBTs as the switching elements based on PWM control technique. The output frequency of the UPS inverter is constant. The schematic diagram of a typical UPS inverter circuit is given in Figure 3.12.

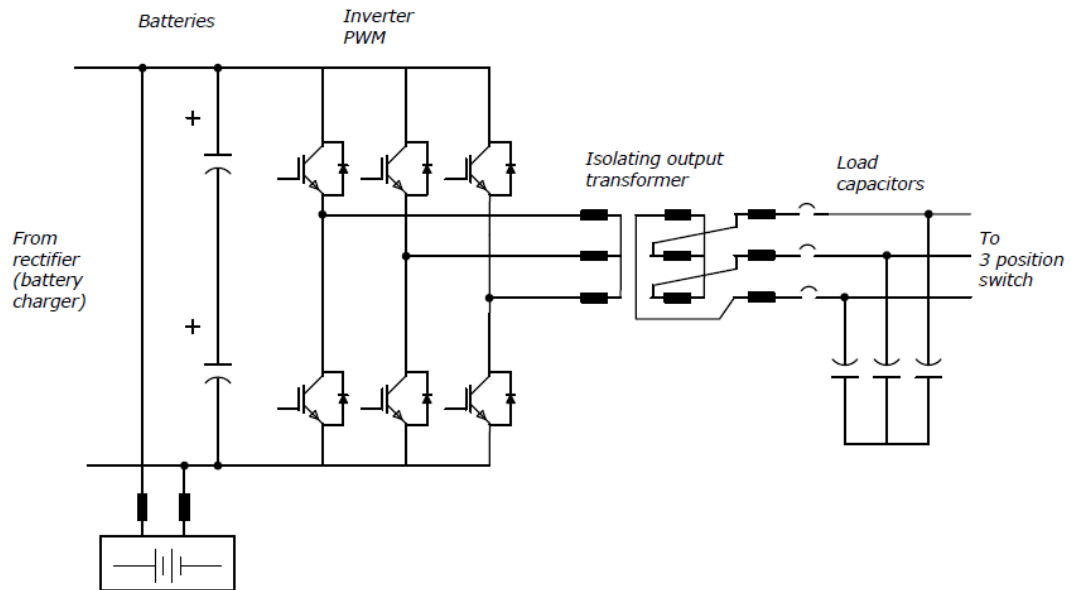


**Figure 3-12 Typical UPS schematic diagram**

The inverter part of the UPS unit is sized for full rated output load. The rectifier is sized to supply full load and simultaneously to charge the batteries. The primary side current comprises current harmonics. The rectifier load is a combination of battery capacitive and inverter inductive load. The analytical derivation of the primary side current is similar to the derivation of the input current for DC rectifiers. For harmonic analysis, the most reliable method of determining current harmonics on the primary side is to carry out harmonic measurements at the place of manufacture and to use this set of data as the source of information on current harmonics.

### 3.3.3 VSDs – LV and MV Application

A Variable Speed Drive System comprises an electric motor, a converter with its control and protection equipment, a supply transformer, harmonic filters and a heat exchanger. Figure 3-13 shows a simplified representation of the VSD system.

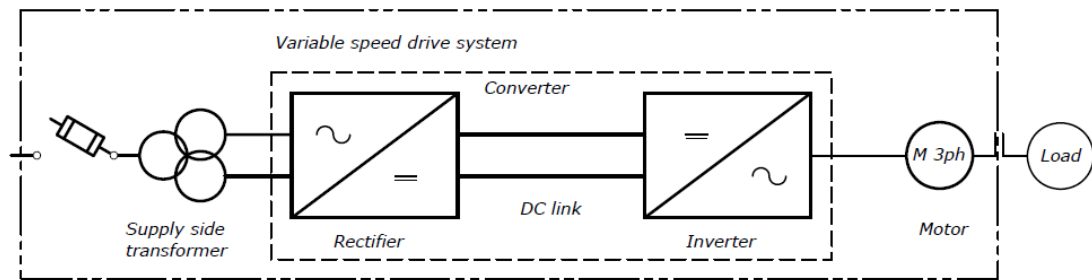


**Figure 3-13 A simple representation of a VSD system**

The VSD system provides variable voltage and variable frequency supply to an electric motor. The converter is a non-linear device as it includes static switches and for this reason is the source of current harmonics. (Bernet, 2000) provides an overview of the power semiconductors currently available on the market. The dominant material used in power electronic switches is silicon. Power switching devices are classified into three categories: diodes, transistors and thyristors. The diodes are classified as Schottky diodes, epitaxial and double diffused pin diodes. Fast switching epitaxial and double diffused pin diodes are used in medium voltage applications ( $V_{br} > 600 \text{ V}$ ). In the transistor range, the IGBTs rated at 600 V, 1200 V, 1700 V, 2500 V and 3300 V and currents of 2400 A are used in medium voltage high power converter circuits. Thyristors are classified as thyristors for phase control, fast thyristors, gate turn-off thyristors (GTOs) and integrated gate turn off thyristors (IGCTs). Conventional thyristors that are turned off by natural commutation are very reliable and are rated up to 12000 V-1500 A and 4800 V – 5000 A. Conventional GTOs are the most widely used gate controlled semiconductors. They are rated up to 6000 V – 6000 A. The improvements made on conventional GTOs such as the gate drive, integration of the inverse diode and change of the turn-off process have led to a introduction of new electronic device IGCT. The IGCTs are rated the same as GTOs up to 6000 V – 6000 A.

A typical VSD converter comprises three parts; a rectifier, a DC link and an inverter. The rectifier is in the front when looking from the supply side and in many references is referred to as ‘a front end’. The front end rectifier converts an AC supply of constant voltage and constant frequency to a DC supply. The converters utilising power diodes or thyristors for switching function are called non-active front ends. The converters utilising IGBTs, GTOs or IGCTs are called active front end

rectifiers as they actively change flow of energy from the supply side into the VSD system and back into the supply system. The DC link comprises a combination of inductor and capacitor circuits acting as an energy storage device providing power to the inverter circuit. Inverters are supplied from a DC link and convert the DC supply to variable voltage and variable frequency AC output. Based on the topology of the inverter supply circuit and commutation energy, the following classification is currently widely accepted within the industry: voltage source inverters (VSI) and current source inverters (CSI).

The voltage source inverters utilise a DC link capacitor which smooths the DC voltage. In addition the DC link usually contains series inductance to limit any transient current that may arise in the inverter supply circuit. The inverter is actively commutated type utilising IGBTs, GTOs or IGCTs. High power applications may utilise SCRs, requiring a complex circuitry to switch off the SCR by forced reduction of the anode voltage. The practical solutions of inverter circuitry based on voltage source commutation principles are subject to numerous patents (refer to website [www.freepatentsonline.com](http://www.freepatentsonline.com) ) and are described in various items of the literature reviewed in Section 2.3 of this thesis.

The voltage and frequency control of the motor supply circuit is achieved using the Pulse Width Modulation (PWM) technique, which is also known as scalar or V/f control. The constant voltage and frequency ratio is used to keep the motor flux constant. The control circuit needs an additional modulator which increases response time. The scalar control cannot control torque. The PWM drives supply frequency and voltage to the motor to produce torque and speed. The supply voltage is converted to DC voltage and current via the rectifier, and the inverter then uses a PWM technique to simulate a sine wave. The voltage and frequency of the supply to the motor will determine the torque and speed of the motor. The speed and torque control via PWM technique cannot accurately control the position of the shaft on the motor. The speed control can go as low as 10%; less than that is not accurate enough. A PWM modulator requires torque and speed response time.

The drives offering control of motor flux and motor torque, utilise Direct Torque Control (DTC) technique. Direct torque control is the most suitable for control of the circuit on 'flying start' which provides ability to catch the spinning load. This is

usually required on fans after loss of power due to a voltage dip. A spinning load is caught immediately without the need for the flux to decay.

Flux vector technique offers control of motor flux and motor torque, with both being controlled separately. The main disadvantage of traditional or closed loop flux vector control is that it requires a tachometer speed feedback from the motor, as the controller needs to know the relative positions of motor flux and data flux. Sensorless or open loop flux vector control technique eliminates tachometer feedback and offers better accuracy than PWM technique. It can produce high torque at low speed.

A typical configuration of a variable speed drive system comprising a VSI inverter is shown in Figure 3-14.

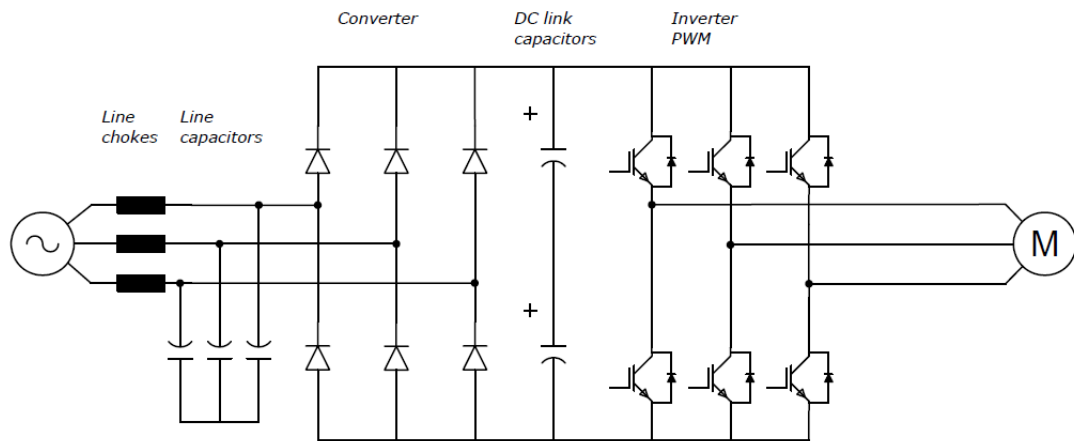


**Figure 3-14 Typical configuration of VSI type VSD system**

Some of the advantages of a typical VSI type variable drive system are as follows (ABB, Switzerland, 2004):-

- The sinusoidal output voltage from the drive supplies induction type motors without a need to de-rate the motor; no additional voltage stress on the motor insulation
- For DTC control, the system can develop full torque at standstill
- Input power factor is close to unity for the entire speed range
- Length of the motor supply cable is almost unlimited

- Elimination of VSD drive voltage torque pulsation
- Reduced motor noise
- Low line side current harmonics
- High drive system efficiency

The most common application of VSI type variable speed drives is for:-

- Drives for pumps, fans, compressors and conveyors
- Drives for mills, winches, cranes and similar drives which require high control accuracy and dynamic response
- High speed motor drives

For medium voltage applications, a typical power range of VSI drive systems is up to 8000 kW for motor voltages of 2.3 to 6.9 kV, frequency range from 0 to  $\pm 200$  Hz and speed control from 0 to 100%. The power range is limited with the DC voltage source which for larger drives should utilise large electrolytic capacitors (ABB, Switzerland, 2004).

The current source inverters utilise a reactor in the DC link which smooths the DC current and stores the energy supplied to the motor. The front end is a controlled (line commutated) rectifier. The inverter is a self-actively-commutated type utilising IGBTs, GTOs or IGCTs. The commutation principle of current commutated inverters is totally different to the commutation mechanism of voltage source inverters. Practical solutions are subject to various patents. The amplitude of the motor current is adjusted by the controlled rectifier. The frequency, which is directly related to motor speed is controlled by the inverter. A typical configuration is shown in Figure 3-15. The CSI type variable drive systems are cost effective and are suitable for a four-quadrant operation. Disadvantages are that operation at low speed is not possible and there is poor power factor at low speed. A typical application is for pumps, blowers and fans.



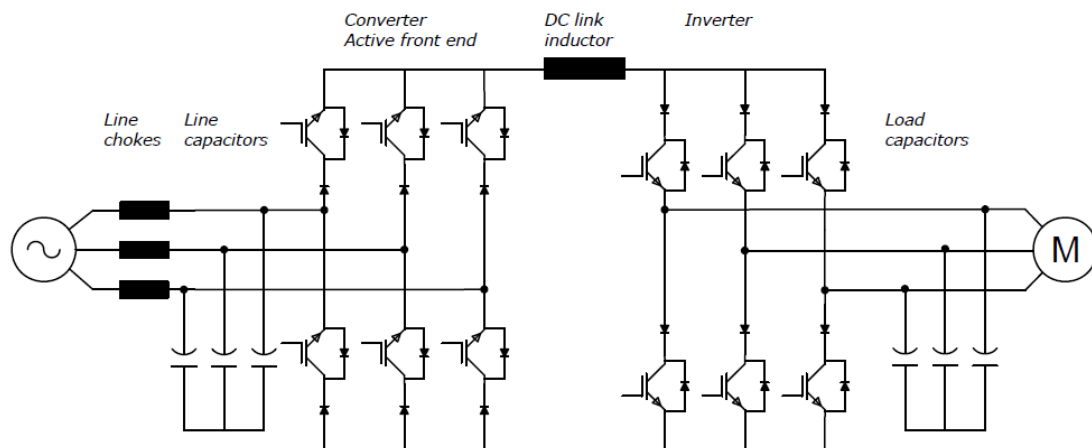


**Figure 3-15 Typical configuration of CSI type VSD System**

As there are so many practical combinations of variable speed drives available on the market, designers of the industrial power system face the problem of how to represent these drives in harmonic analysis. Harmonics generated by variable speed drives are dependent on converter configuration and the load seen by the rectifier. In principle, the characteristic harmonics generated by the rectifier will still be dominant harmonics; however, due to various practical examples of the VSDs, the current harmonic spectrum will be extended to other harmonics and the amplitude of the characteristic harmonics will be different from those calculated for the ideal case.

There are two options open to designers: either specify the maximum limits for current harmonics for non-linear devices or, preferably enter a commercial supply frame agreement with the suppliers and obtain the harmonic current spectrum information, which is based on measurements, before the start of the design process.

### **3.3.4 Electric Process Heaters**

Thyristor controlled electric process heaters, used on off-shore facilities to control the temperature of process liquids such as glycol, are generators of current harmonics and inter-harmonics (IEEE/Cigre, 1997). The process heaters are resistive elements immersed into a tank filled with the process liquid. The heater elements are supplied from a low voltage network. The temperature control of the process liquid is achieved by controlling the amount of electric energy flowing into the heater elements. The most common method of power control is utilisation of thyristor control circuit. Figure 3-16 shows a typical configuration of a process heater power

supply circuit connected in star configuration. A possible variation is to connect the heater elements in delta configuration and install the thyristors in two legs only.

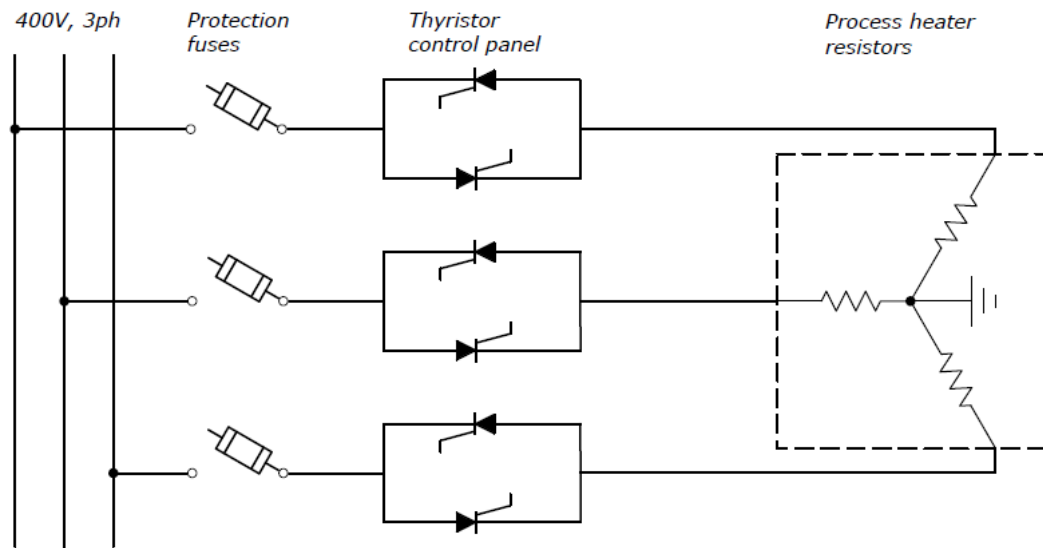


**Figure 3-16 Typical configuration of thyristor controlled process heater**

The power supply to process heaters is controlled via an SCR control panel. The thyristor switching is done in zero current or zero voltage crossing. This method of thyristor control prevents the creation of radio frequency interference signals and system harmonics caused by phase control switching. There are two modes of operation; one is a single cycle mode, the other is burst mode. In the latter, the temperature control is achieved by having the power supply on and off for a preset period of time. For example, the power is switched on for 5 seconds (250 cycles) and then switched off for 5 seconds (250 cycles). In cycling mode the circuit is switched on for a few cycles and then switched off for another few cycles. For example if the temperature is controlled at 75% of power, then the circuit is switched on for three cycles and switched off for one cycle. Burst mode is seen as a load acceptance and load rejection case and is avoided on off-shore facilities having a weak power supply system. The cycling mode is normally utilised on off-shore facilities as it provides tighter temperature control; however this mode of operation injects current inter-harmonics back into the power supply system. The following formulae are derived for 50% duty cycle in single cycle mode. The formulae show that the operation of process heaters in single cycle mode will create sub-harmonics. The sub-harmonics and inter-harmonics generated in the system are dependent on switching cycle ratio.

Figure 3-17 shows current waveform for the 50% duty cycle. The power supply fundamental frequency is designated as  $f$ . The thyristor generated 1 cycle frequency is designated as  $f_0$ .

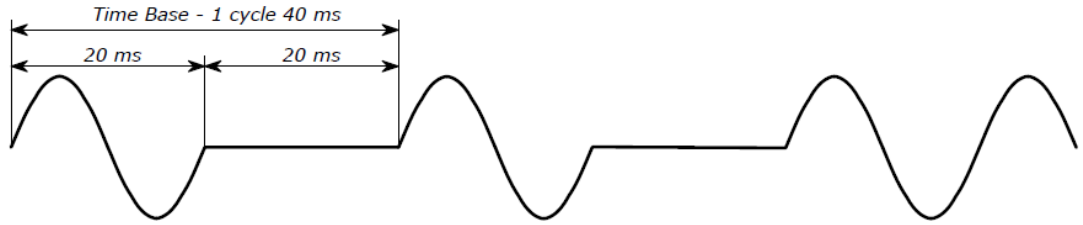


**Figure 3-17 50% duty cycle of thyristor controlled process heater**

$$f_0 = \frac{f}{2} = \frac{50}{2} = 25 \text{ Hz} \quad (3-37)$$

The current that is drawn from the supply circuit can be expressed in terms of frequency  $f_0$ , as:

$$i = I_m \sin 2\omega_0 t, \quad \omega_0 = \frac{1}{T_0} \quad (3-38)$$

$$i(t) = \begin{cases} -I_m \sin 2\omega_0 t, & 0 \leq t \leq \frac{T_0}{2} \\ 0, & \frac{T_0}{2} \leq t \leq T_0 \end{cases} \quad (3-39)$$

$$a_{na} = \frac{2}{T_0} \left[ \int_0^{\frac{T_0}{2}} A \sin(2\omega_0 t) \cos(n\omega_0 t) dt + \int_{\frac{T_0}{2}}^{T_0} 0 \cos(n\omega_0 t) dt \right] \quad (3-40)$$

Applying trigonometric identity of equation (3-30) and substituting in (3-40) we get

$$a_{na} = \frac{2}{T_0} \frac{1}{2} A \left[ \int_0^{\frac{T_0}{2}} \sin(2+n)(\omega_0 t) dt + \int_0^{\frac{T_0}{2}} \sin(2-n)(\omega_0 t) dt \right] \quad (3-41)$$

$$x = (2+n)\omega_0 t \quad dt = \frac{dx}{(2+n)\omega_0} \quad (3-42)$$

$$y = (2-n)\omega_0 t \quad dt = \frac{dy}{(2-n)\omega_0} \quad (3-43)$$

$$a_{na} = \frac{A}{T_0} \left[ \int_{x=0}^{\frac{T_0}{2}} \frac{\sin x}{(2+n)\omega_0} dx + \int_{y=0}^{\frac{T_0}{2}} \frac{\sin y}{(2-n)\omega_0} dy \right] \quad (3-44)$$

$$a_{na} = \frac{A}{T_p} \left[ -\frac{\cos x}{(2+n)\omega_p} t = \frac{T_p}{2} / t = 0 - \frac{\cos y}{(2-n)\omega_p} t = \frac{T_p}{2} / t = 0 \right] \quad (3-45)$$

$$a_{na} = \frac{A}{T_p} \left[ -\frac{\cos x}{(2+n)\omega_p} t = \frac{T_p}{2} / t = 0 - \frac{\cos y}{(2-n)\omega_p} t = \frac{T_p}{2} / t = 0 \right] \quad (3-46)$$

$$a_{na} = \frac{A}{T_p} \left[ -\frac{\cos(2+n)\omega_p t = \frac{T_p}{2} / t = 0}{(2+n)\omega_p} - \frac{\cos(2-n)\omega_p t = \frac{T_p}{2} / t = 0}{(2-n)\omega_p} \right] \quad (3-47)$$

$$a_{na} = \frac{A}{T_p} \left[ \frac{[-\cos(2+n)\omega_p \frac{T_p}{2} + 1]}{(2+n)\omega_p} + \frac{[-\cos(2-n)\omega_p \frac{T_p}{2} + 1]}{(2-n)\omega_p} \right] \quad (3-48)$$

$$a_{na} = \frac{A}{2\pi} \left[ \frac{[-\cos(2+n)\pi + 1]}{(2+n)} + \frac{[-\cos(2-n)\pi + 1]}{(2-n)} \right] \quad (3-49)$$

$$n = 1, a_{1a} = \frac{4}{3\pi} A \quad (3-50)$$

$$n = 2, a_{2a} = 0 \quad (3-51)$$

$$n = 3, a_{3a} = -\frac{4}{5\pi} A \quad (3-52)$$

$$b_{na} = \frac{A}{2\pi} \left[ \frac{[\sin(2-n)\pi]}{(2-n)} - \frac{[\sin(2+n)\pi]}{(2+n)} \right] \quad (3-53)$$

$$n = 1, b_{1a} = 0 \quad (3-54)$$

$$n = 2, b_{2a} = \frac{1}{2\pi} A \quad (3-55)$$

$$n = 3, b_{3a} = 0 \quad (3-56)$$

For  $n = 4, 5, 6$ , etc.  $b_{4a} = 0, b_{5a} = 0, \dots, b_{na} = 0$

$$a_0 = \frac{1}{T_p} \left[ \int_0^{\frac{T_p}{2}} A \sin(2\omega_0 t) dt \right] \quad (3-57)$$

$$a_0 = \frac{T_p}{T_p 4\pi} \left[ -\cos(2\pi) + \cos\left(0 \frac{4\pi}{T_p}\right) \right] \quad (3-58)$$

$$a_n = \frac{A}{4n} [-1 + 1] \quad (3-59)$$

$$a_0 = 0 \quad (3-60)$$

$$i_L = \frac{E_m}{R} \left[ \frac{4}{3\pi} \cos(\omega_0 t) - \frac{4}{5\pi} \cos(3\omega_0 t) + \frac{1}{2\pi} \sin(2\omega_0 t) + \dots \right] \quad (3-61)$$

In equation (3-61) we recognise the following characteristic harmonics and their multiples:-

$$\dots \dots \dots \left[ \frac{4}{3\pi} \cos(\omega_0 t) \right] \quad (\text{sub-harmonic at 25Hz})$$

$$\dots \dots \dots \left[ \frac{4}{5\pi} \cos(3\omega_0 t) \right] \quad (\text{inter-harmonic at 75Hz})$$

The spectrum of harmonic currents is usually provided by equipment manufacturers. The harmonic spectrum is based on measurements and provides all integer harmonics. This information is used as input data in harmonic analysis. The presence of inter-harmonics cannot be directly modelled into commercially available harmonic analysis software such as the widely used software package ETAP.

### 3.4 Practical Issues with System Harmonics and Harmonic Analysis Strategies

#### 3.4.1 Measurements

Practical issues with system harmonics are described in the literature review in Chapter 2 of this thesis. The primary concern with non-linear loads is the generation of distorted current waveforms that are injected back into the system, causing voltage distortion. Applying Fourier's harmonic analysis to voltage and current waveforms enables insight into waveform distortion and the harmonic components that create rotating fields of various frequencies. Each harmonic component will impact on the power system and the effect of each harmonic component is superimposed on each other. Derivation of the harmonic current of a 6-pulse rectifier shows the presence of the fifth and seventh harmonic. The harmonics expressed as  $(2+3n)$ , where  $n = 0, 1, 2, 3, \dots$  will create a negative sequence rotating field. Such fields have rotation opposite to the positive sequence rotating fields, which are caused by  $(1+3n)$  harmonics, where  $n = 0, 1, 2, 3, \dots$ . For this reason it is important to have a full understanding of system harmonics as this will enable analysis and predict the

impact on various electrical components, specifically rotating machines and protection devices working on the principle of rotating fields.

When we carry out harmonic measurements, the process is reduced to capturing voltage and current waveforms. The spectrum analysis based on captured waveforms provides insight into various system harmonics present in the system. Application of a standardised method on capturing voltage and current waveforms and subsequent spectrum analysis will enable direct comparison between various measurements, eliminating system errors.

The voltage and current harmonics in the power system create a number of negative effects. The distorted current will cause increased overheating in resistive components of the network. Voltage distortions cause increased overheating in magnetic circuits due to saturation effect of magnetic material. In the case where the control circuits and protection relays are supplied from a distorted power supply, misoperation and uncontrolled tripping of such devices can cause unexpected plant shutdowns. Negative sequence rotating fields will cause additional overheating in the rotor windings of rotating machines. On smaller isolated power systems, voltage and current distortions caused by non-linear loads are absorbed by the system components. On smaller systems such as off-shore oil and gas facilities, harmonic currents can create vibration issues, when power system frequencies coincide with rotating machinery resonant frequencies, typically around 1500 Hz. These are all well known effects.

Harmonic measurements and harmonic survey are reliable methods employed in determining the level of voltage and current distortions on electrical power systems. However, these reactive methods can be used only when the plant is built and put in operation. A proactive method is harmonic analysis carried out at the design stage. The quality of harmonic analysis is dependent on the quality of the input data and the complexity of the power system model used in analysis. The system design based on load lists and power system simplification strategies compounded with use of typical harmonic source data, which is currently widely used within the industry, will result in poor harmonic study results, (refer to Appendix 3 and Appendix 4 showing results of harmonic measurements used to verify industrial power system design).

The following figures show results of the factory acceptance test and harmonic measurements on UPS units. Both figures show that harmonic measurements can differ from unit to unit, so raises the question of whether "typical" values exist.

Figure 3-18 shows the harmonic spectrum of two identical units, each rated at 60 kVA. The UPS comprises a 12-pulse controlled rectifier and an input filter. The current harmonic spectrum shows the presence of characteristic and non-characteristic harmonics. Both the magnitude and the harmonic spectrum are different.

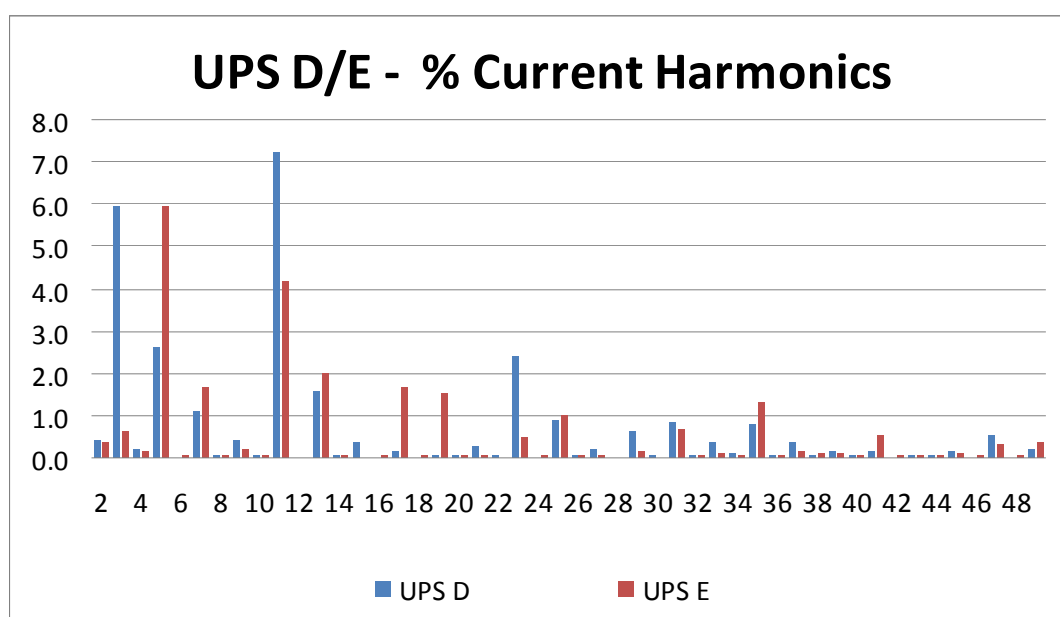


**Figure 3-18 Factory acceptance tests on 60 kVA UPS units**

Figure 3-19 shows % current harmonics for two 220 kVA UPS units. Each unit comprises a 12-pulse rectifier and input filters. The results show different spectrum and levels of non-characteristic harmonics.

To establish a reliable set of input data, we need to understand what the measurements can provide and request that input data provided by equipment manufacturers are supported with a test report. The tests should be carried out in accordance with recognised standard methods, such as those highlighted in IEEE 1159.

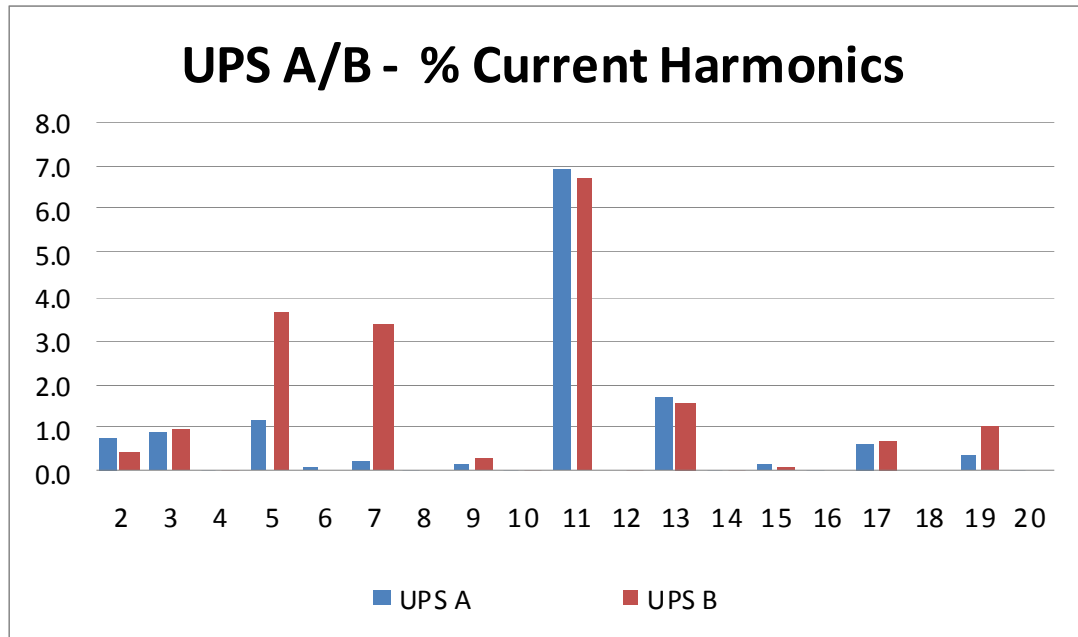


**Figure 3-19 Factory acceptance tests on 220 kVA UPS units**

### 3.4.2 Harmonic Analysis Strategy

Mitigation strategies on how to minimise system harmonics are described in the literature reviewed in Chapter 2 of this thesis. The most effective method is to minimise the use of non-linear loads as much as possible. In case this cannot be achieved, there are a number of measures that can be taken to prevent power system distortions during steady state operation.

One possible measure would be to select a DC rectifier with a higher number of pulses. The 12-pulse rectifier generates harmonics in the system such as 11<sup>th</sup>, 13<sup>th</sup>, 23<sup>rd</sup>, 25<sup>th</sup>, and so on, which, in compares with the 6-pulse rectifier, eliminates the 5<sup>th</sup>, 7<sup>th</sup>, 17<sup>th</sup>, 19<sup>th</sup>, and so on. Therefore UPS systems should incorporate 12-pulse rectifier circuits in order to minimise harmonics.

The LV variable speed drives normally incorporate a 6-pulse rectifier as the front end device. These drives should be selected with input line chokes and input side harmonic filters.



Thyristor controlled electric heaters can be split into two parts, one part to be constantly switched on and another to be switched on and off via the thyristor controlled circuit. This strategy will reduce the total non-linear component of the heater current.

The remaining harmonics in the system should be mitigated via the installation of harmonic filters. The passive harmonic filters are the most cost effective solution. There is limited industry experience in installing active filters on industrial LV systems, especially on remote off-shore facilities where the system reliability and operational flexibility is very important.

Considering the importance of mitigating the effects of non-linear loads on the electrical power system, the current industry practice for conducting harmonic analysis does not always produce the best results. Harmonic analysis requires a good quality power system model and a reliable set of input data.

The development of a good quality power system model should be included in the initial design stage of the project. The model used for harmonic studies is identical to those developed for load flow and short circuit studies and should include the following components:-

- Power generation – all power generators should be modelled, including main power generation and emergency power generators
- Distribution system – system topology should include all MV and LV nodes. The LV nodes should include all three-phase feeder loads. Single-phase loads do not need to be modelled.
- All MV and LV cables should be included in the model, this information can be used to produce power cable schedule.
- All LV and MV motors should be modelled as individual loads, complete with cables
- All MV and LV loads should be modelled as individual loads.

- Harmonic data for each generator, motors, transformers and non-linear loads should be included in power system modelling.

This will enable all components in the system to be considered in harmonic analysis. The use of a good quality model will enable accurate calculation of current and voltage harmonics and will enable selection of suitable mitigation strategies.

### **3.5 Original Contribution**

The following is a summary of original contribution incorporated in this Chapter:-

1. Described typical small oil and gas isolated industrial power systems such as FPSOs and wellhead platforms and described the current design process applied within the industry for such systems.
2. Presented an introduction to current industry standards and critically evaluated the standard approach in the design of electrical power systems. The design process currently prevailing within the industry is a practical approach. However, modern day power plants incorporating a number of non-linear loads require more detailed studies at an early stage of the project cycle. For this reason there is a need to develop alternative methods leading to optimised design.
3. Developed and presented the "design by power system analysis" concept. Highlighted current methodology within the industry for calculating maximum demand (via load list). Identified the short-comings of such an approach and proposed an alternative method which is based on power system analysis software such as ETAP. Each load should be modelled in ETAP and load flow and short-circuit study results used in very early stages of system design. Proposed the inclusion of harmonics studies in the very early stages, at the same time as load flow and short-circuit studies.
4. Highlighted issues associated with power supplies fed from a remote location to a wellhead platform. These supplies are achieved via subsea cables and the most common issue is the selection of the supply voltage and of the cross-sectional area of the cable.

5. Provided the mathematical background for voltage drop calculation for subsea cables and calculated voltage drop curves which can be used for the selection of voltage levels and CSA of cables. Compared the results of manual calculations with those obtained via ETAP power system analysis software.
6. Provided an overview of non-linear loads commonly found on oil and gas offshore facilities and provided analytical formulae of harmonic currents generated by various non-linear loads. Compared theoretical values with measurements and concluded that modelling of harmonic sources should be based on figures obtained by the measurements, not by theoretical values. Otherwise, the results of harmonics analysis could be misleading.
7. Identified loads which generate sub-harmonics and inter-harmonics, provided theoretical background for harmonic currents and challenged the current industry standards which propose a cyclic mode of operation for thyristor controlled electric heaters resulting in the creation of inter-harmonics on the system. Proposed alternative mode of operation based on splitting the major loads into two groups, one with constant load, the other operating in the burst mode.
8. Highlighted issue of representing inter-harmonics and sub-harmonics in power system study (currently only integer harmonics can be simulated in power system study). Provided methodology for obtaining information about harmonic sources based on measurements: factory acceptance tests or vendor data, and harmonic survey using harmonic analyser.
9. Summarised methodology for analysing system harmonics and calculating power system harmonics for an industrial system undergoing significant expansion. The major steps are: obtain harmonic measurements, analyse harmonic measurements, develop power system model, verify model against the measurements and use as a base model for further studies.
10. Analysed new loads, and new harmonic sources, and carried out filter selection study for the power system undergoing expansion.

## **4. POWER SYSTEMS FOR MINERAL PROCESSING PLANTS**

### **4.1 Introduction**

A mineral gold processing plant comprising SAG and ball mills for grinding of process materials is a typical example of an industrial plant with power generation capacity around 100 MW, an order of magnitude larger capacity than a typical off-shore oil and gas facility. Such a plant is typically located in a remote area and includes a power station and a number of load centres. The power generation comprises either coal fired steam turbine or gas turbine driven generators. A diesel fired power station of such a large capacity is not economically viable, however the diesel generation is still employed to complement the operation of the primary power station.

The mineral gold processing plant typically includes a number of load centres concentrated within a particular area, such as:-

- Process area - primary crushing, concentrator, flotation cells
- Non-process area – accommodation village, bore water wells, warehouse, workshops
- Mine site - open pit and/or underground mine

The typical plant comprises a number of non-linear loads. Material handling via conveyors will require a number of variable speed drives in the system, mainly DTC control voltage source inverters due to inherited ability to deliver a full torque at standstill. Centrifugal pumps and electric fans will include variable speed drives, typically current source inverter. There are a small number of UPS system and battery chargers. Electric process heaters and DC motor drives are not common on the mineral processing plants.

The process area is usually the largest load centre which includes ball and SAG mills used for milling and grinding operation. The ball mill will include a VSI drive and a low speed synchronous motor, single or dual pinion coupling. The SAG mill drive will comprise a cyclo-converter and a synchronous ring motor. The SAG mill does not have a gear box for reducing the speed; the speed is controlled directly via the

cyclo-converter. The SAG mill cyclo-converter provides constant torque over entire speed range especially at low speeds down to zero. The negative side of the SAG mill cyclo-converter is that it is a source of current harmonics.

The mineral processing optimisation study is usually carried out by the process engineering team to determine the most optimal size of grinding mills and to define overall electrical loads in the process area. Selection of drive types and optimisation of electrical power system in relation to system harmonics is normally carried out by electrical engineering team. This chapter will analyse system harmonics on an existing plant and evaluate the current design practice within the industry. This analysis will be supported with a functional description of cyclo-converters, a mathematical derivation of cyclo-converter generated inter-harmonic currents, harmonic measurements and measurement of switching transients.

## **4.2 Typical Isolated Power System for Gold Processing Plant**

A typical gold processing plant power system (Figure 4-1) comprises two power stations interconnected via a 33 kV overhead line. The primary power station includes 3 gas turbines with a total capacity of 90 MW (with 2 GTs on). The secondary power station comprises a number of smaller diesel generators with up to 15 MW of power. The distribution of electrical power is carried out at the 33 kV level, which is the highest system voltage. The 33 kV system comprises overhead lines to the primary power station, treatment plant, underground mine and bore water fields. The primary power station 33 kV switchboard incorporates an inter-connector feeder to the secondary power station, 3 generator incomers, 2 feeders to the treatment plant 33 kV switchboard and an overhead line feeder to the bore-fields. The treatment plant 33 kV switchboard is a 2-section board. Each section comprises an incomer, SAG mill feeder, ball mill feeder, 3<sup>rd</sup>/4<sup>th</sup> harmonic filter feeder, 5<sup>th</sup>/7<sup>th</sup> harmonic filter feeder, 2 grinding substation feeders and a wet plant substation feeder. The 3<sup>rd</sup> and 4<sup>th</sup> harmonic filters are C-type while the 5<sup>th</sup> and 7<sup>th</sup> harmonic filters are High Pass type.

A copy of the simplified single line diagram showing the primary power station and treatment plant substation is given in Figure 4-1.

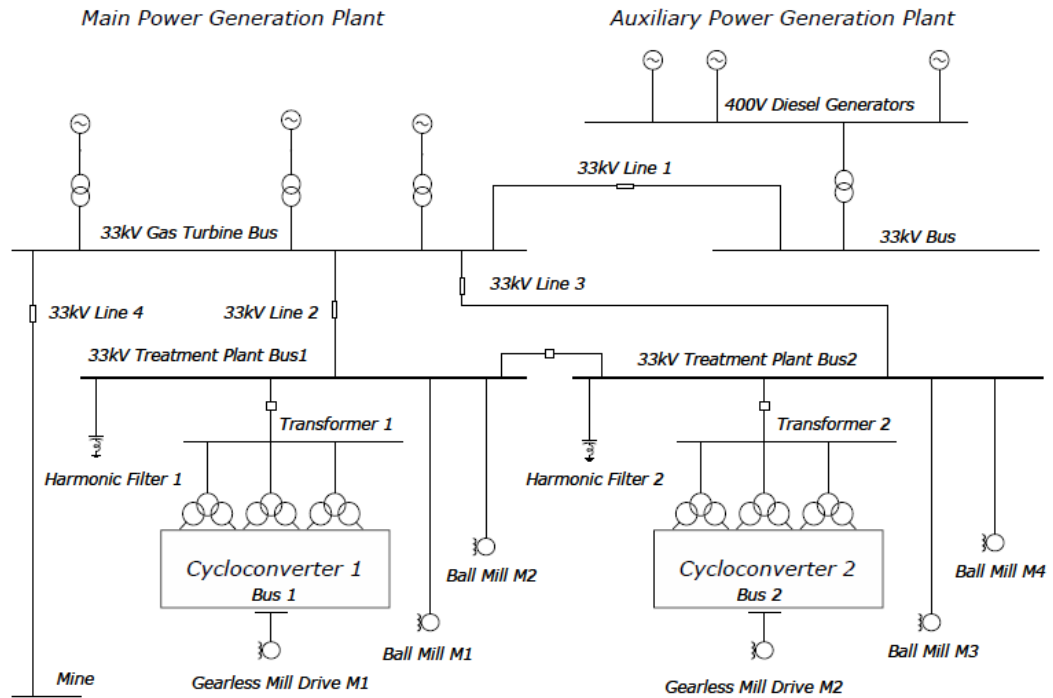


**Figure 4-1 Simplified SLD of primary power station and treatment plant**

### 4.3 Variable Speed Drives for Grinding Mills

#### 4.3.1 General

The largest non-linear load on a mineral processing plant is grinding equipment such as SAG and ball mills. (Ravani von Ow, 2010) reported that the largest SAG mills are up to 36 MW for 44 feet diameter. The ball mills reach today up to 22 MW for 28 feet diameter. The market above 34 feet is at present covered almost completely by the GMD. The SAG mills comprising a synchronous ring motor are driven via cycloconverters. Multilevel voltage source inverters are best suited for a dual pinion ball mill drive with induction machines.

The SAG mill cycloconverters are source of current harmonics and inter-harmonics that have a negative effect on system performance. The harmonic filters installed at MV level are used to mitigate the system harmonics.

#### 4.3.2 Voltage Source Inverters for Ball Mills

Ball mills installed on mineral processing plants are used for fine grinding of the process material. Grinding of materials is achieved inside the rotating mill drum with

the presence of metallic balls. The website [www.metso.com](http://www.metso.com) gives the following technical details of ball mills:

- Size up to 30 ft. x 41 ft. and as much as 30,000 HP
- Feed size is 80% passing 1/4" (6 Mm or finer) for hard ores and 80% passing 1" (25 Mm or finer) for soft ores
- Product size is typically 35 mesh or finer

The ball mills on a typical mineral processing plant are operated at a constant low speed 160 to 200 rpm. They are either driven by a synchronous motor fed directly from MV power supply or by an electric drive system comprising a VSI converter. Mills larger than 18 MW normally incorporate an electric system comprising the gearless mill drive. The synchronous motor is mechanically coupled to the mill via a single or a dual pinion. Mechanical pinion drive system has a limitation on how much torque can be transferred. For the single pinion drives this is limited to 9 MW and dual pinion to 18 MW.

Ball mills are normally run at constant speed and for this reason directly driven synchronous motor application is sufficient. In recent years, the application of a variable speed drive for ball mills indicated that there could be a certain operational benefits during start-up and maintenance operation. The most common variable speed drive topology for ball mills is a voltage source inverter supplying the synchronous motor.

The VSI drives provide a number of benefits, listed as follows:-

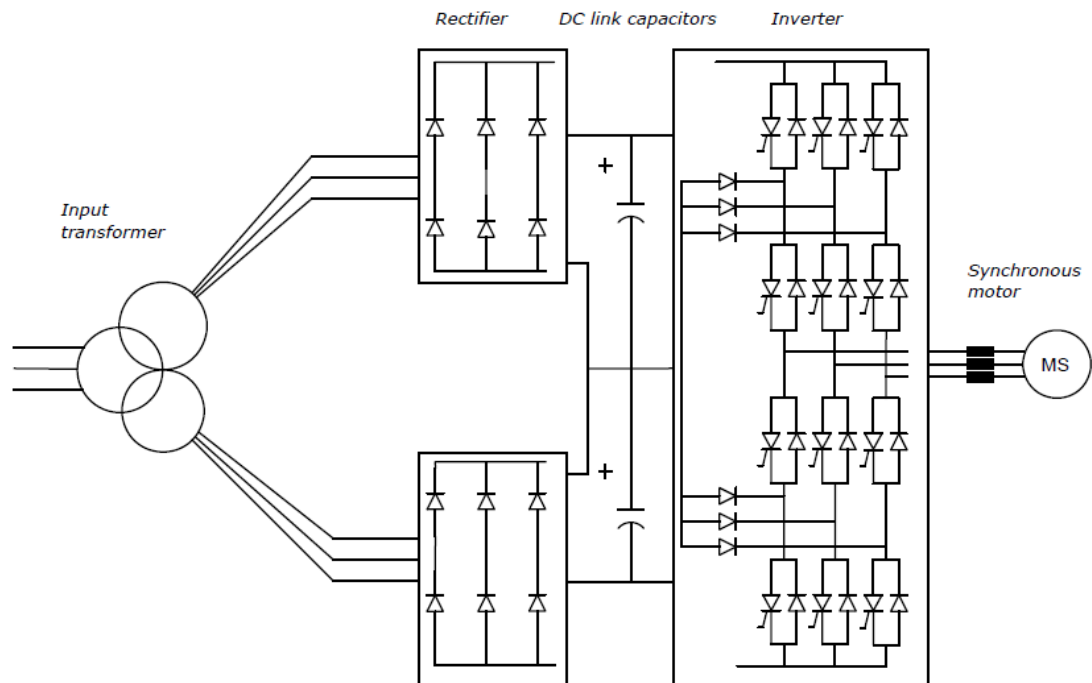
- It can be 2 or 4 quadrant design. The 2 quadrant design comprises a diode rectifier bridge at the front end. The diode bridge has the advantage of having a constant lagging power factor above 0.95 under all conditions. A 4 quadrant rectifier can bring the power factor to 1 and even achieve a leading power factor.
- The DC link prevents any disturbances from the input supply to be transferred to the motor protecting it from network transients and faults. The

capacitor bank located in the DC link smoothes the voltage and supplies reactive power to the motor.

- The self-commutated inverter units use High Voltage Insulated Gate Bipolar Transistors (IGBTs) or Integrated Gate Commutated Thyristors (IGCTs).
- The generation of harmonics to the network is the lowest of all variable speed drives and in most cases no filter is required.

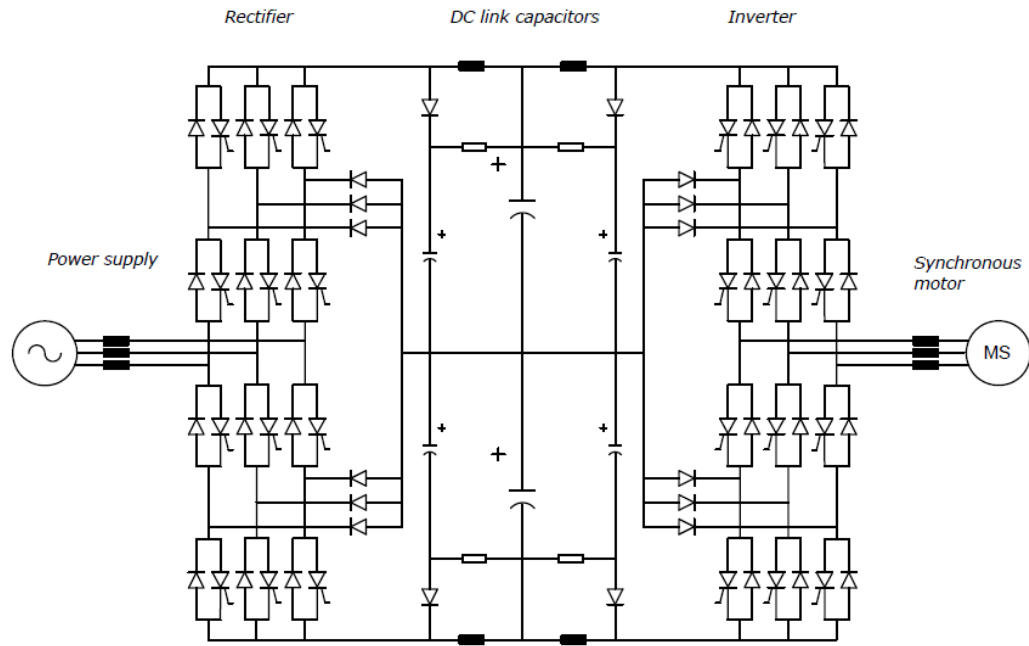
There are some disadvantages such as current de-rating at motor frequencies smaller than 3 Hz because of increased influence of phase current amplitude for thermal load of semiconductors and lower short time overload capability compared to thyristor drives. The VSI converters have a higher number of part count, hence reduced reliability.

Figure 4-2 shows topology of a typical 12-pulse VSI for 2 quadrant operation and Figure 4-3 shows topology of a typical 12-pulse VSI for 4 quadrant operation.



**Figure 4-2** A voltage source inverter with 12-pulse diode rectifier, 2 quadrant operation



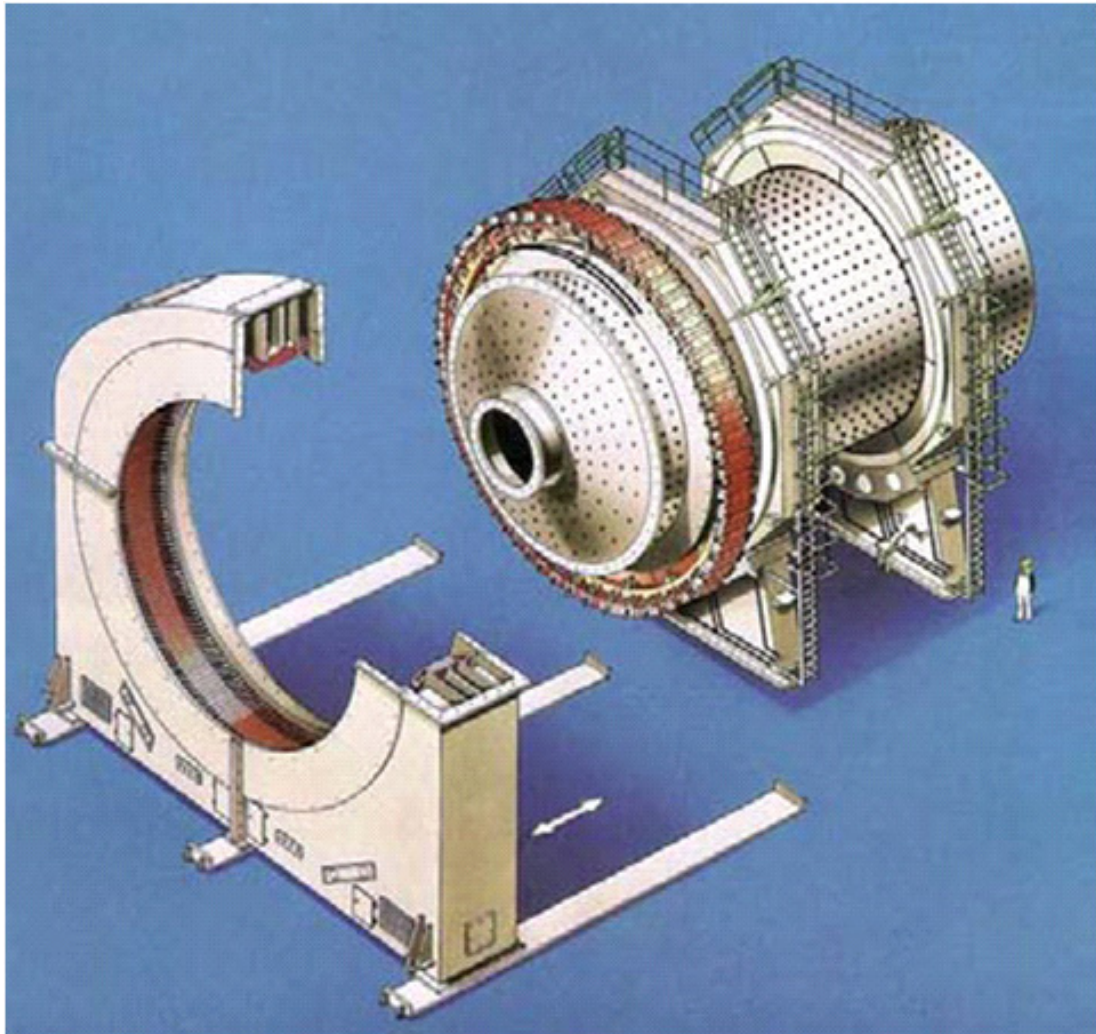


**Figure 4-3** A voltage source inverter with 6-pulse active front end rectifier, 4 quadrant operation

#### 4.3.3 SAG Mill

(Pont, 2005) states that one of the main stages in mineral processing design is optimisation of grinding equipment and grinding circuit due to the energy and maintenance costs. As a result, it is not uncommon that the modern day mineral processing plants utilise large gearless motor drives fed via cyclo-converters. The capacity of around 20 MW is being considered for both the semi-autogenous (SAG) mills and ball mills.

(Wiechmann, 2007) compares alternative converters with regard to their application for gearless drives for grinding mills and concludes that for the gearless mill drives the most suitable type is the cyclo-converter.



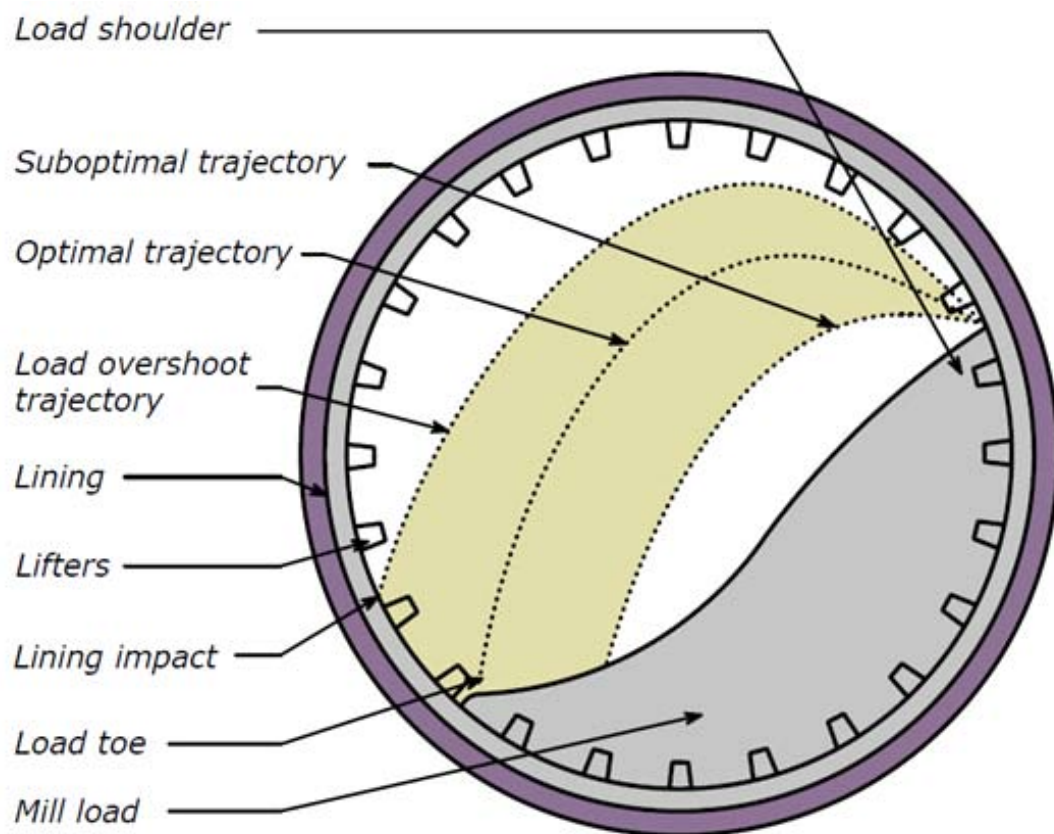
**Figure 4-4 3-D Isometric view of gearless mill motor drive**

Fig. 4-4 shows 3-D isometric view of the SAG mill with gearless motor drive. The electric motor wrapped around the SAG mill is synchronous type. The stator that is normally built in four sections is wrapped around the rotor poles attached directly to the mill. There are two common terminologies referring to SAG mill motors: “ringmotor” and “gearless”. Because the stator is made of a ring form, a common terminology for the synchronous motor is “ringmotor”. As the electromagnetic torque is applied directly to the mill without any gear, another common terminology is “gearless motor drive”.

A typical value of the air gap is 16 mm with tolerance of  $\pm 3$  mm for setting alarms and protections. Rotor poles are subjected to electromagnetic forces and the bolts which tighten individual poles have to be re-tightened in order to maintain the nominal gap of 16 mm. The synchronous motor is fed via a cyclo-converter drive

which controls the torque and operating speed of the mill. The excitation of the synchronous motor is controlled by a 6-pulse controlled bridge.

In large scale mineral processing plants, grinding of mineral ore is carried out with large-diameter rotating mills. This process called “autogenous grinding” is based on the principle where the minerals (rocks) are used as grinding media. On the other hand, semi-autogenous grinding mill (SAG) uses steel balls of typical 5-inch diameter to support the grinding media. Principle of the SAG mill is to carry ore and balls to the maximum height inside the mill and then use the force generated by falling balls to crash the minerals. Figure 4-3 shows the possible trajectories inside the mill.



**Figure 4-5 Possible trajectories of gearless mill drive (Pont, 2005)**

The trajectory which ends at the toe of the load is the most effective for grinding operation. The most efficient range of operation is around 75% - 80% of the critical speed. The critical speed is defined as the speed at which a steel ball remains at the shell of the mill without falling when the centrifugal force equals its weight and is given by:

$$\omega = \sqrt{\frac{2g}{(D-d)}} \quad (4-1)$$

where

- $\omega$  is the critical speed,
- $g = 9.81 \text{ [m/s}^2\text{]}$ ,
- $D$  is the internal mill diameter and
- $d$  is the ball diameter.

If  $d \ll D$ , with  $D$  expressed in [m], a good approximation which gives critical speed in revolutions per minute [rpm] is given by:

$$N_c = \frac{42.2}{\sqrt{D}} \quad (4-2)$$

where

- $42.2$  is the constant,
- $N_c$  is the critical speed [rpm].

For example, a SAG mill with an internal diameter of 11 meters will have a critical speed of 12.72 rpm. Nominal speed of 77% of the critical speed is 9.8 rpm. The bigger the diameter, the lower the nominal speed of rotation (Pont, 2005).

#### 4.3.4 Cyclo-converters for Gearless Mill Drives

The principle of operation of a cyclo-converter is described by (Shepherd, 2004). In brief, cyclo-converters convert AC supply of fixed frequency to an AC output of adjustable but lower frequency. This is achieved with a set of back-to-back or inverse parallel connected static switches such as SCR. Controlled opening and closing of the switches will produce a voltage waveform of desired frequency. Refer to Figure 4-6 showing topology and voltage and current waveform of a 6-pulse phase controlled non-circulating current cyclo-converter.

Phase controlled cyclo-converters in which the firing angle is controlled by gate pulses can vary the output frequency from zero to one third of the input frequency. The envelope cyclo-converters, where static switches remain fully on and conduct for consecutive cycles require compensation circuits at low speeds less than 3% of nominal. For this reason phase controlled cyclo-converters are used for GMD application.

Phase controlled cyclo-converters can be circulating and non-circulating current types. Today all GMD's utilise non-circulating current design. They offer good dynamic response over the entire output range, low starting current and high torque at low loads. Non-circulating current types provide a higher ratio between output and input frequencies compared with circulating current design which limits this ratio to one third. The circulating current design eliminates a dead time of approximately 1 ms which prevents current flow in part of the circuit that is not conducting. The circulating current increases with load and is hard to control and for this reason is not used for GMD drive application.

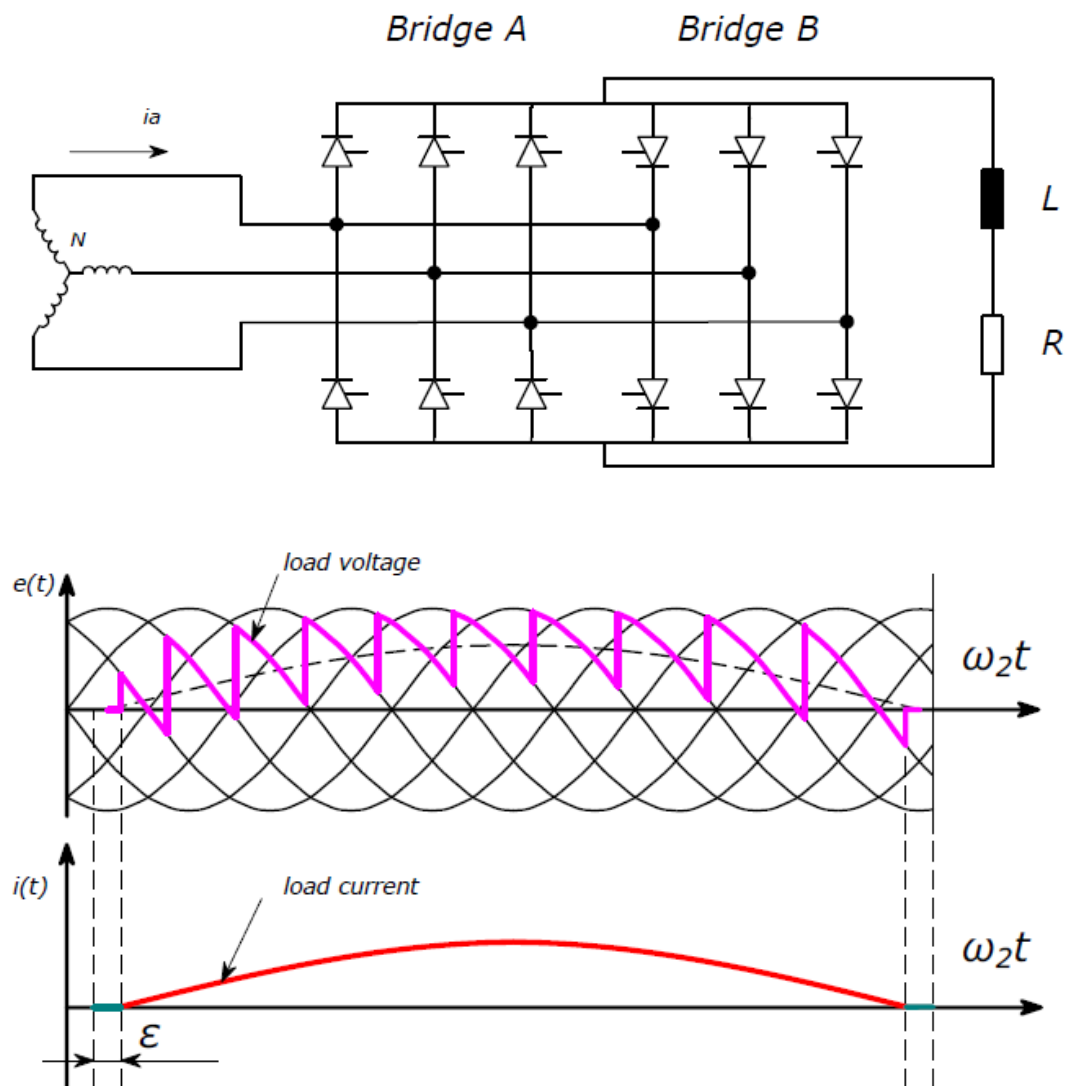
The static switches used in a typical phase controlled cyclo-converter are thyristors controlled via gate pulses to start conduction. All phase controlled cyclo-converters are line commutated to enable natural commutation of the current between successive switching. The cyclo-converter power circuit does not have a DC link. Cyclo-converters provide constant torque over the entire speed range.

(Ahrens, 2007) states that basic design consists of a reversing, direct link, three-phase 6-pulse bridge phase controlled rectifier. For higher power output, the 12-pulse anti-parallel connection is normally used so that higher voltages can be achieved.

The main advantages of cyclo-converters for grinding mill application are summarised by (Wiechmann, 2007) and are as follows:-very high power ratings, very simple and robust, low maintenance and high reliability, wide speed range with high efficiency at all operating points, excellent dynamic performance and surge load capability, low starting current, no contribution to short circuit current, no mechanical connection between motor and mill.

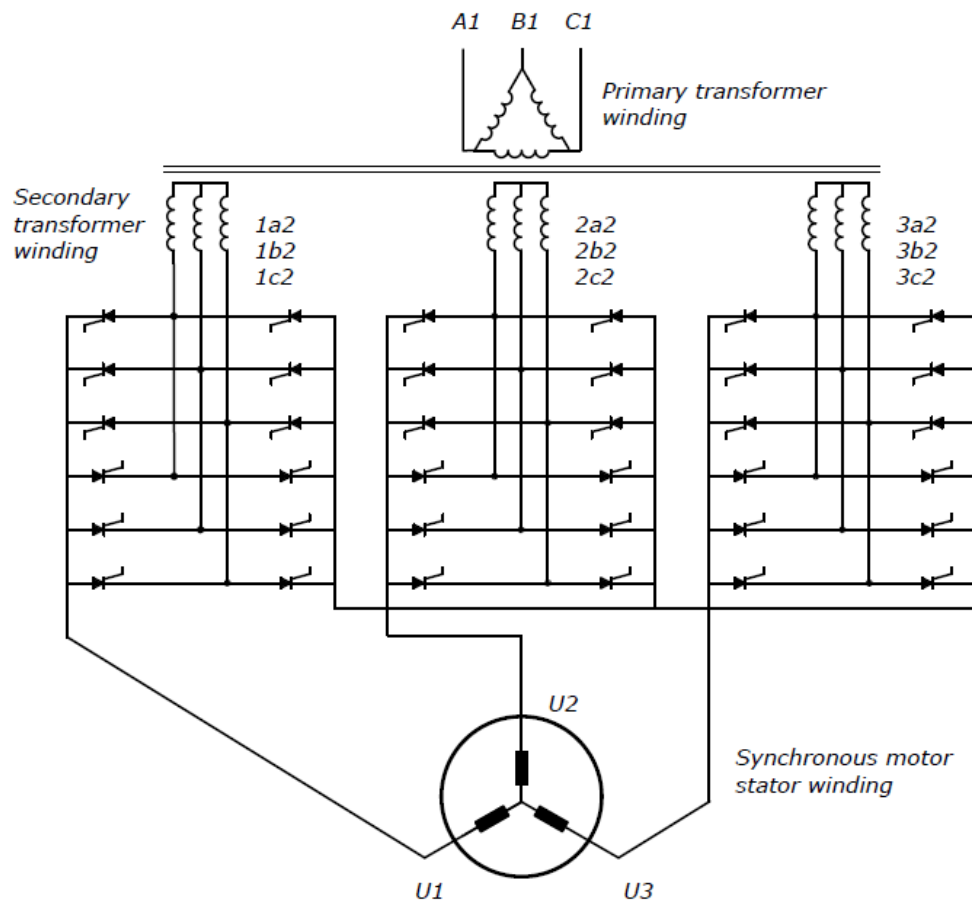
The main disadvantages of the cyclo-converter are poor power factor of about 0.8 and generation of current harmonics in the supply network.

Figure 4-6 shows topology and voltage and current waveform of a 6-pulse three-phase to single-phase cyclo-converter comprising two full pulse bridges connected in anti-parallel configuration. Bridge A will conduct over 2 cycles and then bridge B will conduct over another 2 cycles. A dead time between bridge A and bridge B conduction is required to prevent creation of circulating currents between two bridge groups. By controlling the phase angle and switching cycles we can control the amplitude of the output current and output frequency. In this instance the output frequency is 60% of input frequency.



**Figure 4-6** 6-pulse cyclo-converter

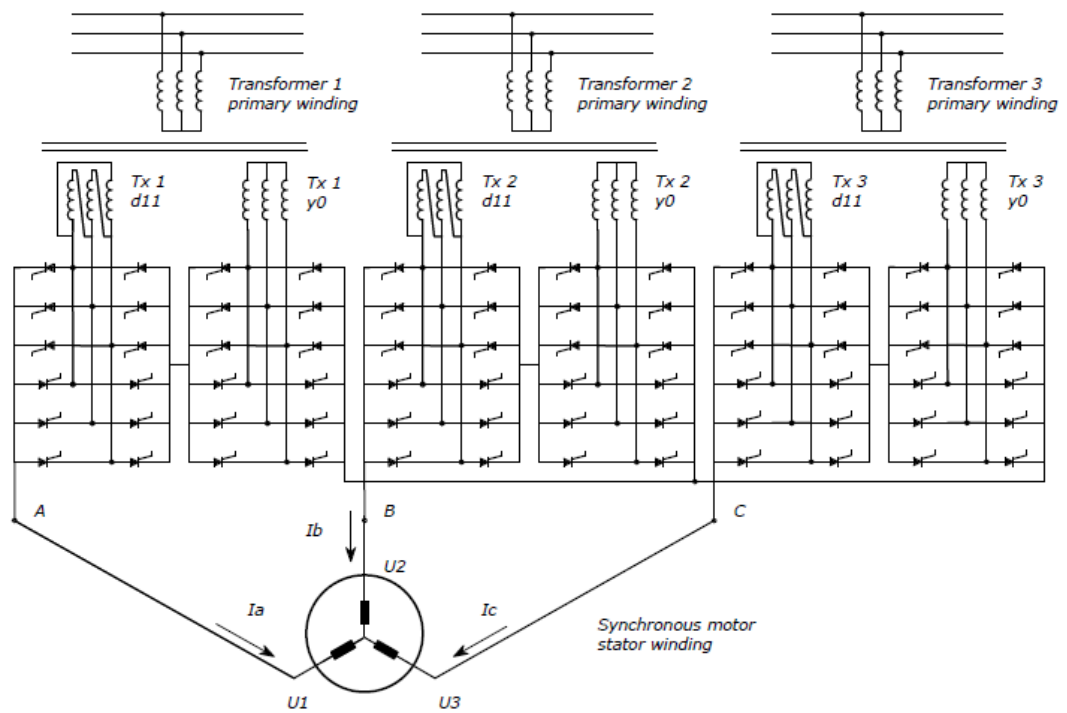
Figure 4-7 shows a typical 6-pulse three-phase cyclo-converter feeding a three-phase synchronous motor.



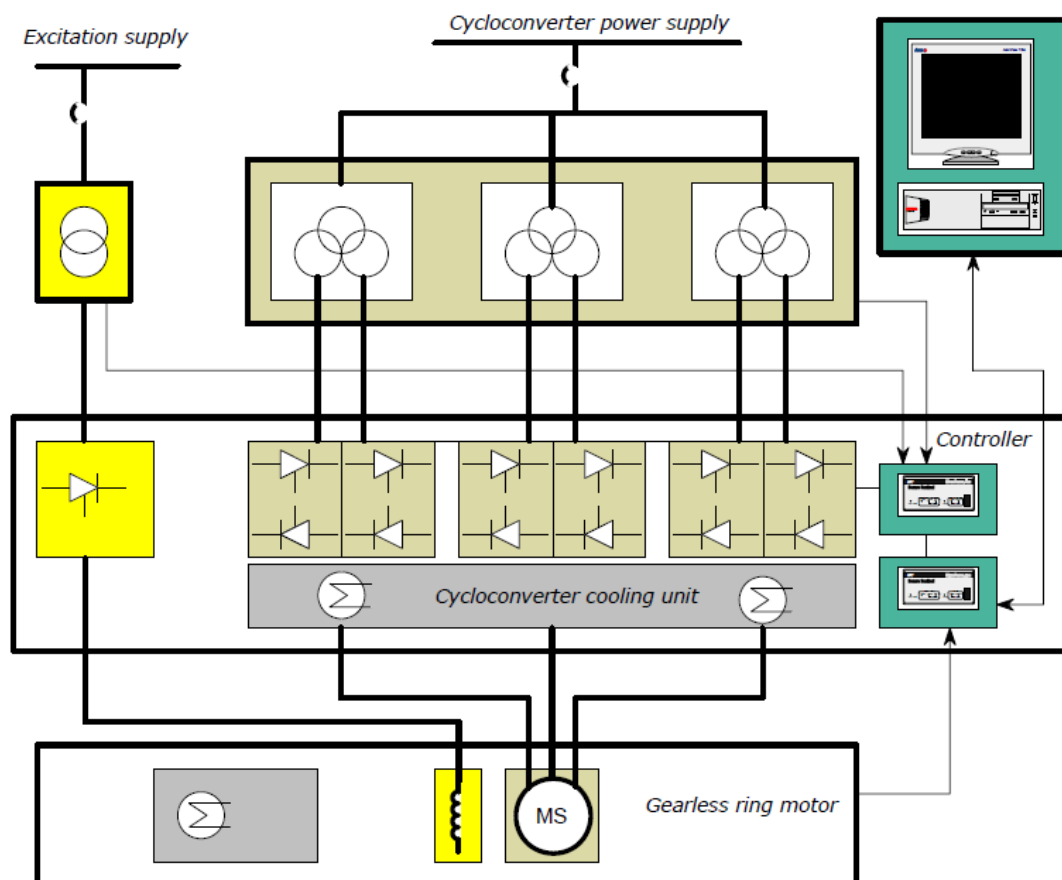
**Figure 4-7 6-pulse cyclo-converter feeding three-phase synchronous motor**

Fig. 4-8 shows a typical 12-pulse cyclo-converter which is achieved by the series connection of two 6-pulse cyclo-converters. Twin 6-pulse cyclo-converter configuration would require a synchronous motor with 2 stator windings. The cyclo-converter control circuit utilises a three-phase current control with feed forward scheme using internal voltages of the machine for better tracking of the three-phase current references. Figure 4-9 shows an overview of a typical 12-pulse cyclo-converter fed GMD system and its components.





**Figure 4-8** 12-pulse cyclo-converter feeding 3-phase synchronous motor



**Figure 4-9** Overview of typical ABB 12-pulse GMD and its components



#### 4.3.5 Theoretical Background

Cyclo-converters are generators of a complex spectrum of current harmonics which are injected back into the supply network. The current harmonic spectrum is comprised of integer harmonics, sub-harmonics (current harmonics with frequency smaller than system frequency) and inter-harmonics (current harmonics of which the frequency is not a multiple of the nominal harmonics). For a 12-pulse cyclo-converter configuration (with a 6-pulse output bridge) a total current as a function of harmonic currents is given as follows:-

$$I_D = \sum_{k=1}^{k=n} \{ I_{(f_h \pm 6kf_o)} + I_{(11f_h \pm 6kf_o)} + I_{(13f_h \pm 6kf_o)} + \dots + I_{f_h} + I_{f_s} + I_{f_A} \} \quad (4-3)$$

where:-

- $I_{(f_h \pm 6kf_o)}$  is a term comprising the characteristic frequency component  $f_h$  and its lateral sidebands.
- $I_{f_h}$  is the fundamental current component of the network side (50 Hz),
- $I_{f_o}$  is the output frequency of the cyclo-converter,
- $k$  is an integer value  $k = 1, 2, 3 \dots$
- $I_{f_s}, I_{f_A}, I_{f_A} \dots$  are non-characteristic harmonic components

The non-characteristic harmonics need to be considered, especially at low-damped networks with high non-linear loads where resonances may exist. A more complex problem arises with multiple cyclo-converter-fed drives operating at different output frequencies.

(Miyairi, 1979) derived formulae for load side voltage waveform harmonics for 6-pulse bridge rectifier and 6-pulse cyclo-converter. The reference paper states that in the 6-pulse three-phase bridge converter, the firing angle of one phase is the same as that of other phases for steady-state DC output. The firing angle of each phase of the 6-pulse three-phase cyclo-converter is controlled so that the output voltage may be the desired AC voltage. Although, from the viewpoint of the output waveform, there is a significant difference between the two converters, the behaviours of them are the

same as each other during the period between the firing of one thyristor and the next. The reference concludes that the bridge converter, may be considered a special type of the cyclo-converter. Refer to Figure 4-10 showing voltage harmonic spectrum of 6-pulse cyclo-converter. Analytical formulae for line side voltage waveforms and voltage harmonic spectrum for 6-pulse bridge rectifier are given in Chapter 3. The load voltage harmonic spectrum of 6-pulse bridge rectifier is show in Figure 3.16.

Derivation of analytical formulae for load side cyclo-converter voltage harmonics as presented by (Miyairi, 1979) is given in further text in this section. Figure 4-10 shows load side current harmonic spectrum of a 6-pulse cyclo-converter.

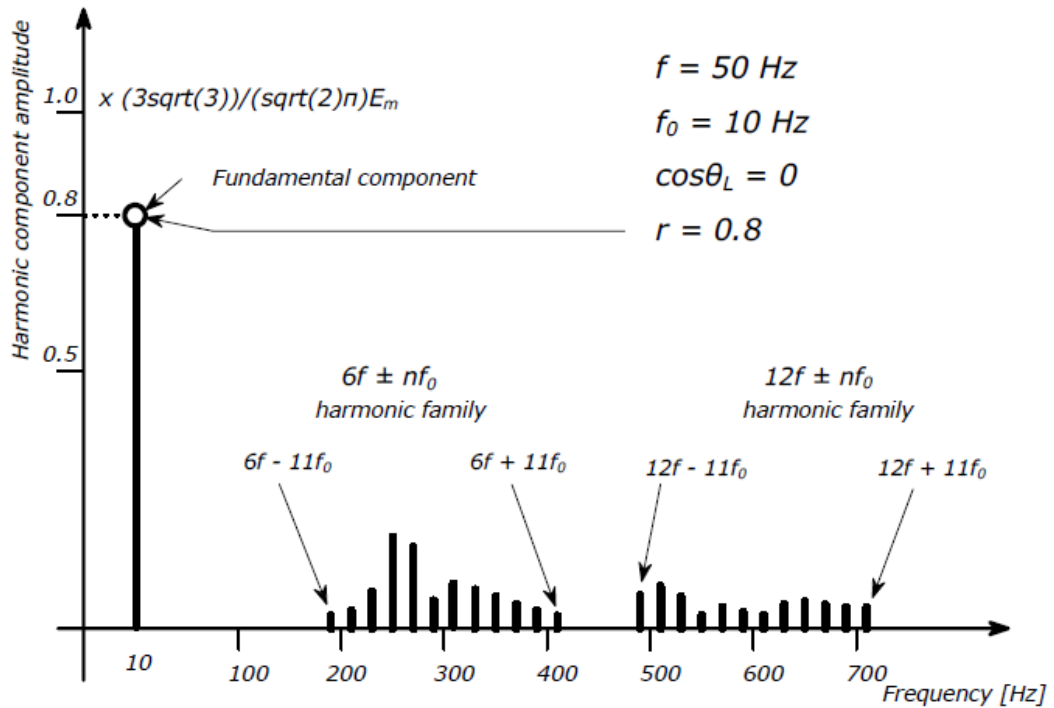


**Figure 4-10** Current harmonic spectrum of 6-pulse cyclo-converter (Miyairi, 1979)

The instantaneous voltage of the cyclo-converter is expressed by using the switching functions  $S_a$ ,  $S_b$ , and  $S_c$ , shown in Figure 4-11 and the mode functions  $M$  and  $M'$  shown in Figure 4-12. Note that the switching functions  $S_a'$ ,  $S_b'$  and  $S_c'$  are defined by the firing angle  $\alpha'$ , refer to equation 4-7.

$$e_{Lo} = (S_a e_a + S_b e_b + S_c e_c)M + (S_a' e_a + S_b' e_b + S_c' e_c)M' \quad (4-4)$$

where

- $M = 1$  and  $M' = 0$  when output current  $i_L$  is positive
- $M = 0$  and  $M' = -1$  when output current  $i_L$  is negative

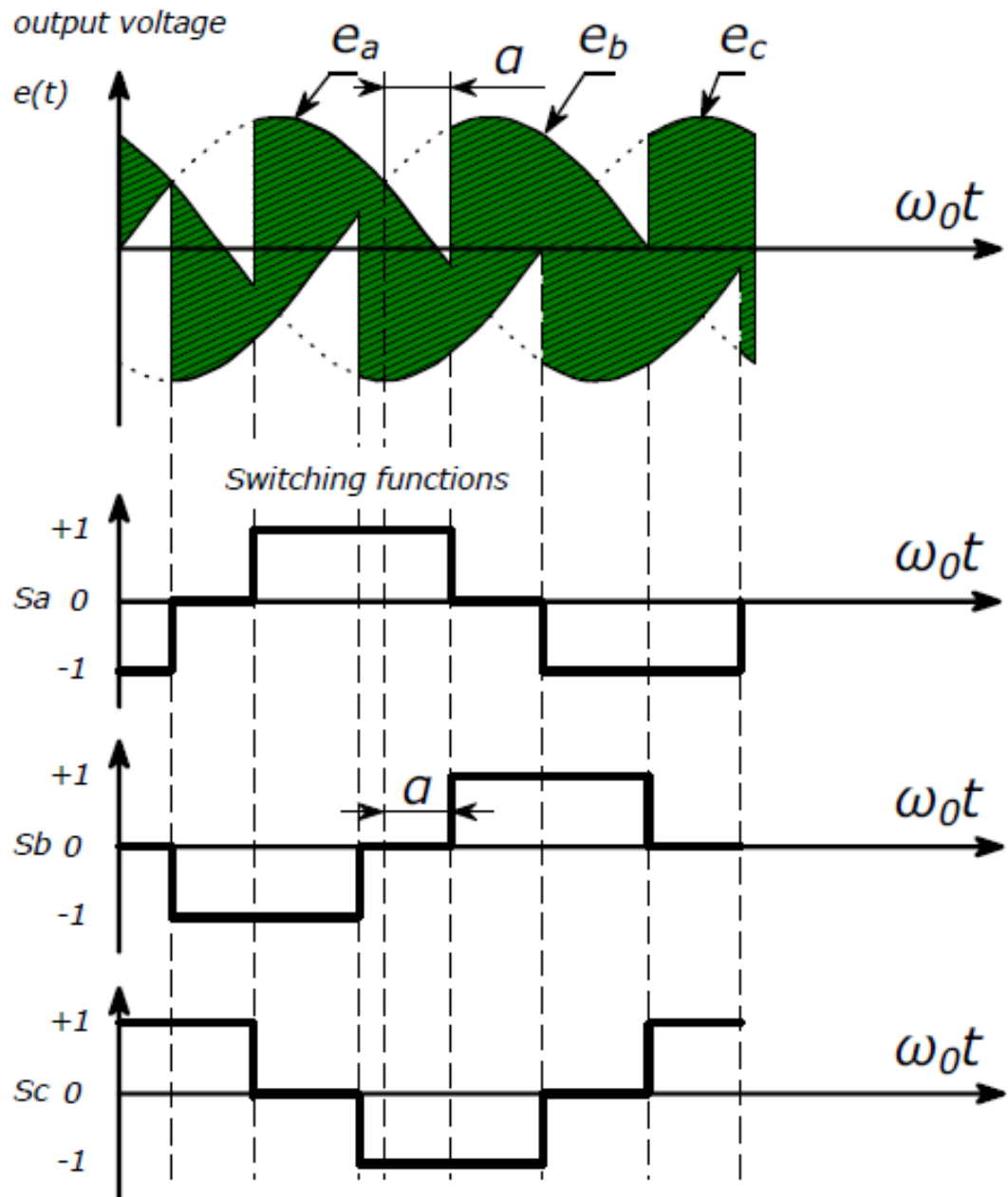
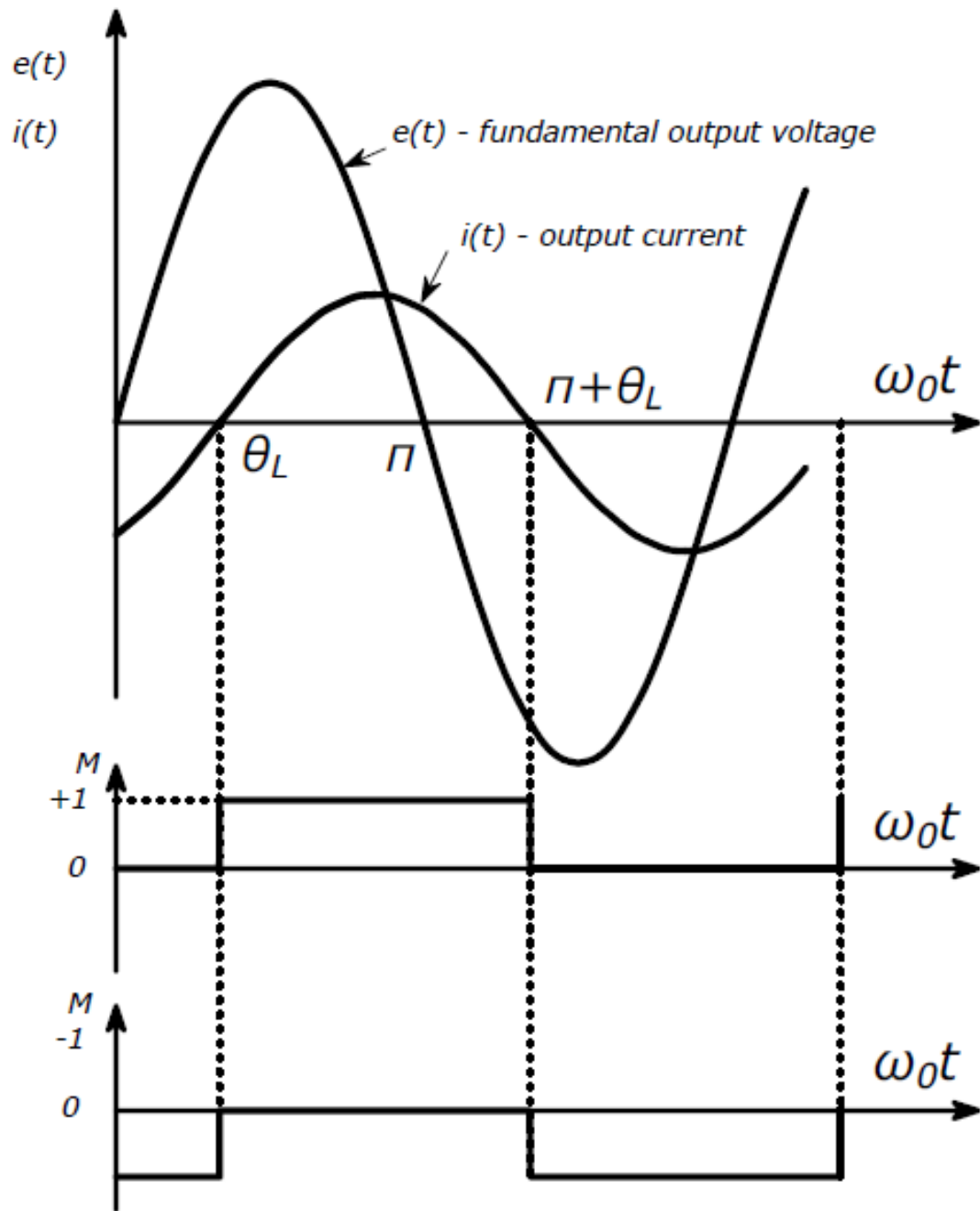


Figure 4-11 Output voltage and switching functions of cyclo-converter  
(Miyairi, 1979)



**Figure 4-12 Fundamental component of output voltage, output current and mode functions (Miyairi, 1979)**

The fundamental output voltage can be expressed as

$$e_{L,f} = E_0 \sin \omega_0 t \quad (4-5)$$

where:-

- $\omega_0$  is equal to  $2\pi f_0$

The mode functions and the firing angles are given by

$$\begin{aligned} M(\omega_0 t) &= 1, & M'(\omega_0 t) &= 0 \\ \alpha(\omega_0 t) &= \cos^{-1}(r \sin \omega_0 t), & \text{when } i_L > 0 \end{aligned} \quad (4-6)$$

$$\begin{aligned} M(\omega_0 t) &= 0, & M'(\omega_0 t) &= -1 \\ \alpha'(\omega_0 t) &= \cos^{-1}(-r \sin \omega_0 t), & \text{when } i_L < 0 \end{aligned} \quad (4-7)$$

where:-

- $r$  is output voltage ratio and defined as the ratio of the amplitude of the output voltage to the maximum DC voltage  $r = E_0 / (3\sqrt{3}E_m/\pi)$ .

The firing angle  $\alpha(\omega_0 t)$  and  $\alpha'(\omega_0 t)$  are periodic functions of period  $1/f_0$  and the switching functions are phase controlled waves as shown in Figure 4-11. The instantaneous output voltage of cyclo-converter is as follows:-

$$\begin{aligned} s_{Lo} = \frac{3\sqrt{3}}{\pi} E_m \left[ \left\{ \cos \alpha + \left( \frac{1}{5} \sin \alpha - \frac{1}{7} \sin 7\alpha \right) \sin 6\omega t \right\} M(\omega_0 t) + \right. \\ \left. \left\{ \cos \alpha' + \left( \frac{1}{5} \sin 5\alpha' - \frac{1}{7} \sin 7\alpha' \right) \sin 6\omega t \right\} M'(\omega_0 t) + \right. \\ \left. \left\{ \left( \frac{1}{5} \cos 5\alpha - \frac{1}{7} \cos 7\alpha \right) \cos 6\omega t + \dots \right\} M(\omega_0 t) + \right. \\ \left. \left\{ \left( \frac{1}{5} \cos 5\alpha' - \frac{1}{7} \cos 7\alpha' \right) \cos 6\omega t + \dots \right\} M'(\omega_0 t) \right] \end{aligned} \quad (4-8)$$

First consider the  $6f \pm nf_0$  harmonic family. The instantaneous voltage of this harmonic family is:

$$s_{Lo}^{6f} = \frac{3\sqrt{3}}{\pi} E_m \{ A(\omega_0 t) \sin 6\omega t + B(\omega_0 t) \cos 6\omega t \} \quad (4-9)$$

$$\begin{aligned} A(\omega_0 t) = \left\{ \frac{1}{5} \sin 5\alpha(\omega_0 t) - \frac{1}{7} \sin 7\alpha(\omega_0 t) \right\} M(\omega_0 t) + \left\{ \frac{1}{5} \sin 5\alpha'(\omega_0 t) - \right. \\ \left. \frac{1}{7} \sin 7\alpha'(\omega_0 t) \right\} M'(\omega_0 t) \end{aligned} \quad (4-10)$$

$$\begin{aligned} B(\omega_0 t) = \left\{ \frac{1}{5} \cos 5\alpha(\omega_0 t) - \frac{1}{7} \cos 7\alpha(\omega_0 t) \right\} M(\omega_0 t) + \left\{ \frac{1}{5} \cos 5\alpha'(\omega_0 t) - \right. \\ \left. \frac{1}{7} \cos 7\alpha'(\omega_0 t) \right\} M'(\omega_0 t) \end{aligned} \quad (4-11)$$

By Fourier analysis equations (4-9) and (4-10) are:-

$$A(\omega_0 t) = A_{s1} \sin \omega_0 t + A_{c1} \cos \omega_0 t + A_{s3} \sin 3\omega_0 t + A_{c3} \cos 3\omega_0 t + \dots \quad (4-12)$$

$$B(\omega_0 t) = B_{s1} \sin \omega_0 t + B_{c1} \cos \omega_0 t + B_{s3} \sin 3\omega_0 t + B_{c3} \cos 3\omega_0 t + \dots \quad (4-13)$$

where:-

$$- A_{sn} = \frac{1}{\pi} \int_0^{2\pi} A(\omega_0 t) \sin n\omega_0 t d(\omega_0 t)$$

$$- A_{cn} = \frac{1}{\pi} \int_0^{2\pi} A(\omega_0 t) \cos n\omega_0 t d(\omega_0 t)$$

$$- B_{sn} = \frac{1}{\pi} \int_0^{2\pi} B(\omega_0 t) \sin n\omega_0 t d(\omega_0 t)$$

$$- B_{cn} = \frac{1}{\pi} \int_0^{2\pi} B(\omega_0 t) \cos n\omega_0 t d(\omega_0 t)$$

$$- n = 1, 3, 5 \dots$$

Substituting (4-10) and (4-11) into (4-9) the following expression is obtained:-

$$\begin{aligned} e_{L\sigma}^{6f} = \frac{3\sqrt{3}}{\pi} E_m \left\{ \frac{1}{2} (A_{c1} - B_{s1}) \sin(6\omega - \omega_0)t + \frac{1}{2} (A_{s1} - B_{c1}) \cos(6\omega - \omega_0)t + \right. \\ \left. \frac{1}{2} (A_{c1} - B_{s1}) \sin(6\omega + \omega_0)t + \frac{1}{2} (B_{c1} - A_{s1}) \cos(6\omega + \omega_0)t + \dots \right\} \end{aligned} \quad (4-14)$$

The rms voltages of the  $6f - f_0$  and  $6f + f_0$  are as follows:-

$$H_{6f-f_0} = \frac{3\sqrt{3}}{\pi} \frac{E_m}{2} \sqrt{\frac{1}{2} \{ (A_{c1} - B_{s1})^2 + (B_{c1} + A_{s1})^2 \}} \quad (4-15)$$

$$H_{6f+f_0} = \frac{3\sqrt{3}}{\pi} \frac{E_m}{2} \sqrt{\frac{1}{2} \{ (A_{c1} + B_{s1})^2 + (B_{c1} - A_{s1})^2 \}} \quad (4-16)$$

The rms value of  $e_{L\sigma}^{6f}$  is as follows:-

$$H_{6f} = \sqrt{\sum_{n=1,3,5,\dots}^{\infty} \left( (H_{6f-nf_0})^2 + (H_{6f+nf_0})^2 \right)} \quad (4-17)$$

$$\begin{aligned} H_{6f} = \\ \frac{3\sqrt{3}}{\pi} \frac{E_m}{2} \sqrt{A_{s1}^2 + A_{c1}^2 + A_{s3}^2 + A_{c3}^2 + \dots + B_{s1}^2 + B_{c1}^2 + B_{s3}^2 + B_{c3}^2 + \dots} \end{aligned} \quad (4-18)$$

by definition of rms the following relationship is valid:-

$$\frac{1}{2\pi} \int_{\theta_L}^{2\pi+\theta_L} A^2(\omega_0 t) d(\omega_0 t) = \frac{1}{2} (A_{s1}^2 + A_{c1}^2 + A_{s3}^2 + A_{c3}^2 + \dots) \quad (4-19)$$

and

$$\frac{1}{2\pi} \int_{\theta_L}^{2\pi+\theta_L} B^2(\omega_0 t) d(\omega_0 t) = \frac{1}{2} (B_{s1}^2 + B_{c1}^2 + B_{s3}^2 + B_{c3}^2 + \dots) \quad (4-20)$$

Since there is a following relationship between  $M$  and  $M'$ , then from (4-10) and (4-11) the following is obtained:-

$$M(\omega_0 t) M'(\omega_0 t) = 0 \quad (4-21)$$

$$A^2(\omega_0 t) + B^2(\omega_0 t) = \left\{ \frac{1}{s^2} + \frac{1}{r^2} - \frac{2}{s \cdot r} \cos 2\alpha(\omega_0 t) \right\} M^2(\omega_0 t) + \left\{ \frac{1}{s^2} + \frac{1}{r^2} - \frac{2}{s \cdot r} \cos 2\alpha'(\omega_0 t) \right\} M'^2(\omega_0 t) \quad (4-22)$$

Combining (4-19), (4-20) and (4-22), the following is obtained:-

$$\begin{aligned} \frac{1}{2\pi} \int_{\theta_L}^{2\pi+\theta_L} \{A^2(\omega_0 t) + B^2(\omega_0 t)\} d(\omega_0 t) = \\ \frac{1}{2\pi} \int_{\theta_L}^{2\pi+\theta_L} \left( \frac{1}{s^2} + \frac{1}{r^2} - \frac{2}{s \cdot r} \cos 2\alpha \right) d(\omega_0 t) + \\ \frac{1}{2\pi} \int_{\theta_L}^{2\pi+\theta_L} \left( \frac{1}{s^2} + \frac{1}{r^2} - \frac{2}{s \cdot r} \cos 2\alpha' \right) d(\omega_0 t) \end{aligned} \quad (4-23)$$

Here from (4-6) and (4-7)

$$\cos 2\alpha(\omega_0 t) = \cos 2\alpha'(\omega_0 t) = 2r^2 \sin^2(\omega_0 t) - 1 \quad (4-24)$$

then

$$\frac{1}{2\pi} \int_{\theta_L}^{2\pi+\theta_L} \cos 2\alpha d(\omega_0 t) = r^2 - 1 \quad (4-25)$$

therefore (4-23) becomes

$$\frac{1}{2\pi} \int_{\theta_L}^{2\pi+\theta_L} \{A^2(\omega_0 t) + B^2(\omega_0 t)\} d(\omega_0 t) = \frac{1}{s^2} + \frac{1}{r^2} - \frac{2}{s \cdot r} (r^2 - 1) \quad (4-26)$$

From (4-19), (4-20) and (4-26)

$$\frac{1}{2}(A_{s1}^2 + A_{c1}^2 + A_{s3}^2 + A_{c3}^2 + \dots B_{s1}^2 + B_{c1}^2 + B_{s3}^2 + B_{c3}^2 + \dots) = \frac{1}{2} + \frac{1}{r^2} - \frac{2}{2 \cdot r}(r^2 - 1) \quad (4-27)$$

Combining (4-18) and (4-27) gives

$$H_{6f} = \frac{3\sqrt{3}}{\pi} E_m \sqrt{\frac{1}{2} \left\{ \frac{1}{2} + \frac{1}{r^2} - \frac{2}{2 \cdot r}(r^2 - 1) \right\}} \quad (4-28)$$

and generally

$$H_{6f} = \frac{3\sqrt{3}}{\pi} E_m \sqrt{\frac{1}{2} \left\{ \frac{1}{(6m-1)^2} + \frac{1}{(6m+1)^2} - \frac{2(r^2-1)}{(6m-1) \cdot (6m+1)} \right\}} \quad (4-29)$$

from (4-8), the rms voltage of the fundamental output component is

$$H_{f0} = \frac{3\sqrt{3}}{\pi} E_m \sqrt{\frac{1}{2\pi} \int_{\theta_L}^{2\pi+\theta_L} (M \cos \alpha + M' \cos \alpha')^2 d(\omega_0 t)} \quad (4-30)$$

$$H_{f0} = \frac{3\sqrt{3}}{\pi} E_m \frac{r}{\sqrt{2}} \quad (4-31)$$

Load side voltage harmonics are reflected on the line side in current waveform as a series of sidebands added to each characteristic harmonic, as expressed in (4-3).

## 4.4 Practical Issues with System Harmonics – Harmonic Measurements

### 4.4.1 Introduction

This section describes the results of harmonic measurements on a mineral gold processing plant, following a major mine upgrade. An extract from a detailed report describing the harmonic measurement project is given in Appendix 3. This section describes the methodology used for the harmonic measurements and discusses typical harmonic system signatures.

(Institute of Electrical and Electronics Engineers, Inc., 1992) recommends that harmonic measurements are performed following system changes or as a part of original design. Harmonic measurements and measurement technique used in a typical industrial power system supplied from the power grid are presented by (Andrews, 1996) and (Sutherland, 1995). The gold processing plant power system is



an isolated system with unique operating regimes and this required development of harmonic measurement methodology suitable for such an isolated system. Characteristic harmonics and impact of cyclo-converter harmonics on a large power system are presented by (Chu, 1989) and (Hill, 1991). The non-fundamental frequency components include higher order harmonics, inter-harmonics and sub-harmonics. Negative effect of the harmonics is additional thermal overheating which may cause accelerated ageing of equipment insulation leading to insulation breakdowns, as pointed out by (Arrilag, et al., 2007), (Institute of Electrical and Electronics Engineers, Inc., 1992) and (Institute of Electrical and Electronics Engineers, Inc., 1995).

The overall scope of the harmonic measurement project comprised the following:-

1. Selection of instruments with the analysis software suitable for capturing three-phase voltage and current waveforms, harmonic spectrum and transient events triggered by major system disturbances;
2. Develop methodology and prepare a detailed test plan for measuring system harmonics at the 33 kV level for various system configurations
3. Harmonic measurements and harmonic analysis for various system configurations such as: SAG mill normal running, creeping and inching modes; (See Appendix 3)
4. Discussion of the results and acceptance criteria, with recommendations for further work on the plant. (See Appendix 3)

#### **4.4.2 Methodology**

The instrument type used for this project was the Dranetz-BMI Power Quality Analyser, Type PX5 PowerXplorer, shown in Figure 4-13. The instrument comprises 4 differential voltage inputs 1-600 Vrms, AC/DC with a 16 bit analogue to digital (A/D) converter. The sampling rate is 256 samples/cycle. Also, each instrument comprises 4 current inputs with optional current probes. The selection was Model TR-2510A 0.1-10A with 16 bit analogue to digital conversion and the sampling rate of 256 samples/cycle as quoted in PowerXplorer™ PX5 USER'S GUIDE DRANETZ-BMI.



**Figure 4-13: Front view of Dranetz PowerXplorer PX5**

The original intention was to carry out the measurements over a period of 1 week by connecting a total of 5-7 instruments. However, such a large number of instruments was not readily available and for this reason, a reduced number of instruments was used over a longer period. Analysis of raw data was carried out using a specialised software package, Dran-View, proprietary software supplied with the instrument for raw data analysis.

The voltage waveforms were measured on the secondary side of the 33 kV bus-bar voltage transformers. The voltage transformers consist of the three single-phase units connected in a 3- phase assembly having voltage ratio  $33000/\sqrt{3}$  to  $110/\sqrt{3}$  per phase. Voltage was measured on both the 33 kV treatment plant and main power station switchboards. Current waveforms were captured on various feeders on the 33 kV switchboard. The current was measured by means of current clamping probes clamped around the CT secondary wires, with one probe per phase. Location of the current measuring points at 33 kV Treatment Plant Switchboard were at each Incomer, Ball Mill Feeders, SAG Mill feeder and the 3<sup>rd</sup>, 4<sup>th</sup>, 5<sup>th</sup>, and 7<sup>th</sup> Harmonic Filter Feeders. The measuring points at 33 kV Power Station Main Switchboard were on each treatment plant feeder, generator incomer, and inter-connector feeder.

Data recorded on a memory card were downloaded onto a hard disk drive on a laptop on a daily basis. A detailed test plan was developed for each switchboard and the connection points were regularly moved around in accordance with the test plan. An extract from the test plan is given in Figure 4-14 for measurements at power station 33 kV switchboard and in Figure 4-15 for measurements at concentrator plant 33 kV switchboard.

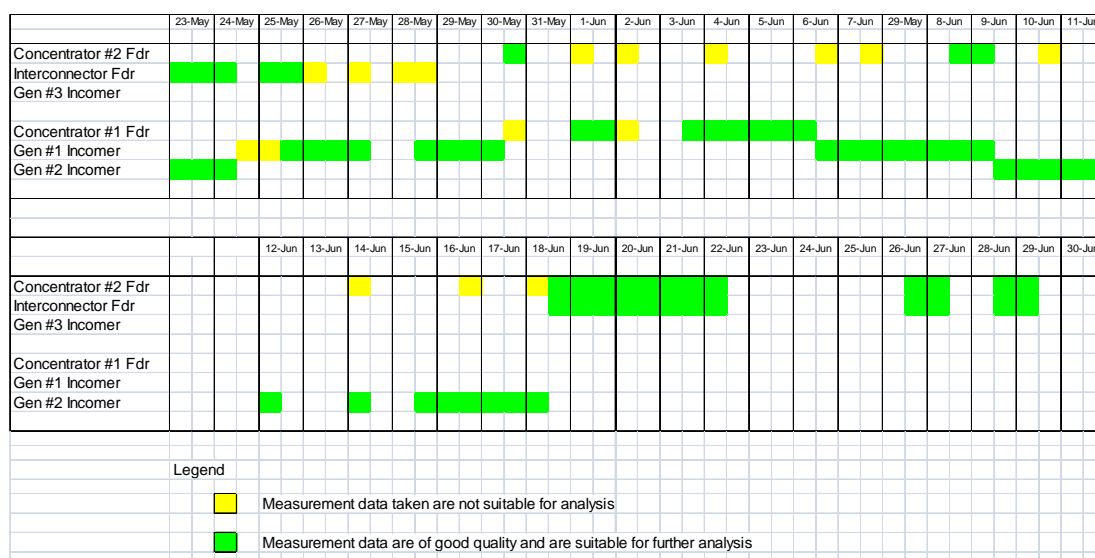


**Figure 4-14 Test plan for measurements at power station 33 kV switchboard**

The acceptance criteria for the power system harmonics were based on the acceptance criteria proposed in (Institute of Electrical and Electronics Engineers, Inc., 1992). The IEEE standard provides limits for both current and voltage harmonics. The philosophy applied for the development of current harmonic limits was based on the harmonic injection limits from individual customers so that they would not cause unacceptable voltage distortion levels for normal system characteristics.

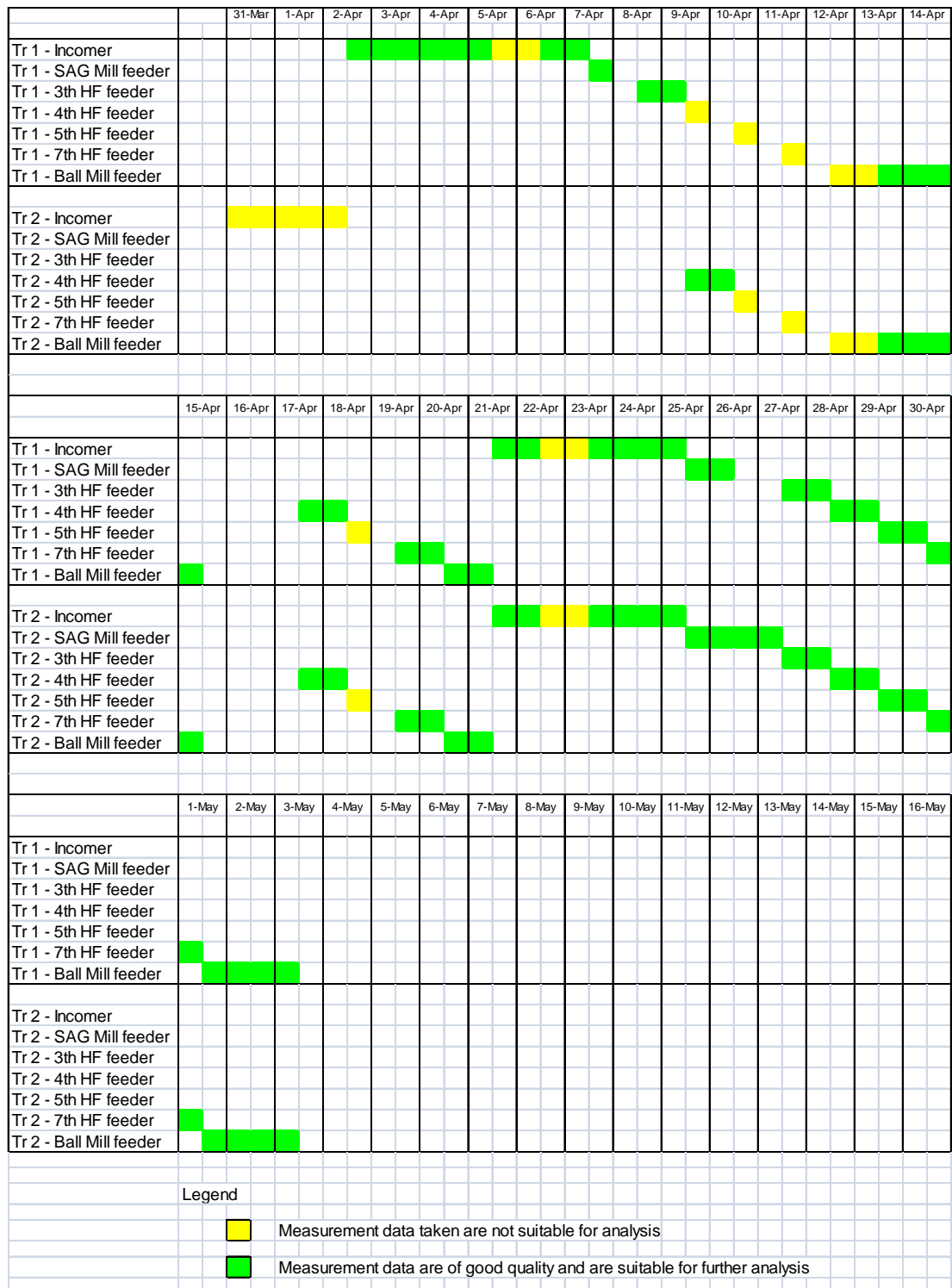


**Figure 4-15 Test plan for measurements at concentrator 33 kV switchboard**

The harmonic voltage distortion on the 33 kV level is a function of the total injected harmonic current and the system impedance at each of the harmonic frequencies. The total injected harmonic current will depend on the number of individual loads, which inject harmonic currents and also on the size of each load.

Individual Harmonic Order	Maximum Harmonic Current Distortion [in % of IL]
3, 5, 7, 9	4.0
11, 13, 15	2.0
17, 19, 21	1.5
23, 25	0.6

**Table 4-1 Current distortion limits – odd harmonics**

Individual Harmonic Order	Maximum Harmonic Current Distortion [in % of IL]
3, 5, 7, 9	4.0
11, 13, 15	2.0
17, 19, 21	1.5
23, 25	0.6

**Table 4-2 Current distortion limits – even harmonics**

The objectives of the current limits are to limit the maximum individual frequency voltage harmonic to 3% of the fundamental and the voltage THD<sub>v</sub> to 5%. Table 4-1 and Table 4-2 summarise the current distortion limits at 33 kV level.

#### **4.4.3 Discussion on Harmonic Measurement Analysis**

Harmonic measurements confirm that cyclo-converters are generators of current harmonics. A typical current waveform, captured during normal operating mode is shown in Figure 4-16. The red phase current waveform is highlighted with a thicker line. If we join the top and bottom peaks of the waveform than we can see that they oscillate with a frequency that is lower than the fundamental frequency. This shows the presence of sub-harmonics in the supply circuit.

## Event Details/Waveforms

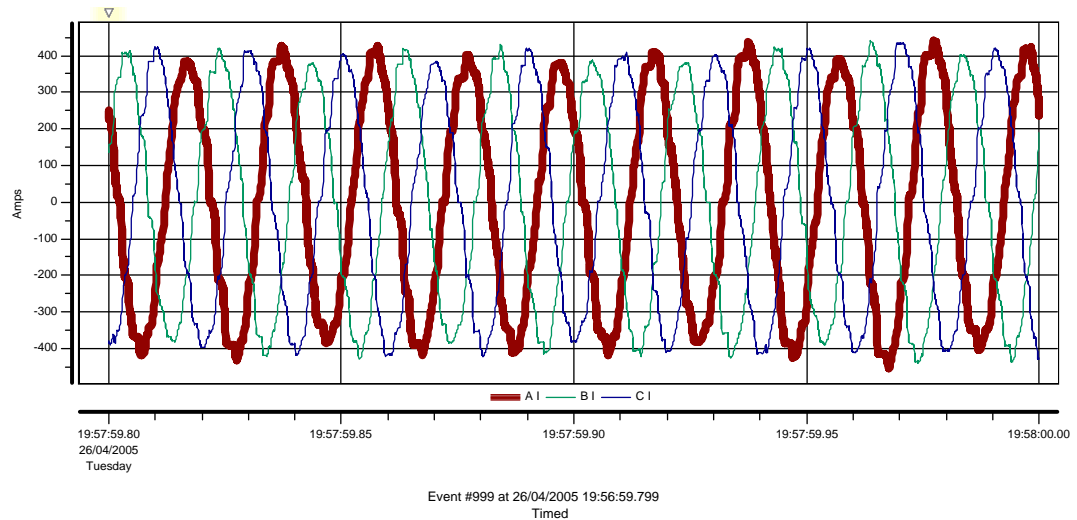


**Figure 4-16 Current waveforms on the supply side of SAG mill cyclo-converter**

The Dran-view software can calculate the full spectra of individual harmonics and inter-harmonics. Figure 4-17 shows full spectra for up to the 50<sup>th</sup> harmonic. The full spectra can be normalised to a full cycle average value and the harmonic spectra for this case are shown in Figure 4-18. The full cycle average value spectra can be used when analysing system harmonics using ETAP software. ETAP cannot accept non-integer values for harmonic sources. Tabulated values of current harmonics can be entered as harmonic source. A list of current harmonic values for the waveform in Figure 4-16 and harmonic spectrum in Figure 4-18 is given in Table 4-3. Figure 4-17 shows that there are a number of inter-harmonics in the current spectra and for this reason the use of single tuned filter should be avoided.

## Waveform harmonics

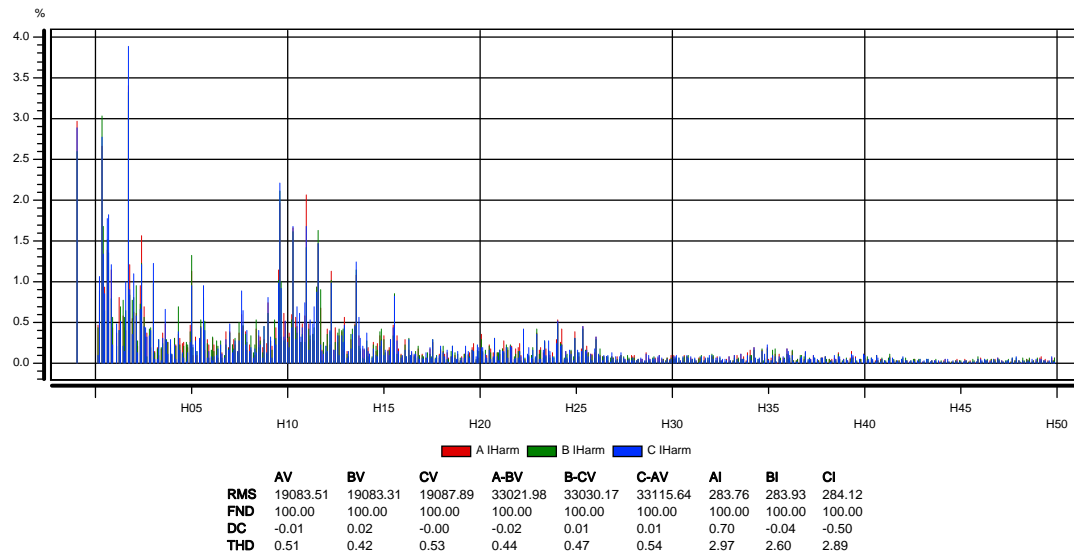


Figure 4-17 Full current harmonic spectra of SAG mill cyclo-converter

## Waveform harmonics

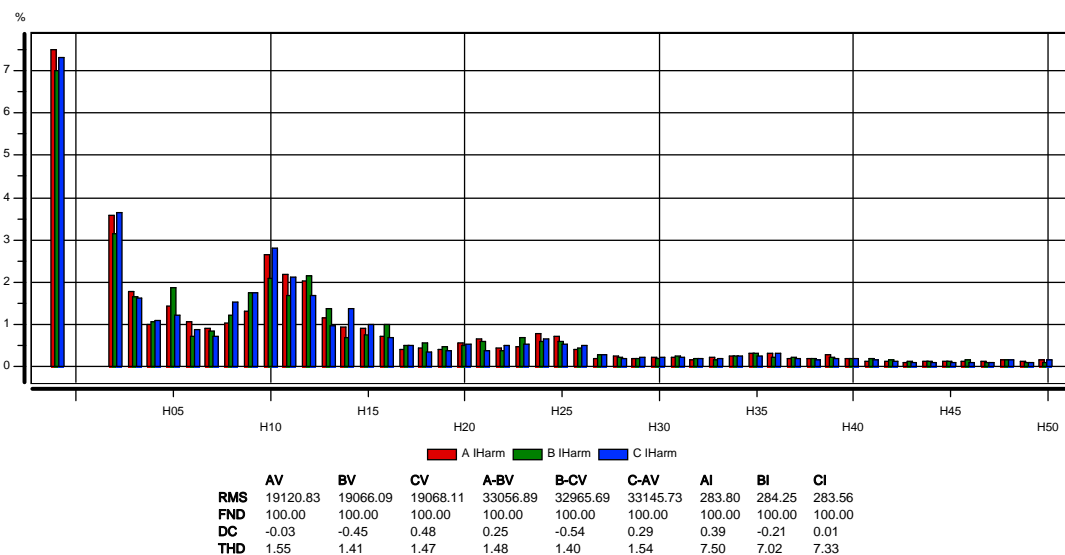


Figure 4-18 Average of one cycle current harmonic spectra of SAG mill cyclo-converter (suitable for ETAP)

Frequency	AIHarmValue[%]	BIHarmValue[%]	CIHarmValue[%]
100	3.585	3.134	3.641
150	1.772	1.655	1.627
200	0.987	1.051	1.086

<b>Frequency</b>	<b>AIHarmValue[%]</b>	<b>BIHarmValue[%]</b>	<b>CIHarmValue[%]</b>
250	1.445	1.853	1.228
300	1.073	0.730	0.869
350	0.901	0.836	0.704
400	1.020	1.218	1.536
450	1.318	1.735	1.740
500	2.655	2.089	2.801
550	2.183	1.691	2.116
600	2.020	2.134	1.676
650	1.154	1.359	0.962
700	0.927	0.694	1.360
750	0.896	0.733	0.997
800	0.716	1.004	0.689
850	0.397	0.497	0.492
900	0.432	0.570	0.330
950	0.394	0.456	0.370
1000	0.553	0.498	0.527
1050	0.642	0.591	0.365
1100	0.426	0.379	0.486
1150	0.476	0.680	0.533
1200	0.781	0.578	0.660



<b>Frequency</b>	<b>AIHarmValue[%]</b>	<b>BIHarmValue[%]</b>	<b>CIHarmValue[%]</b>
1250	0.726	0.596	0.522
1300	0.413	0.433	0.505
1350	0.195	0.287	0.264
1400	0.245	0.204	0.190
1450	0.171	0.173	0.226
1500	0.206	0.172	0.212
1550	0.225	0.259	0.216
1600	0.153	0.194	0.193
1650	0.206	0.155	0.190
1700	0.262	0.260	0.260
1750	0.318	0.307	0.259
1800	0.305	0.209	0.303
1850	0.196	0.206	0.200
1900	0.193	0.192	0.163
1950	0.265	0.208	0.193
2000	0.192	0.185	0.198
2050	0.110	0.190	0.150
2100	0.118	0.147	0.119
2150	0.107	0.115	0.094
2200	0.112	0.122	0.080

Frequency	AIHarmValue[%]	BIHarmValue[%]	CIHarmValue[%]
2250	0.110	0.122	0.094
2300	0.136	0.165	0.104
2350	0.113	0.089	0.088
2400	0.141	0.145	0.151
2450	0.132	0.105	0.097
2500	0.143	0.103	0.140

**Table 4-3 Current harmonics on the SAG mill feeder**

The existing system utilises the high pass 5<sup>th</sup> and 7<sup>th</sup> harmonic filters. Figure 4-19 shows current waveform spectra on the feeder supplying the 7<sup>th</sup> harmonic filter. We can see that majority of the current filtered with this filter are around the 11<sup>th</sup> and 13<sup>th</sup> harmonic.

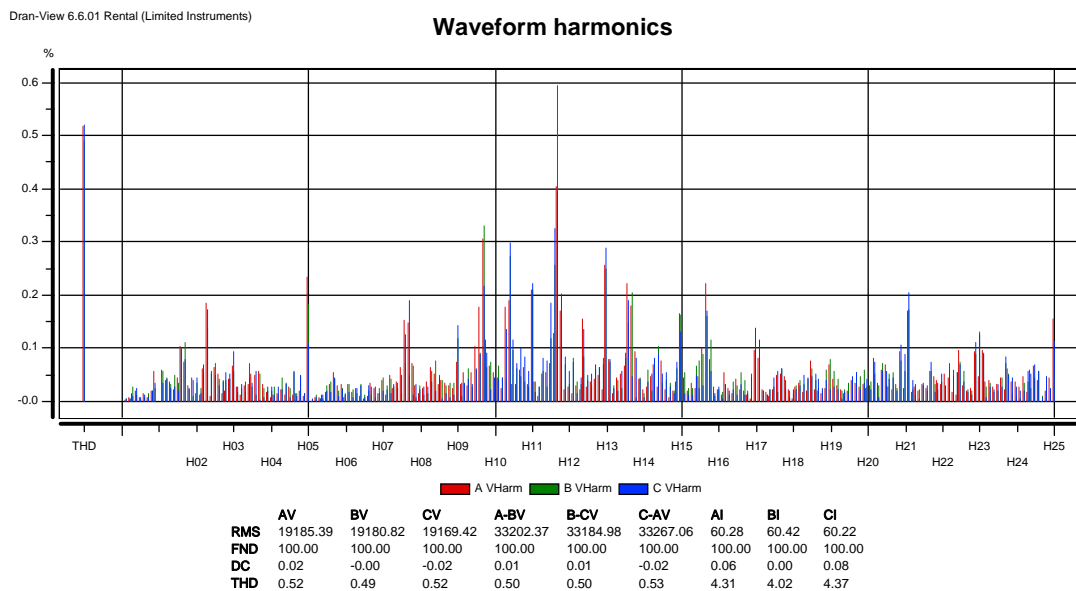


**Figure 4-19 Full current harmonic spectra of the 7<sup>th</sup> harmonic filter**

Figure 4-20 shows full harmonic spectra of the 5<sup>th</sup> harmonic filter. It can be seen that the 5<sup>th</sup> harmonic filter absorbs the fifth harmonic currents generated by the cyclo-converter.

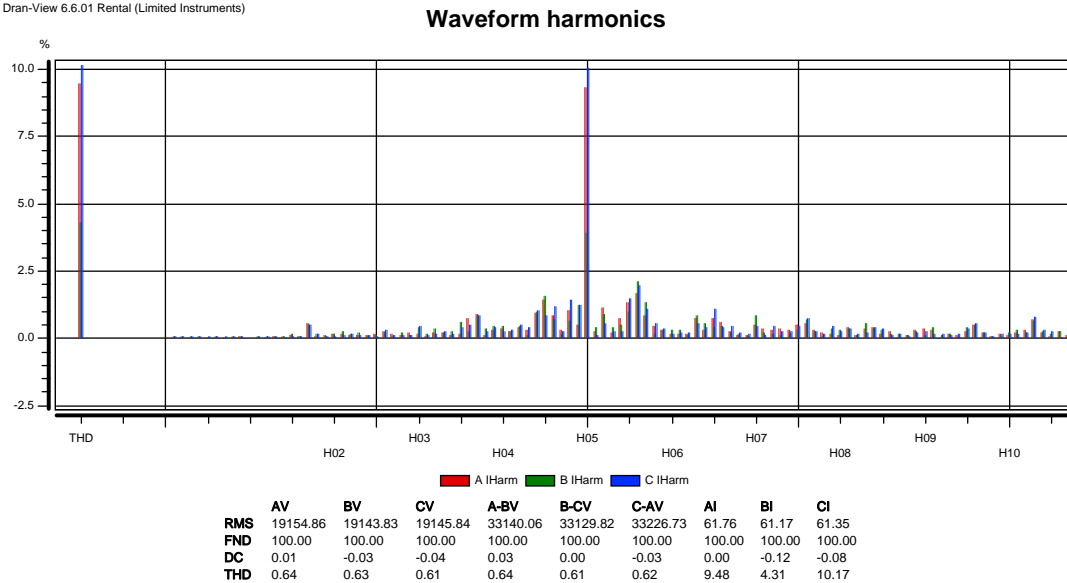


**Figure 4-20 Full current harmonic spectra of the 5<sup>th</sup> harmonic filter**

It can be concluded that both filters perform in compliance with specifications during normal mode of operation.

## 4.5 Practical Issues with System Transients

### 4.5.1 Introduction

This section describes system transients captured on a mineral gold processing plant during harmonic measurements. An extract from the report analysing the system transients is given in Appendix 4. This section describes methodology used for capturing switching transients and discusses typical system transient signatures.

Reference (Institute of Electrical and Electronics Engineers, Inc., 1995) IEEE Std 1159-1995(R2001) IEEE Recommended Practice for Monitoring Electric Power Quality, gives the definition of system transients and system signatures. The standard provides a comprehensive list of all transient types that are normally encountered in an electrical power system; refer to Table 4-4 for list of system disturbances covered in IEEE Std 1159-1995(R2001). The overall scope of the switching transient project comprised capturing voltage and current waveforms at 33 kV level for various system configurations. A brief project scope is listed as follows:-

1. Selection of instruments suitable for measuring three-phase voltage and current transient events triggered by major system disturbances, the same instrument was to be used for harmonic measurements;
2. Selection of a suitable software package compatible with the measuring instrument for further data analysis;
3. Preparation of a detailed test plan for capturing voltage and current transients at the 33 kV system level.

The switching transient project was an integral part of the harmonic measurements described in the previous section and Appendix 3.

Categories	Typical spectral content	Typical duration	Typical voltage magnitude
1.0 Transients			
1.1 Impulsive			
1.1.1 Nanosecond	5 ns rise	< 50 ns	
1.1.2. Microsecond	1 $\mu$ s rise	50 ns-1 ms	
1.1.3 Millisecond	0.1 ms rise	>1 ms	
1.2 Oscillatory			
1.2.1. Low frequency	< 5 kHz	0.3-50 ms	0-4 pu
1.2.2 Medium frequency	5-500 kHz	20 $\mu$ s	0-8 pu
1.2.3 High frequency	0.5-5 MHz	5 $\mu$ s	0-4 pu
2.0 Short duration variations			
2.1 Instantaneous			
2.1.1 Sag		0.5-30 cycles	0.1-0.9 pu
2.1.2 Swell		0.5-30 cycles	1.1-1.8 pu
2.2 Momentary			
2.2.1 Interruption		0.5 cycles- 3 s	< 0.1 pu
2.2.2 Sag		30 cycles-3 s	0.1-0.9 pu
2.2.3 Swell		30 cycles-3 s	1.1-1.4 pu
2.3 Temporary			
2.3.1 Interruption		3 s-1 min	< 0.1 pu
2.3.2 Sag		3 s-1 min	0.1-0.9 pu
2.3.3. Swell		3 s-1 min	1.1-1.2 pu
3.0 Long duration variations			
3.1 Interruption, sustained		> 1 min	0.0 pu
3.2 Undervoltages		> 1 min	0.8-0.9 pu
3.3 Overvoltages		> 1 min	1.1-1.2 pu
4.0 Voltage Imbalance		steady state	0.5-2%
5.0 Waveform distortion			
5.1 DC offset		steady state	0-0.1%
5.2 Harmonics	0-100 <sup>th</sup> H	steady state	0-20%
5.3 Interharmonics	0-6 kHz	steady state	0-2%
5.4 Notching		steady state	
5.5 Noise	broad-band	steady state	0-1%
6.0 Voltage fluctuations	< 25 Hz	intermittent	0.1-7%
7.0 Power frequency variations		< 10 s	

**Table 4-4      Table 2 of IEEE Std 1159-1995(R2000)**

### 4.5.2 Methodology

System configuration and methodology applied for harmonic measurements are described in previous Section 4.4 of this thesis. The transient analysis was based on the same methodology with regard to instrument selection and voltage and current measuring points. The instrument type selected for capturing the system transients was the Dranetz-BMI Power Quality Analyser, Type PX5 PowerXplorer, refer to Figure 4-13 showing front view of the measuring instrument.

PX5 is designed to meet both the IEEE 1159 and IEC 61000-4-30 Class A standards for accuracy and measurement requirements. For example, it can do PQ-optimized acquisition of power quality related disturbances and events. It is designed with a statistical package called Quality of Supply (QOS), with protocols set to determine voltage measurement compliance required for EN50160 monitoring. European standard EN50160 requires that measurement parameters must be within a specified percentage for 95% of the time.

The firmware for the PX5 is contained on internal FLASH memory. It has an operating system capable of performing multiple applications. The PX5 firmware can monitor power quality phenomena and record inrush conditions, carry out long-term statistical studies to establish performance baselines, and perform field-based equipment testing and evaluation for commissioning and maintenance. The firmware integrates an intuitive instrument setup procedure to ensure the capture of all relevant data for additional post process analysis, report writing, and data archiving using other compatible Dranetz-BMI software applications such as DranView®.

The firmware used for the harmonic disturbance monitoring was Ver. V1.8, Build: 0, DB ver.: 0. Dranetz-BMI instruments label rms voltage or current variations as either 'sags' (voltage or current decreases below low limit) or 'swells' (voltage or current increases above high limit) as per IEEE 1159. The voltage disturbances, which are shorter in duration than typical sags and swells, are classified as transients. Two basic types of transients are of special interest:

- impulsive transients characterized by very rapid changes in the magnitude of measured quantities and commonly caused by

capacitors or inductors switching on line, loose wires, lightning, static, and power failures; and

- oscillatory transients defined as a temporary, rapid discontinuity of the waveform. PX5 has extensive recording capabilities for low and medium frequency transients using the following trigger mechanisms:
  - The rms difference cycle-to-cycle
  - Crest or Absolute peak (Instantaneous)
  - Waveshape cycle-to-cycle magnitude/duration variation

Oscillatory transients are types of disturbances usually captured as waveshape faults. PX5 captures pre-trigger and post-trigger waveform cycles. Once a record trigger is detected, instantaneous waveform information is recorded for the prescribed voltage and current channel(s). Disturbance monitoring requires that voltage be continuously sampled and recorded only if the signals exceed specified values. Waveshape changes are only triggerable for voltage transients as the current waveshapes are usually continually changing on a normally operating distribution system. The current is recorded as well to help determine the source of the disturbance.

PX5 is designed with the high speed sampling analogue board that can capture voltage and current transients. High frequency detected transients use special circuitry to detect and capture transients as small as 1 microsecond in duration. These transients can be positive and/or negative values above or below the low frequency waveshape. As these types of disturbances usually exhibit very narrow widths and fast rise and fall times, they are quickly damped by the system.

Switching transient analysis was carried out by means of the DRAN-VIEW software package. DRAN-VIEW is a tool for viewing data on a PC from the Dranetz-BMI analysers such as PowerExplorer PX5. DRAN-VIEW is a Windows compatible program that is used to access and retrieve data from data files stored on disk medium.

### 4.5.3 Discussion on Switching Transient Analysis

Appendix 4 contains a detail description and analysis of the transients captured during harmonic measurements. Analysis showed that starting and stopping of SAG mill drives introduces two types of system transients: the inrush current caused by energising cyclo-converter transformers and voltage transients caused by back-to-back switching of filter capacitor banks.

The sequence of events, leading to switching operations followed by voltage and current waveforms for these two events, is described in detail in Appendix 4. Expanded voltage and current waveforms captured at the time of energising cyclo-converter transformers are shown in Figures 4-21 and 4-22.

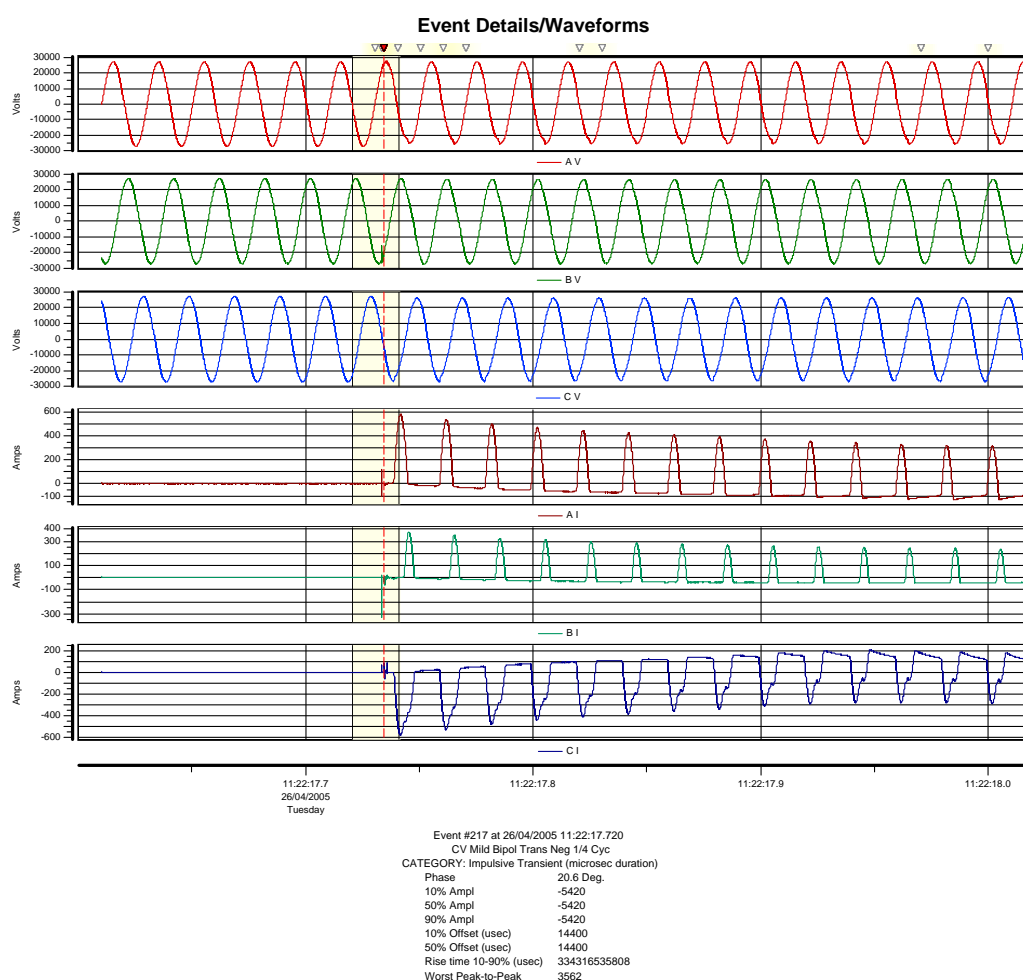


**Figure 4-21 Voltage and current waveforms at time of energising cyclo-converter transformers**



The cyclo-converter circuit comprises a total of three transformers, and at the moment of switching of the circuit breaker, all three transformers are energised at the same time. The signatures show that the inrush current waveform reflects the typical inrush current for a single transformer.

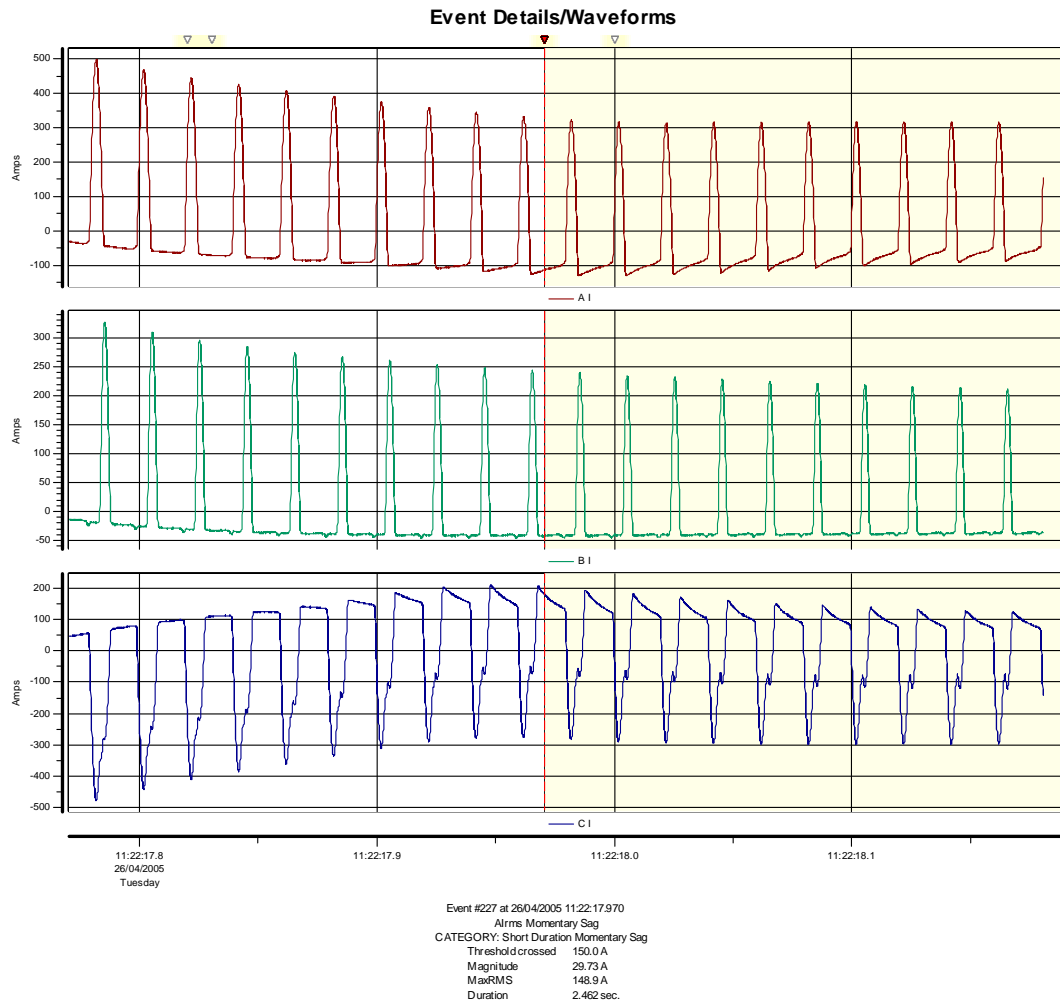


**Figure 4-22 Subsequent cycles of transformer inrush current**

Figure 4-23 shows a voltage waveform captured during back to back switching of the 5<sup>th</sup> harmonic filter. A detailed description of the event is explained in Appendix 4. The back to back switching of capacitor banks will generate voltage transients on the 33 kV network. Capacitor switching and energising of the cyclo-converter transformers have to be limited to a minimum to prevent premature deterioration of equipment insulation.

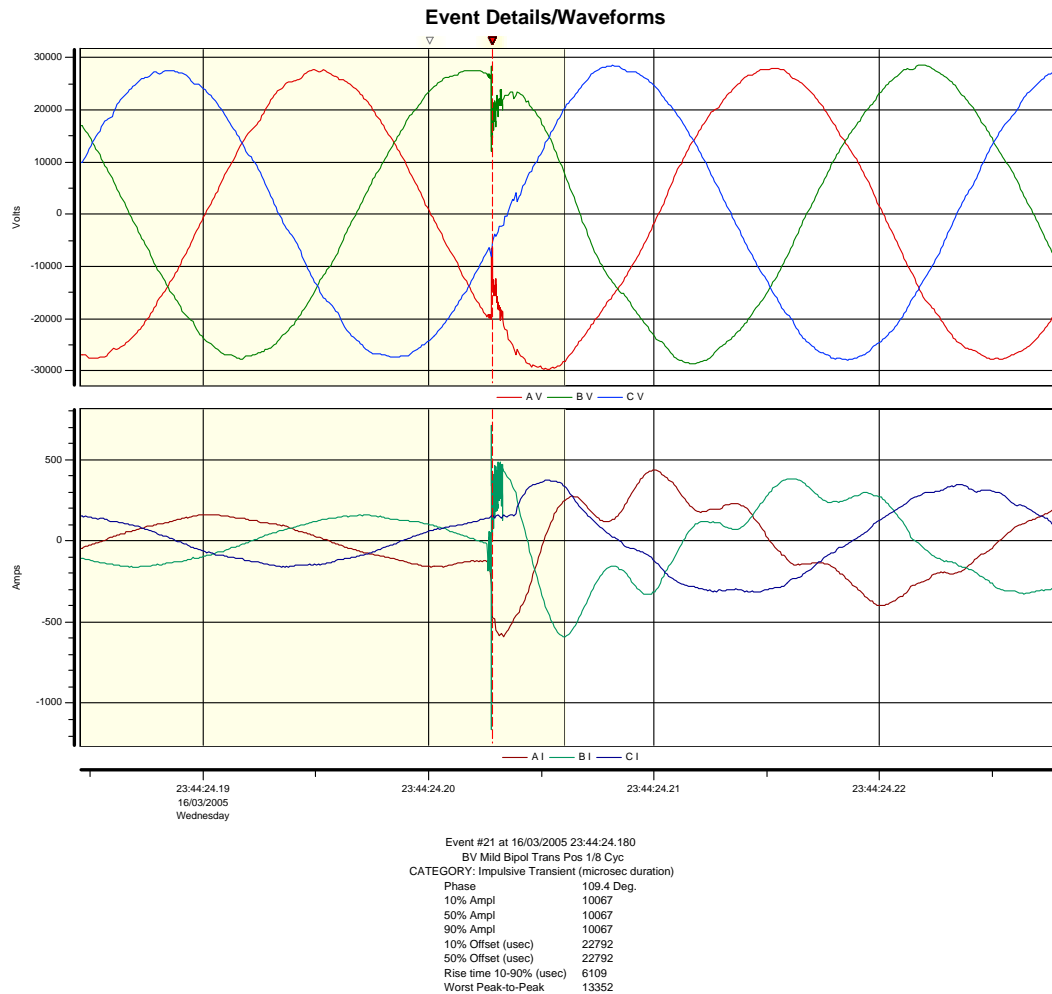


**Figure 4-23 Back-to-back capacitor switching**

#### 4.6 Original Contribution

The following is a summary of original contribution towards the subject matter in this Chapter:-

1. Described a typical mineral processing power system, comprising various load centres and identified loads that are sources of current harmonics.
2. Described modes of operation of SAG mills and provided technical background of SAG mill drives, and formulae for linking speed and diameter of the mill
3. Described a typical 6-pulse cyclo-converter and presented mathematical formulae for calculation of secondary side voltage harmonics as derived by (Miyairi, 1979)

4. Carried out a harmonics survey (measurements) on a large gold processing plant and evaluated suitability of harmonic filters. The plant comprised of two SAG mill cyclo-converters, sources of current harmonics
5. Carried out harmonic measurement analysis and provided harmonic spectrum at various points of the system.
6. Carried out analysis of switching transients on the system; identified over-voltages caused by capacitor bank switching
7. Provided directions on how to analyse the power system and when to carry out complete/overall harmonic analysis study
8. Suggested methodology on how to model in ETAP system harmonics generated by cyclo-converters.

## **5. ISOLATED POWER SYSTEM FOR AN LNG PLANT**

### **5.1 Introduction**

The LNG plant is a typical example of an industrial plant having power generation capacity ranging from a few hundred MW to up to a thousand MW. Typically, LNG plants are located in remote areas and are supplied from their own power station that is not interconnected to the public network. The power generation plants use plant produced natural gas to run gas fired turbines and generate electric energy. A typical LNG plant comprises a number of the production trains, each train ranging from 2 to 5 million tonnes per annum (Mtpa) in capacity.

In Western Australia, currently there is only one producing LNG plant and two additional plants under construction. The producing plant is the Karratha Gas Plant part of the North West Shelf venture. The development is owned by North West Shelf JV and operated by Woodside. The Woodside website <http://www.woodside.com.au> states that the Karratha Gas Plant has an annual LNG production capacity of 16.3 million tonnes and includes five LNG processing trains, four heavily insulated storage tanks each with a gross capacity of 65,000 m<sup>3</sup> and a dedicated LNG jetty with two loading berths. Trains 1, 2 and 3 each have an annual production capacity of 2.5 million tonnes while Trains 4 and 5 can produce up to 4.4 million tonnes. The Karratha Gas Plant is located in the North West Interconnected System (NWIS), however the plant power system is isolated and not interconnected to the NWIS. The plant operates its own power plant with a total installed power generation capacity of 240 MW (reference 2010 Electricity Generation Tables – Office of Energy).

The Pluto LNG plant which is currently under construction is 90% owned and operated by Woodside and is scheduled to come into production in 2011. The Woodside website <http://www.woodside.com.au> states that the initial phase of the Pluto LNG Project will comprise an off-shore platform in 85 m of water, connected to five subsea wells on the Pluto gas field. Onshore infrastructure is a single LNG processing train with a forecast production capacity of 4.3 Mtpa. The Pluto LNG plant is physically located in close proximity to the Karratha Gas Plant and the NWIS systems. The plant has its own power station and is isolated from the NWIS

and the Karratha Gas Plant. The total installed power generation capacity is 160 MW.

The Gorgon development is the second plant currently under construction and is the largest single resource natural gas project in Australia's history. The Gorgon Project is a joint venture of the Australian subsidiaries of Chevron (approximately 47%), ExxonMobil (25%), Shell (25%), Osaka Gas (1.25%), Tokyo Gas (1%) and Chubu Electric (0.41%). The Gorgon development is located on Barrow Island which is an A class nature reserve. The LNG plant will initially comprise 3 LNG trains, each capable of producing nominally 5 Mtpa of LNG, with the first gas expected for delivery in 2014. The LNG plant will operate its own gas fired power station comprising five 130 MW GE Frame-9 gas turbines ( <http://fossilfuel.energy-business-review.com> ). The total installed power generation capacity will be 650 MW. In addition, GE will supply equipment including three main refrigerant compression trains driven by six Frame-7 gas turbines.

The largest electrical loads on an LNG plant are gas refrigerant compressor helper motors. In the past those compressors would be fully gas turbine driven, however the recent trend is to incorporate a hybrid configuration including a helper motor. The next move within the industry is to replace gas compressors with all electric refrigeration gas compressors. The outcome is that the LNG plant power generation systems will need to be of even larger capacity.

## **5.2 Power system description**

### **5.2.1 Typical Single Line Diagram**

Only two companies in the world, Shell and Conoco Phillips Cascade, are licence holders for the technology needed to design an LNG plant. Operators and owners of LNG plants purchase a licence to design and build the plant, which is executed by expert engineering companies. In the past Shell licence has been used by the following engineering companies: MW Kellogs, Foster Wheeler, Technip, Snamprogetti and their joint venture partners. Bechtel Oil and Gas has used the technology offered by Conoco Phillips Cascade (Nahan, 2010).

(Martinez, 2005) presented a schematic diagram of the Conoco Phillips LNG production process. A copy of the schematic diagram as presented by (Martinez, 2005) is shown in Figure 5-1. The schematic shows three compressors used in the refrigerant cycle: propane, ethylene and methane compressors. The propane and ethylene compressors are coupled to the same shaft, while the propane refrigerant compressor is driven separately. Those compressors are gas turbine driven incorporating a helper motor of up to 25 MW to cover for site temperature variations. Refrigerant compressors comprising a helper motor and a variable speed drive are the largest electrical loads on the LNG plant.

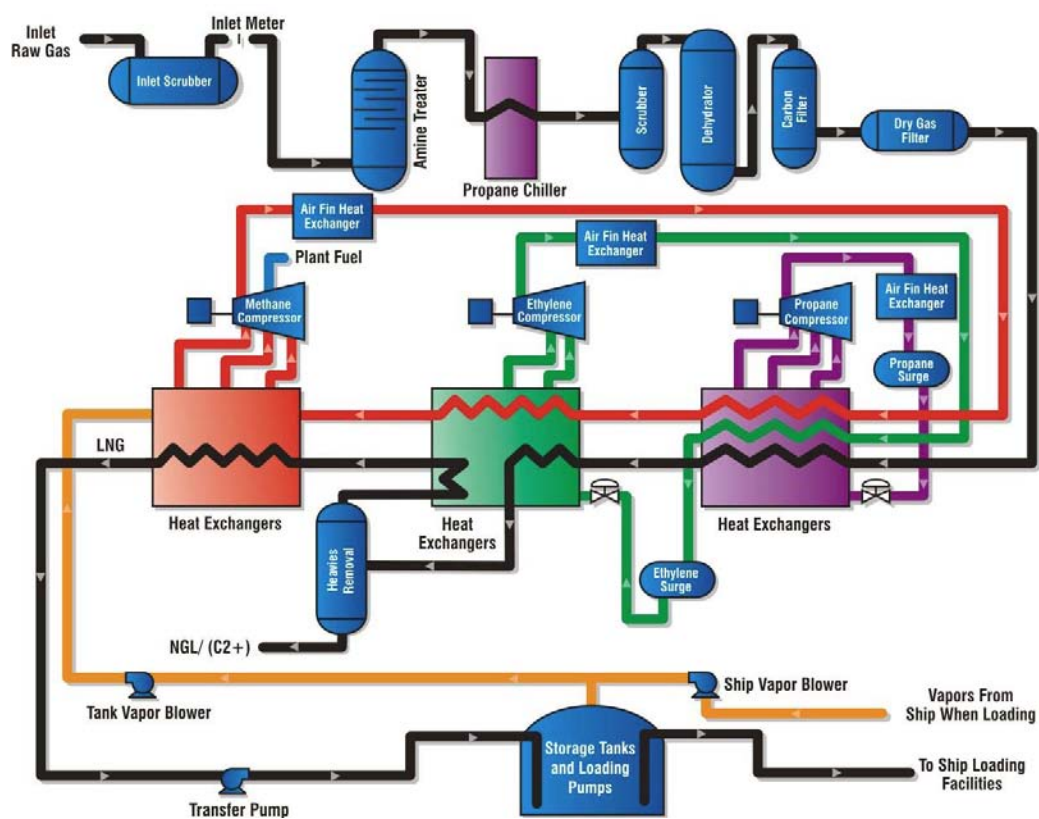


**Figure 5-1 Schematic of Conoco Phillips LNG process (Martinez, 2005)**

Engineering companies implement the licence technology of the process plant into practical design. The design of the plant is their primary role and the sizing and design of the electrical power generation and distribution systems are part of the process.

The electrical design process starts with the development of a single line diagram. Similar to mineral processing plant a typical LNG plant comprises a number of load

centres. The major load centre is the LNG process plant comprising production trains. The power system is designed so that each train has its own radial distribution network. This ensures that should the distribution system supplying one of the trains be out of service, the operation of the remaining trains will not be affected.

A typical single line diagram of the LNG plant is given in Figure 5-2. For simplicity the diagram shows a single train operation. The system configuration has similarities with mineral processing plants (refer to Fig 4-1): the power generation is centralised in a single power station, the system is a radial system comprising dual feeders to the process area and either single or dual feeds to other load centres.

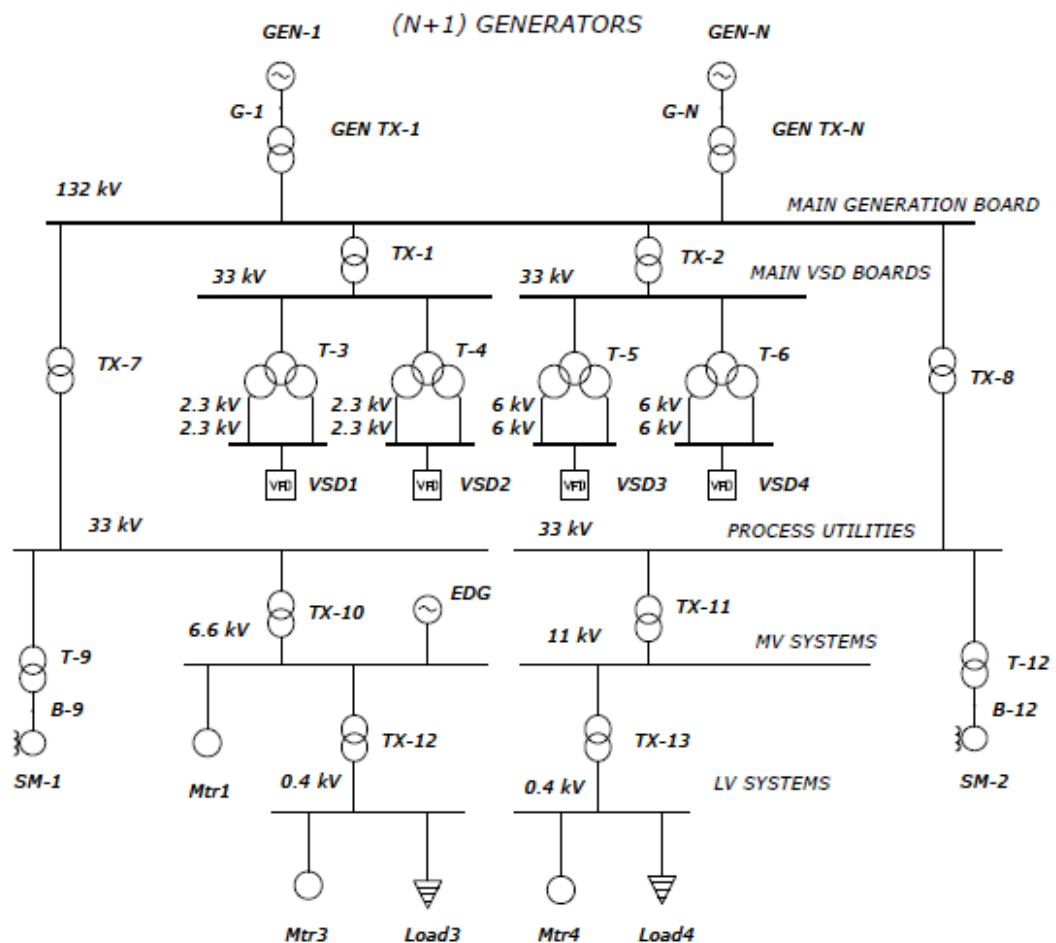


**Figure 5-2 Typical LNG plant SLD (Wilson, 2006)**

The power is generated at 11 kV and stepped-up via a generator transformer to 132 kV for further distribution. The step-up voltage is dependent on the system fault level. For example 33 kV switchgear rated at 40 kA has a maximum fault level of 2,283 MVA. The power generation is limited to approximately one eleventh of that

about 275 MVA. Generation plants of overall capacity larger than 275 MW require higher voltage, such as 132 kV.

The 132 kV is distributed to the LNG production area and is stepped down to 33 kV. The 33 kV distribution is used to supply LNG process trains and some of the remote areas such as accommodation village / township, LNG jetty and bore water fields. The 33 kV switchboard is split into two sections. The process area refrigeration compressor motors, due to their capacity, are fed directly from the 33 kV switchboard. The 33 kV is stepped down to 6.6 kV to feed medium voltage motors. The 6.6 kV (or in some cases 33 kV) is stepped to 690 or 400 V for low voltage distribution.

Low voltage distribution comprises two voltage levels, 690 V and 400 V. The 690 V distribution system is used for supplying the low voltage motors as it offers reduced cable cross sectional area for the same motor size. The 400 V distribution system is used for supplying the low voltage general power and lighting distribution boards.

The LNG plant electrical system will include an essential switchboard, similar to an FPSO power system, which will provide supply to all critical services in case the main power generation is shut down. This switchboard is not shown on the typical SLD in Figure 5.2. The essential services system consists of a vital power system which is supplied via UPS units and the main feed to those UPS units is from the essential board. System description and discussions related to essential and vital power systems on off-shore facilities (refer Section 3.3.1) is applicable to essential systems on LNG plants.

### **5.2.2 Engineering Specifications and Design Process**

The design process described in this section is based on practical observations of the design process currently used within the LNG industry. Of special interest are observations related to non-linear loads and the way they are managed throughout the design process.

The process applied in the design of electrical power system on an LNG plant follows the same principles as those used on off-shore oil and gas facility and other similar industrial plants. Engineering standards and equipment specifications used



for off-shore plants are complemented with minor additional requirements that are specific to the LNG plants, such as buried cables, and large refrigeration compressor drives. A set of engineering standards and philosophies is developed by plant operators and engineering companies during the develop phase of the project and they are used throughout the project for the selection of equipment and engineering design.

The design process is based on key single line diagrams, and load list and load balance calculations. Refer to Section 3.2.2 of this thesis for a sample load balance calculation sheet. Engineering guidelines established by the project team provide direction to the design team on how to design equipment and installations. A massive quantity of electrical equipment and related information is managed via integrated data base systems producing automatic schedules and lists. The process starts with plant layout and the identification of load centres. The load centres are then split into functional areas which are fed from the common nodes to enable selective shedding. Redundancy level is defined and a sufficient number of feeders provided to supply various load centres. It should be observed that non-linear loads are not identified and taken into consideration in load balance calculations as the load balance calculation is carried out for the nominal power frequency.

Power system studies, both static and dynamic are carried out in support of the design. Static studies are comprised of load flow, short circuit and harmonic studies. Preliminary harmonic studies are carried out during the develop phase and detailed studies are carried out towards the end of detail (execute) design phase. Such a late study is driven by the lack of vendor data available to the project team at the beginning of the develop phase. For power system studies, the system configuration given in key single line diagrams is shown in the power system model and the results are used to define major equipment parameters. LV and MV loads are usually grouped and presented as lumped loads. Numerous other assumptions are made in order to enable a quick power system study.

The concern with the existing design process is that non-linear loads are neglected in early stages of the design process and their impact on the power system is evaluated towards the end of the detail design phase.

The current trend within the LNG industry is the establishment of a frame agreement between the plant owners and operators with equipment suppliers. Such agreements define equipment types that will be supplied and used on the facility, and consequently all equipment parameters can be defined well before the plant design is started. This trend is specifically attractive for the proposed design by power system analysis concept.

To carry out design by power system analysis, the entire equipment library can be established and supplied to the project team before the start of the project. The project team then needs to follow inputs from the process engineers regarding system loads and use the library to design the power system. The power system model can then be established from the very early stages of the design, enabling modelling of the power system with finite detail. All LV loads can be modelled as individual loads, and each LV cable can be modelled in the network. The load flow studies would immediately highlight issues with overloading equipment. The short circuit studies would provide comprehensive set of short circuit currents. And most importantly, harmonic studies can be run for the entire system configuration.

Power system analysis software packages have developed to the point where they can manage a large number of nodes. Personal computers are powerful enough to provide fast calculation results. The format of printouts can then be shaped to provide comprehensive equipment schedules and bill of materials. The repetitive nature of LNG trains enables quick model generation and yet provides a powerful tool to drive the design.

It is recommended that the approach utilising design by power system analysis philosophy is fully evaluated and developed in further research work. Such research would require a collaborative agreement with LNG operators and access to proprietary design information.

Major types of non-linear loads found on a typical LNG plant are explained in further sections of this chapter, for reference.

### **5.3 Non-linear loads**

#### **5.3.1 Variable Speed Drives and UPS Systems**

The largest non-linear load on a typical LNG plant is a gas compressor helper motor comprising a synchronous motor coupled to the gas compressor and a variable frequency drive. There are two different technologies for large variable speed drive systems currently available on the market: Load Commutated Inverter (LCI) and Voltage Source Inverter (VSI), further described in Sections 5.3.2 and 5.3.3, respectively.

A number of variable speed drive systems are provided to supply low voltage and medium voltage motors for process pumps and fans. A typical variable drive system includes a low voltage motor and a variable frequency drive. Due to the large number of variable speed drives on the plant, a cost effective solution will drive the selection of variable speed drives for pumping and air cooling fan application.

Variable frequency drives are either voltage source or current source inverters utilising the pulse width modulation technique. The speed control uses the V/f control technique alleviating the need for a speed feedback loop. Special applications may require flux vector control. The rectifier circuit includes a 6-pulse diode bridge rectifier. The DC link incorporates both a capacitor and a reactor to limit the current and smooth the inverter supply voltage. The inverter utilises IGBTs with free-wheeling diodes. Generation of primary side current harmonics is mitigated with the installation of the supply side filters. Refer to Section 3.4 describing variable speed drives used on off-shore facilities; the same types are used on LNG plants.

The UPS systems on LNG plants are used to supply power to vital components such as the process control supply and telecommunication systems. Refer to section 3.5 of this thesis for the description of a typical UPS system used on off-shore facilities. The same observations are applicable to the UPS systems used on LNG plants.

#### **5.3.2 LCI Driven Compressors**

The Load Commutated Inverter (LCI) feeding synchronous motor can deliver large amounts of power at high efficiency. A typical LCI comprises a phase controlled rectifier bridge on the front end, a DC link with an inductor that smoothens the ripple

current and an output inverter. It can be built in 4 quadrant operating mode. Simple and reliable thyristors are used in both rectifier and inverter circuits (Kleiner, 2003).

A typical configuration of a 12-pulse LCI converter supplying a synchronous motor is shown in Figure 5-3.

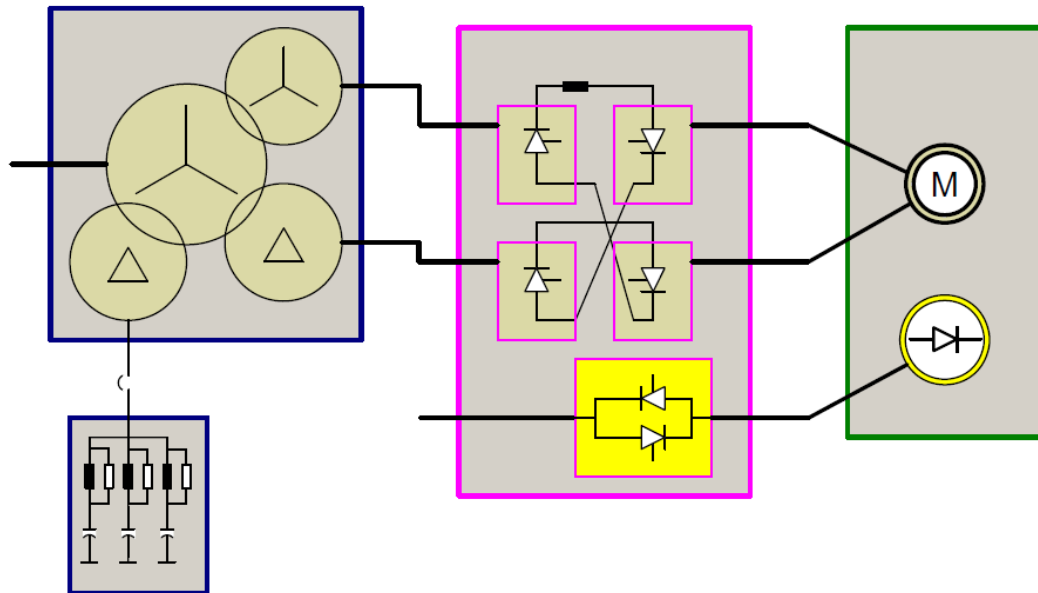


**Figure 5-3 12-pulse LCI arrangement with harmonic filter (Siemens)**

An LCI incorporates thyristors in the inverter circuits, which cannot be turned off by applying external gate signals; turning off the thyristors is achieved via an external circuit forcing the reverse-biased voltage across the device for a minimum specified time period. The natural turn-off process is supported with a leading power factor from the load side (Kwak, 2005).

Commutation of the output inverter is achieved by the induced EMF of the synchronous machine (Colby, 1985). Energy required for commutation of the thyristors in the inverter circuit is supplied by the load. Natural commutation supported from the load is only possible if the load current leads the output voltage, or when the load power factor is leading. If the load is an induction motor the leading power factor is achieved by installing power factor capacitors connected in parallel with the induction motor on the load side, as the motor is unable to provide a leading power factor (Kwak, 2005). If the LCI is driving a synchronous motor, the motor then runs overexcited providing a leading power factor.

The DC link contains a reactor which stores the energy converted by the front end rectifier. The energy stored in the reactor is used to supply the inverter. This source is seen by the inverter as a constant current source.

The LCI drive is seen by the supply network as a source of current harmonics. The current harmonic spectrum is similar to the harmonic spectrum of the CSI drives described in Chapter 3. Mitigation techniques include designs with 12, 18 and 24 pulse rectifiers complemented with the installation of harmonic filters.

An alternative to LCI would be current source inverters utilising GTO in inverter circuits. However LCI's have several advantages over the GTO CSI, such as higher voltage blocking ability, smaller on-state voltage drop, better cost effectiveness, and greater reliability (Kwak, 2005).

Possible arrangement of an LCI drive is shown in Figure 5-4.

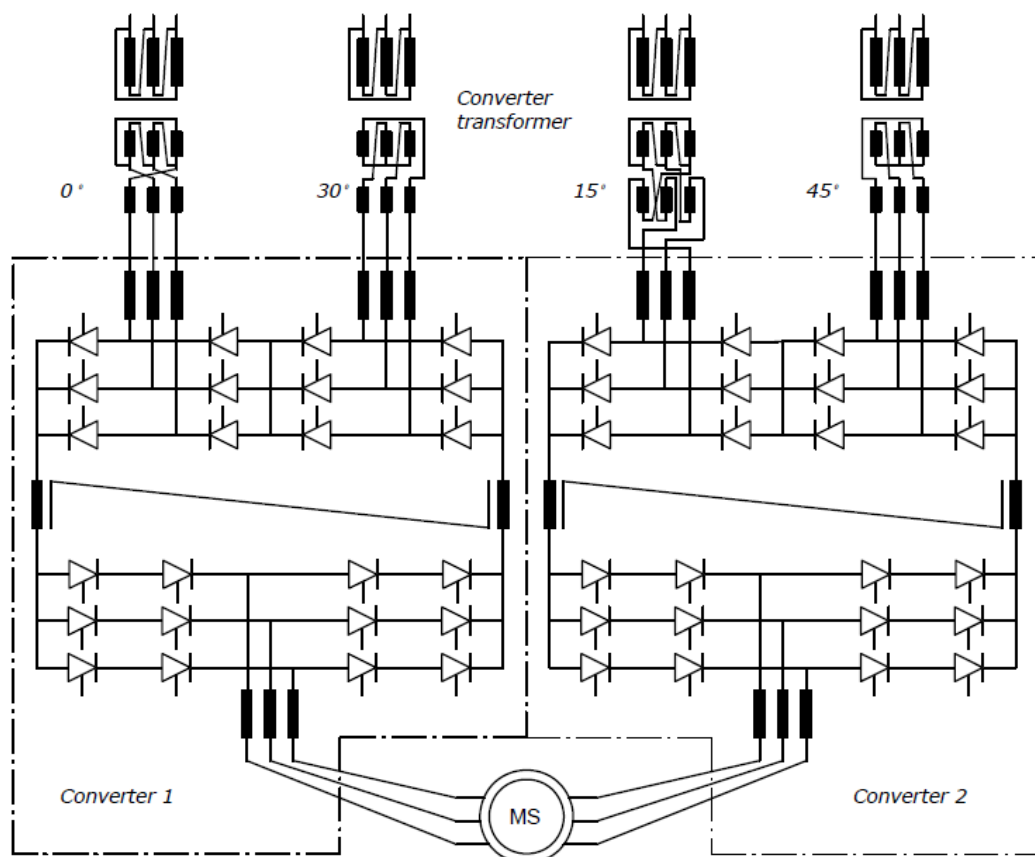


**Figure 5-4 Thyristor converter power circuit**

Figure 5-4 shows a typical configuration of a 24-pulse LCI converter. The LCI rectifier is supplied from the mains via an isolating transformer. The purpose of the transformer is to provide an appropriate voltage level to the converter, isolate the LCI from the supply network and provide an input impedance that will limit fault currents inside the converter (Wade, 1983).

The LCI drive can be applied to large fan, pump and refrigerant compressor drives. Large compressor drives in excess of 25 MW are predominantly LCI, as they provide the highest efficiency of any electric drive, as well as offering soft electrical and mechanical start and regenerative braking.

### 5.3.1 VSI Driven Compressors

There is a large variety of topologies to feed variable speed medium voltage induction or synchronous machines. The following combinations are possible: thyristor Current Source Inverters (CSI); PWM-CSIs applying conventional GTOs; multi-level inverters on the basis of low voltage IGBTs and three-level VSIs with IGCTs; high voltage IGBTs and GTOs.

Voltage Source Converters comprise a rectifier, DC link with capacitor and inverter. VSI type converters rectify the input power and store the energy in a DC link utilising capacitors. The inverter section of the VSD will see this source as constant voltage source.

The most common topology is the pulse width-modulated (PWM) voltage-source inverter (VSI). The VSI provides a simple and effective motor control as the power circuit can be operated over wide ranges of load frequency and voltages. Furthermore, the popular space vector PWM techniques for the VSI have been well established to obtain a direct control of the magnitude and phase of the output voltage.

The VSI, based on fast-switching insulated gate bipolar transistors (IGBTs), has disadvantages for high power applications due to substantial switching losses and high  $\frac{dv}{dt}$  of the PWM operation, leading to hazardous overvoltages and

electromagnetic interference problems. The VSI fed from a diode rectifier prevents regeneration of the output power back to supply utility (Kwak, 2006).

The VSI converters are becoming price competitive compared with LCI and cyclo-converters. Today VSI converters, employing PWM control, range from 0.5 MVA to 10 MVA. Voltage source converters offer reduced line harmonics, a better power factor, smaller filters and a higher system efficiency. These converters use IGBTs, IGCTs and multilevel topology. Thyristors for phase control, fast thyristors, Gate Turn Off thyristors (GTOs) and Integrated Gate Commutated Thyristors (IGCTs) have a latching structure where charge carriers are injected from the anode and cathode. GTO based Voltage Source Converters and Current Source Inverters are replaced by PWM Voltage Source Inverters using IGCTs or IGBTs (Bernet, 2000).

The introduction of new products by different manufacturers shows, that there is a trend towards PWM controlled 3L-NPC-VSIs. The high reliability, low losses, low costs and the wide range of the switch power of the IGCTs available on the market make the IGCT an alternative choice for medium voltage drives.

The VSI drive consists of an input transformer, a converter using IGCTs/thyristors, a DC link capacitor, switched voltage waveform output, an output filter (no individual input filter required) and a standard motor up to 6.9kV (induction or synchronous motor).

The VSI drives are made up of modular power electronic building blocks. Possible arrangements of a VSI drive are shown in Figures 5-5, 5-6, 5-7 and 5-8. Figure 5-5 shows a 24-pulse VSI arrangement offered by ABB. Figure 5-6 shows a 30/36-pulse VSI arrangement offered by Siemens. Figure 5-7 shows VSI with reverse conducting IGCTs for a 3.3 kV drive offered by ABB. Figure 5-8 shows a VSI configuration with IGBTs for a 3.3 kV motor offered by ABB.

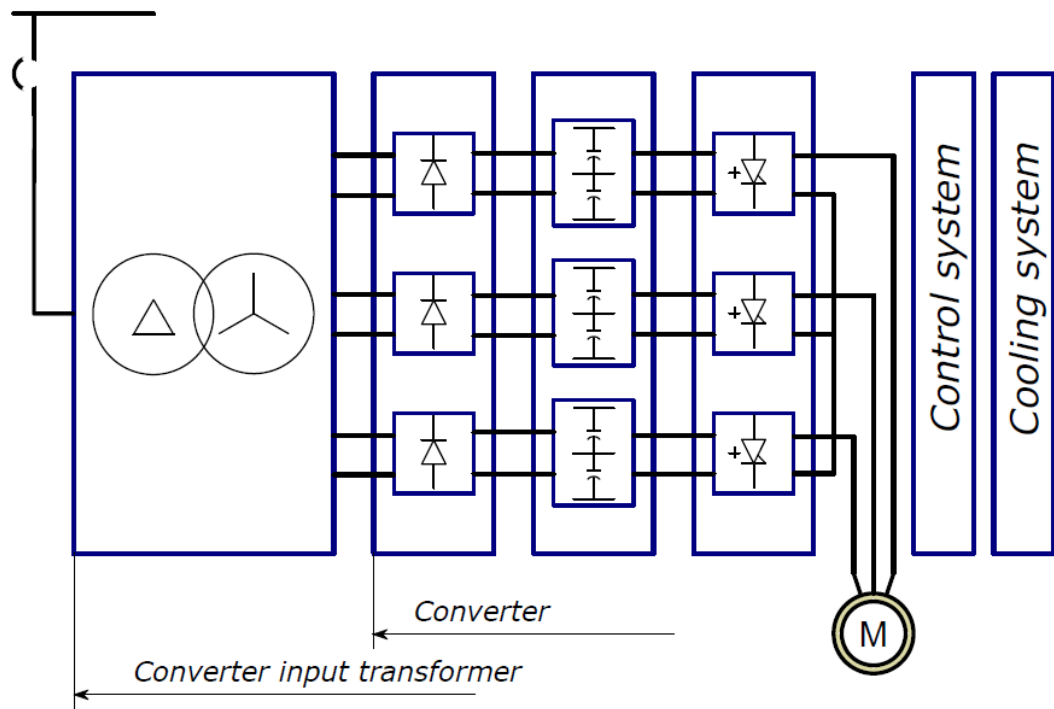


**Figure 5-5 24 pulse VSI arrangement (ABB)**

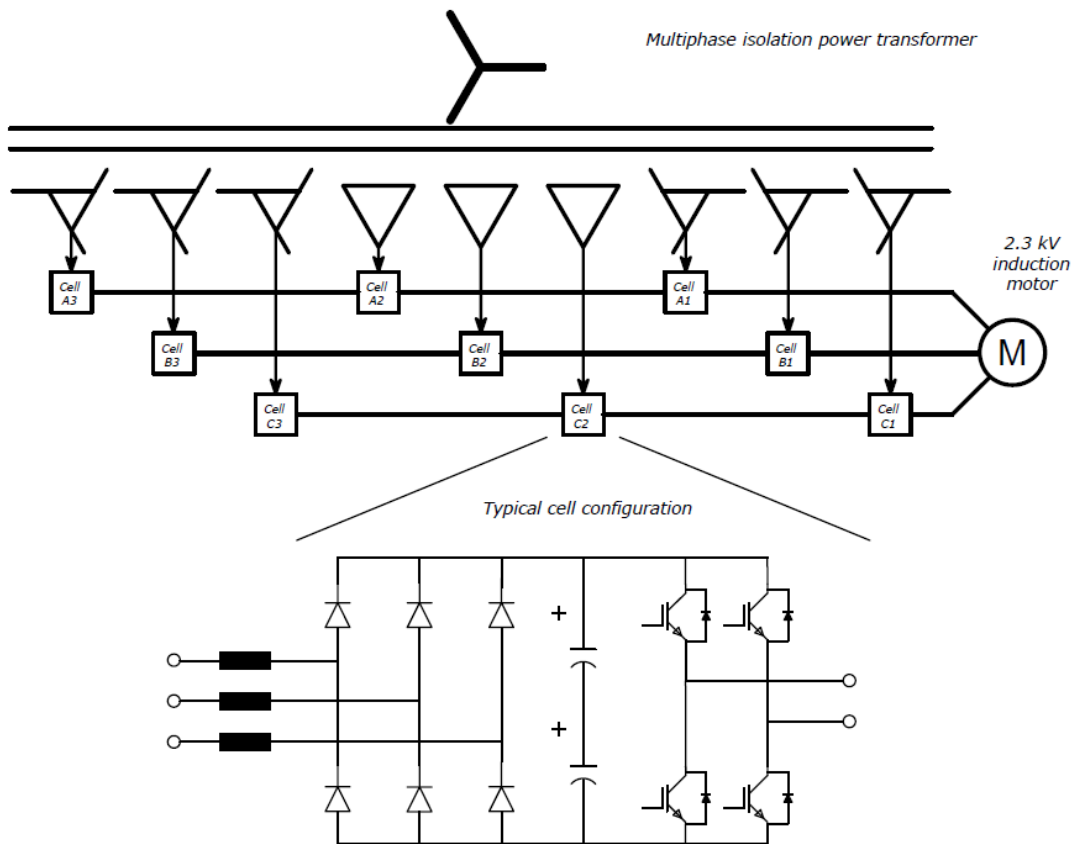


**Figure 5-6 30/36-pulse VSI arrangement (Siemens, Perfect Harmony)**



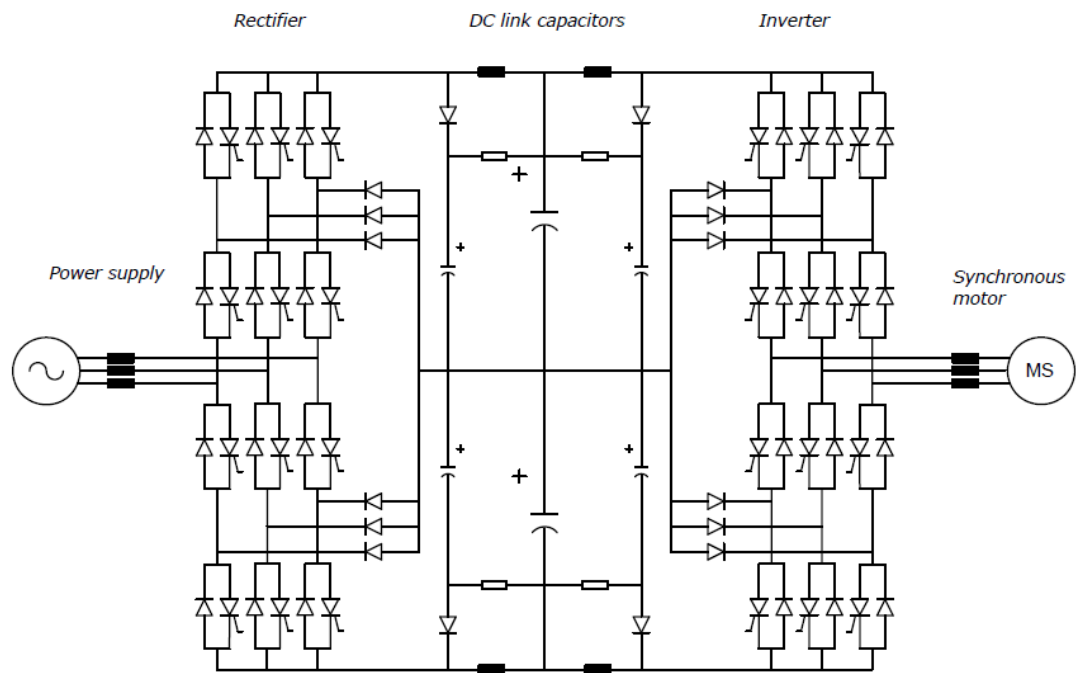


**Figure 5-7 VSI with reverse conducting IGBTs for a 3.3 kV drive**

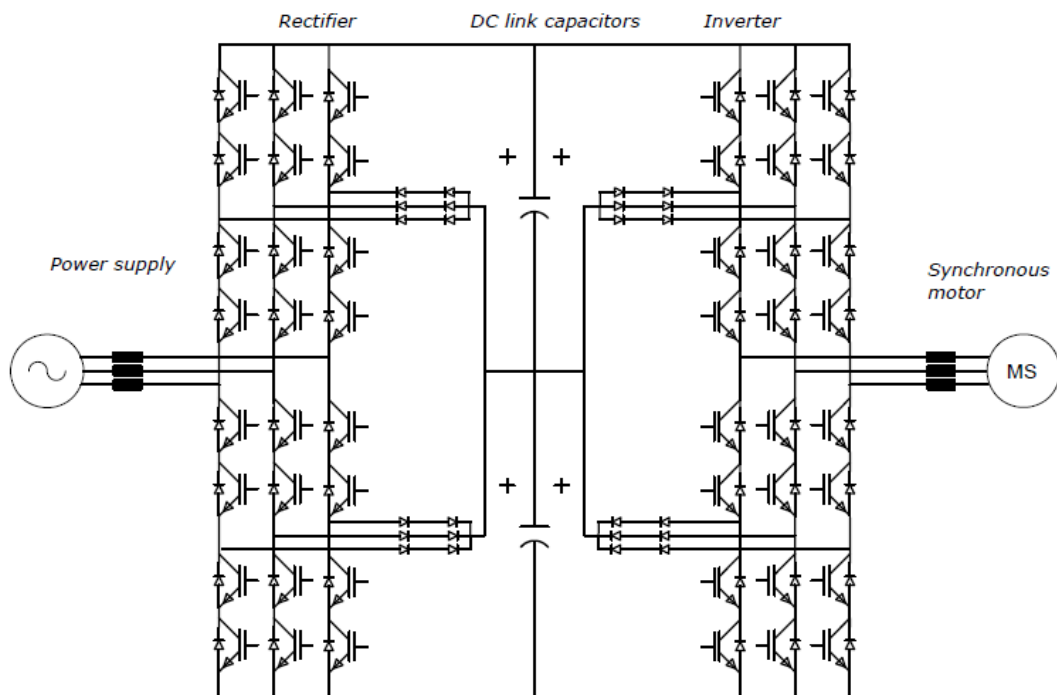


**Figure 5-8 VSI with IGBTs for a 3.3 kV motor**

## **5.4 Practical Issues with System Harmonics**

### **5.4.1 Mitigation Strategy**

A most effective mitigation strategy is the elimination of non-linear loads by design. This is not an option for LNG plants as the current trend within the industry is to increase both the number and size of variable speed drives in order to improve operational efficiency (Guyomard, 2010), (Martinez, 2005). For this reason the LNG plants comprise both a large number of smaller variable speed drives and large variable speed drivers for compressor motor drives. The variable speed drives comprising static switches are non linear loads and are the major generators of current harmonics on LNG power systems.

Numerous mitigation strategies minimising the impact of current harmonics have been employed on industrial systems (Wade, 1983), (Arrilag, et al., 2000), (Natarajan, 2005) and some of them are directly applicable to LNG plants. An isolated power system for an LNG plant, when compared with other industrial power systems, includes more large LCI drives and for this reason harmonic issues on LNG plant are specific to this type of industry.

Generation of harmonics produced by non-linear loads can be minimised by specifying and selecting the right type of non-linear equipment. Prior knowledge collected through operational experience (Guyomard, 2010) is implemented in equipment specifications, which are regularly reviewed and updated by operators and passed onto engineering companies. It has been observed that the LNG industry is very conservative, and only proven equipment is used in the design. This usually results in the implementation of older but very reliable technologies.

On LNG plants, low voltage variable speed drives for fan and pump applications are PWM drives utilising voltage source inverters for two quadrant operation. The voltage source inverters are described in section 3 of this thesis. The voltage source inverters are provided with input filters and for this reason inject a level of current harmonics complying with IEC recommendations (Standards Australia International, 2001). This is the most common mitigation strategy employed today, each drive is supplied with its own harmonic filter. This solution will result in good power factor control as every individual load will be compensated at its source. In addition to the

implementation of input filters the following mitigation strategies can be considered for LV systems supplying variable speed drives:-

- Install harmonic filters on the common LV node to cater for a group of variable speed drives supplied from the common node (multi drop connection of variable speed drives).
- Utilise 12-pulse rectifiers instead of 6-pulse and eliminate characteristic harmonics - this strategy is generally implemented on medium voltage drives.
- Consider installation of active front end variable speed drives units applicable for four quadrant operation designed specifically to limit line side harmonics
- Install active harmonic filters on the LV bus

The UPS systems are specified for 12-pulse operation and the inclusion of primary side filters. The measurements of harmonic currents on the primary side during factory acceptance testing shows that the level of current harmonics is significantly reduced with the implementation of the 12-pulse rectifier circuits (refer to Section 3). With large units, the implementation of 18 or 24 pulse converters should be considered wherever possible.

Electric heaters utilising zero current crossing will produce inter-harmonics. The electric heaters reach sizes around 1 MW. The design strategy on large electric heaters is to split the unit in two sections, one part to be constantly switched on via a contactor and another to be switched on and off using thyristor switches.

Medium voltage variable speed drives for fan and pump applications are PWM drives utilising either voltage or current source inverters. The difference between these two variable speed drives is explained in Section 3 of this thesis. In comparison, for PWM control system, voltage source inverters produce less current harmonics on the primary side. This is due to the energy stored in DC capacitor circuit that is being used as the voltage source for the inverter circuit. These drives generate characteristic harmonic currents which are fed back into the system.

Medium voltage variable speed drives for compressor application are explained in previous sections. LCI are predominantly used in such applications. In this instance

the installation of harmonic filters on an MV bus is the best mitigation strategy. An industry standard for MV drives is to utilise 12-pulse rectifiers. Larger units utilise 18 and 24-pulse configurations, as described in Section 5.3.2.

The mitigation strategies are confirmed through harmonic analysis and in order to provide good understanding on system harmonics it is recommended that each non-linear load is modelled as an individual load, complete with cables and filters. This information will need to be sourced from equipment vendors and the request to supply the harmonic spectrum for each drive can be incorporated in the frame agreement.

Medium voltage drives for compressor motors offer proven LCI technology. The current harmonics produced by LCI drives are mitigated through the installation of passive harmonic filters on the supply bus. The filter selection process is discussed in the following section. Another possible mitigation strategy is the further development of VSI technology that will result in reduced line side harmonics and eliminate the need for passive harmonic filters. This research is currently being carried out by equipment manufacturers in collaboration with oil and gas companies and it is recommended for future consideration.

#### **5.4.2 Filter Selection**

The filter selection process on LNG plant is limited to the selection of harmonic filters installed on buses supplying compressor motors (refer to Figure 5-2 in Section 5.1 of this thesis). Harmonic filters perform a dual purpose; they improve the power factor and act as a current harmonic sink for the range of frequencies for which they are designed. The level of voltage harmonics on LV buses is controlled via various mitigation strategies described in Section 5.3.1.

The first step in any filter selection study is to determine the level of current and voltage harmonics in the system. The LNG plant is an isolated power system and the system is free from any external harmonics commonly found on the public network. According to (Paice, 1996) the LNG power system can be classified as Type 1, which provides a fully balanced power supply. The level of harmonics on the power system can be established, depending on the stage of plant development, either by analysis or measurements. For new plants, analysis is the only possibility. For the

existing plants, undergoing expansion, harmonic measurements should be taken (refer to Appendix 1), and the power system model verified against the measurements (refer to Appendix 2). The power system model verified by measurements is then used as a tool to determine the level of system harmonics on the expanded system.

The acceptable level of voltage harmonics on each LV and MV bus is detailed in the engineering specifications. Power system analysis will provide the level of voltage harmonics at each switchboard. If the voltage levels are exceeded, then mitigation strategies should be implemented to bring the level of harmonics to acceptable levels.

The quality of power system modelling plays an important role in calculating the resonant frequency of the power system. The system with no capacitive load will have a linear impedance vs. frequency curve. The system with a capacitive component will show a resonant frequency. This is a natural system resonant frequency. The slope of the impedance curve and system resonant frequency will change when further capacitive loads such as harmonic filters are introduced into the system. The power system model developed during the design stage is used for harmonic analysis and filter selection study.

The filter selection process carried out on a typical industrial plant is given in Appendix 5. The principles highlighted in Appendix 5 are applicable to LNG plants. It is recommended that the filter selection process for LNG plant be the subject of further research, carried out in collaboration with engineering companies designing LNG plant. Analytical formulae for various filter configurations and filter design are explained by (Natarajan, 2005).

## **5.5 Original Contribution**

The following is a summary of original contribution presented in this Chapter:-

1. Provided an introduction to LNG power systems and described a typical LNG plant electrical power system, consisting of a large number of variable speed drive systems which are a source of current harmonics.

2. Described a typical design process and showed that the design process currently employed within the LNG industry is based on the design process used on smaller systems, such as oil and gas off-shore facilities.
3. Proposed a new design process based on design by power system analysis approach and using power system analysis software. Computers and power system analysis software packages have both developed to a level that enables the manipulation of large volumes of data. Design by power system analysis would provide an accurate representation of an electrical power system and enable power system analysis.
4. Described design challenges related to medium voltage variable speed drives and explained differences between VSI and LCI technologies used for compressor motor drives.
5. Described a typical 12-pulse LCI (Load Commutated Inverter) and provided a typical configuration of the drive system.
6. Described a typical VSI (Voltage Source Inverter), showed typical configurations and listed their advantages and disadvantages.

## **6. CONCLUSIONS AND RECOMMENDATIONS**

### **6.1 Original Contribution**

A list of original contribution statements presented in this thesis is given at the end of each chapter. This section repeats those statements for each section. The definition of original contribution relates to activities carried out independently as part of this research work. The original contribution does not imply that such processes and the topics presented in this thesis have not been covered in previous work by other researchers.

The following original contribution was presented in Chapter 3:-

1. Described typical small oil and gas isolated industrial power systems such as FPSOs and wellhead platforms and described current the design process applied within the industry for such small systems.
2. Presented introduction to current industry standards and critical evaluation of the standard approach in the design of electrical power systems. The design process currently adopted within the industry is a practical approach; however, modern day power plants incorporating a number of non-linear loads require more detailed studies at an early stage of the project cycle. For this reason there is a need to develop alternative methods leading to optimised design.
3. Developed and presented design by power system analysis concept. Highlighted current methodology within the industry on how to calculate maximum demand (via load list). Identified short-comings of such an approach and proposed an alternative method which is based on power system analysis software such as ETAP. Each load should be modelled in ETAP and load flow and short-circuit study results should be used in the very early stages of system design. Proposed that harmonic studies be included in the very early stages and run at the same time as load flow and short-circuit studies.
4. Highlighted issues associated with power supplies fed from a remote location to a wellhead platform. These supplies are achieved via subsea cables and the

most common issue is the selection of supply voltage and the cross-sectional area of the cable.

5. Provided mathematical background on the voltage drop calculation for subsea cables and calculated voltage drop curves which can be used for selection of voltage levels and CSA of cables. Compared results of manual calculation with the results obtained via ETAP power system analysis software.
6. Provided an overview of non-linear loads commonly found on oil and gas offshore facilities and provided analytical formulae for harmonic currents generated by various non-linear loads. Compared theoretical values with measurements and concluded that modelling of harmonic sources should be represented with figures obtained by the measurements, not by theoretical values. In the latter case the results of harmonics analysis could be misleading.
7. Identified loads which generate sub-harmonics and inter-harmonics and provided theoretical background on harmonic currents. Challenged the current industry standards which propose a cyclic mode of operation for thyristor controlled electric heaters because it results in the creation of inter-harmonics on the system. Proposed alternative methods for splitting the major loads into two groups, one with constant load, the other operating in the burst mode.
8. Highlighted the issue of how to represent inter-harmonics and sub-harmonics in power system study (currently only integer harmonics can be simulated in power system study).
9. Provided a methodology for obtaining information about harmonic sources based on measurements, factory acceptance tests or vendor data, and harmonic surveys using a harmonic analyser.
10. Summarised a methodology for analysing system harmonics and the calculation of power system harmonics for an industrial system undergoing significant expansion. The major steps are: harmonic measurements, analysis of harmonic measurements, development of a power system model, verification of the model against the measurements and its use as a base for further studies.



11. Analysed new loads, new harmonic sources and carried out a filter selection study for the power system undergoing expansion.

The following is a summary of original contribution towards the subject matter in Chapter 4:-

12. Described a typical mineral processing power system, consisting of various load centres and identified loads that are sources of current harmonics.
13. Described modes of operation of SAG mills and provided the technical background of SAG mill drives and formulae for linking the speed and diameter of the mill
14. Described a typical 6-pulse cyclo-converter and presented mathematical formulae for the calculation of secondary side voltage harmonics as derived by (Miyairi, 1979).
15. Carried out a harmonics survey (measurements) on a large gold processing plant and evaluated the suitability of harmonic filters. The plant comprised two SAG mill cyclo-converters, sources of current harmonics
16. Carried out harmonic measurement analysis and provided a harmonic spectrum at various points of the system.
17. Carried out analysis of switching transients on the system and identified over-voltages caused by capacitor bank switching
18. Provided directions on how to analyse the power system and when to carry out complete/overall harmonic analysis study
19. Suggested methodology on how to model in ETAP the system harmonics generated by cyclo-converters.

The following is a summary of original contribution towards the subject matter in Chapter 5:-

20. Provided an introduction to LNG power systems and described a typical LNG plant electrical power system, consisting of a large number of variable speed drive systems which are a source of current harmonics.
21. Described a typical design process and showed that the design process currently employed within the LNG industry is based on the design process used on smaller systems, such as oil and gas off-shore facilities.
22. Proposed a new design process based on design by power system analysis approach and using power system analysis software. Computers and power system analysis software packages have both developed to a level that enables the manipulation of large volumes of data. Design by power system analysis would provide an accurate representation of an electrical power system and enable power system analysis.
23. Described design challenges related to medium voltage variable speed drives and explained differences between VSI and LCI technologies used for compressor motor drives.
24. Described a typical 12-pulse LCI (Load Commutated Inverter) and provided a typical configuration of the drive system.
25. Described a typical VSI (Voltage Source Inverter), showed typical configurations and listed their advantages and disadvantages.

## **6.2 Recommendations for Further Work**

The following are recommendations for further work. :-

1. Harmonic Measurements - It was found during this research that obtaining harmonic measurements from existing facilities is a tedious process as it requires significant resources, both human and equipment. Logistically, it is hard to implement; isolated industrial plants are in remote areas and it is hard to provide sufficient labour and equipment for the measurements. Usually a compromise must be made to minimise the amount of time for the survey. Measurement points are not easily accessible, and it requires plant shutdown to avoid live work. Alternatively, if live work is allowed, it is a safety hazard that

has to be controlled before the task is started. There is the potential to trip the plant and cause production loss, which either puts additional pressure on the project team or prevents the system operators giving permission to carry out such measurements. For this reason further research should be concentrated on: finding a method of monitoring system harmonics on-line; selection of measurement points; device selection; communication protocols; selection of best system configuration; and reporting of system harmonics which are measured on the system.

2. Design by Power System Analysis Approach - This study proposed an alternative method to approach industrial plant design by organising all design office activities around power system analysis software such as ETAP. Further research should develop a complete design model for the design process, provide check points and request level of accuracy of input data to achieve desired output accuracy. This model would change the existing design office demography by placing a greater emphasis on professional engineers' output and would organise design deliverables around the power system analysis software reports. This is especially important for LNG plants, where access to design system is controlled by operators and large engineering companies.
3. Modelling of Harmonic Sources and Data Collection - Non-linear loads are a source of current harmonics. The harmonic spectrum measured on the finished product is different from analytical results. This is because of tolerances on both device components and control circuits controlling power switching devices. In addition, some loads such as cyclo-converters and thyristor controlled electric heaters produce sub-harmonics and inter-harmonics. Further work should focus on data collection techniques for both factory acceptance testing and harmonic surveys on live plants. Data collected during these activities should be compiled in a data base and used for modelling purposes. Power system analysis software would carry out harmonic analysis for integer harmonics. Research should be directed into the area proposing an alternative harmonic analysis which would take into consideration non-linear loads generating non-integer harmonic sources.

## **7. BIBLIOGRAPHY**

**ABB, Switzerland** A Guide to Standard Medium Voltage Variable Speed Drives Part 1: Questions and Answers and Medium Voltage Variable Speed Drive Selection [Conference]. - [s.l.] : ABB Publication, 2004.

**ABB, Switzerland** A Guide to Standard Medium Voltage Variable Speed Drives Part 2: Choosing a motor control platform and drive system [Conference]. - [s.l.] : ABB Publication, 2004.

**Ahrens M, Gonser, J** Technical and Commercial Benefits of Gearless Mill Drives for Grinding Applications [Conference] // SME Annual Meeting. - Denver, CO : ABB Reprint, 2007.

**Akagi H, Takahashi, I & Nabae, A** 'Input Current Harmonics and Fundamental Reactive Power of Cyclo-converters' [Article] // Electrical Engineering in Japan. - 1981. - No. 5 : Vol. 101. - pp. 85-92.

**Amemiya Y & Kanamura, Y** 'Improvement of Power Factor of Series-Connected Cyclo-converters' [Article] // Electrical Engineering in Japan. - 1978. - No. 6 : Vol. 98. - pp. 65-71.

**Andrews D, Bishop, MT & Witte, JF** 'Harmonic Measurements Analysis and Power Factor Correction in a Modern Steel Manufacturing Facility' [Article] // IEEE Transactions on Industry Applications. - 1996. - May/June. - No. 3 : Vol. 32. - pp. 617-624.

**AREVA T&D** Network Protection and Automation Guide [Book]. - Paris : Areva, 2005. - pp 1-497.

**Arrilag J [et al.]** Power System Harmonic Analysis [Book]. - New York : John Wiley & Sons, Inc, 2000. - Vols. pp 1-418.

**Arrilag J and Watson RW** Power System Harmonics [Book]. - New York : John Wiley & Sons, Inc, 2007. - Vols. pp 1-418.

**Azbill DC, Propst, JE, Catlett, RE** "A Case Study of Replacing Steam Turbines with LCI-Type Variable-Speed Drives" [Article] // IEEE Transaction on Industry Applications. - 1990. - Nov/Dec. - No. 6 : Vol. 26. - pp. 1086-1094.

**Benedict E, Collins, T, Gotham, D, Hoffman, S, Karipides, D, Pekarek, S, Ramabahdran, R** Losses in Electric Power Systems [Book]. - West Lafayette, Indiana : Purdue University, 1992. - Vols. pp 1-90.

**Bernet S** Recent Developments of High Power Converters for Industry and Traction Applications [Conference] // IEEE Transaction on Power Electronics. - Foz do Iguaçu, Brazil : IEEE, 2000.

**Bomvinsinho** [Conference]. - 2010.

**Chattopadhyay AK, Rao, J** A Generalized Method of Computer Simulation for Induction Motors with Stator Current Discontinuities and its Application to a Cyclo-converter-Fed Drive [Article] // IEEE Transactions on Industry Applications. - 1980. - March/April. - No. 2 : Vol. vol.. - pp. 234-241.

**Choi S, Enjeti, PN, Lee, HH & Pitel, IJ** 'A New Active Interphase Reactor for 12-pulse Rectifiers Provides Clean Power Utility Interface' [Article] // IEEE Transactions on Industry Applications. - 1996. - November/December. - No. 6 : Vol. 32. - pp. 1304-1311.

**Chu RF & Burns, JJ** 'Impact of Cyclo-converter Harmonics' [Article] // IEEE Transactions on Industry Applications. - 1989. - May/June. - No. 3 : Vol. 25. - pp. 427-435.

**Colby RS, Lipo, TA, Novotny, DW** A State Space Analysis of LCI Fed Synchronous Motor Drives in the Steady State [Article] // IEEE Transactions on Industry Applications. - 1985. - July/August. - No. 4 : Vol. IA 21. - pp. 1016-1022.

**Daniel F, Chaffai, R & Al-Haddad, K** 'A New Modulation Technique for Reducing the Input Current Harmonics of a Three-Phase Diode Rectifier with Capacitive Load' [Article] // IEEE Transactions on Industry Applications. - 1997. - September/October. - No. 5 : Vol. 33. - pp. 1185-1193.

**Das JC** Power System Analysis - Short Circuit Load Flow and Harmonics [Book]. - New York, NY : Marcel Dekker, Inc., 2002. - Vol. pp .

**De La Rosa FC** Harmonics and Power Systems [Book]. - Boca Raton, FL : CRC Press, 2006. - Vols. pp 1-.

**De Rosa F, Langella, R, Sollazzo, A & Testa A** 'Waveform Distortion Caused by High Power Adjustable Speed Drives Part I: High Computational Efficiency Model' [Article] // ETEP. - 2003. - November/December. - No. 6 : Vol. 13. - pp. 347-354.

**Department of Mines and Petroleum** [Article] // Petroleum in Western Australia. - Perth : Department of Mines and Petroleum, 2010. - September.

**Dionise TJ, Lorch, V, Brazil, BJ** Power Quality Investigation of Back-to-Back Harmonic Filters for a High-Voltage Anode Foil Manufacturing Facility [Article] // IEEE Transactions on Industry Applications. - 2010. - March/April. - No. 2 : Vol. 46. - pp. 694-702.

**Esmail EH & Erickson, R** 'Single Switch 3 ph PWM Low Harmonic Rectifiers' [Article] // IEEE Transaction on Power Electronics. - 1996. - March. - No. 2 : Vol. 11. - pp. 338-346.

**Ewanchuk J, Salmon, J, Knight, AM** Performance of a High-Speed Motor Drive System Using a Novel Multilevel Inverter Topology [Article] // IEEE Transactions on Industry Applications. - 2009. - September/October. - No. 5 : Vol. 45. - pp. 1706-1714.

**Fielding G & Elkateb, MM** Economics, Design and Emergency Control of Electrically-Interconnected Off-shore Gas/Oil Installations [Conference] // IEE International Conference in Power System Control, Operation and Management. - Hong Kong : [s.n.], 1991. - Vols. pp. 907-913.

**Fukao T, Matsui, M** Basic Characteristics of Cyclo-converter for Linking Commercial and High-Frequency Distribution Lines [Article] // IEEE Transactions on Industry Applications. - 1987. - September/October. - No 5 : Vol. IA 23. - pp. 927-936.

**Grainger JJ and Stevenson WD Jr** Power System Analysis [Book]. - New York : McGraw-Hill, Inc, 1994. - Vol. I.

**Guyomard R, Dessogne, D, Martinot, B, Thibaut, E** 20 years of Experience in VSDs for High Power Compressors of Steam Crackers [Conference]. - 2010.

**Hammond PW** A Harmonic Filter Installation to Reduce Voltage Distortion from Static Power Converters [Article] // IEEE Transactions on Industry Applications. - 1988. - January/February. - No. 1 : Vol. 24. - pp. 53-58.

**Hazel T, Condamin, I & Audemard, F** 'No-risk In-service Training' [Article]. - 2006. - May/June. - pp. 56-66.

**Hill WA, Ho, EYY & Neuzil, I** 'Dynamic Behaviour of Cyclo-converter System' [Article] // IEEE Transactions on Industry Applications. - 1991. - July/August. - No. 4 : Vol. 27. - pp. 750-755.

**Howell KB** Principles of Fourier Analysis [Book]. - Boca Raton, FL : Chapman & Hall/CRC, 2001. - Vols. pp 1-769.

**IEEE/Cigre** Interharmonics in Power Systems [Conference] // IEEE Interharmonic Task Force, Cigré 36.05/CIRED 2 CC02 Voltage Quality Working Group. - 1997.

**Institute of Electrical and Electronics Engineers, Inc.** IEEE Std 1159-1995(R2001) IEEE Recommended Practice for Monitoring Electric Power Quality [Book]. - New York, NY : Institute of Electrical and Electronics Engineers, Inc., 1995. - Vols. pp 1-70.

**Institute of Electrical and Electronics Engineers, Inc.** IEEE Std 141-1993 IEEE Recommended Practice for Electrical Power Distribution for Industrial Plants [Book]. - New York, NY : Institute of Electrical and Electronics Engineers, Inc., 1994. - Vols. pp 1-750.

**Institute of Electrical and Electronics Engineers, Inc.** IEEE Std 399-1997 IEEE Recommended Practice for Industrial and Commercial Power System Analysis [Book]. - New York, NY : Institute of Electrical and Electronics Engineers, Inc., 1998. - Vols. pp 1-483.

**Institute of Electrical and Electronics Engineers, Inc.** IEEE Std C57.110-1998 IEEE Standard Practice for Establishing Transformer Capability when Supplying Nonsinusoidal Load Currents [Book]. - New York, NY : Institute of Electrical and Electronics Engineers, Inc, 1999. - Vols. pp 1-39.

**Institute of Electrical and Electronics Engineers, Inc.** IEEE Std C57.18.10-1998 IEEE Standard Practices and Requirements for Semiconductor Power Rectifier Transformers [Book]. - New York, NY : Institute of Electrical and Electronics Engineers, Inc., 1998. - Vols. pp 1-61.

**Institute of Electrical and Electronics Engineers, Inc.** IEEE-Std 519-1992 IEEE Recommended Practices and Requirements for Harmonic Control in Electrical Power System [Book]. - New York, NY : Institute of Electrical and Electronics Engineers, Inc., 1992. - Vols. pp 1-93.

**Ishihara K, Katayama, S, Kokubu, T, Yasaka, M, Kurosawa, R** Application of New Drive Systems for Plate Mill Drives [Article] // IEEE Transactions on Industry Applications. - 1986. - March/April. - No 2 : Vol. IA 22. - pp. 345-351.

**Jorg P, Scheuer, G, Wikstrom, P** A Higher Level of Efficiency - Five Level Frequency Converter for MV [Conference] // ABB Review. - [s.l.] : ABB Publication, 2007. - pp. 26-31.

**Kadar L, Hacksel, P & Wikston, J** 'The Effect of Current Voltage Transformers Accuracy on Harmonic Measurements in Electric Arc Furnace' [Article] // IEEE Transactions on Industry Applications. - 1997. - May/June. - No. 3 : Vol. 33. - pp. 780-783.

**Kennedy PS** 'Design and Application of Semiconductor Rectifier Transformers' [Article] // IEEE Transactions on Industry Applications. - 2002. - July/August. - No. 4 : Vol. 38. - pp. 927-933.

**Khan S** Industrial Power Systems [Book]. - Boca Raton, FL : CRC Press, 2008. - pp 1-446.

**Kleiner F, Rausch, S, Knabe, J** Increase Power and Efficiency of LNG Refrigeration Compressor Design - All Electric Driven Plants [Conference] //



Hydrocarbon Processing / ed. USA Gulf Publishing. - USA : [s.n.], 2003. - pp. 67-69.

**Kusko A & Peeran, SM** 'Application of 12-pulse Converters to Reduce Electrical Interference and Audible Noise from dc Motor Drives' [Article] // IEEE Transactions on Industry Applications. - 1993. - January/February. - No. 1 : Vol. 29. - pp. 153-160.

**Kwak S, Tiloyat, HA** "A Hybrid Solution for Load-Commutated-Inverter-Fed Induction Motor Drives" [Article] // IEEE Transaction on Industry Applications. - 2005. - Jan/Feb. - No. 1 : Vol. 41. - pp. 83-90.

**Kwak S, Tiloyat, HA** Multilevel Converter Topology Using Two Types of Current-Source Inverters [Article] // IEEE Transactions on Industry Applications. - 2006. - November/December. - No. 6 : Vol. 42. - pp. 1558-1564.

**Liang X, Faried, SO, Ilohonwu, O** Subsea Cable Applications in Electrical Submersible Pump Systems [Article] // IEEE Transactions on Industry Applications. - 2010. - March/April. - No. 2 : Vol. 46. - pp. 575-583.

**Liang X, Jackson, WM** Influence of Subsea Cables on Off-shore Power Distribution Systems [Article] // IEEE Transactions on Industry Applications. - 2009. - November/December. - No. 6 : Vol. 45. - pp. 2136-2144.

**Martinez Meher-Homji, CB, Paschal, J, Eaton, A** All Electric Motor Drives for LNG Plants [Conference] // Gastech 2005. - Bilbao, Spain : Copyright Conoco Philips, 2005.

**McGranaham MF, Mueller, DR** Designing Harmonic Filters for Adjustable-Speed Drives to Comply with IEEE-519 Harmonic Limits [Article] // IEEE Transactions on Industry Applications. - 1999. - March/April. - No. 2 : Vol. 35. - pp. 312-318.

**McSharry PJ, Hamer, PS, Morrison, D, Nessa, J, Rigsby, JG** Design, Fabrication, Back-to-Back Test of 14 200-HP Two-Pole Cylindrical Rotor Synchronous Motor for ASD Application [Article] // IEEE Transactions on Industry Applications. - 1988. - May/June. - No. 23 : Vol. 34. - pp. 526-533.

**Mendes de Seixas FJ & Barbi, I** 'A 12 kW Three-Phase Low THD Rectifier with High-Frequency Isolation and Regulated DC Output' [Article] // IEEE Transaction on Power Electronics. - 2004. - March. - No. 2 : Vol. 19. - pp. 371-377.

**Merhej SJ, Nichols, WH** Harmonic Filtering for Off-shore Industry [Article] // IEEE Transactions on Industry Applications. - 1994. - May/June. - No. 3 : Vol. 30. - pp. 533-542.

**Miyairi S, Akagi, H, Fukao, T, Fujita, M** Equivalence in Harmonics between Cyclo-converters and Bridge Converters [Article] // IEEE Transactions on Industry Applications. - 1979. - January/February. - N0. 1 : Vol. IA 15. - pp. 92-99.

**Nahan MD** The Potential for the Development of a Centre of Excellence in LNG Industry Design in Western Australia [Report]. - Perth : State Law Publisher, 2010.

**Natarajan R** Power System Capacitors [Book]. - Boca Raton, FL : CRC Press, 2005. - Vol. pp .

**Neft CL, Chauder, CD** Theory and Design of a 30-hp Matrix Converter [Article] // IEEE Transactions on Industry Applications. - 1992. - May/June. - N0. 3 : Vol. 28. - pp. 546-551.

**Norrnga S, Meier, S, Ostlund, S** A Three-Phase Soft-Switched Isolated AC/DC Converter without Auxiliary Circuit [Article] // IEEE Transactions on Industry Applications. - 2008. - May/june. - No. 3 : Vol. 44. - pp. 836-844.

**Paice DA** Power Electronic Converter Harmonics [Book]. - Piscataway, NJ : IEEE Press, 1996. - Vols. pp 1-199.

**Peeran SM, Cascadden, WP** Application, Design, and Specification of Harmonic Filters for Variable Frequency Drives [Article] // IEEE Transactions on Industry Applications. - 1995. - July/August. - No 4 : Vol. 31. - pp. 841-847.

**Perreault DJ & Kassakian, JG** 'Effects of Firing Angle Imbalance on 12-Pulse Rectifiers with Interphase Transformers' [Article] // IEEE Transaction on Power Electronics. - 1995. - May. - No. 3 : Vol. 10. - pp. 257-267.

**Pont J, Rodriguez, J, Valderrama, W, Sepulveda, G, Chavez, P, Cuitino, B, Gonzalez, P & Alzamora, G** Current Issues on High-Power Cyclo-converter-fed gearless Motor Drives for grinding Mills [Conference]. - 2005.

**Quirt RC** 'Voltages to Gound in Load-commutated Inverters' [Article] // IEEE Transactions on Industry Applications. - 1988. - May/June. - No. 3 : Vol. 24. - pp. 526-530.

**Ravani von Ow Tatiana, Bomvisinho, Leandro** Use of the Latest Technology to Overcome the Demands of Mill [Article] // ABB Publication. - 2010.

**Rodríguez JR, Pontt, J, Newman, P, Musalem, R, Miranda, H, Moran, L, Alzamora, G** Technical Evaluation and Practical Experience of High Power Grinding Mill Drives in Mining Applications' [Article] // IEEE Trransaction on Industry Applications. - 2005. - May/June. - 3 : Vol. 41. - pp. 866-874.

**Sakui M & Fujita, H** 'An Analytical Method for Calculating Harmonic Currents of a Three-Phase Diode-Bridge Rectifier with DC Filter' [Article] // IEEE Transaction on Power Electronics. - 1994. - November. - No. 6 : Vol. 98. - pp. 631-637.

**Salor O, et al** Electrical Power Quality of Iron and Steel Industry in Turkey [Article] // IEEE Transactions on Industry Applications. - 2010. - January/February. - No. 1 : Vol. 46. - pp. 60-80.

**Sankaran C** Power Quality [Book]. - Boca Raton, FL : CRC Press, 2002. - Vols. pp 1-.

**Schaefer J** Rectifier Circuits: Theory and Design [Book]. - New York : John Wiley & Sons, Inc, 1965. - Vols. pp 1-220.

**Schmidtke B** Multiple Harmonic Filters Over Six Phases of Expansion in a 170-MW Plant [Article] // IEEE Transactions on Industry Applications. - 2009. - May/June. - No. 3 : Vol. 45. - pp. 1175-1179.

**Shahrodi EB & Dewan, SB** 'Steady State Characteristics of the 6-pulse Bridge Rectifier with Input Filter' [Article] // IEEE Transactions on Industry Applications. - 1985. - November/December. - No. 6 : Vols. 1A-21. - pp. 1418-1423.

**Shepherd W & Zhang, L** Power Converter Circuits [Book]. - New York, NY : Marcel Dekker, Inc., 2004. - Vols. pp 1- 527.

**Shimizu T, Jin, Y & Kimura, G** 'DC Ripple Current Reduction on a Single-Phase PWM Voltage-Source Rectifier' [Article] // IEEE Transactions on Industry Applications. - 2000. - September/October. - No. 5 : Vol. 36. - pp. 1419-1429.

**Standards Australia International** AS 3000: Wiring Rules [Book]. - 2007.

**Standards Australia International** AS/NZS 61000.3.6:2001 Electromagnetic Compatibility (EMC)- Part 3.6 Limits - Assessment of Emission Limits for Distorting Loads in MV and HV Power Systems (IEC 61000-6-3, MOD) [Book]. - Sydney : Standards Australia International Ltd, 2001. - Vols. pp 1-60.

**Standards Australia International** AS/NZS 61000.3.7:2001 Electromagnetic Compatibility (EMC)- Part 3.7 Limits - Assessment of Emission Limits for Fluctuating Loads in MV and HV Power Systems (IEC 61000-3-7:1996, MOD) [Book]. - Sydney : Standards Australia International Ltd, 2001. - Vols. pp 1-40.

**Standards Australia International** HB 264-2003 Power Quality - Recommendations for the Application of AS/NZS 61000.3.6 and AS/NZS 61000.3.7 [Book]. - Sydney : Standards Australia International Ltd, 2003. - Vols. pp 1-103.

**Steinke JK** Use of an LC Filter to Achieve a Motor-friendly Performance of the PWM Voltage Source Inverter [Article] // IEEE Transactions on Energy Conversion. - 1999. - September. - No. 3 : Vol. 14. - pp. 649-654.

**Suh Y, Steimer, PK** Application of IGCT in High-Power Rectifiers [Article] // IEEE Transactions on Industry Applications. - 2009. - September/October. - No. 5 : Vol. 45. - pp. 1628-1636.

**Sutherland PE** 'Harmonic Measurements in Industrial Power Systems' [Article] // IEEE Transactions on Industry Applications. - 1995. - January/February. - No. 1 : Vol. 31. - pp. 175-183.

**Tadakuma S, Tamura, Y** Current Response Simulation in Six-Phase and Twelve Phase Cyclo-converters [Article] // IEEE Transactions on Industry Applications. - 1979. - July/August. - No 4 : Vol. IA 15. - pp. 411-420.

**Thasananutariya T, Chatratana, S** Planning Study of Harmonic Filter for ASDs in Industrial Facilities [Article] // IEEE Transactions on Industry Applications. - 2009. - January/February. - No. 1 : Vol. 45. - pp. 295-302.

**The Australian Petroleum Production and Exploration Association** Key Statistics 2010 [Article] // Key Statistics 2010. - Perth : The Australian Petroleum Production and Exploration Association, 2010.

**Timple W** Cyclo-converter Drives for Rolling Mills [Article] // IEEE Transactions on Industry Applications. - 1982. - July/August. - No 4 : Vol. IA 18. - pp. 400-404.

**Tischler K** The Behaviour of Cyclo-converter for Gearless Drive under Abnormal Electrical Conditions [Conference] // Workshop SAG. - Vina del Mar, Chile : Siemens, 2003.

**Verma V, Singh, B** Genetic-Algorithm-Based Design of Passive Filters for Off-shore Applications [Article] // IEEE Transactions on Industry Applications. - 2010. - July/August. - No. 4 : Vol. 46. - pp. 1295-1303.

**Verma V, Singh, B, Chandrs, A, Al-Haddad, K** Power Conditioner for Variable-Frequency Drives in Off-shore Oil Fields [Article] // IEEE Transactions on Industry Applications. - 2010. - March/April. - No. 2 : Vol. 46. - pp. 731-739.

**Wade CA, Crane, DR** Reliability Features of Large Load Commutated Inverter Drives and Some Cautions in Their Application [Article] // IEEE Transactions on Industry Applications. - 1983. - July/August. - No. 4 : Vol. IA 19. - pp. 534-540.

**Western Power** Technical Rules for The South West Interconnected Network [Book]. - Perth : Western Power, 2007. - Vols. pp 1-202.

**Wiechmann H, Tischler, K** Comparison of Alternative Converters with Regard to their Application for Gearless Drives for Grinding Mills [Conference] // Workshop SAG. - Vina del Mar, Chile : Siemens, 2007.

**Wilson RC, Dall, CL, Smith, KS** Electrical Network Design Studies for Natural Gas Liquefaction Plants [Article]. - 2006.

**Winn JK & Crow, DR** 'Harmonic Measurements Using a Digital Storage Oscilloscope' [Article] // IEEE Transactions on Industry Applications. - 1989. - July/August. - No. 4 : Vol. 25. - pp. 783-788.

**Zargari NR, Xiao, Y, Wu, B** 'A Multilevel Thyristor Rectifier with Improved Power Factor' [Article] // IEEE Transactions on Industry Applications. - 1997. - September/October. - No. 5 : Vol. 33. - pp. 1208-1213.

**Zhezhelenko I, Sayenko, Y, Baranenko, T** Frequency Converters as Generators of Interharmonics [Conference] // 9th International Conference - Electrical Power Quality and Utilisation. - Barcelona : [s.n.], 2007.

Every reasonable effort has been made to acknowledge the owners of copyright material. I would be pleased to hear from any copyright owner who has been omitted or incorrectly acknowledged.

## **8. APPENDIX 1 - HARMONIC MEASUREMENTS ON AN INDUSTRIAL PLANT**

### **8.1 Introduction**

A harmonic measurement study was initiated to determine the level of voltage and current harmonics on the main MV plant switchboard. The Main Switchboard comprises a 22kV incomer feeder fed from the WPC 132kV substation via a step down transformer. The board comprises 12 outgoing feeders including one supplying a 6-pulse rectifier.

The purpose of the harmonic measurement project was to establish baseline voltage harmonic levels at the 22kV bus for the existing plant (The Plant) and to determine the level of current harmonics on various 22kV feeders fed from the existing 22 kV main switchboard.

The aim of this project is to get a better understanding of the distribution of current harmonics and to establish the harmonic sources and sinks. Ultimately, the objective of this project is to establish acceptance criteria and determine if the level of current and voltage harmonics is within the established acceptance criteria.

### **8.2 Background**

The power supply to the rectifier is provided via a 22kV feeder, fed from the main substation. The maximum demand of the rectifier circuit is approximately 7.5 MW.

The rectifier transformer feeds a 6-pulse rectifier which is a source of current harmonics. There are no harmonic filters at the rectifier (rectifier and transformer), they are installed on the main 22kV switchboard. Currently, the plant is undergoing expansion of its capacity and as part of the expansion project, the harmonic measurement study was initiated to determine the level of voltage and current harmonics on the 22 kV bus.

### **8.3 Purpose**

The governing industrial standards for harmonic control in the electrical power system, IEEE Std 519-1992, recommends that harmonic measurements are

performed following system changes and re-examined from time to time to determine system behaviour and performance.

A negative effect of the harmonics is additional thermal overheating which may cause accelerated ageing of the equipment insulation, leading to insulation breakdowns, unscheduled shutdowns and loss of production. Harmonics can also interfere with communication signal lines, cause nuisance tripping and system shutdowns.

In line with IEEE recommendations, the aims of the harmonic measurement project are as follows:-

- To establish baseline voltage harmonic levels at the 22kV bus for the existing plant,
- To determine the level of current harmonics on various 22kV feeders fed from the existing 22kV Main Switchboard,
- To get a better understanding of the distribution of current harmonics and to establish the sources and sinks of the harmonics,
- To obtain data through measurements in order to confirm the results of the power system harmonic analysis, that will be performed following completion of the harmonic measurements, but prior to the completion phase of the plant expansion project ,
- To establish acceptance criteria and therefore to determine if the level of current and voltage harmonics are within the established acceptance criteria,

This report includes the results of harmonic measurements that were carried out from Dec 14 2007 to Jan 11 2008 on the plant electrical power system.

#### **8.4 Scope**

The following scope was applied to the harmonic measurement project:-

- Collect single line diagrams, schematics, termination and wiring diagrams of the 22kV Main Switchboard,



- Evaluate drawings and establish measurement points,
- Prepare a test plan and identify the number of people required for the project,
- Visit the site and verify the test plan by identifying connection points at the 22kV switchboard,
- Organise work permits and connect the test instrument as per the test plan,
- Download the data measured on a daily basis,
- Carry-out harmonic analysis,
- Submit a report with recommendations - The report will include the methodology that was applied during measurements, it will summarise the results of analysis and provide recommendations for further works.

## **8.5 Methodology**

### **8.5.1 Harmonic Measurements**

The site work was carried out in accordance with the plant's permit to work system and the relevant HSE procedures. The personnel involved in the initial set-up of the test instrument and the regular daily data collection activity attended a compulsory half day induction at The Plant prior to commencement of work on the site.

The technical recommendations for the selection of instruments, test probes and test methodology for a typical industrial plant as reported in various textbooks and technical papers were reviewed and applied to this project. The references for the relevant papers are included in the report.

The selection of the test instrument and number of instruments used for monitoring of the harmonics was discussed with operations. It was decided that one instrument would be used over a period of 4 weeks. The selected instrument matched all of the selection criteria and it was readily available from a local instrument hire company.

The test instrument used for this project was Dranetz-BMI Power Quality Analysers, Type PX5 PowerXplorer. The harmonic analyser is equipped with 4 differential

voltage inputs of 1-600Vrms, AC/DC with a 16 bit analogue to digital (A/D) converter. The sampling rate is 256 samples/cycle. Also, the instrument comprises 4 current inputs with optional current probes. The probe selected was a Model TR-2510A 0.1-10A with a 16 bit analogue to digital conversion with a sampling rate of 256 samples/cycle.

### **8.5.2 Voltage and Current Measuring Points**

The 22 kV voltage was measured via the 22 kV bus voltage transformers. The voltage transformer set consists of three single-phase units connected in a three-phase assembly with a voltage ratio of  $22000/\sqrt{3}$  to  $110/\sqrt{3}$  per phase. The bus VTs are physically located in Panel 5.

The termination points used to connect the test instrument are located in Panel 5, at terminal block TS-1. Phase L1 was terminated at terminal 16, phase L2 at terminal 18 and phase L3 at terminal 20. The neutral wire was terminated in the marshalling panel, physically located next to the 22kV switchboard assembly, at terminal block KP, terminal No 118.

The voltage was measured at only one point throughout the measurements and that was at the 22kV plant switchboard as described in the previous 2 paragraphs.

Feeder currents were measured on various feeders at the 22kV switchboard. Each feeder current was measured via current clamping probes clamped around the CT secondary wires, with one probe per phase. The current was measured on the following feeders at the 22 kV Main Switchboard.

- Panel 10      CT-1, 300/1    Rectifier feeder
- Panel 4      CT-2, 900/5    Incomer
- Panel A      CT-1, 150/1    Feeder to Power factor Correction Unit
- Panel 7      CT-1, 150/1    Plant Feeder # 1
- Panel 0      CT-1, 75/1    Plant Feeder # 2

A detailed test plan was developed and the measurements were executed in accordance with the plan.

Voltage and current snapshots, captured via the power analyser, were stored in electronic format on a memory card as per the settings. The total capacity of the memory card was 128MB which was sufficient for storing the harmonic snapshot captured every minute over 24 hours. For this reason the memory card had to be cleared every day.

Raw measurement data were downloaded onto a hard disk drive on a lap-top on a daily basis (except on Christmas Day and Boxing Day). During Christmas Day and Boxing Day the periodic journal interval was increased to 5 minutes.

### **8.5.3 Harmonic Analysis**

Voltage and current waveforms captured by the power analyser were used for further harmonic analysis. Analysis was carried out using a specialised software package, Dran-View, supplied by Dranetz for analysis of the raw data.

The software is accompanied by a User's Guide which explains all of the features of the software package and instructions on how to install and use the software. The software package provides a Fast Fourier Transform (FFT) function, enabling calculation of the harmonic spectrum from base waveforms.

The base waveform captured during steady state conditions and then stored by the Power Analyser consists of a total of 10 waveforms per channel.

### **8.5.4 Acceptance Criteria**

Access to the SWIS electrical distribution system operated by Western Power is regulated through the Access Code. The Access Code requires Western Power to publish Technical Rules. Section 2 of the Technical Rules describes the technical performance requirements of the power system, and the obligations of the Network Service Provider to provide the transmission and distribution systems that will allow these performance requirements to be achieved. It sets out criteria for the planning, design and construction of the transmission and distribution systems.

With regards to harmonic levels, the Technical Rules state that under normal operating conditions, the harmonic voltage in networks with a system voltage of less than or equal to 35 kV must not exceed the planning levels shown in Table 1 of the Rules.

Odd harmonics Non-multiple of 3		Odd harmonics Multiple of 3		Even harmonics	
Order h	Harmonic voltage %	Order h	Harmonic voltage %	Order h	Harmonic voltage %
5	5	3	4	2	1.6
7	4	9	1.2	4	1
11	3	15	0.3	6	0.5
13	2.5	21	0.2	8	0.4
17	1.6	>21	0.2	10	0.4
19	1.2			12	0.2
23	1.2			>12	0.2
25	1.2				
>25	$0.2 + 0.5 \cdot 25/h$				
Total harmonic distortion (THD): 6.5 %					

**Table 8-1      Table 1: Distribution planning levels for harmonic voltages**

The planning limits are based on AS/IEC Standard 61000-3-6, which defines the acceptable level of voltage harmonics. The point of common coupling between the Plant and Western Power is at 132 kV and harmonic measurements at the 22 kV level are not used to determine if the system harmonics comply with the current access agreement between the plant operator and WPC.

The IEEE Standard 519-1992 provides harmonic limits for current and voltage. The philosophy applied for the development of current harmonic limits was based on the following criterion: to limit the harmonic injection from individual customers so that they will not cause unacceptable voltage distortion levels for the normal system characteristics.

The harmonic voltage distortion on the 22kV level is a function of the total injected harmonic current and the system impedance at each of the harmonic frequencies. The

total injected harmonic current will depend firstly, on the number of individual loads which inject harmonic currents and secondly on the size of each load.

The objectives of the current limits are to limit the maximum individual frequency voltage harmonic to 3% of the fundamental and the voltage THDv to 5%.

The following table summarises the current distortion limits as set out in IEEE Std 519-1992 which can be applied to the 22kV level. The ratio of the system maximum short circuit current to maximum demand load current is less than 20.

Odd harmonics		Even harmonics	
Order h	Harmonic current %	Order h	Harmonic current %
3	4.0	2	1.0
5	4.0	4	1.0
7	4.0	6	1.0
9	4.0	8	1.0
11	2.0	10	1.0
13	2.0	12	0.5
15	2.0	14	0.5
17	1.5	16	0.5
19	1.5	18	0.375
21	1.5	20	0.375
23	0.6	22	0.375
25	0.6	24	0.125
27	0.6	26	0.125

**Table 8-2 Current distortion limits as per IEEE Std 519**

## **8.6 Results of the Harmonic Analysis**

The time plot diagrams in Figure 8-1 indicates that the 22kV system voltage was steady and maintained within +5% and - 2.5% of the nominal voltage.

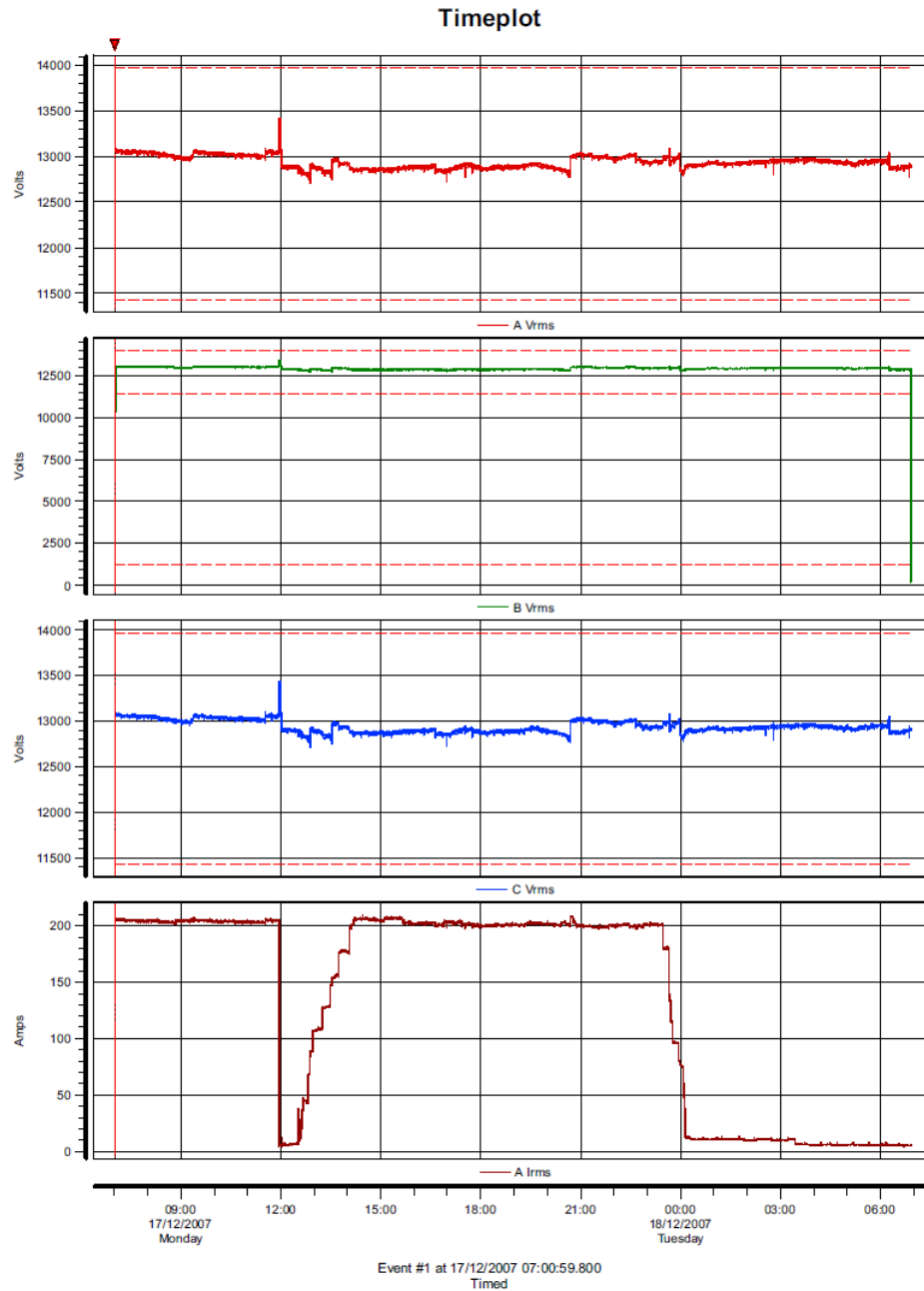


**Figure 8-1 Voltage and current time-plot over 24 hour period**

The Voltage THD time plot in Figure 8-2 shows that the voltage THD does not exceed 2.5% for the maximum plant load. This is well below the planning level of 6.5%. The harmonic spectrum plots indicate that the most dominant harmonics are 5th, 7th, 11th, 13th,... indicating that they are caused by a 6-pulse rectifier. The voltage waveforms indicate the existence of voltage notches. There are 6 notches, 2 per each phase in each cycle. This is caused by the same 6-pulse rectifier.

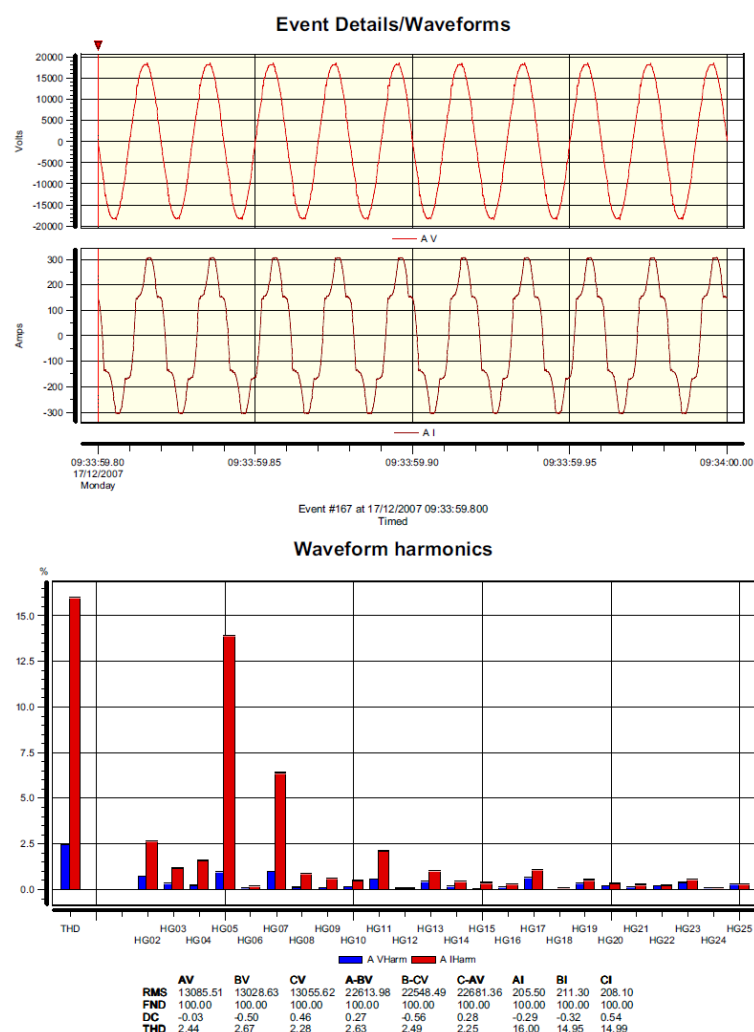


**Figure 8-2 Voltage and current time-plot over 24 hour period**

The measurements show that the largest load on the 22kV Main switchboard was the rectifier load. It can be seen that the load current was around 200 A. The Current THD was around 16%. The 5th harmonic is approximately 13%, 7th is 6%, 11th is 2%, 13th is 1%, 17th is 1% and 19th is 0.5%. The most dominant harmonic numbers in the feeder circuit are typical for a 6-pulse rectifier.

The harmonics generated by the rectifier plant non-linear load are mainly absorbed by the PFC unit. The current harmonics on the PFC feeder are shown in Figure 8-3. It can be seen that the PFC feeder current under steady state conditions is around 135A. The 5th harmonic absorbed by the PFC is approximately 11%, 7th is 3.5%, 11th is 1%, 13th is 1%,... The PFC absorbs all spectrum of current harmonics, however the most significant ones are the 5th and 7th harmonics.

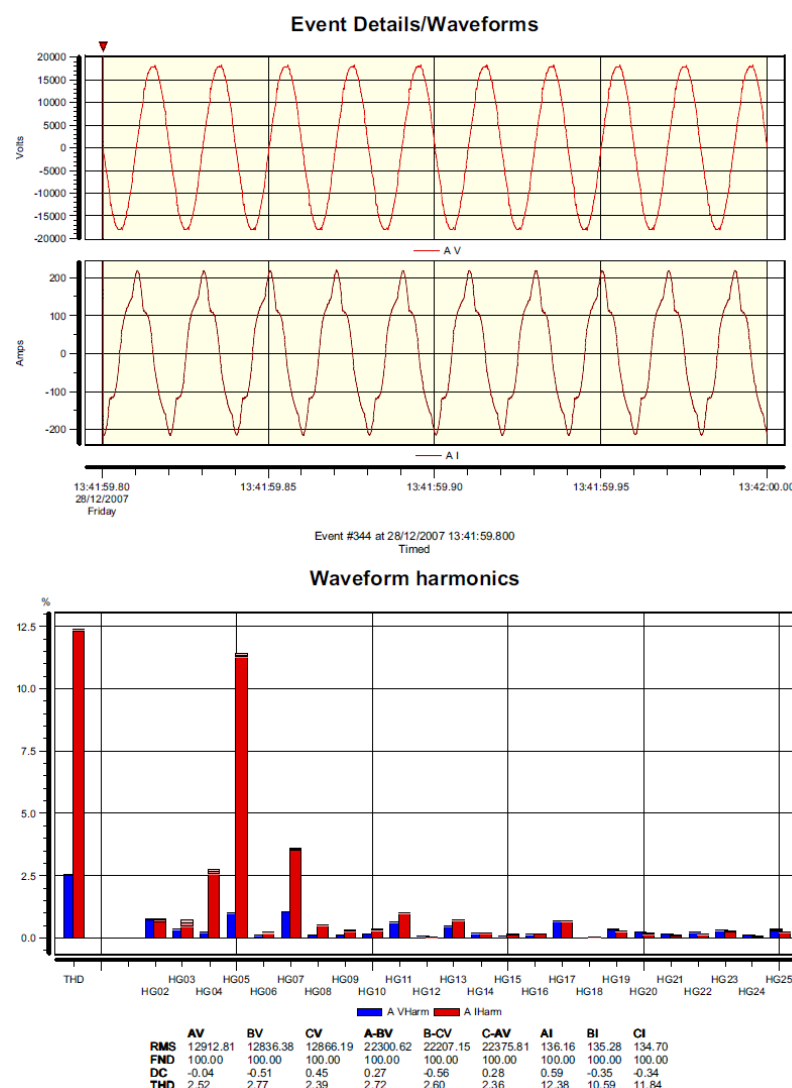


**Figure 8-3 Voltage and current time-plot over 24 hour period**

## 8.7 Discussion of Results

The harmonic currents are generated by non-linear loads. The most significant single non-linear load on the 22kV system is a 6-pulse rectifier. The harmonic currents generated by the 6-pulse rectifier are sent back to the main 22kV bus. A significant part of the harmonic currents is absorbed by the power factor correction unit, which acts as a harmonic filter and the rest of the harmonic currents are sent back to the Western Power network.

The results show that individual voltage harmonic distortion and total voltage harmonic distortion on the 22kV bus do not exceed the planning levels listed in Table 1. The maximum voltage THD is only 2.5%, which is well within the planning



limit of 6.5%. In the same way, each individual harmonic is well below the level in Table 1.

The plant meets the planning criteria regarding voltage harmonics and there is sufficient capacity within the system to absorb an additional level of current harmonics before the voltage planning levels are exceeded. It is not possible to predict the remaining capacity load available purely on these results.

The level of the current harmonic on the incomer feeder is within the limits set by IEEE and listed in Table 2. This is usually not achievable for 6-pulse rectifier loads without additional filtering. The plant has a set of harmonic filters on the 22kV bus which prevent the current harmonic levels as set-out by IEEE from being exceeded.

## **9. APPENDIX 2 - POWER SYSTEM MODELLING AND HARMONIC ANALYSIS**

### **9.1 Introduction**

The harmonic measurements carried out on The Plant are summarised in Appendix 1 of this thesis. The purpose of this study is to develop a power system model, carry out harmonic analysis for the existing power system, and verify the model against the measurements. This model will then be used as a basis for further harmonic studies.

### **9.2 Purpose**

Harmonic measurements indicated that the most significant source of current harmonics on the plant power system is the plant rectifier feeder. The measurements showed that the majority of the current harmonics were absorbed by a single tuned PFC unit located at the main 22kV switchboard, and that the total harmonic distortion figure on the main 22kV bus was well within the recommended planning level of 6.5%. It was found that the level of current and voltage harmonics on the existing system were not a concern.

The purpose of this study is to develop a power system model for the existing system, and to verify the model against the harmonic measurements. The study aims to test model sensitivity for various operating configurations that were captured during harmonic measurements. For each case, the results of harmonic analysis will be verified against harmonic measurements.

The voltage distortion caused by the harmonic currents, is a function of both the system impedance, and the amount of harmonic current injected into the system. Power system harmonic studies are a cost effective way to analyse system performances, as they take into consideration the non-linear nature of system loads and can easily be performed for various system configurations.

### **9.3 Scope**

#### **9.3.1 Data Collection**

The existing system consists of various components such as switchboards, transformers, cables, motors and rotating and static loads. Data collection was limited to the equipment types, listed below. The list indicates the source of the data collected for each of the equipment types:-

- 132kV Western Power infinite network – previous system study
- 132/22kV transformer, 22kV earthing transformer, 22/3.3 kV transformers, 22/.433 kV transformers – nameplate data
- 22kV switchboards, 415V MCCs – nameplate data and single line diagrams
- 22kV cables – single line diagram
- 22kV PFC – data sheets
- 415V PFCs – 3 line schematics and nameplate data
- Motor loads and shunt loads – load list, site survey
- Non-linear loads – site survey (harmonic measurements)

Data collection was co-ordinated between the operations and engineering teams. Equipment data sheets and single line diagrams were provided by the engineering team. Site survey and collection of nameplate data was carried out by the project team.

#### **9.3.2 System Modelling**

The system configuration, or network topology, that was used in the model, was based on the plant single line diagrams. Only the major components of the system, which are shown in the single line diagrams, were modelled. The parameters of the system components were selected to reflect static system modelling requirements and were expanded to cover harmonic analysis studies.

### **9.3.3 Harmonic Analysis Study**

The following harmonic analysis study cases were carried out for the purpose of model verification. Each study case represents a typical snapshot of the power system based on data captured during harmonic measurements.

- Study case 1 – Normal operation, normal running plant load, 22kV rectifier feeder and power factor correction capacitor feeder both switched on. The 6-pulse rectifier load was modelled with a set of harmonic currents and harmonic angles.
- Study case 2 – Normal operation, normal running plant load, 22kV rectifier feeder and power factor correction capacitor feeder both switched on. The 6-pulse rectifier load was modelled with a set of harmonic currents. Harmonic angles were set to zero.

The harmonic study report for each study case contains a full list of harmonic voltages at each network bus and harmonic currents at the branches.

## **9.4 Methodology**

### **9.4.1 Assumptions**

The ETAP software package is widely used within the industry and the calculation methods used in ETAP are based on the relevant industry standards. The package supports the equivalent IEEE and IEC models.

Operations Technology, Inc. (OTI), designers and developers of ETAP, work under the strict Quality Assurance program and the OTI company is Registered to ISO 9001, Certificate No A3147 UL. The Quality Assurance Plan covers an extensive process of verification and validation throughout the lifecycle.

As stated by OTI, the verification and validation method for ETAP is quite extensive consisting of thousands of test cases that encompass each and every calculation module, user interface, persistence, reports, plots, and library data. The test cases include a comprehensive comparison of study results and system performances against hand calculations, field measurements, industry standards (ANSI/IEEE, IEC,

UL) and other established methods, in order to ensure and verify ETAP's technical accuracy and performance stability.

The quality assurance process, as described by OTI, guarantees validity of the results, so an independent validation exercise has not been carried out. Sample validation cases for ETAP harmonic analysis are available from the ETAP website at [www.etap.com](http://www.etap.com).

#### **9.4.2 Data Collection**

The data used for the study were classified as either site or final vendor data. Vendor data were listed on equipment data sheets, performance data sheets and engineering drawings. The final test data recorded on test certificates, where available, have been utilised in the study.

The results of the harmonic measurements were taken from the results of harmonic measurement project described in Appendix 1. The project team carried out a site survey and collected the nameplate data for power transformers and major switchboards. The data were summarised and stored in the power system model, under the information tab for each component.

#### **9.4.3 Power System Modelling**

Modelling of the key components of the electrical power system was carried out in accordance with the relevant IEEE standards and the ETAP modelling technique.

Distribution transformers were modelled as 2-winding transformers. The transformer model was based on an equivalent impedance circuit. The positive sequence impedance was divided equally between the primary and secondary winding. The negative sequence impedance was assumed to be 100% of the positive sequence impedance. The value of impedance was taken from the data sheet and a typical X/R ratio was selected from the ETAP library. The transformation ratio of an ideal transformer was entered into the model.

Cables were modelled as passive elements, represented by an equivalent impedance model for short overhead lines. Positive sequence impedance was represented as line impedance comprising a resistance and reactance component. The capacitance of the

cable was neglected. Zero sequence impedance was equal to the positive sequence impedance.

The MV and LV loads on each bus were modelled as a composite load comprising of a group motor load and static load. The ratio of rotating to static loads varied for different MCCs; on average the rotating load was 80% and static load was 20%.

#### **9.4.4 Harmonic Analysis Calculation Method**

The harmonic analysis study was carried out using the ETAP Power System Analysis Software. The package comprises a number of analysis modules integrated into a single package. The package modules used for the harmonic study utilised a common model comprising positive and zero sequence impedances of the network components. The model is best described as a static model and all impedances of the system were calculated at a nominal frequency of 50 Hz.

The power system impedances of the static model used in the load flow study were expressed at the fundamental frequency of 50 Hz. In harmonic analysis these impedances were varied as a function of frequency, and for an integer multiple of the fundamental frequency the system was represented with the equivalent impedance.

Non-linear loads were modelled as ideal current sources at multiple frequencies (Norton's impedance across the source was neglected). The system was subjected to current injections at multiple frequencies and the network was solved for voltage and current at each frequency separately. The total voltage or current in an element was then found either by a root-mean-square sum or arithmetic sum, using the principle of superposition.

### **9.5 Harmonic Analysis and Model Verification**

#### **9.5.1 General**

The switchboards, transformers and circuit breakers were identified with their unique tag numbers which correspond to tag numbers shown on the single line diagram. This approach enabled direct identification of the system components shown in the model. Electrical switchboards and MCCs were shown with a line symbol. The

132kV network was connected to the 22kV switchboard via the 132/22kV transformer.

The 22kV switchboard was interconnected with the 3.3 kV and 415V switchboards via the 22/3.3 and 22/.433 power transformers, respectively. Each transformer was modelled as a 2 winding transformer. Transformer connection symbols were shown next to each transformer component symbol. The vector group was shown in the transformer schedule. The 22kV feeder cables were shown with a cable symbol. Each cable was given an ID number. The loads on each section of the 3.3 kV and 415V MCCS, were combined into a lumped load and shown as a composite load, one composite load per switchboard section. The composite loads on LV MCCs were selected as 80% motor loads and 20% static loads. The 22kV PFC was modelled as a single tuned filter.

The first level of model verification was carried out via a load flow study. The load flow calculation identified any inaccuracies, errors, omissions or inconsistencies of the input data. The load flow study confirmed input data consistency. It also indicated good correlation of the measured and calculated data.

### **9.5.2 Harmonic Analysis – Case 1**

Harmonic analysis was carried out using the base model. The loads were normal running plant loads as per the load flow study. The 22kV rectifier feeder and power factor correction capacitor feeder were both switched on.

The 6-pulse rectifier was modelled with a set of harmonic currents and angles, determined by harmonic measurement analysis: Event #1050 at 16/12/2007 00:54:59.800 Timed, refer to Figure 9-1. The tabulated data are listed in Table 9-1.

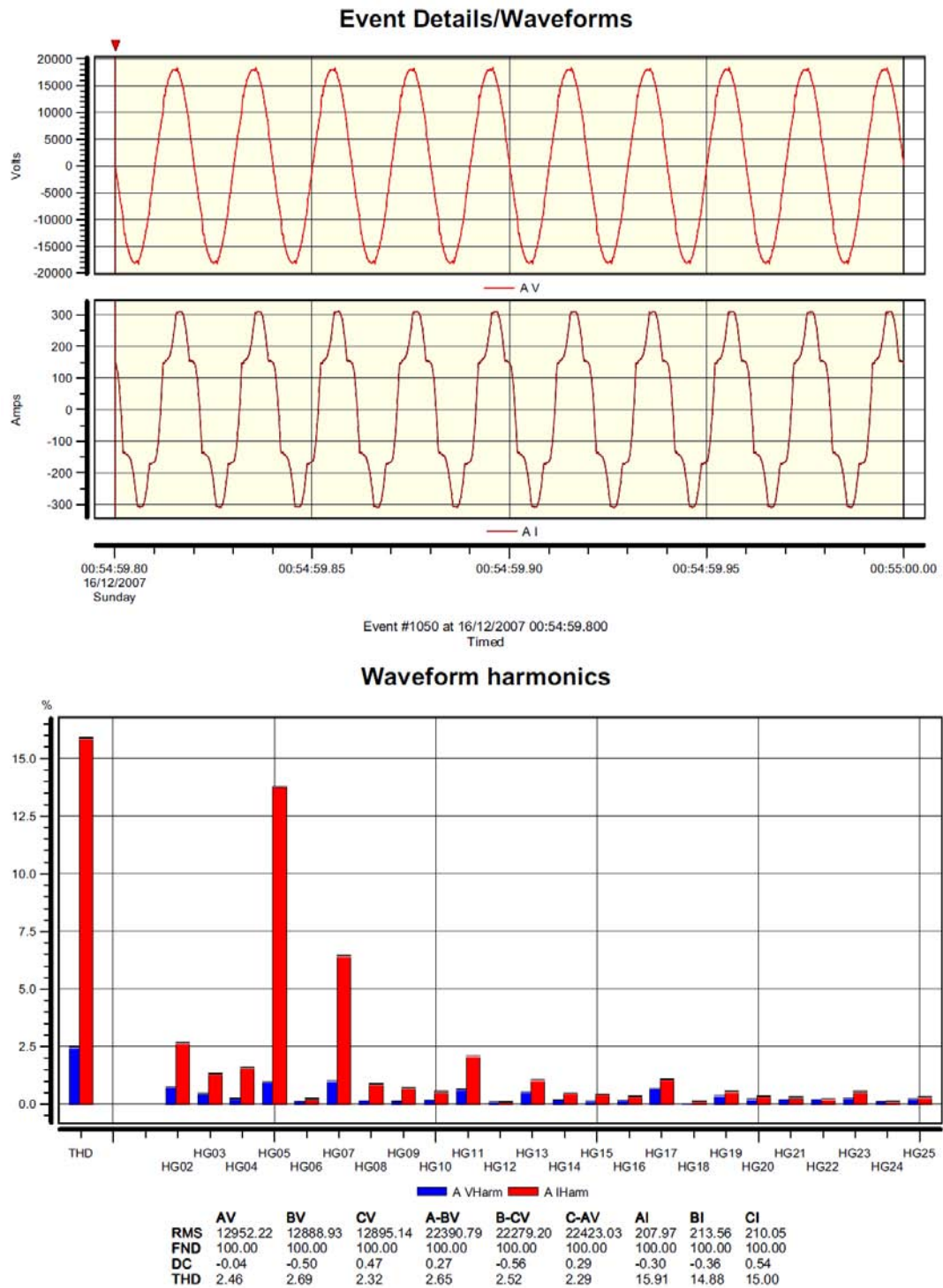


**Figure 9-1 Voltage and current time-plot on rectifier feeder**

X-Data	AIHarmMax[%]	A°IHarmMax[Deg]
THD	15.933	
H02	2.7006	0.7127
H03	1.3462	189.99
H04	1.6086	125.2



<b>X-Data</b>	<b>AIHarmMax[%]</b>	<b>A°IHarmMax[Deg]</b>
H05	13.807	241.7
H06	0.24288	236.16
H07	6.447	15.426
H08	0.9213	337.8
H09	0.7139	206.41
H10	0.5534	108.72
H11	2.1288	237.2
H12	0.09715	279.08
H13	1.07	347.7
H14	0.4879	304.4
H15	0.4343	169.94
H16	0.3503	80.59
H17	1.0972	197.84
H18	0.1333	242.82
H19	0.5612	331.2
H20	0.3529	274.52
H21	0.30743	134.33
H22	0.23716	54.15
H23	0.5489	160.9
H24	0.1295	215.21
H25	0.31211	295.51

**Table 9-1 Harmonic source input data**

The measured data are typical for the maximum demand load, captured during the harmonic measurements.

The harmonic load flow printout shows that current THDi on the rectifier feeder is 15.4% (based on 214A at 22kV). The harmonic filter PF-501 absorbs 11.42 THDi (based on 144.9A at 22kV). A total of 3.2% of THDi is injected back into the SWIS (based on 85.4A at 132kV). The harmonic measurements indicate 16% THDi on the rectifier feeder, 11% THDi on the power factor capacitor feeder, and 4% on the incomer (measured at 22kV side). This shows a good correlation between the data measured and simulation. It was observed that the current waveform on the rectifier feeder deviated from the current waveform captured during measurements. For this

reason the input data were varied and a separate case study (Case 2 below) was performed in order to get better correlation with measured data.

The frequency scan indicates that the existing harmonic filter is a single tuned filter. The tuned frequency is set at 200 Hz, a safe margin from the most dominating fifth harmonic.

### 9.5.3 Harmonic Analysis - Case 2

Harmonic analysis was carried out using the base model. The loads were normal running plant loads as per the load flow study. The 22kV rectifier feeder and power factor correction capacitor feeder were both switched on.

The base model was the same one as used in case study 1. The difference between cases 1 and 2, is that the harmonic source of the 6-pulse rectifier was modelled with all harmonic angles set to zero.

Analysis showed that the current waveform on the rectifier plant feeder closely matches the current waveform captured during measurements, refer to Figure 9-2.

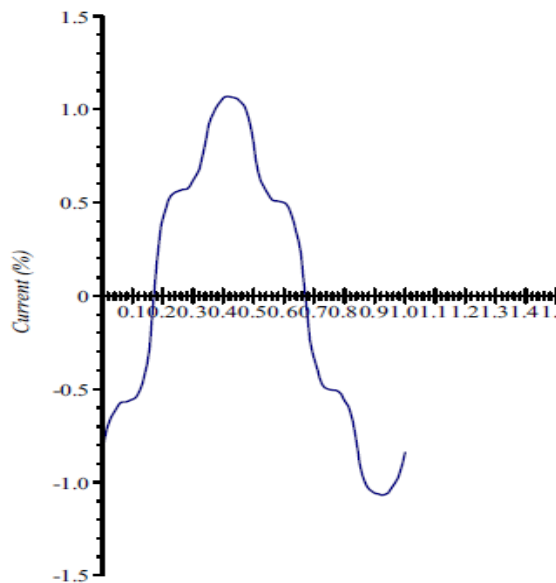


**Figure 9-2 ETAP simulation - rectifier feeder current waveform**

## **9.6 Discussion of Results**

The power system harmonic analysis involved modelling the frequency characteristics of different components of the power systems, and computing harmonic parameters, such as harmonic current, harmonic voltage and THD, at various buses and branches. Harmonic analysis identified problems associated with the existing harmonics, and provided a tool to simulate and test any modifications to the power system.

The ETAP harmonic analysis module consisted of two analytical methods, the load flow and harmonic frequency scan methods. Both methods were used, and both methods employed the same impedance based model.

The load flow study verified model parameters, and eliminated any inconsistencies, errors or omissions of the input data. The load flow study results showed a good correlation with plant site data.

The results of the harmonic analysis were dependent on the harmonic source and harmonic currents injected into the system. Results of case study 1 and 2 showed that the harmonic waveform was dependent on harmonic angles.

## **9.7 Conclusions and Recommendations**

The power system model was developed using the ETAP power system analysis software package. The model topology was based on the plant single line diagram and incorporated major switchboards, power transformers, 22kV cables, harmonic filter and various loads. The system components were modelled in accordance with IEEE/IEC recommendations.

Input data of the system components were based on equipment data sheets and nameplate data collected during a site survey. The loads were based on site measurements.

The model input data were verified by load flow study. Harmonic analysis was carried out for maximum plant running load. Typical harmonic source data selected from harmonic measurements were used in the study. Harmonic source currents were

injected at the 22kV rectifier feeder bus. Harmonic voltages were calculated at each system bus and harmonic currents were determined for each branch.

The results were compared with harmonic measurements. It was concluded that a simplified model verification methodology confirmed good correlation between calculated and measured data. The model developed in this study can be used as a base model for further harmonic studies.

## **10. APPENDIX 3 - HARMONIC MEASUREMENTS ON A MINERAL PROCESSING PLANT**

### **10.1 Introduction**

This Appendix covers the following scope of the harmonic measurement project:-

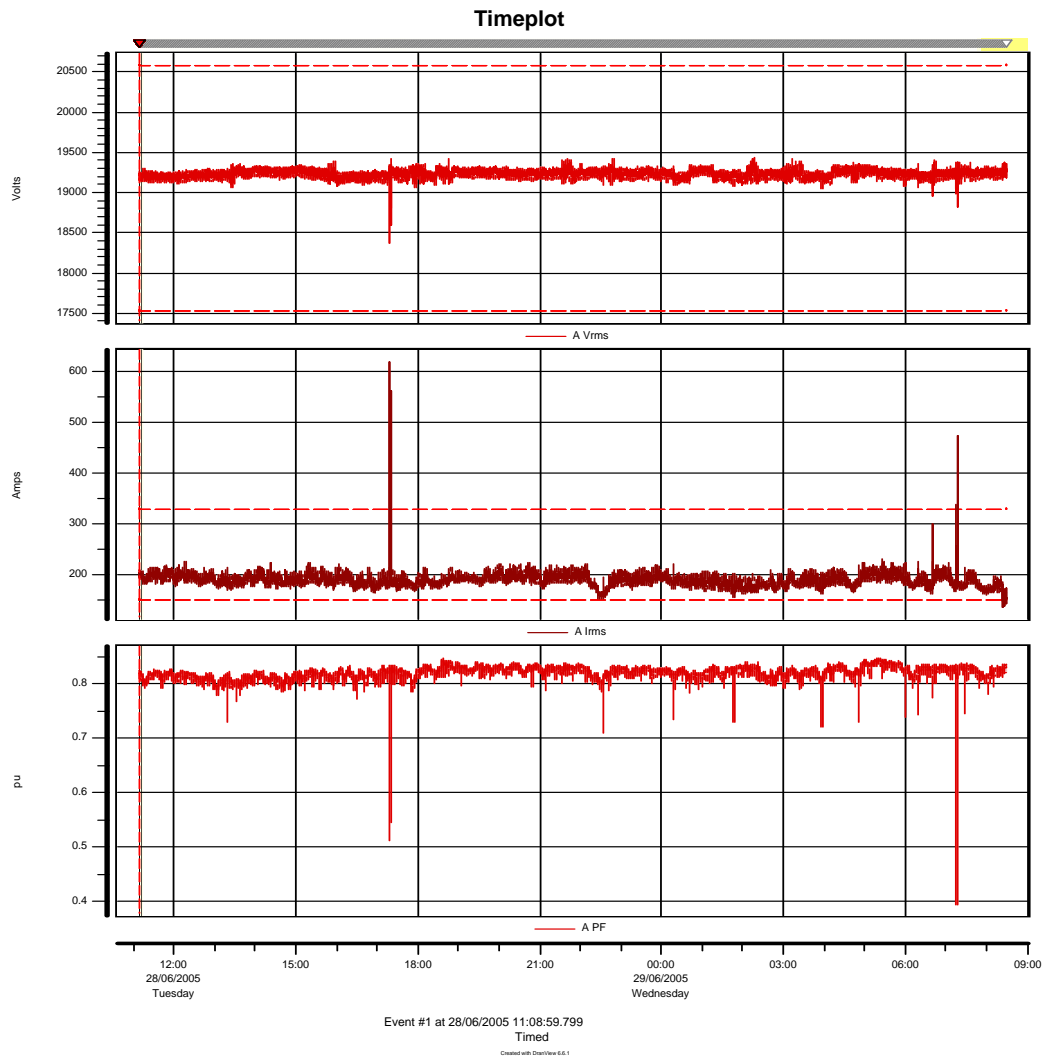
1. Harmonic measurements and harmonic analysis for various system configurations such as SAG mill normal running, creeping and inching modes;
2. Discussion of the results and acceptance criteria with recommendations for further works.

### **10.2 Harmonic Analysis for Normal Mode of Operation**

The normal mode of operation has the following system configuration:-

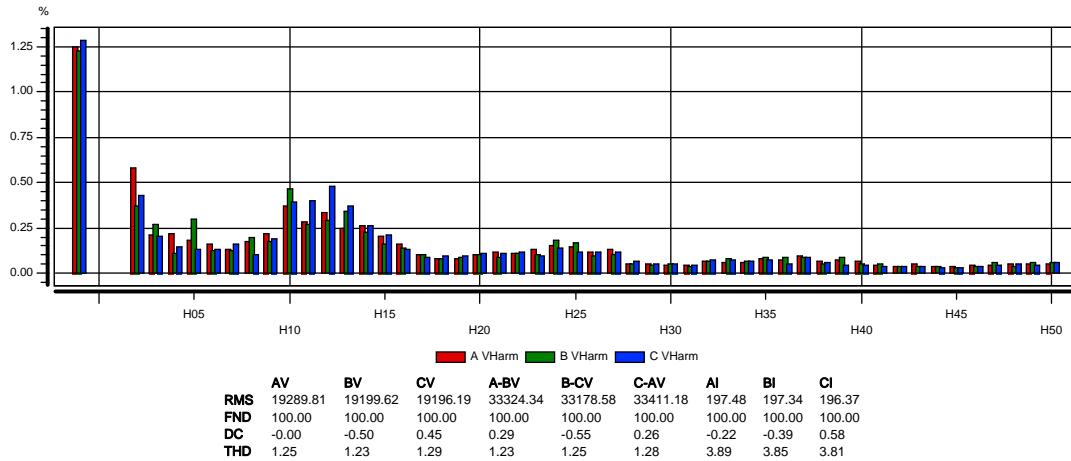
- 2 gas turbines and secondary power station on line
- 2 generator incomers and all feeder breakers on the primary power station 33 kV switchboard are closed
- At the treatment plant switchboard the bus tie circuit breaker open and all incoming and outgoing feeder breakers closed, both train 1 and 2 SAG mills and ball mills running.

For harmonic analysis at the power station main switchboard, the results of analysis comprising voltage and current time plots, voltage and current waveforms and the waveform harmonics are attached in the figures below. The time plot diagram, Figure 10-1 shows voltage, current and power factor of the red phase captured from 11:00am on 28/06/05 to 09:00am on 29/06/05 on the inter-connector feeder.

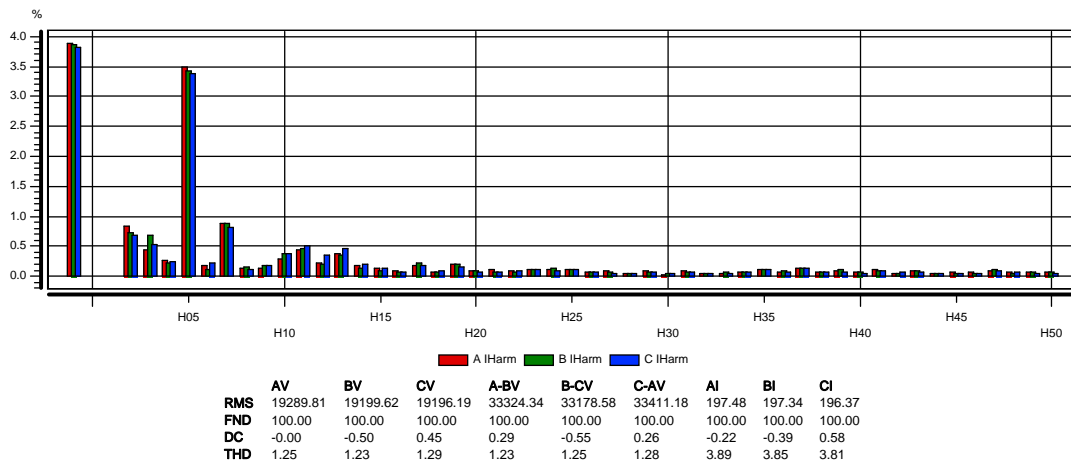


**Figure 10-1 Timeplot of electrical parameters**

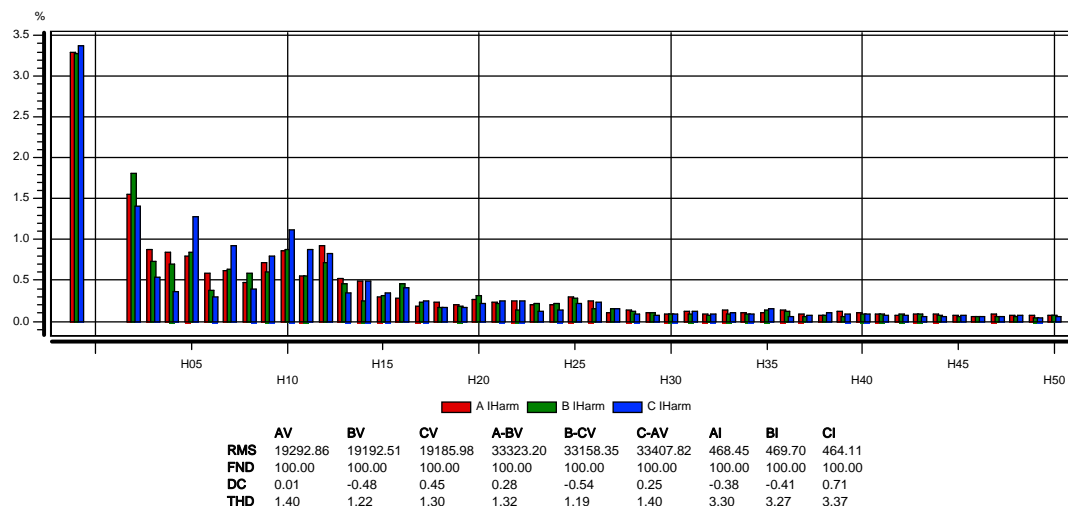
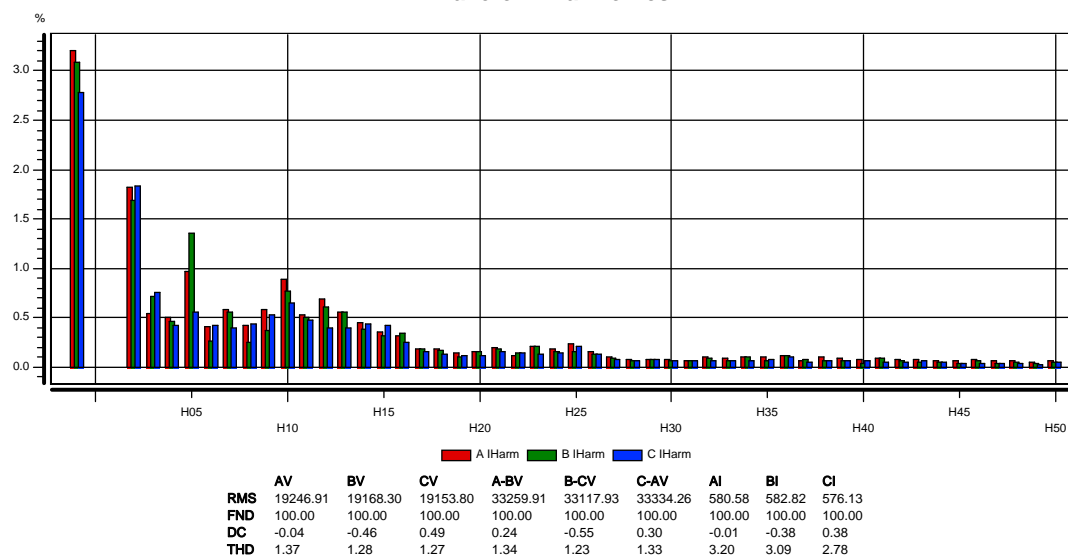
The typical harmonic spectrum, Figure 10-2 recorded at 19:58:59 on 28/06/05 shows that the total THDv is below 1.5%. The individual harmonics are below 0.5%. The most dominant harmonics are grouped between the 10<sup>th</sup> and 13<sup>th</sup> and around the 2<sup>nd</sup>, which indicates that the harmonics are mainly caused by operation of the SAG mill cyclo-converters.

**Waveform harmonics****Figure 10-2 Voltage harmonics on the 33 kV switchboard**

The total THDi on the inter-connector feeder, Figure 10-3 is around 4% (the rms value of current is 200A) with the 5<sup>th</sup> harmonic being the most dominant, around 3.5%, followed by the 7<sup>th</sup> harmonic, around 1%. The source of the harmonics is a 6-pulse variable voltage variable frequency drive on the inter-connector feeder.

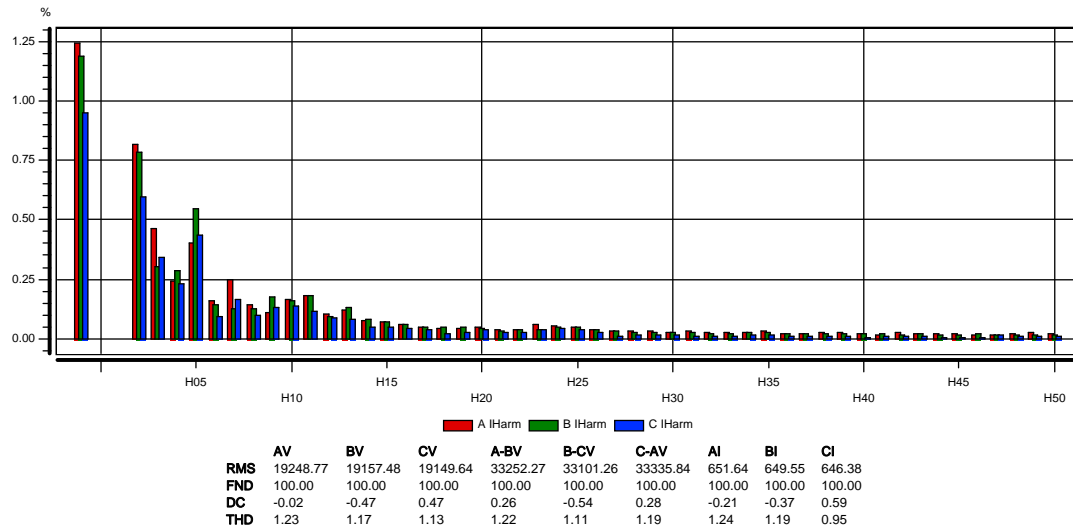
**Waveform harmonics****Figure 10-3 Current harmonics on inter-connector feeder**

The current harmonics on the Train 1 and Train 2 feeders, Figures 10-4 and 10-5 are similar in magnitude. The THDi is less than 3.5% (the rms value of a feeder current is around 500A). The most dominant harmonics are concentrated around the 2<sup>nd</sup> harmonic indicating presence of sub-harmonics generated by the SAG mill cyclo-converters.

**Waveform harmonics****Figure 10-4 Current harmonics on train 1 feeder****Waveform harmonics****Figure 10-5 Current harmonics on train 2 feeder**

The harmonic spectrum on GT#1 incomer is shown in Figure 10-6. The THDi is less than 1.5% (rms current of the incomer is 550A). Most of the harmonics are concentrated around the 2<sup>nd</sup> and the 5<sup>th</sup> harmonic. This indicates that GTs consume the sub-harmonics generated by the SAG mill cyclo-converters; however it does not have any detrimental effect on the safe and reliable operation of the generator.



**Waveform harmonics****Figure 10-6 Current harmonics on a GT**

Harmonics at the Treatment Plant Main Switchboard are of special interest as the SAG mill cyclo-converters are fed from the Treatment Plant 33 kV Switchboard. The time plot diagram, Figure 10-7, shows voltage, current and the power factor of the red phase recorded from 09:00am on 21/04/05 to 09:00am on 22/04/05 on the train 1 incomer feeder. It can be seen that the voltage was steady with a number of the switching events over the 24 hour period. During the normal operation, with both SAG mill and ball mill running, the power factor on the train 1 incomer was steady and around the unity power factor. When both the SAG mill and ball mill were shut down the power factor changed to 0.6 leading. This is due to the 3<sup>rd</sup> and 4<sup>th</sup> harmonic filter being kept on line with no other significant load connected to the switchboard.

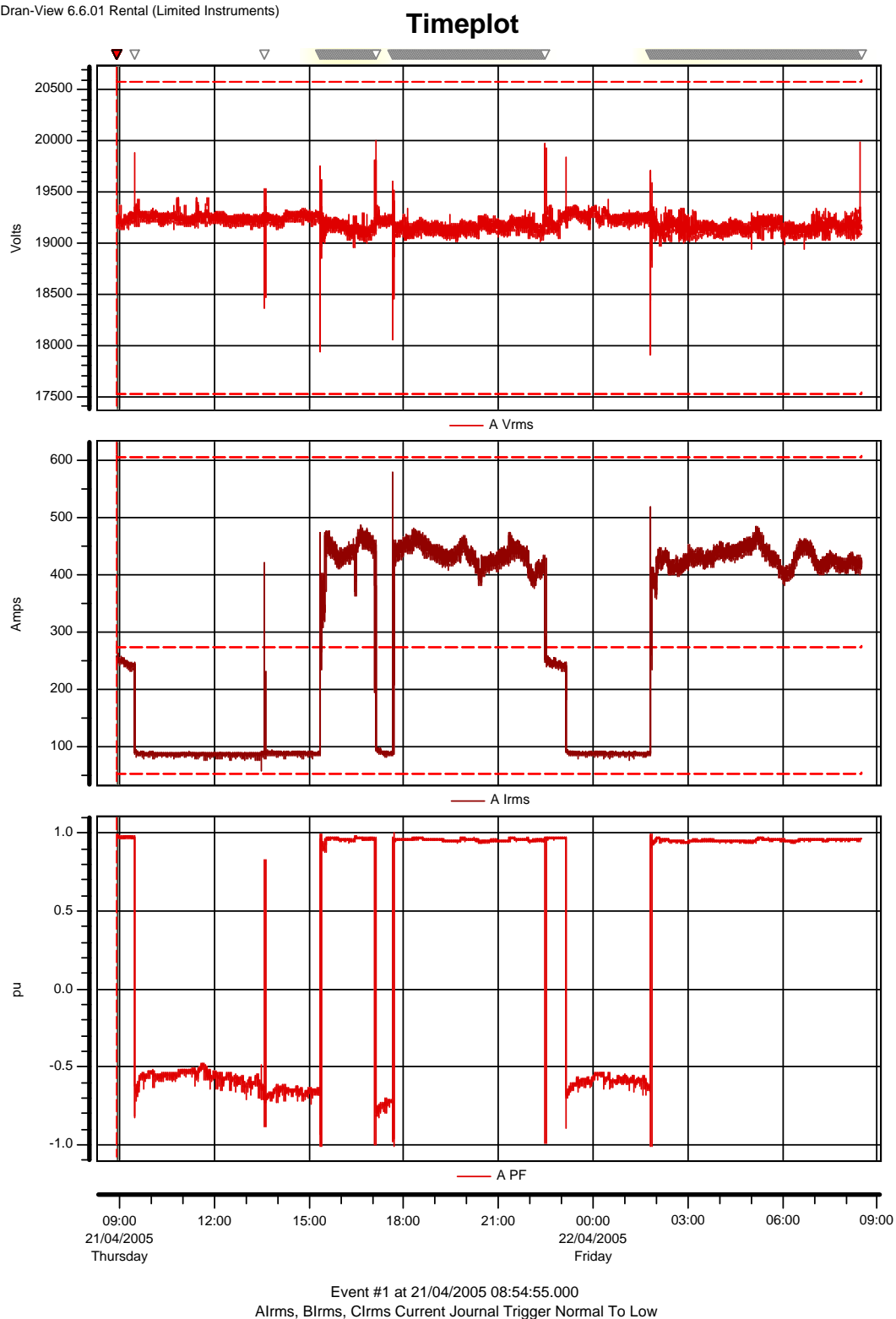


**Figure 10-7 Voltage, current and power factor timeplot**

The typical voltage harmonic spectrum as recorded at 07:11:59 on 22/04/05 is shown in Figure 10-8 below. The total THDv is below 1.5%. The individual harmonics are below 0.5%, with exception of the 11th harmonic slightly exceeding 0.5%. The most

dominant harmonics are grouped between the 10<sup>th</sup> and 13<sup>th</sup> and around the 2<sup>nd</sup>, which indicates that the harmonics are mainly caused by operation of the SAG mill cyclo-converter.

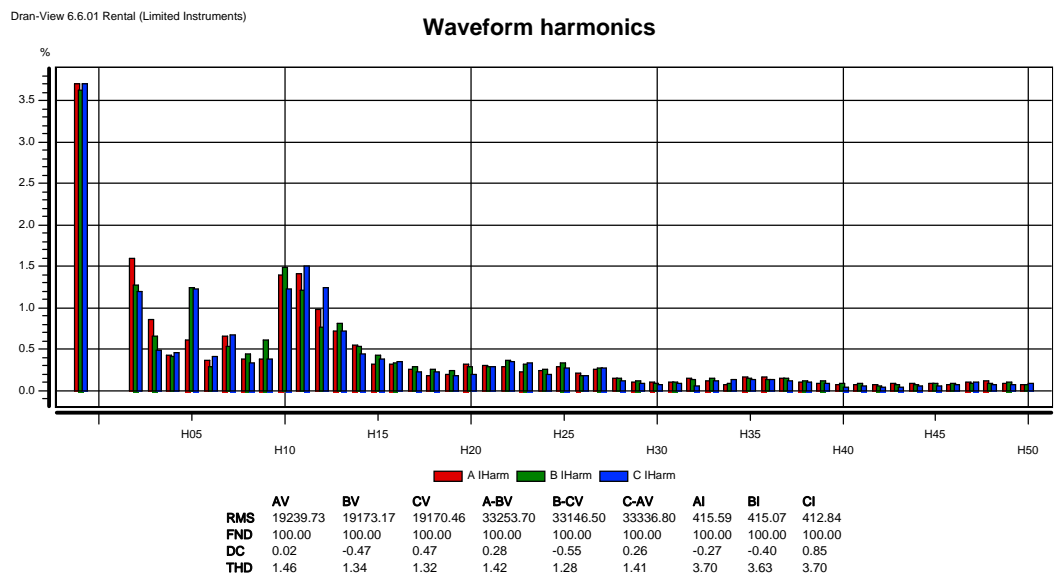


**Figure 10-8 Voltage harmonics**

The typical voltage waveform and harmonic spectrum on the SAG mill feeder, Figures 10-9 and 10-10 recorded at 07:22:59 on 25/04/05 show a total THDi of 8% (the rms value of feeder current is around 250A). The most dominant harmonics are concentrated between the 10<sup>th</sup> and 13<sup>th</sup> and around the 2<sup>nd</sup> indicating the presence of sub-harmonics.

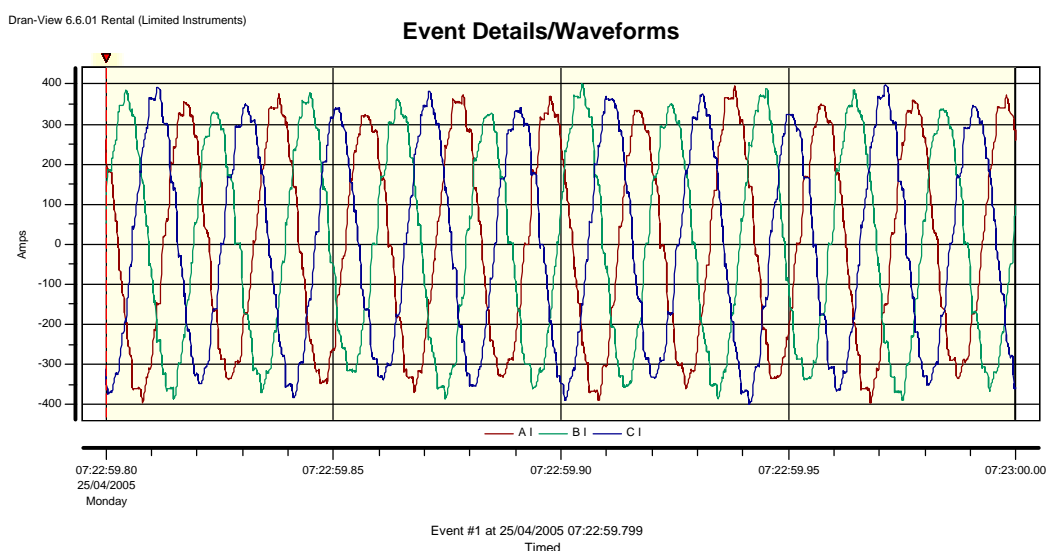


**Figure 10-9 Current waveform on SAG mill feeder**

## Waveform harmonics

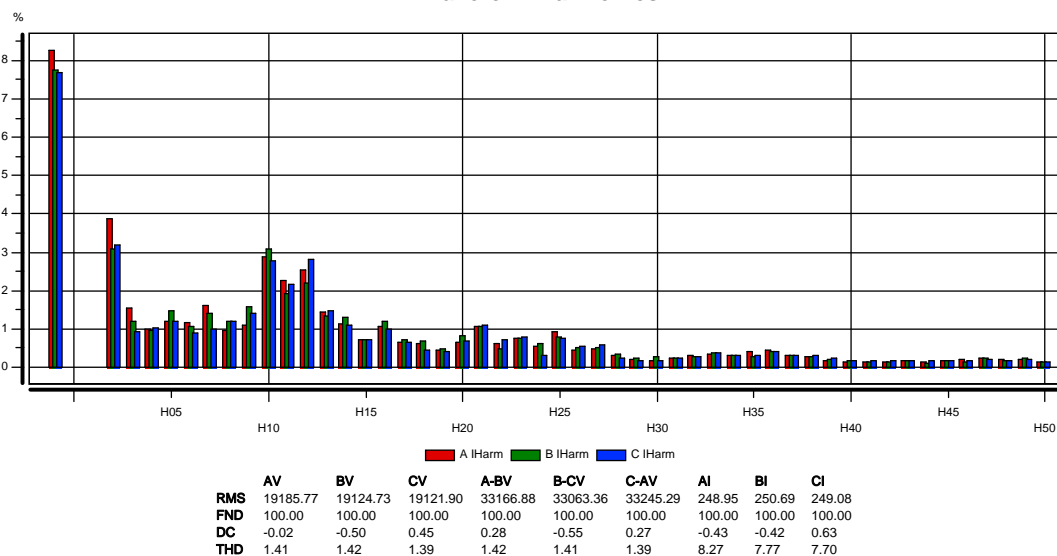
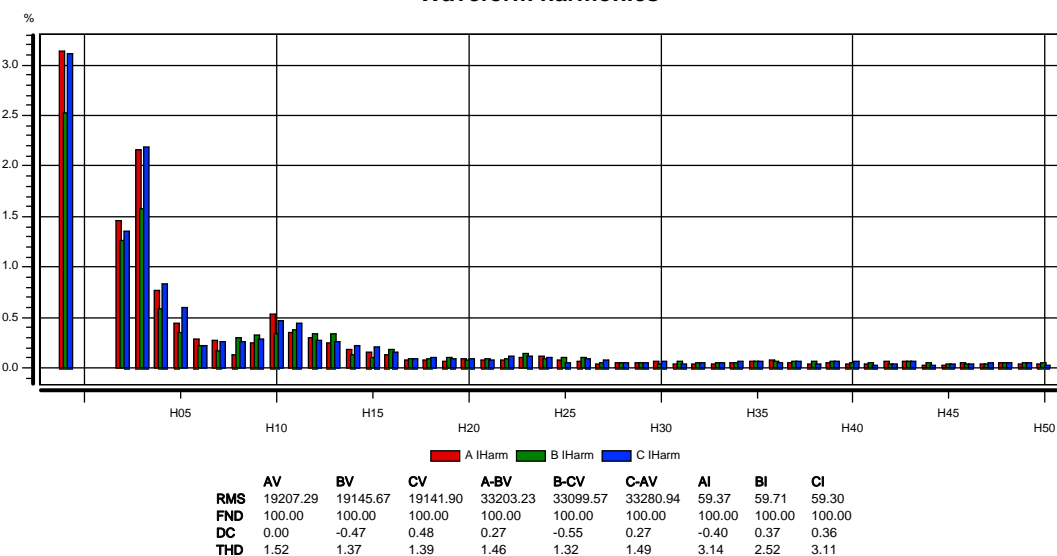


Figure 10-10 Current harmonics on SAG mill feeder

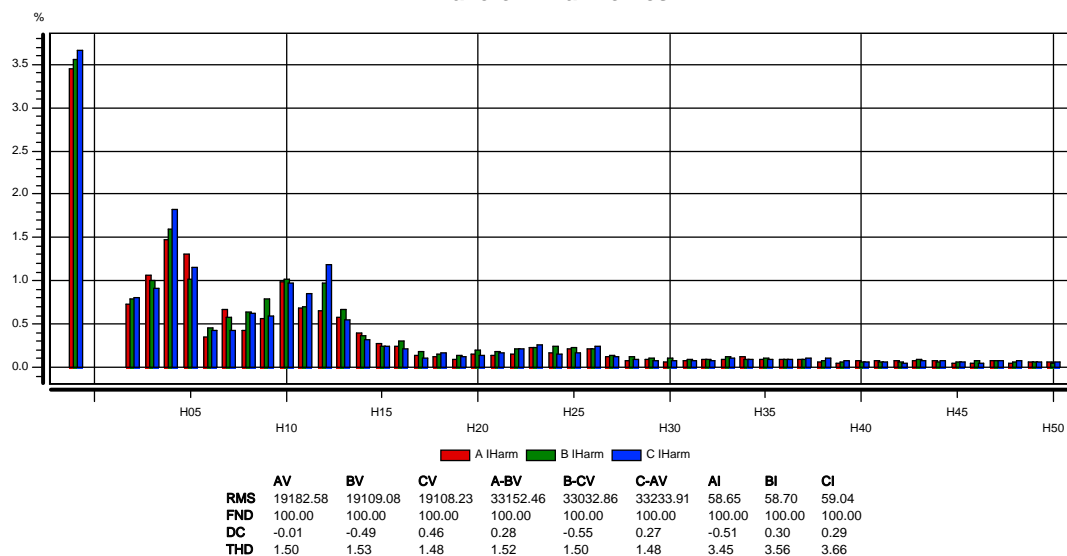
The 3<sup>rd</sup> harmonic filter, Figure 10-11 consumes less than 3% of THDi (rms current is 60A) of which the most dominant individual harmonics are 3<sup>rd</sup> and 2<sup>nd</sup>.

## Waveform harmonics

Figure 10-11 Current harmonics on the 3<sup>rd</sup> harmonic feeder

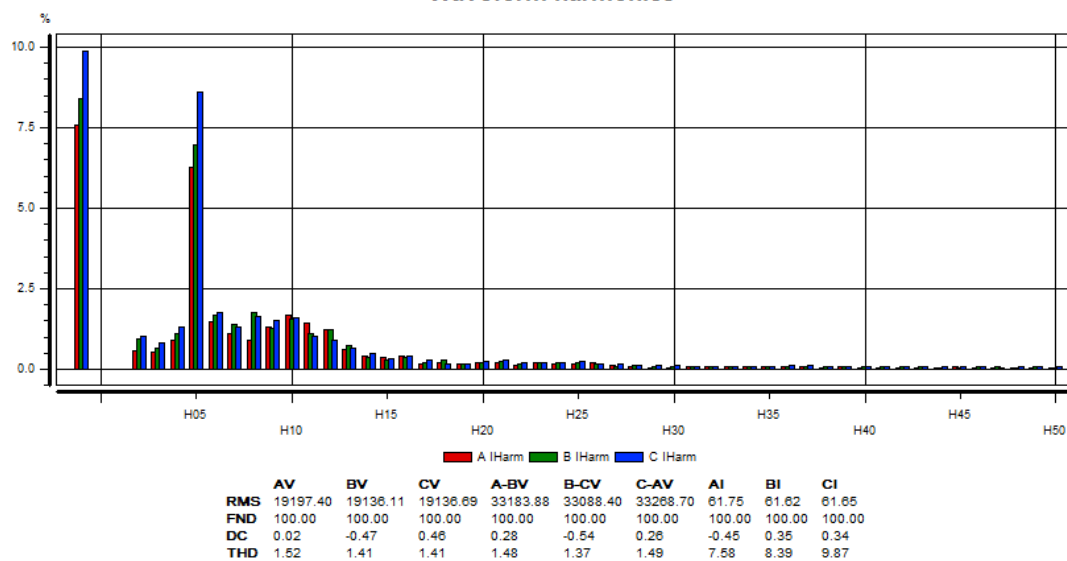
The 4<sup>th</sup> harmonic filter, Figure 10-12 consumes around 3.5% of THDi (rms current is 60A) of which the most dominant are the 4<sup>th</sup> and 5<sup>th</sup> harmonics.

## Waveform harmonics

Figure 10-12 Current harmonics on the 4<sup>th</sup> harmonic feeder

The 5<sup>th</sup> harmonic filter, Figure 10-13 consumes around 10% of the THDi (rms current is 60A) with the most dominant 5<sup>th</sup> harmonic at around 7.5%.

## Waveform harmonics

Figure 10-13 Current harmonics on the 5<sup>th</sup> harmonic feeder

The 7<sup>th</sup> harmonic filter, Figure 10-14 consumes a total of 12.5% of THDi (rms current is 60A). The most dominant harmonics are grouped between the 10<sup>th</sup> and 13<sup>th</sup> harmonics.

## Waveform harmonics

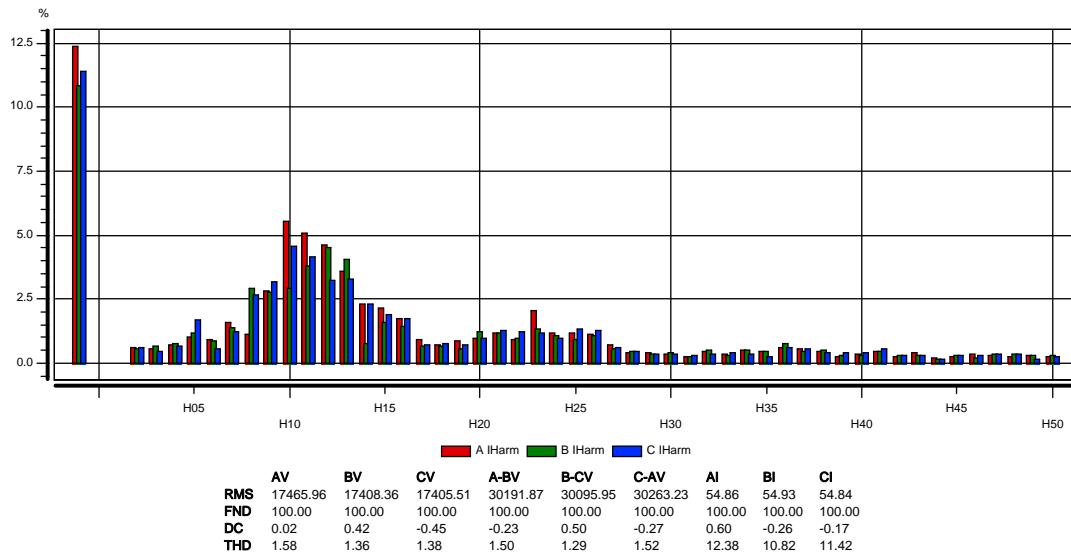


**Figure 10-14 Current harmonics on the 7<sup>th</sup> harmonic feeder**

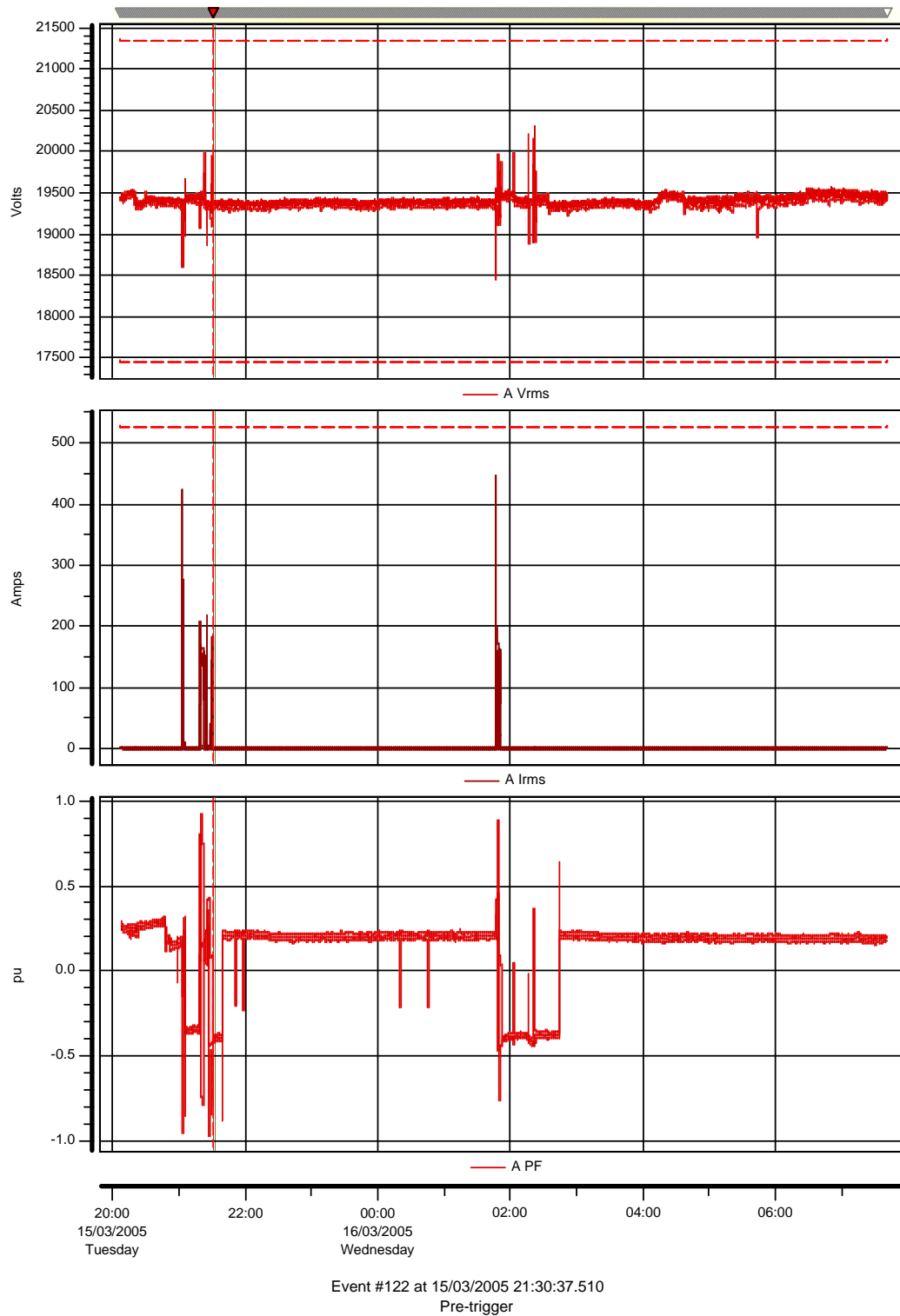
### 10.3 Harmonic Analysis for Inching Mode of Operation

Inching mode of operation is utilised during regular SAG mill maintenance and is best described with the following system configuration:-

- 2 gas turbines and secondary power station on line
- 2 generator incomers and all feeder breakers on the primary power station 33 kV switchboard are closed
- Treatment plant 33 kV switchboard bus tie breaker open and all incomer and feeder breakers closed
- One of the trains has both SAG mill and ball mill running in normal operating mode; the other train is shut down and the SAG mill is run in inching mode when required:-

Harmonics at Treatment Plant Main Switchboard - The time plot diagram, Figure 10-15 shows voltage, current and power factor of the red phase recorded from 20:00 on 15/03/05 till 07:00 on 16/03/05 on the Train 1 switchboard. It can be seen that the voltage was steady with 2 inching cycles recorded during this period.

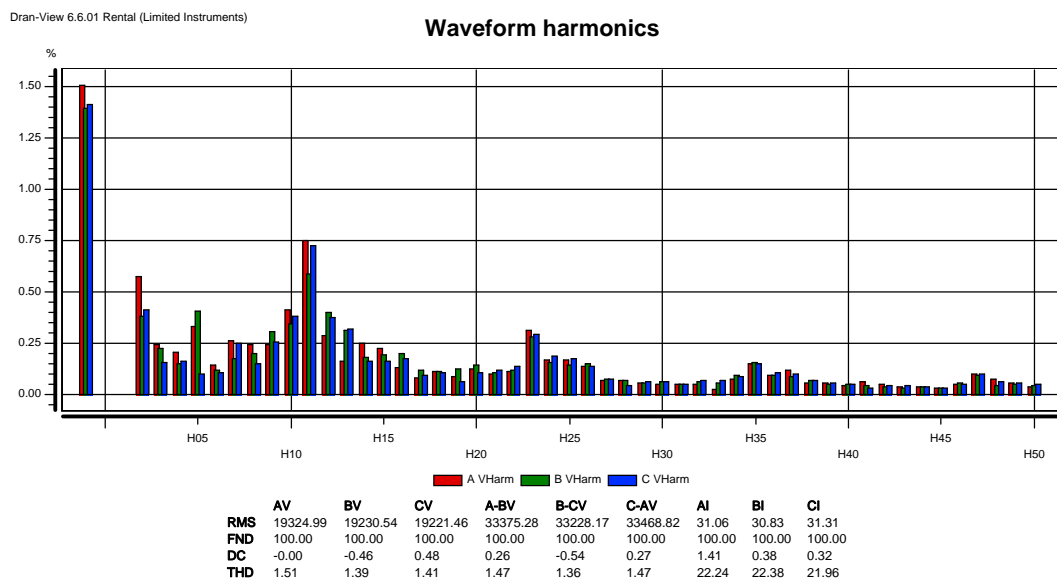
## Timeplot



**Figure 10-15 Voltage, current and power factor timeplot**

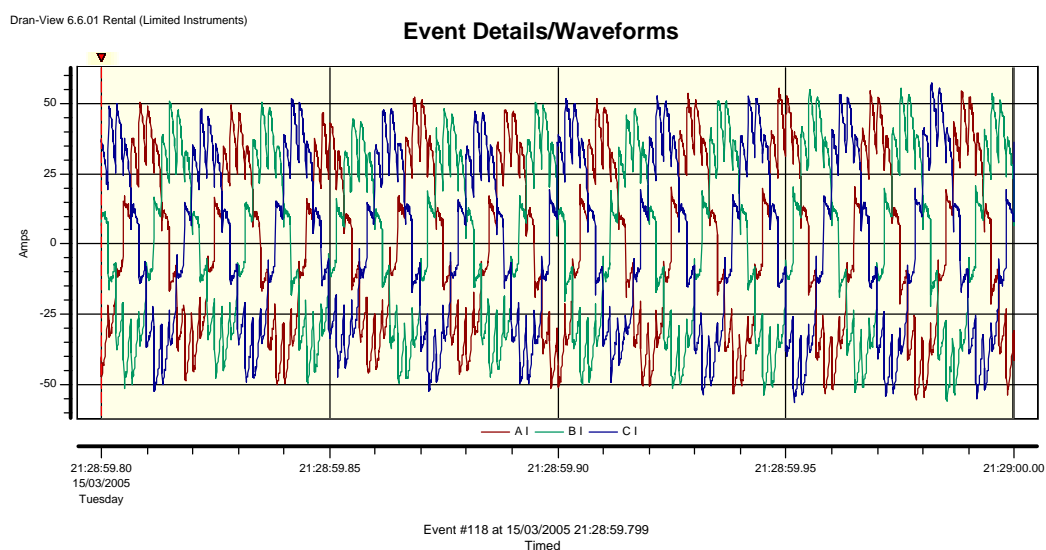
The typical harmonic spectrum, Figures 10-16 recorded at 21:28:59 on 15/03/05 show that the total THD<sub>v</sub> is below 1.5%. The individual harmonics are below 0.75%. The most dominant harmonics are grouped between the 10<sup>th</sup> and 13<sup>th</sup> and around the

2<sup>nd</sup>, which indicates that they are mainly caused by operation of the SAG mill cyclo-converter. The voltage harmonics recorded on the 33 kV switchboard are well within the recommended maximum value of 5% (under 1.5%). The individual voltage harmonics are less than the recommended 3%, (under 0.5%).



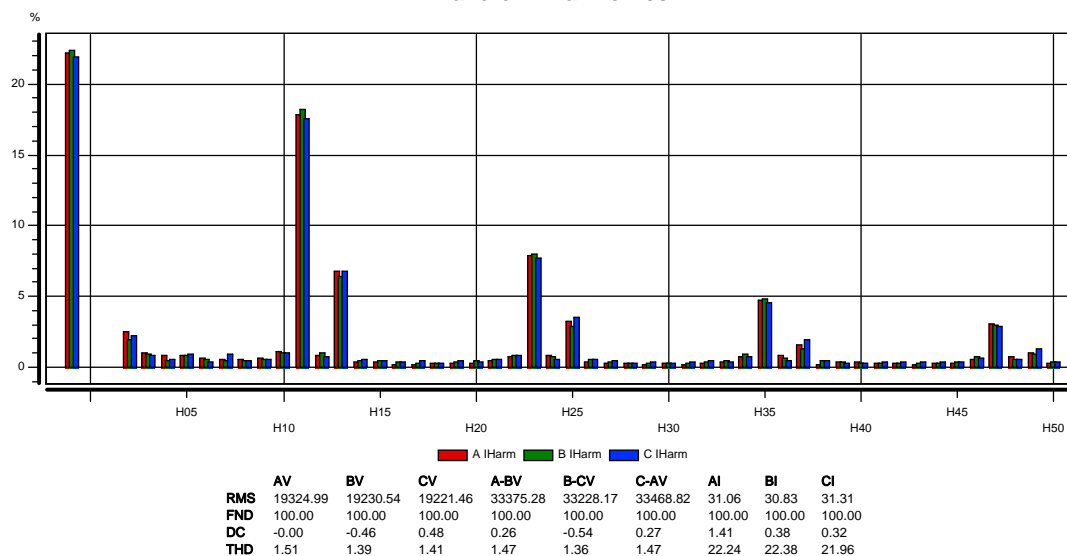
**Figure 10-16 Voltage harmonics at the 33 kV switchboard**

The current waveform and the harmonics on the SAG mill feeder are shown in Figures 10-17 and 10-18, respectively. The current harmonics have a total THDi of 23% (the rms value of feeder current is around 30A). The most dominant harmonics are the 11<sup>th</sup> and 13<sup>th</sup>.

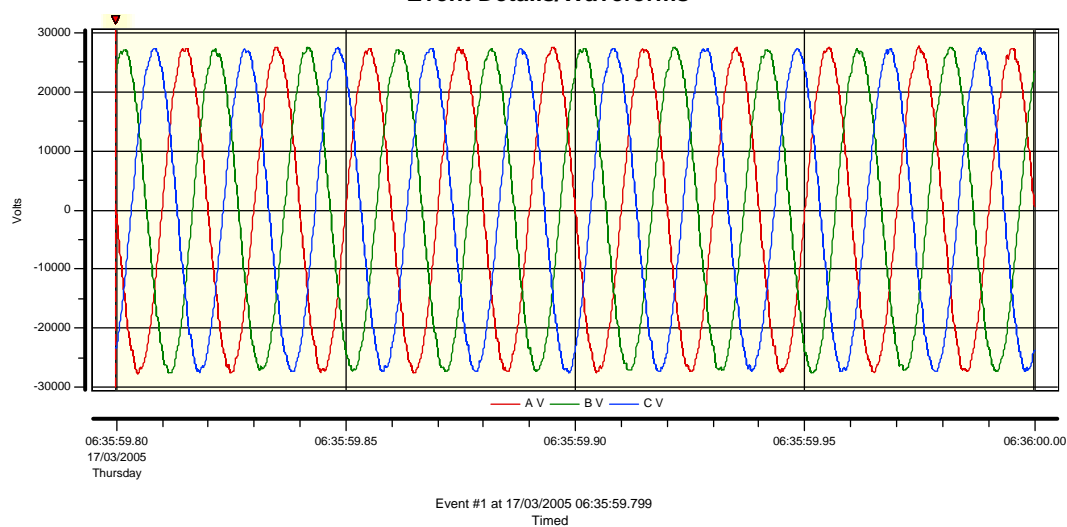


**Figure 10-17 Current waveform on SAG mill feeder**



**Waveform harmonics****Figure 10-18 Current harmonic spectrum**

The current waveform and harmonics on train 1 incomer are shown in Figure 10-19 and 10-20, respectively.

**Event Details/Waveforms****Figure 10-19 Current waveform on Incomer**

## Waveform harmonics

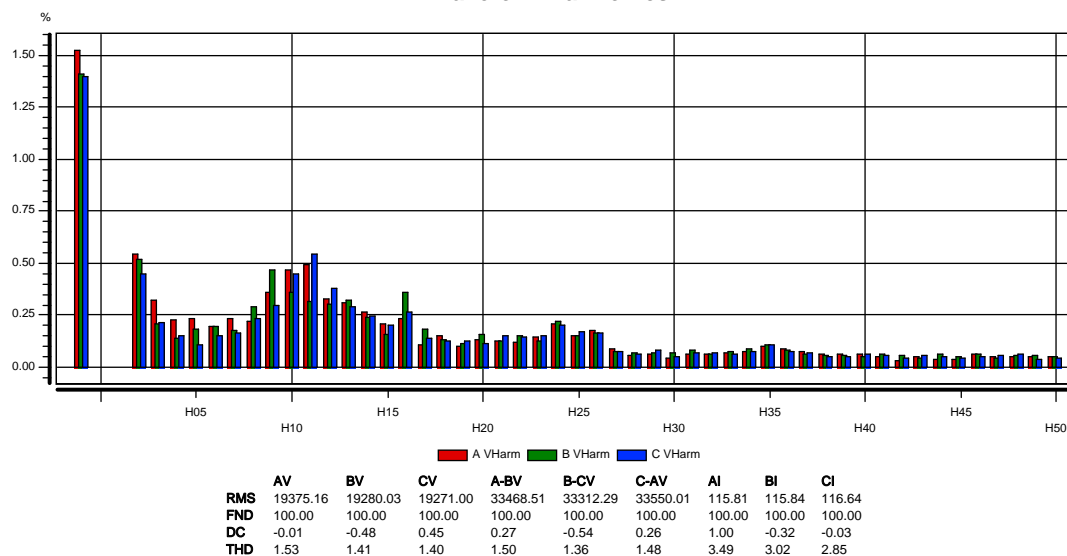
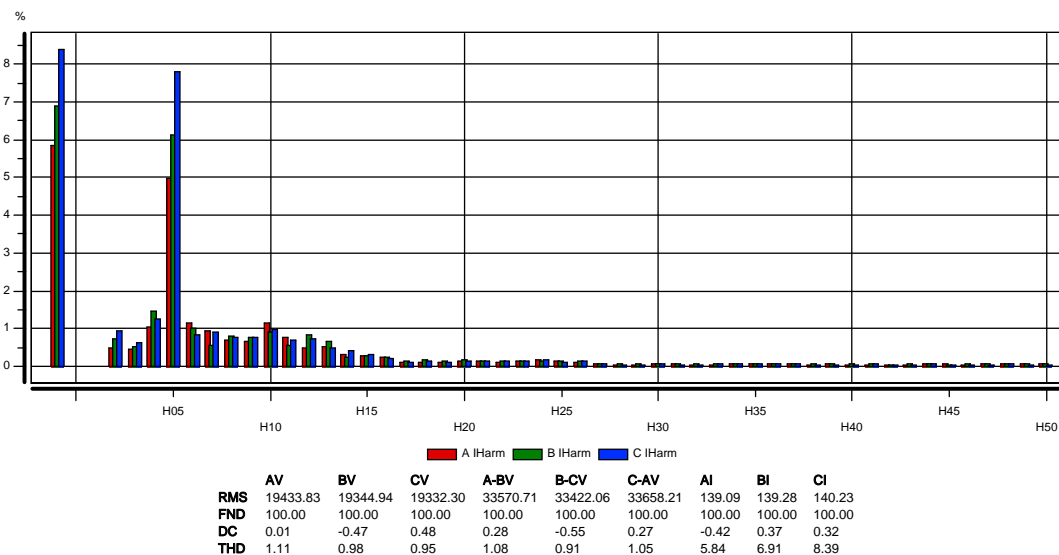


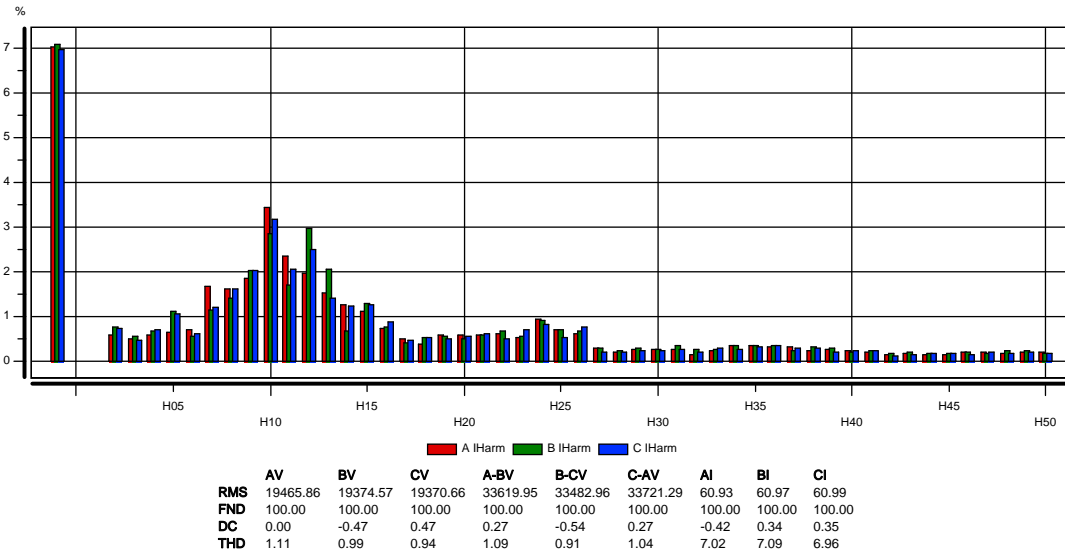
Figure 10-20 Current harmonic spectrum

The harmonics have a total THDi of less than 4% (the rms value of feeder current is around 160A). The most dominant harmonic is the 5<sup>th</sup>. It can be concluded that the current harmonics are absorbed by the harmonic filters. The 5<sup>th</sup> harmonic filter, Figure 10-21 consumes around 8% of the THDi (rms current is 150A) with the most dominant 5<sup>th</sup> harmonic at around 8%.

## Waveform harmonics

Figure 10-21 5<sup>th</sup> harmonic filter harmonic spectrum

## Waveform harmonics

Figure 10-22 7<sup>th</sup> harmonic filter harmonic spectrum

## 10.4 Discussion of Results

The results of harmonic measurements show that during the steady state conditions and for the normal mode of operation, the voltage and current harmonics at 33 kV level are below maximum allowable limits. The harmonic filters and associated capacitors perform well and in accordance with the acceptance criteria. At the 33 kV switchboards the total measured voltage harmonic distortion is less than 1.5% THDv. For normal mode of operation, the power factor measured on incomers of the 33 kV treatment plant switchboard is approximately 0.97%. This means that the harmonic filters provide adequate reactive power compensation.

The SAG mills generate various current harmonics and inter-harmonics with a total THDi of approximately 8% (225A nominal current). The most dominant harmonics are the inter-harmonics grouped around the nominal frequency and from the 10<sup>th</sup> to 12<sup>th</sup> harmonic frequency. The current harmonics on the inter-connector feeder are around 4% THDi (200A nominal), the most dominant is the 6<sup>th</sup> harmonic, approximately 3.5%.

The 3rd harmonic filters absorb 3% of THDi (60A nominal), mainly the 2<sup>nd</sup> and 3<sup>rd</sup> harmonics. The 4th harmonic filters absorb 3.5% of THDi (60A nominal), mainly the 4<sup>th</sup> and 5<sup>th</sup> harmonics. The 5<sup>th</sup> harmonic filters absorb 10% of THD (60A nominal), of which almost three quarters is the 5<sup>th</sup> harmonic. The 7<sup>th</sup> harmonic filters absorb 12%

of THDi (60A nominal), the most dominant harmonics are from 9<sup>th</sup> to 13<sup>th</sup>. The rms current on the 5<sup>th</sup> harmonic filter feeder is almost 2.5 times its nominal current (measured rms current is 150A, nominal current is 60A). This finding requires further investigation.

During normal mode of operation the total voltage harmonic distortion on the 33 kV system is below 1.5% THDv. The voltage harmonics recorded on the 33 kV power station switchboard are well within the recommended maximum value of 5% (under 1.5%). The individual voltage harmonics are less than recommended 3%, (under 0.5%).

During inching mode, the 5<sup>th</sup> harmonic filter draws 2.5 times nominal current. It is suspected that the system may be experiencing harmonic resonance, which requires further investigation.

## **11. APPENDIX 4 - SWITCHING TRANSIENTS**

### **11.1 Switching Transient Analysis - General**

Switching transient analysis was performed for 2 operating modes, normal mode of operation and a single train operation. System configuration under normal mode of operation is described in Appendix 3, Section 10.2.

The typical start-up sequence of one of the process trains is as follows, note that the 3<sup>rd</sup> and 4<sup>th</sup> harmonic filters are already switched on

- Start ball mill motor
- Run ball mill motor for a few minutes
- Switch on the 5<sup>th</sup>/7<sup>th</sup> harmonic filters
- Close the SAG mill circuit breaker and energise transformers
- Run the SAG mill

### **11.2 Normal Mode of Operation**

#### **11.2.1 Inter-Connector Feeder on Power Station Main Switchboard**

The time plot diagram, Figure 11-1 shows voltage and current of the red phase recorded from 11:00am on 28/06/05 to 09:00am on 29/06/05 on the inter-connector feeder. The voltage was steady with a few switching events, the most significant event occurring between 17:00 and 18:00 on 28/06/05.

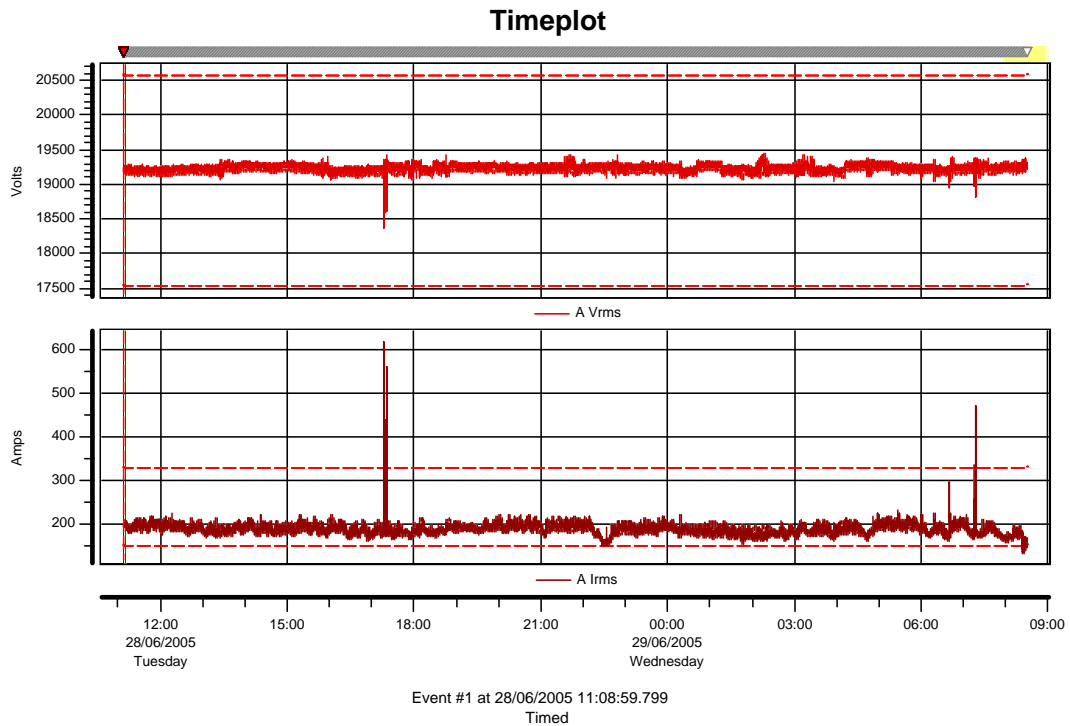


**Figure 11-1 Voltage and current timeplot**

Further analysis revealed that the following events occurred in that period:-

1. Event #371, Figure 11-2 at 28/06/2005 17:17:04 AV Misc Phase 1.323 Deg. –  
The voltage rms graph shows a voltage drop of 5% and current transients over a period of 3-4 cycles.

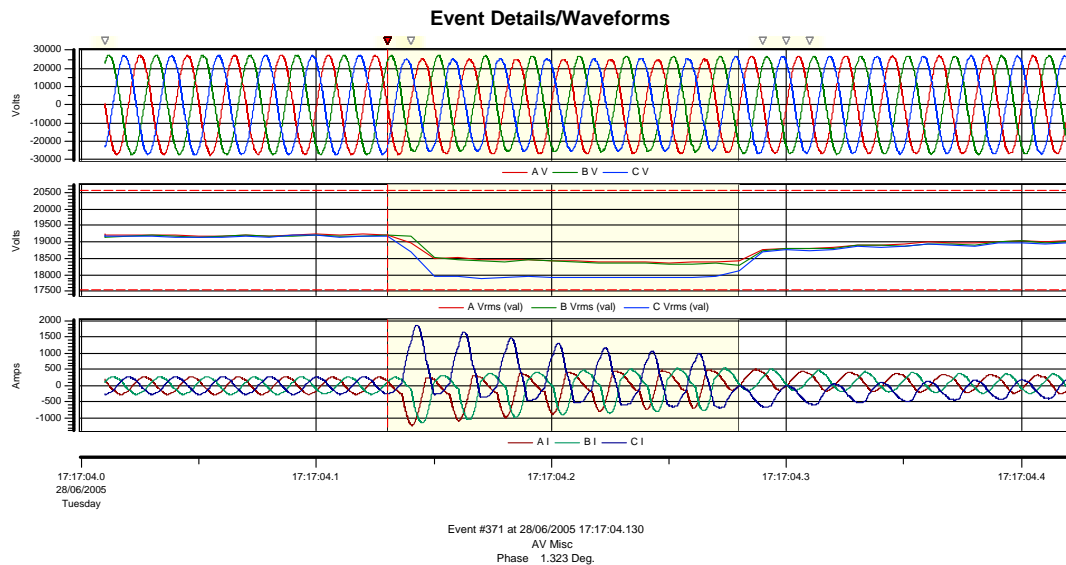


**Figure 11-2 Voltage and current waveforms**

2. Event #382, Figure 11-3 at 28/06/2005 17:20:14 Airms Instantaneous Swell, category: Short duration instantaneous swell, threshold crossed 330A.

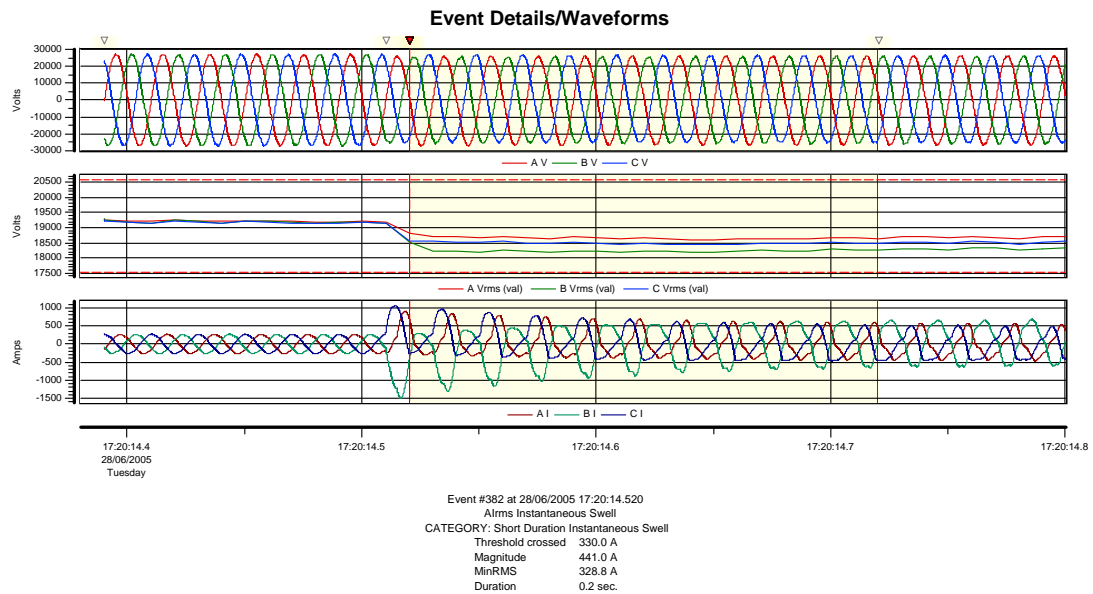


**Figure 11-3 Voltage and current waveforms**

Reconstruction of the events indicated that the Event#371 captured an unsuccessful start and the Event#382 captured a successful start-up of the winder motor. Both events are characterised with a high transient current, typically 6 times the motor nominal current. The measurements demonstrate that system disturbances during the start-up of the winder motor do not cause a significant impact on the system.

### 11.2.2 Train 2 Feeder on Power Station Main Switchboard

The time plot diagram, Figure 11-4 shows voltage and current of the red phase recorded from 05:00 to 20:00 on 09/06/05 at the train 2 feeder. The voltage time plot curve shows a steady voltage indicating a series of transient events around 08:00 and 12:00.

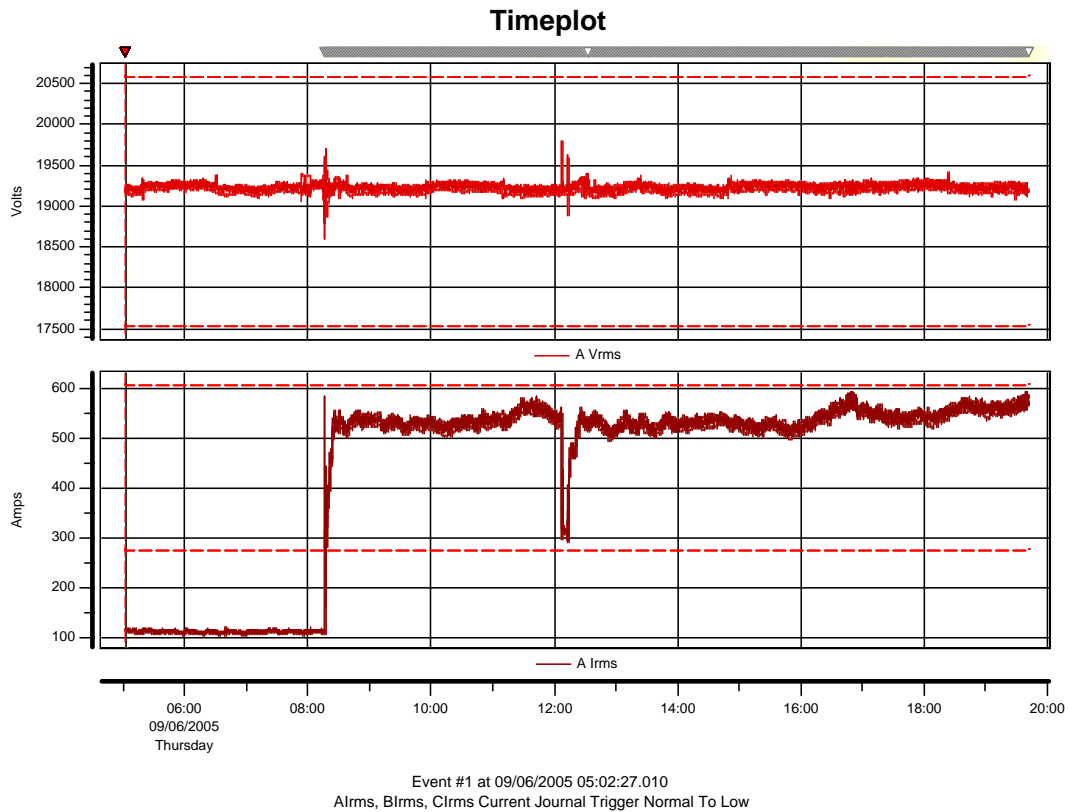


**Figure 11-4 Voltage and current timeplot**

Figure 11-4 shows that shortly after 08:00am the current increased from 100A to 400A and then to 550A, indicating start-up of both ball and SAG mills. At around 12:00 the current dropped to 300A for a short period of time and then it was increased back to 550A. This corresponds to a temporary loss and start-up of the SAG mill as shown in the following events:-

1. Event #8, Figure 11-5 at 09/06/2005 08:16:43 Post-trigger. – This event shows start-up of the ball mill. The voltage rms graph shows a voltage drop of 8% and current transients over a period of 6-8 cycles.



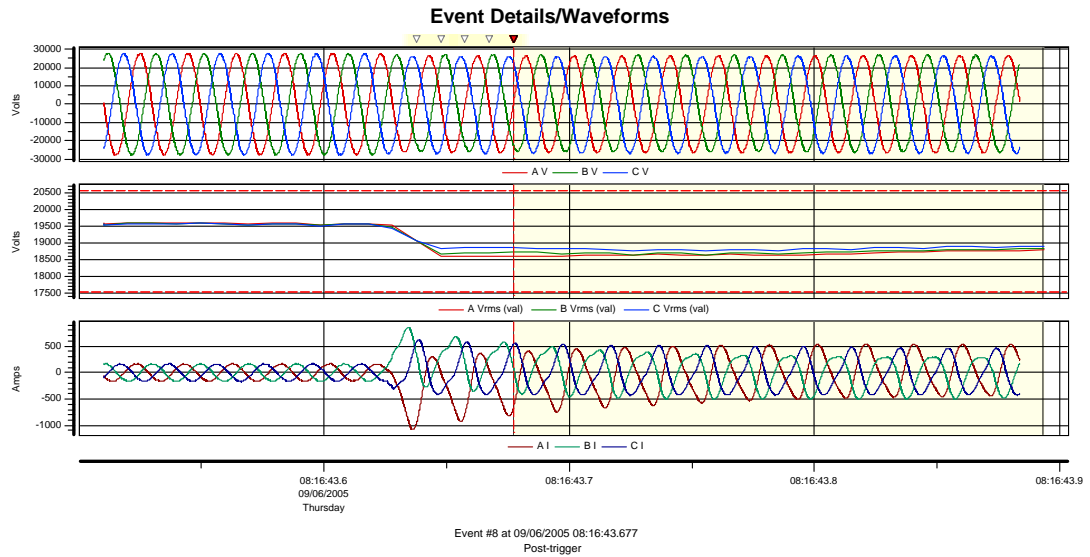


**Figure 11-5 Event #8 voltage and current waveforms**

2. Event #26, Figure 11-6 at 09/06/2005 08:17:34 Intermediate waveform – The voltage rms plot shows low frequency voltage oscillations caused by ball mill load fluctuations. The load current is changing from 250 Apeak to 500 Apeak. The total voltage harmonic distortion is less than 1.25%.

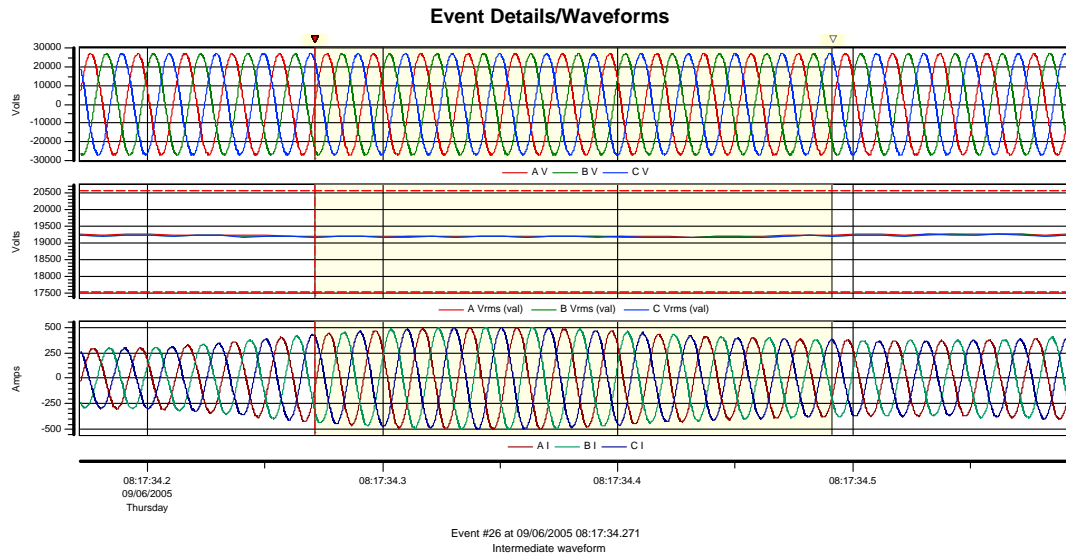


**Figure 11-6 Event #26 voltage and current waveforms**

3. Event #31 Figure 11-7 at 09/06/2005 08:17:55 AVRmsDev Normal to High threshold crossed 952.0 – This event shows the voltage and current waveforms during switching of the 5<sup>th</sup> and 7<sup>th</sup> harmonic filters.

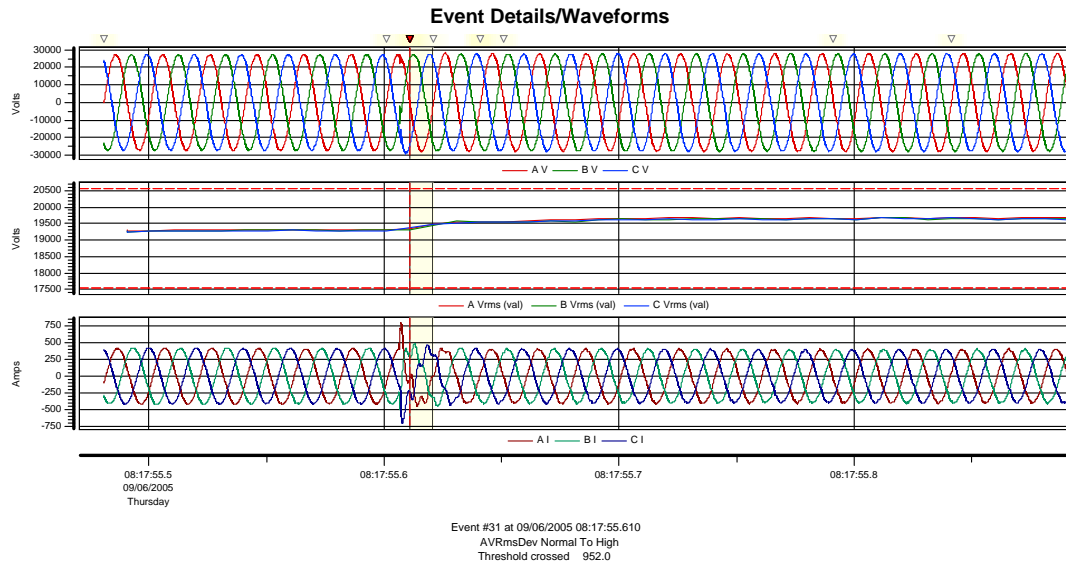


**Figure 11-7 Event #31 voltage and current waveforms**

The yellow marker was enlarged and shown in Figure 11-8. The switching of the capacitor banks is characterised by high frequency oscillations and the waveform captured in this event is typical for back-to-back capacitor switching. The voltage rms curve shows the rms voltage increase of 3-4%. This voltage would be reduced back to its nominal settings after a few seconds by the AVR action.

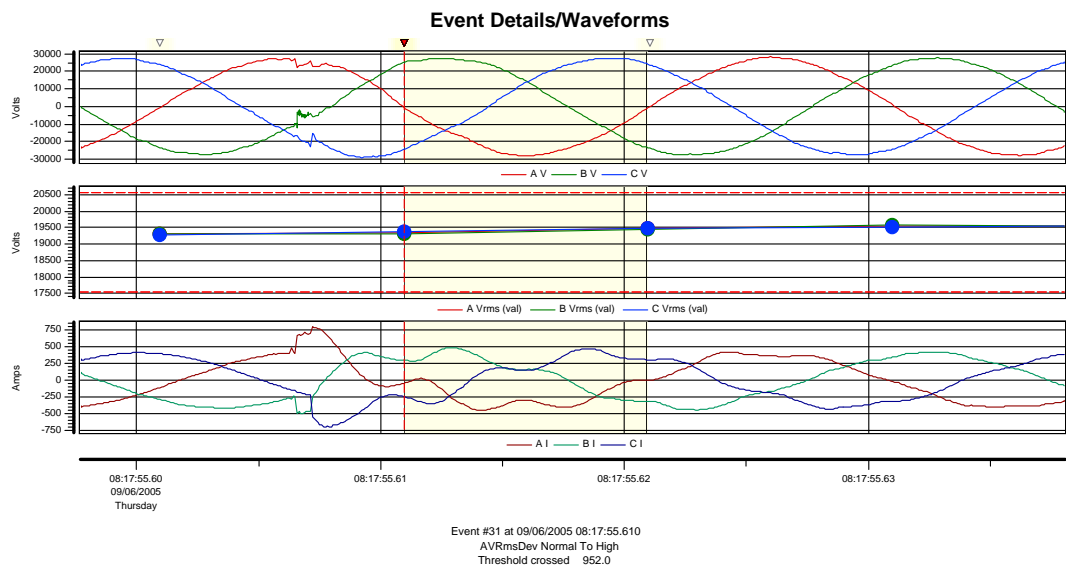


**Figure 11-8 Event #31 waveform close look-up**

## 11.3 Single Train Operation

### 11.3.1 General

In the case where one of the GT is lost and the whole system is supplied by a single GT, only a single train operation can be maintained. A series of events was captured during the single train, single GT operation. The bus tie on the 33 kV switchboard was open in this mode of operation.

### 11.3.2 Train 2 SAG Mill Feeder on Treatment Plant Main Switchboard

The time plot diagram, Figure 1-19 shows voltage, current and power factor of the red phase recorded from 08:00am on 26/04/05 to 08:00am on 27/04/05 at switchboard 388SB001 on the train 2 SAG mill feeder.

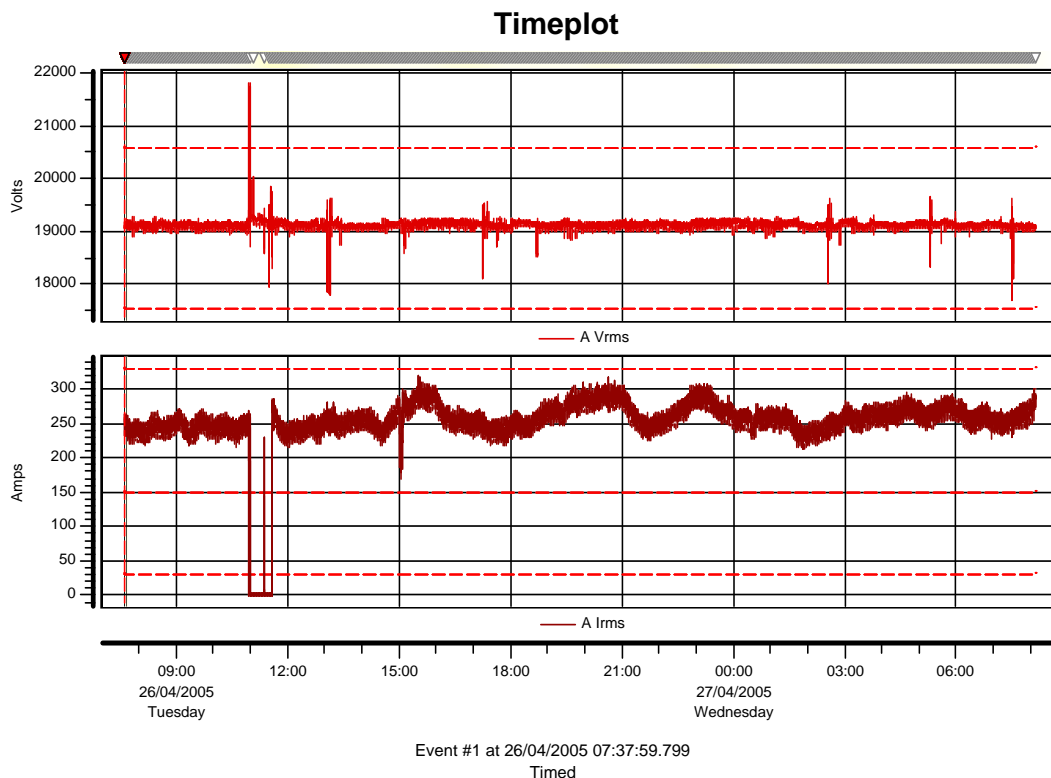


**Figure 11-9 Voltage and current timeplot**

The daily power PPS data recorded by the power station showed that train 1 was shut down shortly after 3:00am and the system was supplied from a single GT until 13:00pm the same day. The events that occurred from 11:00am to 12:00am are of interest as they represent a single train single GT operation. The most significant

event occurred around 11:00am. The typical waveforms captured during the start-up sequence of the train 2 SAG mill and switching of the capacitor banks are shown in the following events:-

1. Event #202, Figure 11-10 at 02/05/2005 07:47:54 Pre-trigger. – This event shows a shut-down of the train 2 SAG mill. The voltage rms graph shows a voltage increase of 3% following the loss of the SAG mill, which gradually increases to 6% of its rated value. This second voltage step increase occurred approximately 10 cycles from the loss of the SAG mill, caused by loss of the ball mill. The voltage level on the 33 kV system increased by an additional 6% to a total of 12%. Such a voltage level is a not desirable and can cause premature failure of any 33 kV equipment supplied from the 33 kV system.

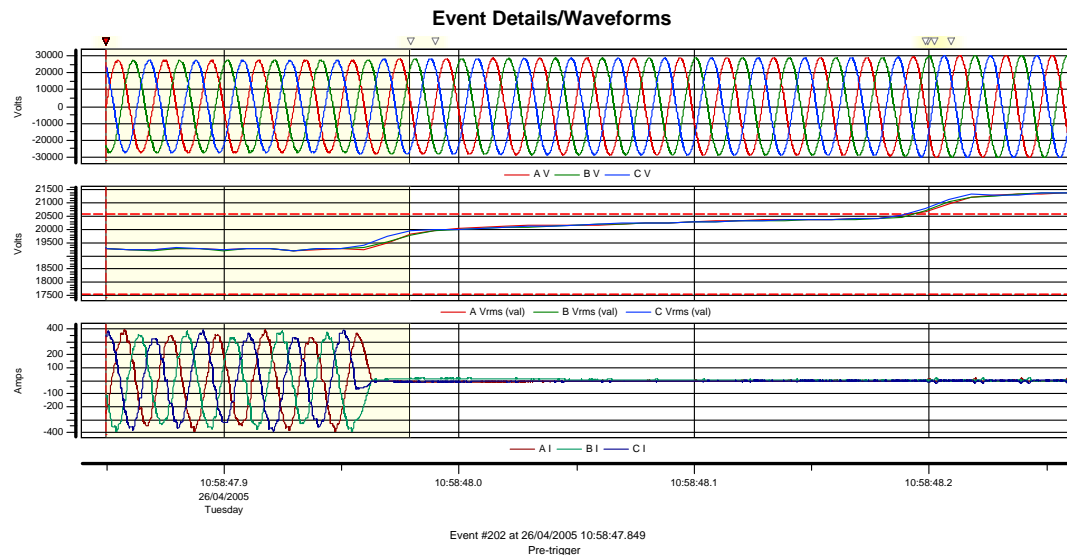


**Figure 11-10 Event#202 voltage and current waveforms**

2. Event #212, Figure 11-11 at 26/04/2005 10:58:54 Intermediate waveform – This event shows the switching off of the 5<sup>th</sup>/7<sup>th</sup> harmonic filters on train 2. The rms voltage drops down by 5-7%.

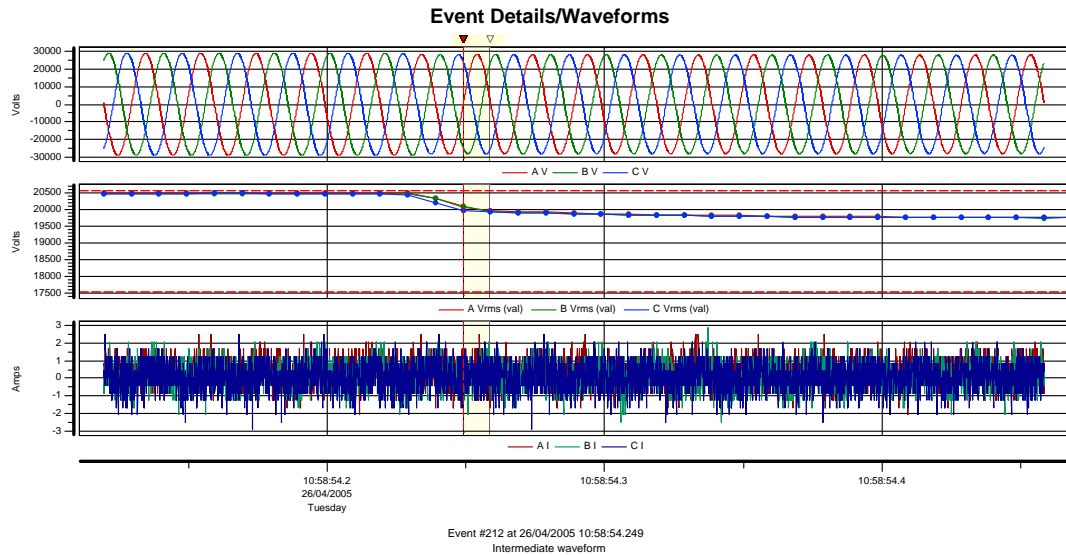


**Figure 11-11 Event#212 voltage and current waveforms**

3. Event #226, Figure 11-12 at 26/04/2005 11:22:17 Intermediate waveform – This event shows a specific time measurement of switching on the SAG mill circuit breaker and energisation of the SAG mill transformers. The current waveform shows a very high transformer inrush current. During the transient period lasting 20-30 cycles the voltage drops to 95% of its nominal value.

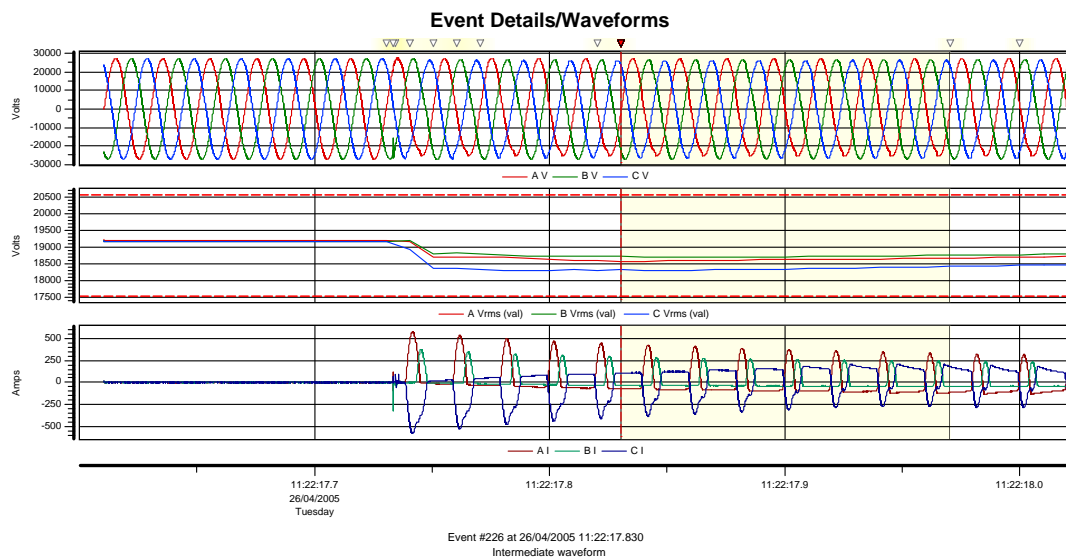


**Figure 11-12 Event#226 voltage and current waveforms**

4. Event #259 Figure 11-13 shows voltage and current waveforms during the running of the SAG mill. The current waveform shows significant distortion.

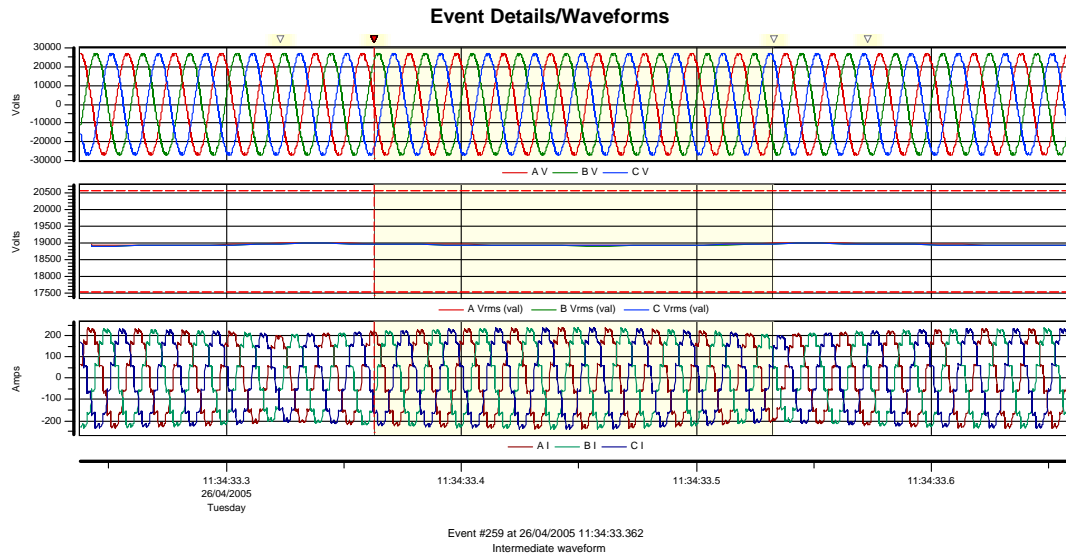


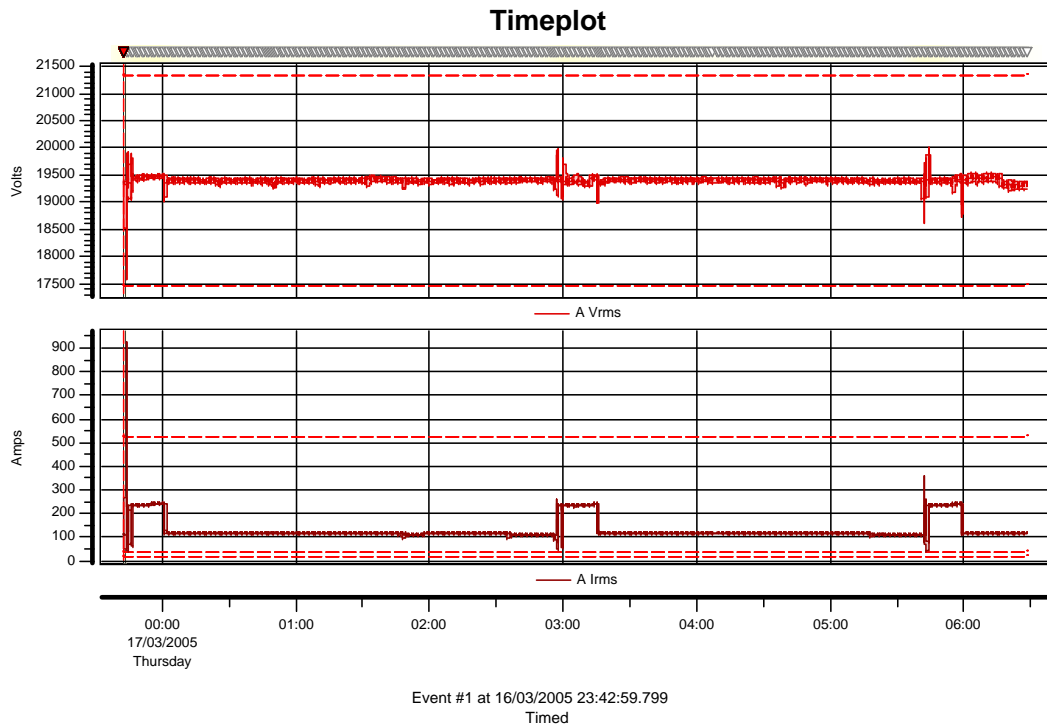
**Figure 11-13 Event#259 voltage and current waveforms**

## **11.4 Train 1 SAG Mill Inching Mode of Operation**

### **11.4.1 Train 1 Incomer**

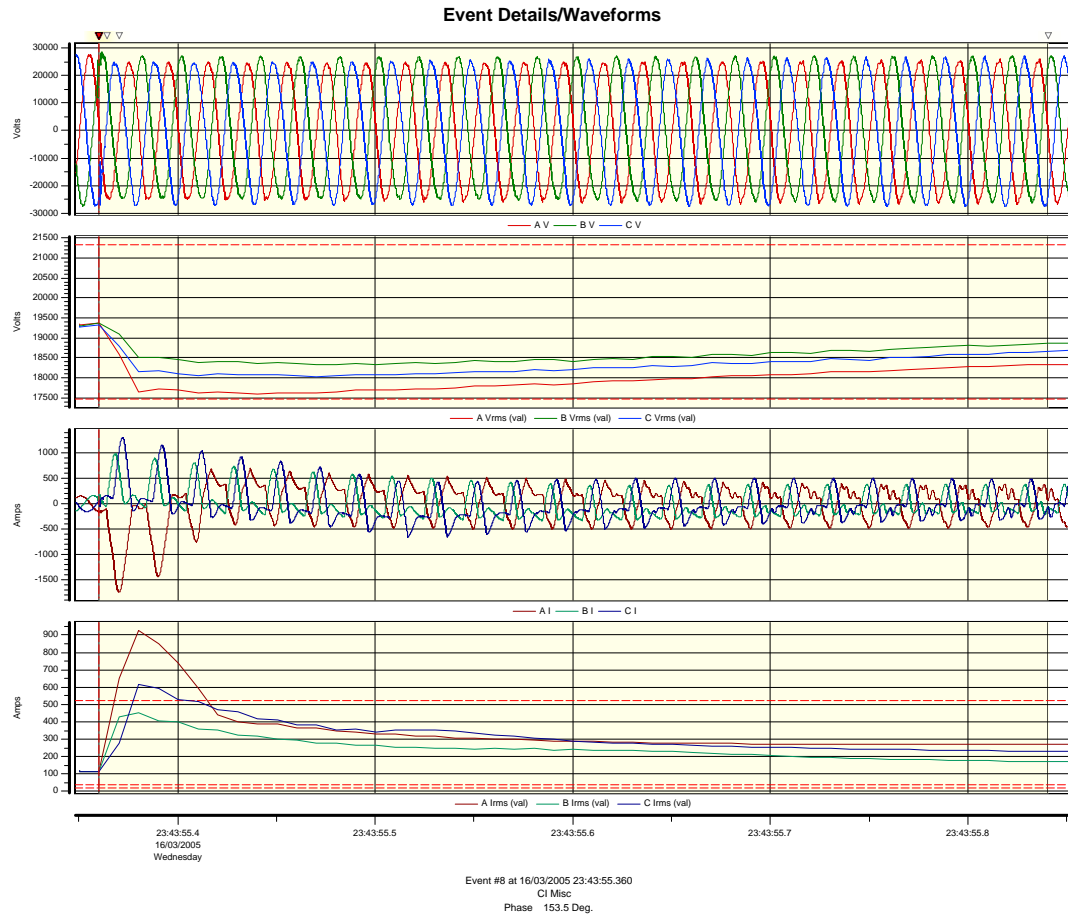
System configuration under inching mode of operation is described in Appendix 3, Section 10.3 of this thesis. Results of analysis, comprising voltage and current time plots and voltage and current transient waveforms, are given in figures below. The voltage waveforms were measured on section A of the board and current waveforms were measured on the train 1 incomer. At the time when train 1 was in maintenance mode, train 2 was running under normal mode of operation, the 33 kV switchboard bus tie breaker was open and 2 GTs were on line.

Figure 11-14 shows voltage, current and power factor time plot from 23:30 on 16/03/05 to 06:30 on 17/03/05. A total of 3 inching cycles was captured in this period.



**Figure 11-14 Voltage and current timeplot**

1. Event #8 Figure 11-15 at 16/03/2005 23:43:55 CI Misc – This event shows closing of the SAG mill feeder breaker and energising of the SAG mill transformers. The switching transients show high inrush currents due to transformers being energised. The inrush current in the SAG mill feeder causes voltage drop which under worst case conditions can fall below 10% of the nominal voltage. The inrush current transients last up to 100 cycles, during which the initial voltage drop slowly recovers back to the nominal value. The generator AVR's are not effective for this type of disturbance.



**Figure 11-15 Event#8 voltage and current waveforms**

2. Event #226 in Figure 11-16 at 16/03/2005 23:44:24 Pre-trigger – This event shows the switching of the 5<sup>th</sup> and 7<sup>th</sup> harmonic filters on train 1. It can be seen that at the time of the harmonic filter switching operation, there is a short duration transient current flowing in the incomer. This current causes high frequency voltage oscillations that last for less than  $\frac{1}{4}$  of the cycle. The high frequency voltage oscillations are seen by the entire system and potentially may damage equipment insulation. The bus voltage increases by 2-3%. This voltage drops back to its nominal value within a few seconds as a result of the generator AVR operation.



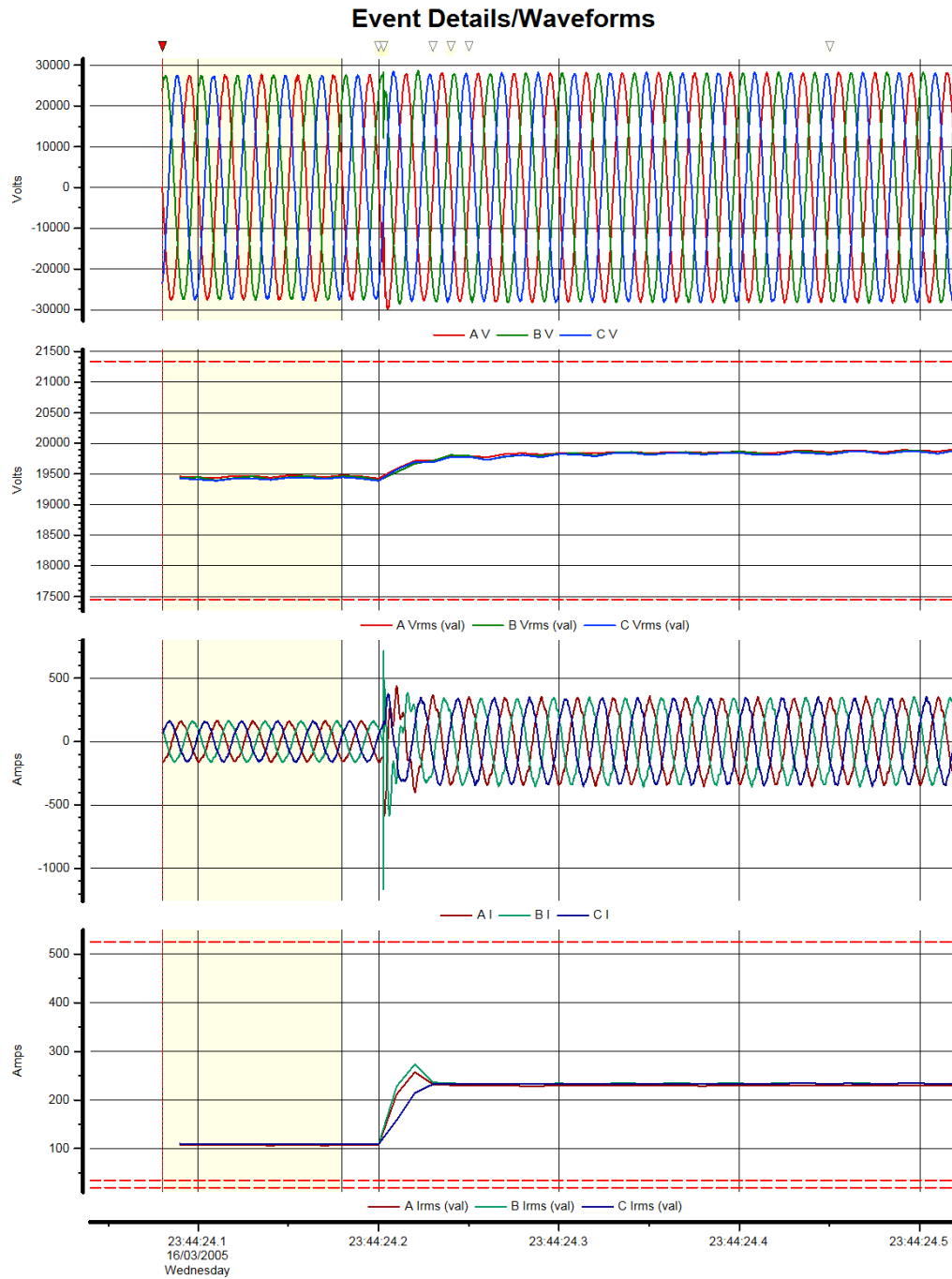


**Figure 11-16 Event#226 voltage and current waveforms**

3. Event #73 Figure 11-17 at 17/03/2005 00:01:06 Pre-trigger – This event shows transients during switching of the harmonic feeder breaker. There are no voltage and current oscillations during this switching operation.

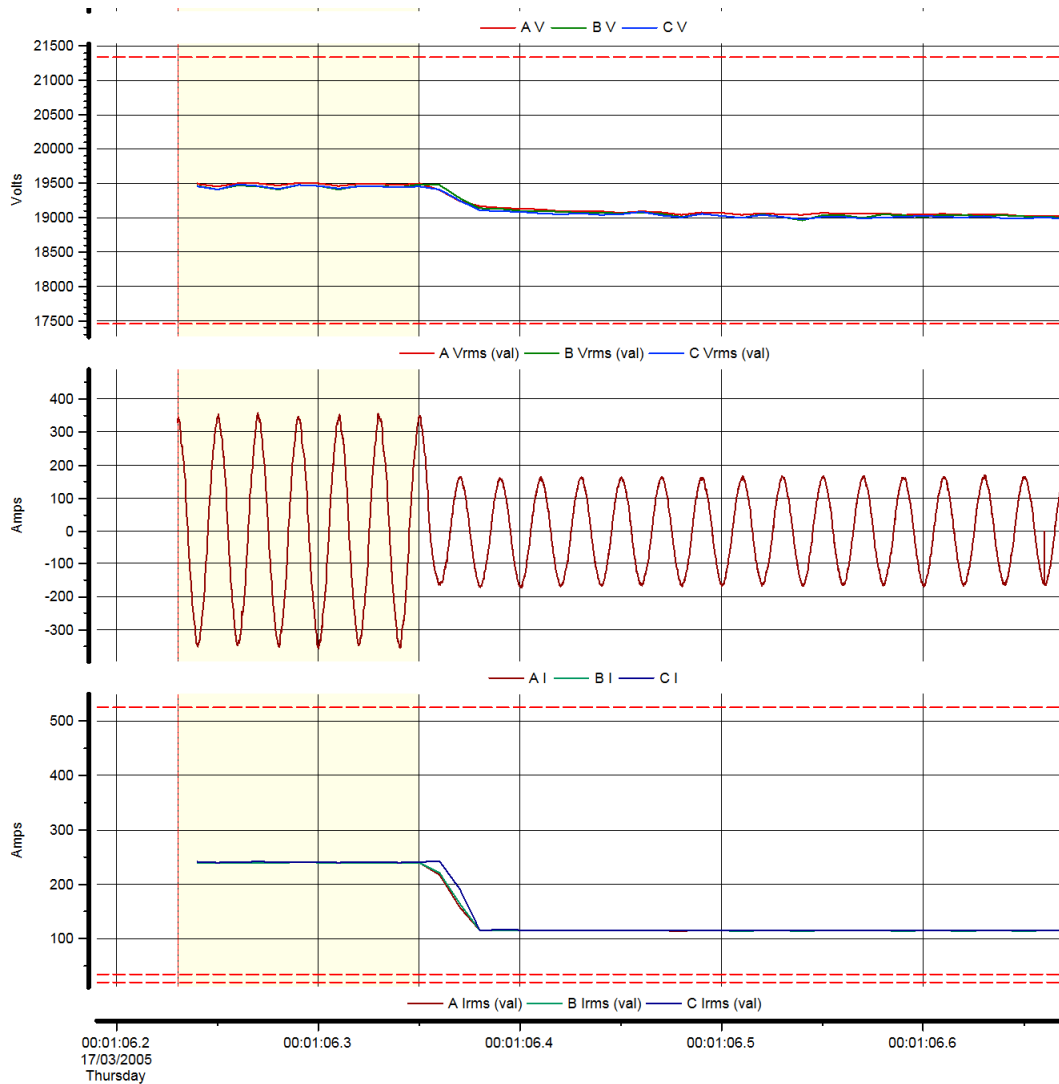


**Figure 11-17 Event#73 voltage and current waveforms**

The system voltage drops down by 2-3% and is brought back to the nominal value by the generator AVRs within a few seconds. The opening of the SAG mill circuit breaker does not cause any switching transients.

#### 11.4.2 Train 1 SAG Mill Feeder

The time plot diagram, Figure 11-18 shows voltage and current of the red phase recorded from 20:00 on 15/03/05 to 07:00 on the following day on the train 1 SAG mill feeder. The voltage time plot curve shows 2 inching cycles captured during this time period.

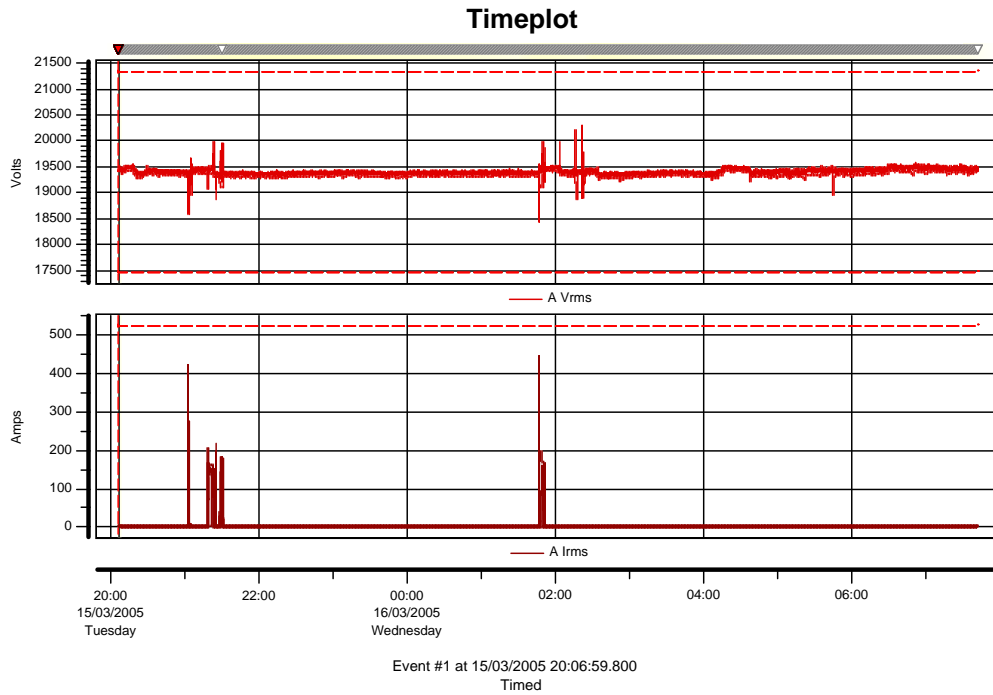


**Figure 11-18 Voltage and current timeplot**

The typical waveforms captured during the start-up sequence of the train 2 ball and SAG mills and the switching of the capacitor banks are shown in the following events:-

1. Event #65, Figure 11-19 at 15/03/2005 21:03:00 Waveforms – This event shows the closing of the SAG mill feeder breaker and the energising of the SAG mill transformers. The same comments apply as for Event#8.

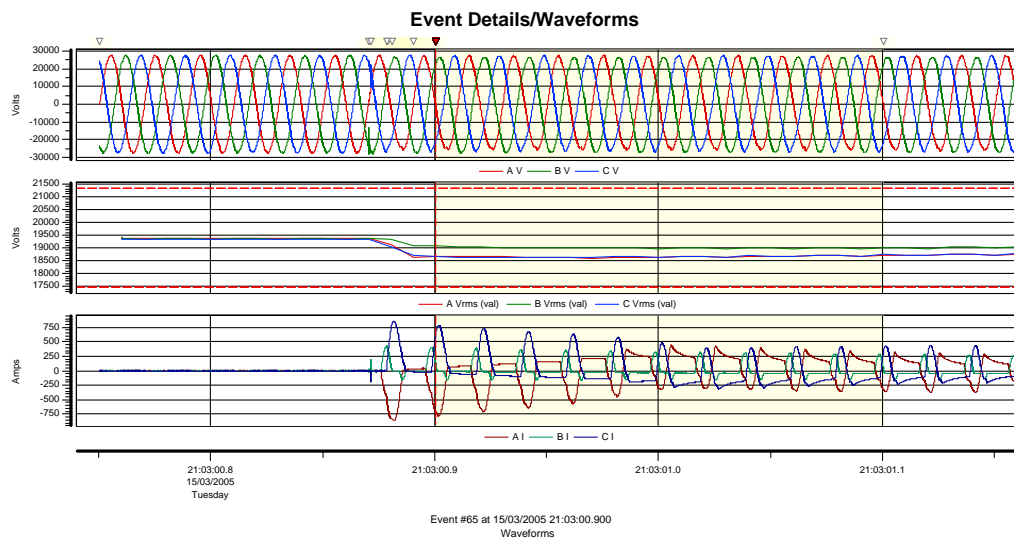


**Figure 11-19 Event#65 voltage and current waveforms**

2. Event #73 Figure 11-20 at 15/03/2005 21:05:24 CV mild bipolar Trans Neg 1/8 Cyc, Category: impulsive transient (microsec duration) – This event shows the closing of the 5<sup>th</sup> and 7<sup>th</sup> harmonic filter breaker on train 1. It can be seen that at the time of the harmonic filter switching operation, there is a short duration transient current flowing in the incomer. This current causes high frequency voltage oscillations that last for less than ¼ of the cycle. The high frequency voltage oscillations are seen by the entire system and potentially may damage equipment insulation. Also, following the switching operation, the bus voltage increases by 2-3%. This voltage drops back to its nominal value within a few seconds as a result of the generator AVR operation.

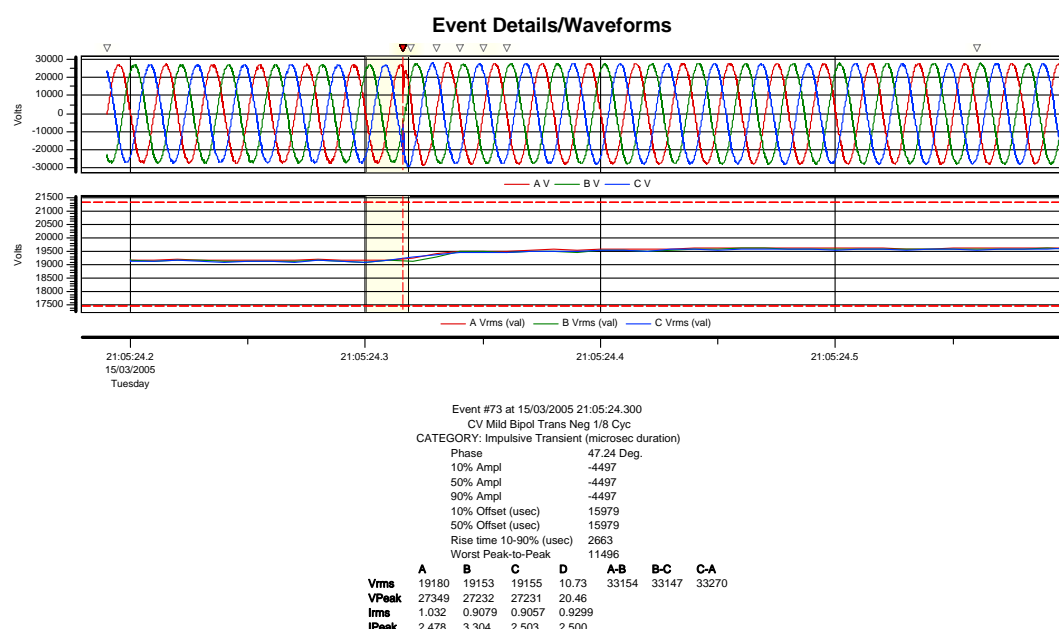


**Figure 11-20 Event#73 voltage and current waveforms**

3. Event #118, Figure 11-21 at 15/03/2005 21:28:59 timed – This event is not a transient event; it shows voltage and current waveforms of the SAG mill feeder during inching mode. The voltage harmonic spectrum indicates that the total voltage harmonic content is less than 1.5% and it is within the prescribed limits.

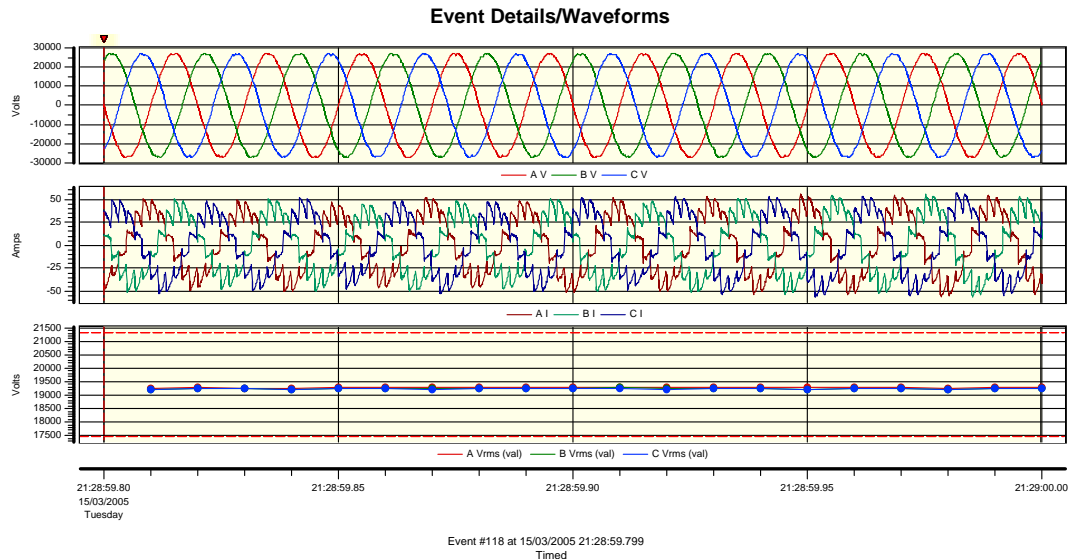


**Figure 11-21 Event#118 voltage and current waveforms**

4. Event #122, Figure 11-22 at 15/03/2005 21:30:37 Pre-trigger – This event shows transients following opening of the SAG mill feeder breaker. There are no voltage and current oscillations during this switching operation; however the system voltage increases by 3-4%. The voltage is brought back to its nominal value by the generator AVRs.

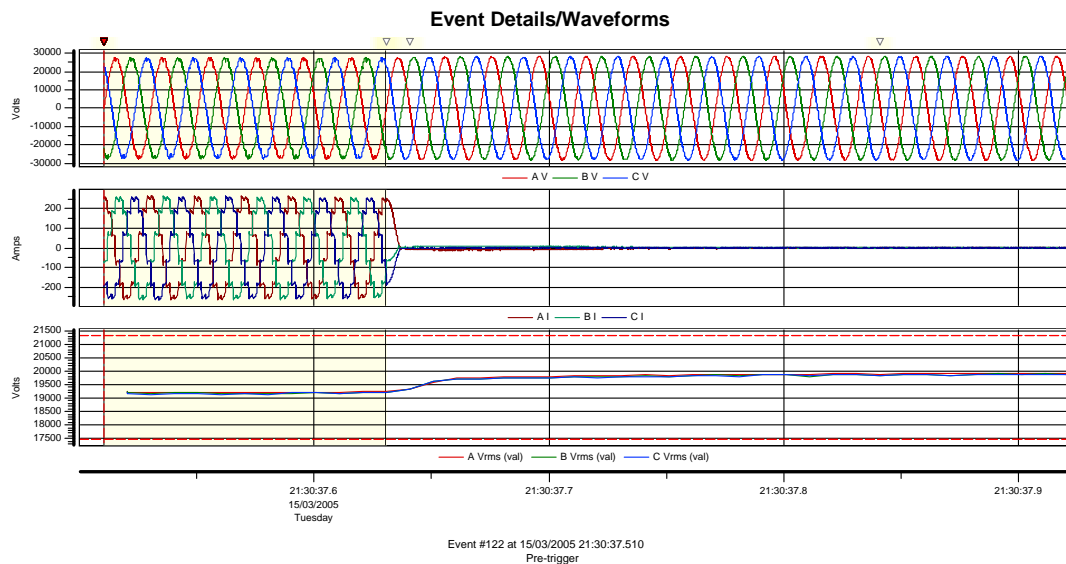


**Figure 11-22 Event#122 voltage and current waveforms**

5. Event #447, Figure 11-23 at 16/03/2005 02:21:27 waveforms – This event shows the system transients following the opening of the 5<sup>th</sup>/7<sup>th</sup> harmonic filter

feeder breaker. The system voltage drops by 6-7%. The voltage is brought back to its nominal value by the generator AVRs.

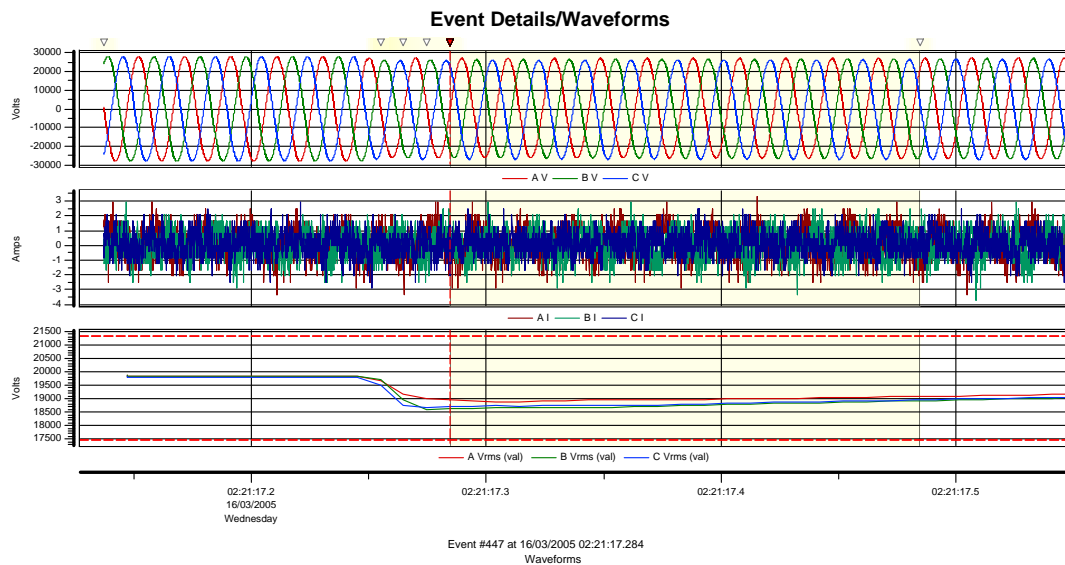


**Figure 11-23 Event#447 voltage and current waveforms**

## 11.5 Discussion of Results

The gold processing plant power system is a relatively simple system and voltage and current waveforms captured during the switching operations fit into typical signatures expected on systems with capacitor banks, large induction motors and transformers.

The largest single load on the inter-connector feeder is the winder motor and major disturbances are caused by the start-up of the winder motor. Analysis showed that during the motor start-up the load current increases to a peak of 1500A causing instantaneous voltage drop of approximately 5%. It can be concluded that the system is robust enough to accept the winder motor load and the starting of such a large load does not cause any significant disturbances to the system. Voltage drop of 5% is well within the system tolerances for transient conditions.

The switching of the capacitor banks is characterised by high frequency oscillations and the waveform captured during this event was typical for back-to-back capacitor switching. The system voltage increased by 3-4%. The voltage dropped back to its nominal value after a few seconds as a result of AVR operation.

During normal mode of operation, there were a very high number of the 5<sup>th</sup>/7<sup>th</sup> capacitor switching operations on both production trains. The 5<sup>th</sup>/7<sup>th</sup> harmonic filters are switched out every time the SAG mill is stopped. They are switched-in every time the SAG mill is ready for start-up. If the SAG mill start-up is not successful, then the capacitors are switched out to be switched in again a few minutes later. The voltage transients caused by the capacitor switching are present on the entire 33 kV system. Such a large number of switching operations is impacting the integrity of the 33 kV system and also the integrity of capacitor circuit breakers which are designed for a limited number of switching operations. For these reasons, the switching frequency should be minimised. Further investigation is required to determine the optimal switching procedure.

Shut-down of the train 2 SAG mill and the ball with the 3<sup>rd</sup> and 4<sup>th</sup> capacitor banks left energised increases the system voltage to 12% of its rated value before the generator AVRs start reducing this voltage back to its initial value.

Start-up of the SAG mill is characterised by the energisation of the SAG mill transformers. The current waveform shows a high transformer inrush current during the transient period lasting 20-30 cycles. The voltage drops to 95% of the nominal voltage. While transformers are designed to withstand short circuit forces caused by the inrush currents, the number of switching operations should be minimised in order to preserve their integrity.

The switching transient analysis project, described in this paper, captured voltage and current waveforms on the 33 kV system for various system configurations.

The system disturbances that are frequently encountered on the system, and for this reason cause concern are summarised as follows:-

- Switching in of the 5<sup>th</sup>/7<sup>th</sup> harmonic filters on both train 1 and train 2 as it produces a high frequency voltage and current oscillations which impact the power system integrity.
- Energising of SAG mill transformers – this event is characterised by a high inrush current which impacts the integrity of the SAG mill transformers.

The system is designed to handle the above disturbances (voltage and current waveforms prove it); however the concern here is directed towards the high number of switching operations. For this reason it is recommended that the switching sequence logic is reviewed and a new switching logic be implemented into the plant DCS system.



## **12. APPENDIX 5 - HARMONIC FILTER SELECTION STUDY**

### **12.1 Introduction**

Harmonic analysis and the harmonic filter selection study for The Plant (refer Appendix 1) is the last phase of the harmonic analysis project which commenced in December 2007. In this study, the base model developed in ETAP was expanded to include the new network configuration as advised by the project design team.

The system was modelled based on the project's single line diagrams and load list. The network configuration reflected normal operating conditions and the loads were maximum running plant loads. The industrial power system was shown as two radial networks with a common node established at the 132kV bus. The main objective of this study is to develop a conceptual design for new harmonic filters. The key filter parameters proposed in this study will be subject to review and optimisation by the suppliers.

### **12.2 Background**

The new system configuration is split into two radial networks. The common node is at the 132kV point of common coupling with the Western Power network. The plant radial network is fed from the 132kV node, via the existing 132/22kV transformer, to the existing 22kV switchboard. The power supply to the plant is further distributed via a number of radial feeders.

The rectifier plant is fed from the same 132kV node, via the existing spare 132/22kV transformer, to a new 22kV switchboard. The new 22kV switchboard comprises 3 feeders, one feeder to the existing 6-pulse rectifier plant, one feeder to the new 12-pulse rectifier plant and a separate feeder to a new harmonic filter.

A bus tie is provided between the new and old switchboards to enable supply of both radial networks via a single 132/22kV transformer. This link is provided as a contingency measure in case one of the two 132/22kV transformers is out of service. It should be noted that operation of the plant under such conditions would reduce the operational capacity of the plant.

The combined plant and rectifier electrical power system has to satisfy the requirements of the power factor and individual harmonic levels set out by the project. The harmonic analysis study was conducted to calculate the system power factor and individual harmonic levels on each radial network.

This report provides a summary of the harmonic analysis study and provides a conceptual design for harmonic filters on both the rectifier and the plant radial networks. The harmonic analysis study was performed using the ETAP software package, and was an extension of the power system modelling and harmonic measurements work carried out as part of the overall harmonic analysis study.

### **12.3 Purpose**

The purpose of this study was to analyse the distribution of harmonic currents and voltages on the combined electrical power system. The new system configuration and parameters were set-out by the expansion project design team.

The aim of analysis was to develop a conceptual design for the Harmonic Filtering system for the combined plant and rectifier radial networks. Harmonic analysis was done to confirm that the proposed concept would improve the system power factor and reduce the level of individual harmonics to acceptable levels. The study was carried out to define the basic parameters of the Harmonic Filtering system which would be provided to prospective vendors for review. It is expected that equipment vendors will carry out a final selection of the filter type, optimisation of filter parameters and detailed design of the harmonic filter. This study was to provide a cost effective solution.

### **12.4 Scope and Objective**

The combined power factor correction and harmonic filter unit has to satisfy the requirements of the Technical Rules (referenced in Section 5.2 of this report) with regards to individual voltage harmonics.

The power factor on the 22kV system should be maintained in the range of 0.95 to 1.00, lagging for normal operating conditions, as set in the project design criteria.

The combined power factor correction and harmonic filter unit should satisfy the following design criteria:-

- Harmonic filters are to be installed at a 22kV system level
- Only one harmonic filter feeder on each 22kV switchboard
- Individual voltage harmonics on 22kV switchboards are to be within Western Power's distribution planning levels as listed in the Technical Rules, Table 2.4.
- Harmonic filters should provide good system damping of the parallel resonance

Harmonic analysis is to be carried out for the following system configuration. This configuration represents normal operating conditions:-

1. The 132kV power supply will be fed from Western Power SWIS network.
2. The bus tie between the 22kV switchboards will be open, meaning that the 132/22kV power transformers will not be running in parallel.
3. The bus coupler on the 3.3 kV switchboards will be open, thus the 22/3.3 kV transformers will not be paralleled.
4. Bus couplers on the 415V switchboards will be open, meaning that the 22/0.433 kV transformers will not be running in parallel.
5. All loads will be at maximum demand as per the project load list calculation.

## **12.5 Methodology**

### **12.5.1 Assumptions**

The harmonic sources used in the study are harmonic sources produced by the existing 6-pulse rectifier and a new 12-pulse rectifier. All other harmonic sources such as variable speed drives are ignored.

The reason for this approach is that the 6-pulse and 12-pulse rectifiers connected to the rectifier network generate significant harmonics and any other non-linear load on the system is considered insignificant for a typical industrial system.

### **12.5.2 Electrical Network Modelling**

An electrical network developed using ETAP, for load flow and short circuit studies, was used as a base model for harmonic analysis. The base model is described in Appendix 1.

The electrical network was configured as per the plant single line diagram. The 132kV network was represented as an infinite bus. The fault levels of the infinite bus were based on WPC planning levels as at 2010. The 2010 maximum fault levels were used for harmonic analysis. The maximum three-phase short circuit current was 29.1kA and the single-phase was 30.8kA.

The 22 kV switchboards, 3.3 kV MCCs and 415 V MCCs were represented as bus nodes. The maximum bus voltage on the 132 kV and 22 kV system was set to 110% of the nominal voltage. The maximum bus voltage on the 3.3 kV and 415 V system was set to 106%. The upper voltage limits employed in the study were as per the Technical Rules.

The voltage total harmonic distortion limits on systems 22kV and below were set to 6.5% as per the Technical Rules.

Power transformers were modelled as two winding transformers. The nameplate rated values, such as voltage levels and impedances were used in the model. All taps were set to zero and no harmonic sources were assigned to transformers. On the 20/27MVA transformers, the 22kV bus was the regulated bus, and auto tap changer on the primary 132kV side was assigned to regulate the voltage on the associated 22kV bus.

### **12.5.3 Harmonic Analysis**

Harmonic analysis was carried out using the ETAP software package and all of the standard features available through ETAP were employed during analysis. The

ETAP Harmonic Analysis module employs two analytical methods, the Harmonic Load Flow method and Harmonic Frequency Scan method.

## 12.6 Harmonic Levels on the Existing Network

### 12.6.1 Objectives

The main objective of Case 1 was to determine the level of voltage and current harmonics on the combined electrical network, with no power factor correction capacitors and harmonic filters installed on the system. The results would indicate whether there would be any need to install power factor correction capacitors and harmonic filters.

### 12.6.2 Harmonic Study Results

The target power factor and calculated power factors on the 22kV SG-501 and SG-502 switchboards are summarised in Table 12.1. It can be seen that on both of the 22kV switchboards the system power factor is lower than the power factor specified in the design criteria. The power factor on both buses has to be improved in order to satisfy the project requirements.

Bus Tag Number	Nominal voltage [kV]	Target power factor (Technical Rules) (p.u.)	Load flow current and power factor (I [A] @p.u.)
SG-501	22	0.95	436A@0.83
SG-502	22	0.95	501A@0.90

**Table 12-1 Power factor for the existing network**

The voltage harmonic spectrum on SG-502, calculated in Case 1, is shown in Figure 12.1 alongside the planned voltage harmonic levels. The results show that individual harmonic levels exceed the planning levels for the 11<sup>th</sup>, 13<sup>th</sup>, 23<sup>rd</sup>, 35<sup>th</sup>, 37<sup>th</sup>, 47<sup>th</sup> and 49<sup>th</sup> harmonics, which are the characteristic harmonics of a 12-pulse rectifier.

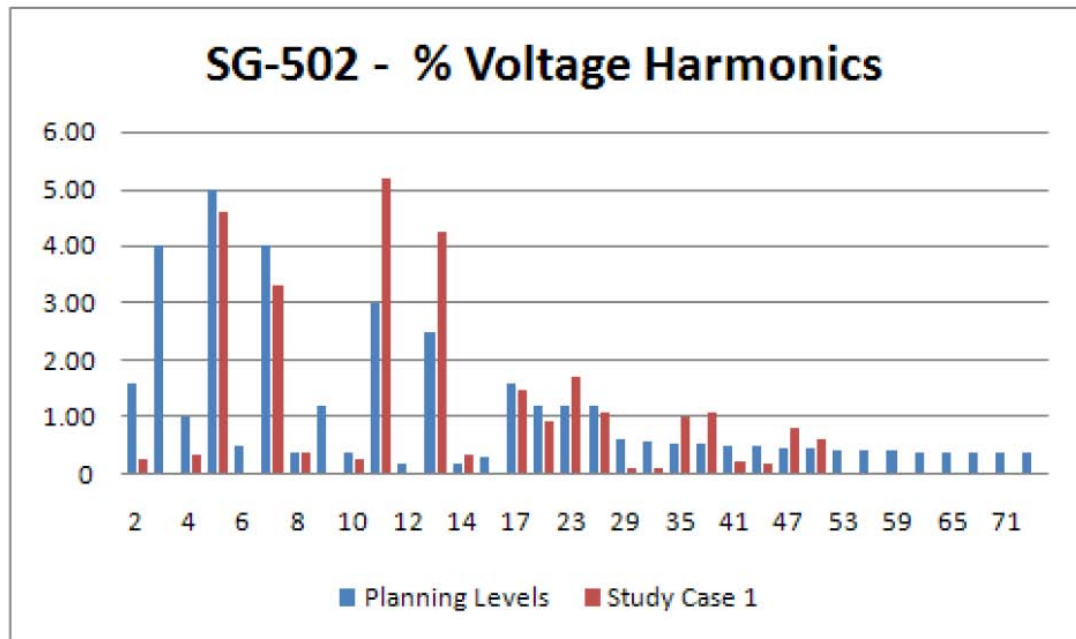


**Figure 12-1 Voltage harmonics on SG-502 for case 1**

The voltage harmonics on SG-501 are equal to zero as there are no harmonic sources on the plant radial network. The study shows that the plant network is independent of the harmonic sources located on rectifier network. This case shows that the individual harmonic level criteria specified by the project were not met on the rectifier radial network, and for this reason this network requires installation of harmonic filtering devices.

## **12.7 Filter Selection Study**

### **12.7.1 Objectives**

The main objective of Case 5 was to develop a conceptual design for a new filter on the rectifier network and determine the level of voltage and current harmonics. The aim was to show that each individual voltage harmonic would satisfy the project design criteria.

### **12.7.2 Filter Type Selection**

The study evaluated 3 filter combinations: a single tuned filter, a high-pass single filter, and the combination of a single tuned and a high pass filter. Each filter combination was fed via a single feeder. The feeder to PF-501 was connected to SG-501. The new harmonic filter was connected to the rectifier network at SG-502.

### Single tuned filter

Conceptually, this filter was similar to the existing filter but with 1000 kVAr reactive power per phase. The filter was tuned to 200 Hz. The filter capacitance was 19.73 $\mu$ F and filter inductance was 32.1mH. The Q factor of the filter was assumed to be 0.93.

The results of harmonic analysis are shown in Figure 12.2. This figure shows that individual harmonic levels for the 5th and 7th harmonics are well within design criteria. The individual harmonic levels exceed the planning levels for the 11th, 13th, 23rd, 35th, 37th, 47th and 49th harmonics, which are mainly the characteristic harmonics of a 12-pulse rectifier. The results clearly show that a single tuned filter would not provide a satisfactory solution. Higher order harmonics would require a high pass filtering device.

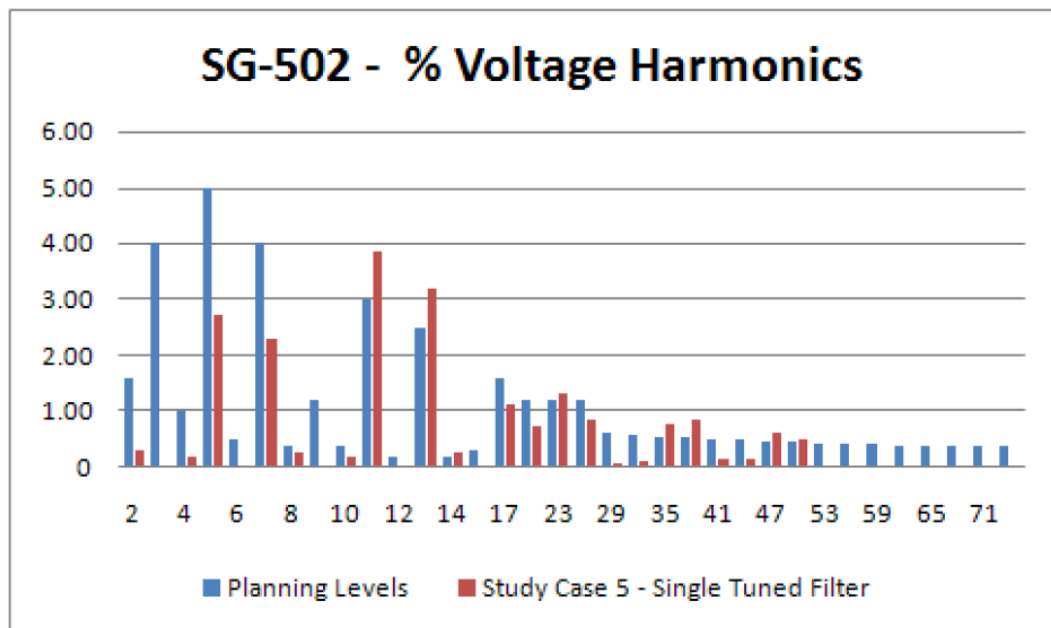


**Figure 12-2 Voltage harmonics on SG-502 with the single tuned filter**

### Option High-pass filter

The ETAP harmonic filter editor screen dump showing a High-Pass (damped) filter and its parameters, is shown in Figure 12.3. The filter comprises of 1000 kVAr capacitors per phase. Inductor L1 impedance was selected to tune the filter to the 5th harmonic. Filter damping resistance was selected to reduce impedance at higher frequencies and mitigate higher order harmonics.

**Figure 12-3 Harmonic filter parameters – ETAP input data**

The results of harmonic analysis are shown in Figure 12.4, showing that individual harmonic levels are all within planning levels except for the 11<sup>th</sup> harmonic. The individual harmonics starting from the 17<sup>th</sup> harmonic and higher are significantly reduced. Lower order harmonics such as the 5<sup>th</sup>, 7<sup>th</sup> and 13<sup>th</sup>, are marginally lower than the planning level harmonics. This solution does not provide a robust design margin for the most significant harmonics on the system and for this reason is not recommended for implementation.

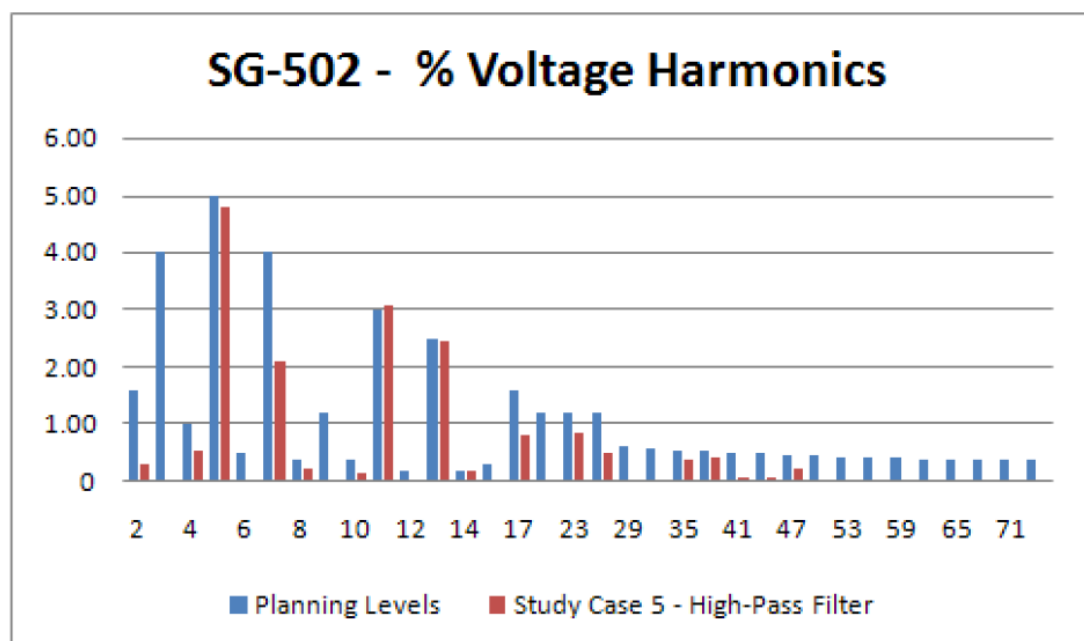


**Figure 12-4 SG-502 voltage harmonics with the high-pass single filter**



### Combination of a single tuned and a high pass filter

The concept of combining a single tuned filter and a high-pass (damped) filter met the design criteria for each individual harmonic. The new harmonic filter selected for the rectifier network was a combination of a Single Tuned Filter SG-502A and a High-Pass (damped) type SG-502B. The single tuned filter SG-502A was comprised of the following parameters:

- 600 kVAr reactive power per phase.
- The filter was tuned to 4.7<sup>th</sup> harmonic.
- The filter capacitance was 11.84  $\mu$ F and filter inductance was 38.74 mH.
- The Q factor of the filter was assumed to be 0.93.

The following parameters were selected for the high-pass (damped) filter SG-502B:

- 400 kVAr reactive power per phase.
- The filter was tuned to 6.7<sup>th</sup> harmonic.
- The filter capacitance was 7.89  $\mu$ F and filter inductance was 28.6 mH.
- The reactor Q factor of the filter was assumed to be 0.93.
- The damping resistor was selected based on the filter factor  $Q_f = 2$  and was calculated to be 125 ohms.

The target power factor and calculated power factors on the 22kV switchboards, SG-501 and SG-502, are summarised in Table 12.2. It can be seen that the system power factor is 0.96, the same on both switchboards.

Bus Tag Number	Nominal voltage [kV]	Target power factor (Technical Rules) (p.u.)	Load flow current and power factor (I [A] @p.u.)
SG-501	22	0.95	383A@0.96
SG-502	22	0.95	477A@0.96

**Table 12-2 Load factor for case 5**

The calculated voltage harmonics on SG-502 and the maximum planning levels are shown in Figure 12.5. showing that all individual harmonic levels are within the recommended planning levels. The voltage harmonics on SG-501 are equal to zero as there are no harmonic sources on the plant radial network.

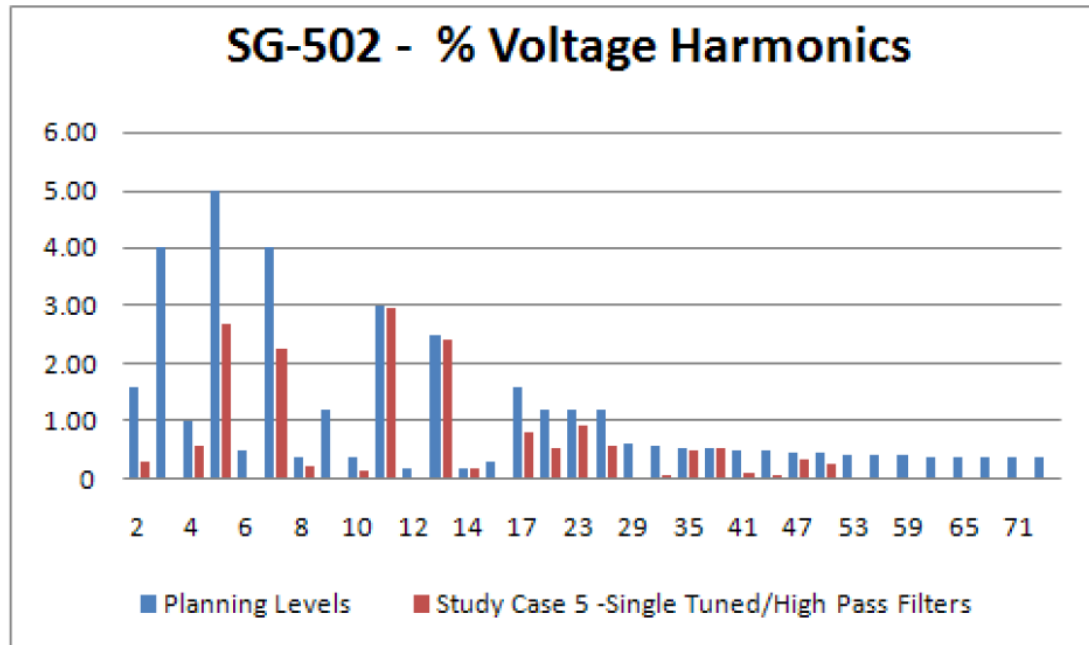


**Figure 12-5 Voltage harmonics on SG-502 for case 5**

The impedance diagram for SG-501 confirms that the filter PF-501 is tuned to 4.3<sup>rd</sup> harmonic. The impedance diagram for SG-502 shows that the filter PF-502A is tuned to 4.7<sup>th</sup> harmonic and that parallel resonance is at 200 Hz. Optimisation of filter parameters should include consideration of various high pass filter parameters, resulting in increased filtering of the 11<sup>th</sup> and 13<sup>th</sup> harmonics.

## 12.8 Discussion of Results

### 12.8.1 Power Factor Correction

The results of Case 1 indicate that the expanded rectifier-plant power system without harmonic filtering devices does not meet the power factor design criterion. The power factor on the Plant radial network at the 22 kV switchboard SG-501 was calculated to be 0.83, at maximum running load of 436 A. The design criterion set by the project is 0.95 or better. In order to improve the power factor from 0.83 to above

0.95, some 4500 kVAr reactive capacitor power would need to be installed on the network.

On the other hand, the rectifier radial network power factor at the 22 kV switchboard SG-502 was calculated to be 0.9, at maximum running plant load of 501A. In order to improve the power factor from 0.9 to over 0.95, some 3000 kVAr reactive capacitive power should be installed.

Installation of reactive power on the plant network does not impact on the power factor of the rectifier radial network, and vice versa. Hence, the two radial networks are independent, and solutions developed for each network can be analysed independently.

Case 5 analysed the power system with a new harmonic filter installed on the rectifier network. The filter reactive power was 1000 kVAr per phase (total of 3000 kVAr). The results showed that the system power factor with the new filter was 0.96. The same filter reduced the level of individual harmonics to acceptable levels.

### **12.8.2 Harmonic Filters**

The project design criteria developed for this study is based on Western Power planning levels. The individual voltage harmonic levels set out by the project are the 22 kV system levels, one level below the point of common coupling. The assumption made in this Study is that if the harmonic levels are satisfied at a 22 kV level, then they will also be satisfied on the 132 kV side. In addition, it is easier for the rectifier plant to measure the harmonics at the 22 kV side, than at the 132 kV side as access to the 132 kV substation is restricted to authorised Western Power personnel.

Case 1 indicated that for the power system with no harmonic filters installed on either the plant or rectifier networks, the individual harmonic levels are exceeded on the rectifier network. Individual harmonics on the plant network are almost non-existent and are well below the acceptable limits.

A 6-pulse rectifier and 12-pulse rectifier, which are sources of harmonic currents, were connected to the rectifier network. There were no harmonic sources on the plant network. Case 5 showed that a proposed new filter combination, which is to be installed on rectifier network, comprising of a single tuned filter and a high-pass

filter with damped resistor, would mitigate system harmonics to acceptable levels. The filter combination comprises 600 kVAr reactive capacitive power on the single tuned filter and 400 kVAr reactive capacitive power on the high pass filter. The damped resistor is rated at 125 ohms. This is only a conceptual design solution. Further verification and a filter parameter optimisation study will need to be carried out by prospective vendors.